ISSN 0973-8916

Current Trends in Biotechnology and Pharmacy

Volume 13 Issue 2 April 2019

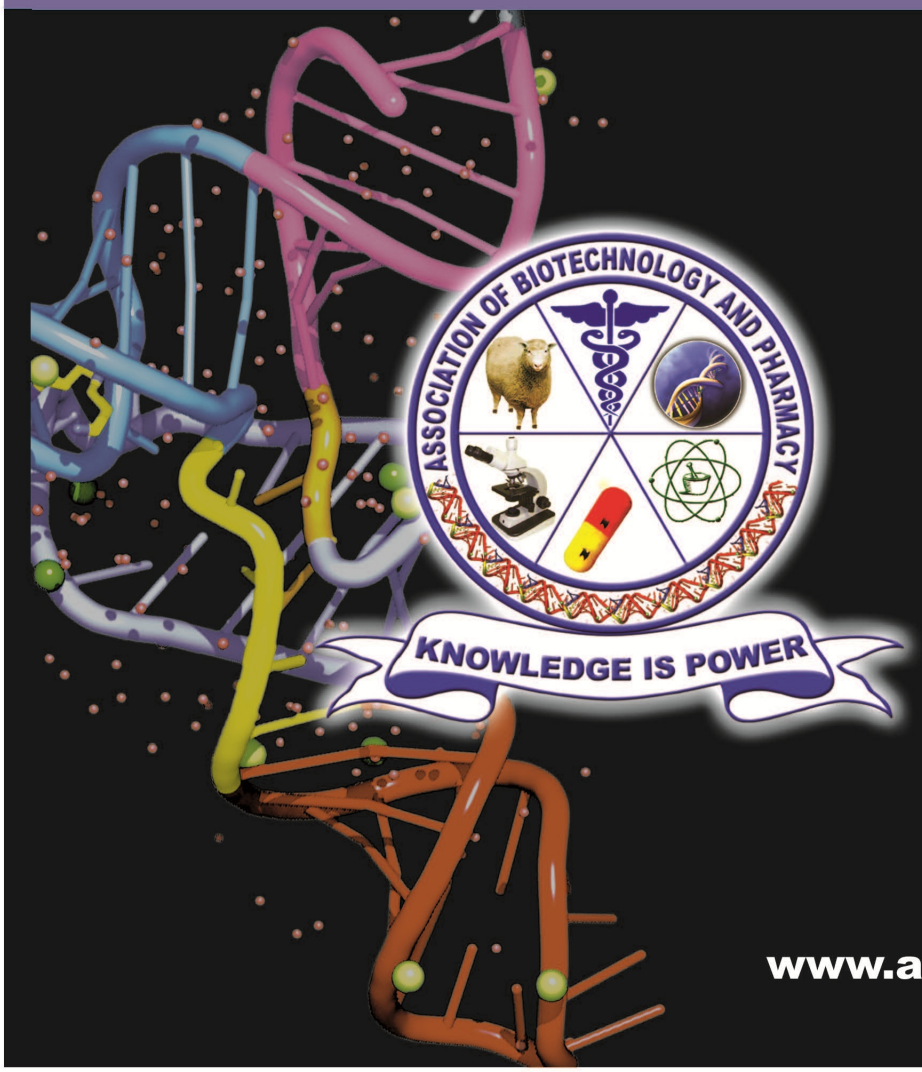

www.abap.co.in

Current Trends in Biotechnology and Pharmacy
ISSN 0973-8916 (Print), 2230-7303 (Online)

www.abap.co.in

ISSN 0973-8916

Current Trends in Biotechnology and Pharmacy

(An International Scientific Journal)

Volume 13 Issue 2 April 2019

www.abap.co.in

Indexed in Chemical Abstracts, EMBASE, ProQuest, Academic SearchTM, DOAJ, CAB Abstracts, Index Copernicus, Ulrich's Periodicals Directory, Open J-Gate Pharmoinfonet.in Indianjournals.com and Indian Science Abstracts.

Current Trends in Biotechnology and Pharmacy
Vol. 13 (2) April 2019, ISSN 0973-8916 (Print), 2230-7303 (Online)

Association of Biotechnology and Pharmacy

(Regn. No. 28 OF 2007)

The *Association of Biotechnology and Pharmacy (ABAP)* was established for promoting the science of Biotechnology and Pharmacy. The objective of the Association is to advance and disseminate the knowledge and information in the areas of Biotechnology and Pharmacy by organising annual scientific meetings, seminars and symposia.

Members

The persons involved in research, teaching and work can become members of Association by paying membership fees to Association.

The members of the Association are allowed to write the title ***MABAP*** (Member of the Association of Biotechnology and Pharmacy) with their names.

Fellows

Every year, the Association will award Fellowships to the limited number of members of the Association with a distinguished academic and scientific career to be as Fellows of the Association during annual convention. The fellows can write the title ***FABAP*** (Fellow of the Association of Biotechnology and Pharmacy) with their names.

Membership details

(Membership and Journal)		India	SAARC	Others
Individuals	– 1 year	Rs. 600	Rs. 1000	$100
	LifeMember	Rs. 4000	Rs. 6000	$500
Institutions	– 1 year	Rs. 1500	Rs. 2000	$200
(Journal only)	Life member	Rs.10000	Rs.12000	$1200

Individuals can pay in two instalments, however the membership certificate will be issued on payment of full amount. All the members and Fellows will receive a copy of the journal free.

Association of Biotechnology and Pharmacy
(Regn. No. 28 OF 2007)
#5-69-64; 6/19, Brodipet
Guntur – 522 002, Andhra Pradesh, India

Current Trends in Biotechnology and Pharmacy
Vol. 13 (2) April 2019, ISSN 0973-8916 (Print), 2230-7303 (Online)

Current Trends in Biotechnology and Pharmacy

ISSN 0973-8916

Volume 13 (2) **CONTENTS** **April 2019**

Research Papers

Review Papers

Current Trends in Biotechnology and Pharmacy
Vol. 13 (2) April 2019, ISSN 0973-8916 (Print), 2230-7303 (Online)

Information to Authors

The *Current Trends in Biotechnology and Pharmacy* is an official international journal of *Association of Biotechnology and Pharmacy*. It is a peer reviewed quarterly journal dedicated to publish high quality original research articles in biotechnology and pharmacy. The journal will accept contributions from all areas of biotechnology and pharmacy including plant, animal, industrial, microbial, medical, pharmaceutical and analytical biotechnologies, immunology, proteomics, genomics, metabolomics, bioinformatics and different areas in pharmacy such as, pharmaceutics, pharmacology, pharmaceutical chemistry, pharma analysis and pharmacognosy. In addition to the original research papers, review articles in the above mentioned fields will also be considered.

Call for papers

The Association is inviting original research or review papers and short comunications in any of the above mentioned research areas for publication in Current Trends in Biotechnology and Pharmacy. The manuscripts should be concise, typed in double space in a general format containing a title page with a short running title and the names and addresses of the authors for correspondence followed by Abstract (350 words), 3 – 5 key words, Introduction, Materials and Methods, Results and Discussion, Conclusion, References, followed by the tables, figures and graphs on separate sheets. For quoting references in the text one has to follow the numbering of references in parentheses and full references with appropriate numbers at the end of the text in the same order. References have to be cited in the format below.

Mahavadi, S., Rao, R.S.S.K. and Murthy, K.S. (2007). Cross-regulation of VAPC2 receptor internalization by m2 receptors via c-Src-mediated phosphorylation of GRK2. Regulatory Peptides, 139: 109-114.

Lehninger, A.L., Nelson, D.L. and Cox, M.M. (2004). Lehninger Principles of Biochemistry, (4th edition), W.H. Freeman & Co., New York, USA, pp. 73-111.

Authors have to submit the figures, graphs and tables of the related research paper/article in Adobe Photoshop of the latest version for good illumination and allignment.

Authors can submit their papers and articles either to the editor or any of the editorial board members for onward transmission to the editorial office. Members of the editorial board are authorized to accept papers and can recommend for publication after the peer reviewing process. The email address of editorial board members are available in website www.abap.in. For submission of the articles directly, the authors are advised to submit by email to krssrao@abap.co.in or krssrao@yahoo.com.

Authors are solely responsible for the data, presentation and conclusions made in their articles/research papers. It is the responsibility of the advertisers for the statements made in the advertisements. No part of the journal can be reproduced without the permission of the editorial office.

Current Trends in Biotechnology and Pharmacy
Vol. 13 (2) 102-111, April 2019, ISSN 0973-8916 (Print), 2230-7303 (Online)

Genome-wide Identification and Characterization of *Hsp70* gene family in Pearl millet (*Pennisetumglaucum*)

Kummari Divya[1,2], P. B. Kavi Kishor[2],Nagaraju Maraka[2], Pooja Bhatnagar-Mathur[1], Prashanth Singam[2], Vincent Vadez[1] and Palakolanu Sudhakar Reddy[1]*
[1]International Crops Research Institute for the Semi-Arid Tropics (ICRISAT), Patancheru, Hyderabad 502 324, India
[2]Department of Genetics, Osmania University, Hyderabad 500 007, India
*For Correspondence - p.sudhakarreddy@cgiar.org; palakolanusreddy@gmail.com

Abstract

Heat shock proteins (Hsps) are a class of molecular chaperons which are crucial for protein folding, assembly, and translocation in many normal cellular processes. They stabilize proteins and membranes, and can assist in protein refolding under stress conditions in plants. Pearl millet (*Pennisetum glaucum*) is highly abiotic stress tolerant, but its Hsps have not been characterized. In the present study, *PgHsp70* genes were retrieved and gene information analyzed in order to characterize their structure, localization and functions. Genome-wide screening using the tools of bioinformatics identified 18 *PgHsp70* genes in the pearl millet genome which have been categorized into four subfamilies depending on their cellular localization such as endoplasmic reticulum, mitochondria, chloroplast and cytoplasm. Number of introns ranged from 0-11 in *PgHsp70* family genes and the genes are located across 1 to 7 chromosomes. Phylogenetic analysis of *Hsp70s* revealed that they are closely related to *Sorghum Hsp70s*. Promoter analysis showed the presence of *cis*-acting elements such as GCN4, HSE, LTR, MBS, ABRE, MYB, and TC Aassociated with abiotic stress conditions indicating the involvement of these genes in the abiotic stress. Under vapour pressure deficit (VPD) conditions, leaf and root tissues of VPD-sensitive ICMR 1152 line, showed mild expression and in the presence of high VPD, VPD-insensitive ICMR1122 *PgHsp70* genes showed high expression in leaf and root tissues in comparison with VPD-sensitive line. Gene *PgcHsp70-1* displayed high transcript level under high VPD conditions. These results expand our horizon of understanding of the structure and function of *Hsp70s*, especially under abiotic stress conditions which can further be validated and employed in breeding programs and genetic engineering.

Key words: Abiotic stress, Hsps, heat shock proteins, pearl millet, Hsp70 family,*Vapour pressure deficit*

Introduction

Pearl millet (*Pennisetum glaucum*) is the sixth most important cereal crop plant grown in different areas of the world (1). A member of Poaceae family, pearl millet is usually grown well in the arid and semi-arid regions. It is used as food, forage, fuel and construction material (2). The crop accounts for 95% production from the developing countries, India being its largest producer covering an area of 9.8 million hectares (1,3). It is high in carbohydrates, protein and mineral, and hence suitable for animal and human consumption (4,5,6). Plants have developed many stress tolerance mechanisms to cope with adverse conditions. To protect themselves against high temperature stress conditions, plants produce several kinds of heat shock proteins

(Hsps) and heat shock factors (6,7,8,9,10). *Hsp70* class is an important one, among the eukaryotic cells. Hsp70 class proteins have a chaperonic function and prevent the accumulation of unfolded proteins. They also guide proper folding as well as help in the translocation of proteins in an ATP-dependent manner (11, 6, 12). Based on cellular localizations (mitochondria, chloroplasts, endoplasmic reticulum and cytoplasm), 4 subgroups of *Hsp70* have been noticed(6).The number of *Hsp70* genes identified in crop plants vary, for example 18 have been detected in *Arabidopsis* (13), 32 in rice (14), 20 in *Populus* (15), 61 in *Glycine max* (15), 27 in pepper (16), 27 in *Setaria* (17), 29 in *Brachypodium* (18) and 48 in *Sorghum bicolor* (unpublished data).

Pearl millet genomic sequence information (19) aided the present genome-wide screening, identification and characterization of *PgHsp70* gene family. The information about the Hsp gene family number, their cellular and chromosomal localization and also the characterization of the promoter sequences along with tissue specific expressions of the genes under varied abiotic stress conditions are vital for subsequent use of these genes to generate abiotic stress tolerant lines. Multiple sequence alignment of these genes helps in phylogenetic tree construction and their evolutionary tendencies. Present study identifies the number of *Hsp70* class of genes in the whole pearl millet genomes, their cellular and chromosomal localization, promoter sequence analysis and the gene expression data extraction in different tissues under different VPD conditions in the pearl millet crop. This may help ultimately in crop breeding programs aimed at developing stress tolerant lines.

Materials and Methods

Identification and retrieval of *PgHsp70* genes in *Pennisetum glaucum:* In the present study, *Oryza* (14), *Arabidopsis* (13) and *Sorghum* (Nagaraju et al unpublished data) *Hsp70* gene sequences were retrieved from NCBI databaseand searched their homologs in pearl millet genome using TBLASTN. Genscan (http://genes.mit.edu/GENSCAN.html) program was employed in order to identify and retrieve the coding sequences as well as protein sequences.

Nucleotide sequence analysis and characterization: Chromosomal locations of *PgHsp70s* were determined with the information obtained from Gramene data base and NCBI. Gene intron-exon structures were studied using Gene Structure Display Server (http://gsds.cbi.pku.edu.cn) (20). Chromosomal localizations were also found out. PAL2NAL software was employed to identify the number of synonymous and non-synonymous sites, their substitutions rates and dN/dS were calculated for the *PgHsp70* orthologs and paralogs (21).

Protein analysis: For *insilico* characterization of proteins, different bioinformatics tools were employed. Total number of amino acids, instability index, protein molecular weight (MW) and isoelectric point (pI) were found out by blasting protein sequences using Expasy ProtoParam. For finding out cellular localization, Wolf PSORT II was used (16). Conserved motifs were identified using MEME suit (22). Multiple alignment of the protein sequences were performed using CLUSTALW. Amino acid sequences of *PgHsp70s* along with their related plant species were taken to construct phylogenetic tree using MEGA 6.0 (23).

Promoter analysis of *PgHsp70* genes: The upstream regions of *PgHsp70* genes were extracted from pearl millet genome and regulatory elements of these genes were retrieved. Putative *cis*-acting regulatory elements of the promoter sequences in both forward and reverse strands were analyzed using Plant CARE database (24). *Hsp70* genes expression pattern in VPD tolerant and susceptible Pearl millet genotypes: To explore the expression of *PgHsp70* family genes under low VPD, high VPD and tissue specific expression in leaf and root tissues was extracted from the our earlier transcriptome data.

Results

***PgHsp70* putative protein identification, classification and cellular localization in**

***Pennisetumglaucum*:** Eighteen putative *PgHsp70* genes were identified in a search by Blast with the homologs of *A. thaliana*, *O.sativa* and *S. bicolor* against pearl millet genome in Gramene database. Based on the presence of these genes in different cellular compartments, PgHsp70s were further sub-divided into 4 groups. In group I *PgcHsp70,* 12 proteins in cytoplasm/nucleus, in group II PgBipHsp70, 3 proteins in endoplasmic reticulum, in group III PgmtHsp70, 2 in mitochondria, and in group IV *PgcpHsp70,* 1 in the chloroplast were localized (Table 1).

Chromosomal localization and gene structure analysis of PgHsp70 genes: *PgHsp70* genes were noticed across all the 7 chromosomes. On chromosomes 1, 2, 3, 4, 5, 6, and 7 (Table 1), 4, 4, 1, 1, 3, 2 and 3 genes were noticed respectively. Structure of *PgHsp70* genes revealed that *PgcHsp70-1* and *PgbipHsp70-15* contain no introns but*PgbipHsp70-14* contains 11. With few exceptions, *PgbipHsp70* contains maximum number of introns.

Characterization and motif distribution of PgHsp70 proteins: In PgHsp70proteins, amino acids ranged from 543 (*PgcHsp70-5*) to 848 (*PgcHsp70-2*). Similarly, pI values ranged from 4.8 (*PgcHsp70-3*) to 8.28 (*PgcHsp70-5*), molecular weights from 59773.3Da (*PgcHsp70-5*) to 93777.37Da (*PgcHsp70-2*) and instability index from 25.64 (*Pgbip Hsp70-15*) to 44.19 (*PgcHsp70-11*) (Table 1). *PgHsp70* proteins werefound localized in the chloroplast, cytoplasm, mitochondria and endoplasmic reticulum with the highest localizationin the cytoplasm(Table 1).Motif 3 at N-terminus and motif 9 and 10 at C-terminus were foundhighly conserved across the whole *PgHsp70* protein family (Fig. 4).The number of amino acids of DBDs in *PgHsp70* proteins ranged from 1 *(PgcHsp70-3)* to 689 *(PgcHsp70-11).*

Phylogenetic analysis and estimation of non-synonymous and synonymous substitution rates in PgHsp70 genes: In the present investigation,out of a total of 7 paralogous events, only one regional duplication (*PgHsp70-3*/ *PgHsp70-16*) was noticed on chromosome 1 and the remaining as segmental duplication events (Fig.2). All the paralogs exhibited non-synonymous substitution (d_N) to synonymous substitution (d_S) ratios above 1, indicating positive/ Darwinian selection pressure (Table 2 and Fig. 2). Out of 12 orthologous events, 9 were observed with S*orghum*, 2 with *Oryza* and 1 with *Arabidopsis* indicating the evolutionary relationship between *Sorghum* and *Pennisetum*. Of the 12 orthologous events,only one (*PgcHsp70-4*(Pgl_GLEAN_ 10006422)/ Sb01g010460) showedd_N/d_S ratio less than 1, suggesting purifying selection whilethe remaining follows the positive/Darwinian selection (Table 3and Fig. 3).

Promoter analysis: Promoter analysis of PgHsp70sshowedvaried*cis*-elements which are categorized into biotic and abiotic stress-responsive elements (DRE, DPBF, MYB, MYC, GT1C, HSE, LTRE, WBOX), light-responsive elements (I Box), hormone-responsive elements (ABA, ERE, ABRE, GARE), tissue-specific elements (CCGTCC-box), and otherelements (Skn, KST1, DOF).

Expression analysis of Hsp70 genes in VPD tolerant and susceptible pearl millet genotypes: To explore the expression of *PgHsp70* family genes under low VPD, high VPD and tissue specific expression in leaf and root tissues was extracted from our earlier transcriptome data. PgcHsp70-4 exhibited the least expression under all conditions in both the leaf and root tissues. Whereas, *PgcHsp70-1* showed maximum expression in all the conditions in comparison to other genes. Rest of the genes *PgcHsp70-2*,*PgcHsp70-3*, *PgcHsp70-5* and*PgcHsp70-16* exhibited mild expressions in both leaf and root tissues with the highest expression in high VPD, followed by low VPD and control conditions.In high VPD stress conditions,VPD insensitive ICMR-1122 cultivar showed higher expression in leaf and root tissues in comparison withVPD sensitive ICMR-1152 cultivar. In low VPD and normal conditions also, VPD insensitiveICMR-1122 showed higher transcript levels in leaf and root tissue when compared to VPD sensitiveICMR-1152 (Fig. 5).

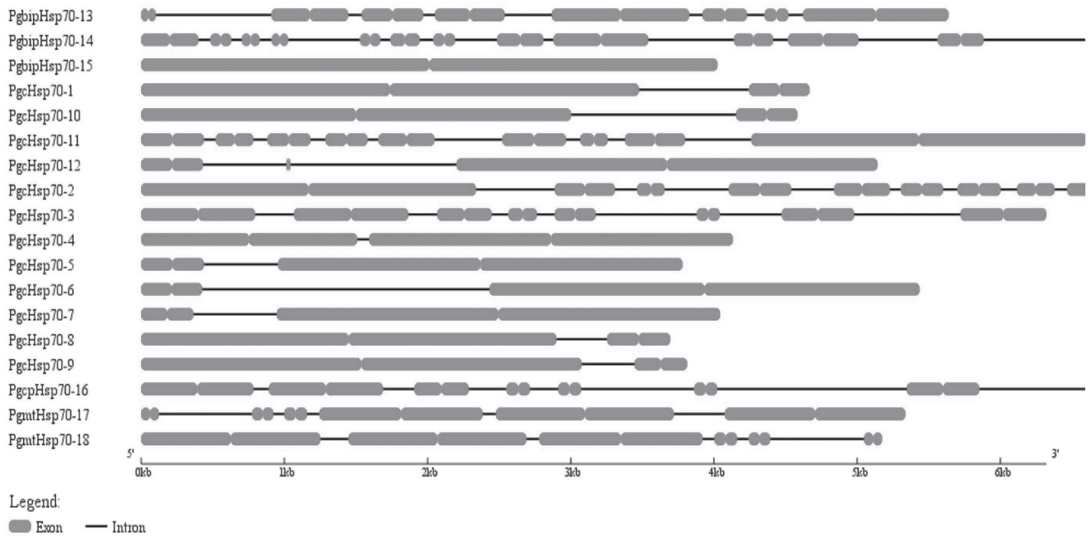

Fig. 1. Intron-exon distribution pattern across *PgHsp70* gene family

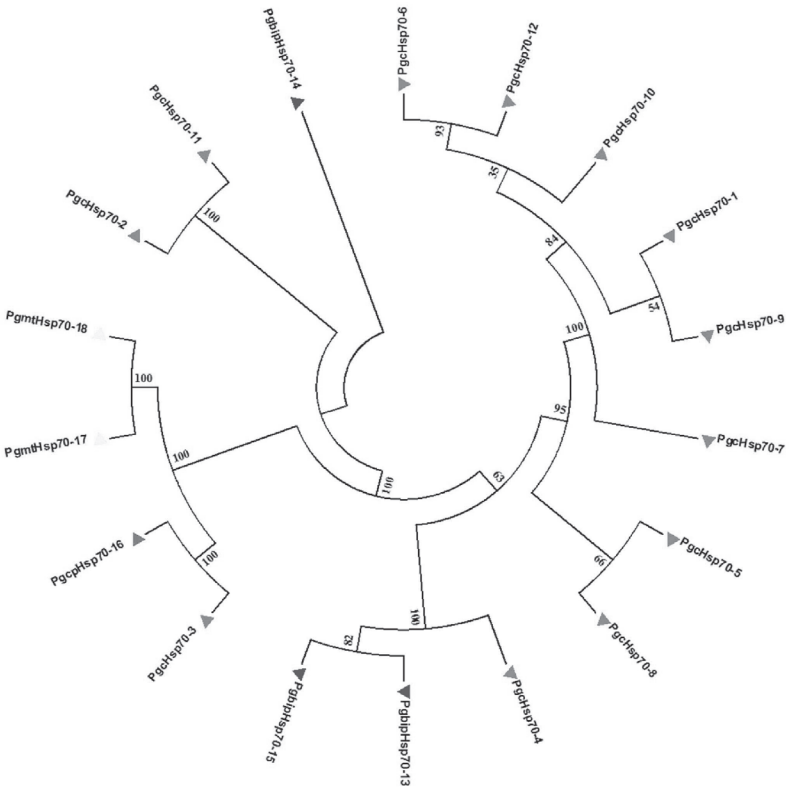

Fig. 2: Phylogenetic tree showing paralogous relation within *PgHsp70* gene family

Vol. 13 (2) 102-111, April 2019, ISSN 0973-8916 (Print), 2230-7303 (Online)

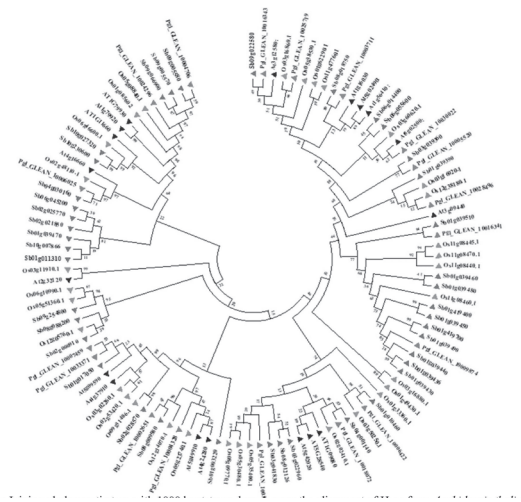

Fig. 3: Neighbor-Joining phylogenetic tree with 1000 bootstraps, based upon the alignment of Hsps from *Arabidopsis thaliana*, *Sorghum bicolor*, *Oryza sativa* and *Pennisetum glaucum.* Numbers on branches represent bootstrap values. At- *Arabidopsis thaliana*, Zm- *Zea mays*, Sb- *Sorghum bicolor*, Os- *Oryza sativa* and Pg-*Pennisetum glaucum*

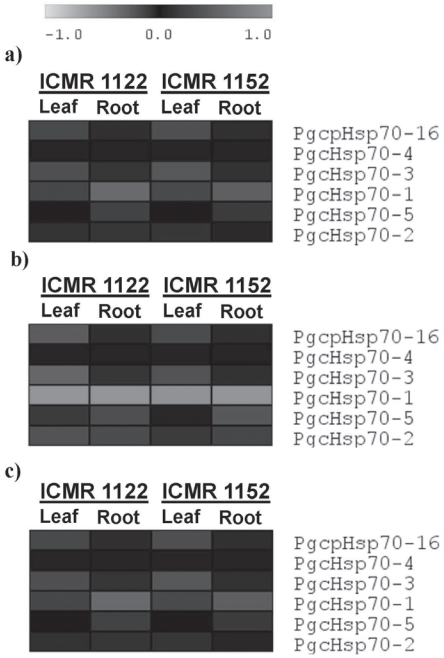

Fig. 5. Expression levels of *PgHsp70* genes in different conditions a) Low VPD, b) High VPD and c) Tissue specific expression

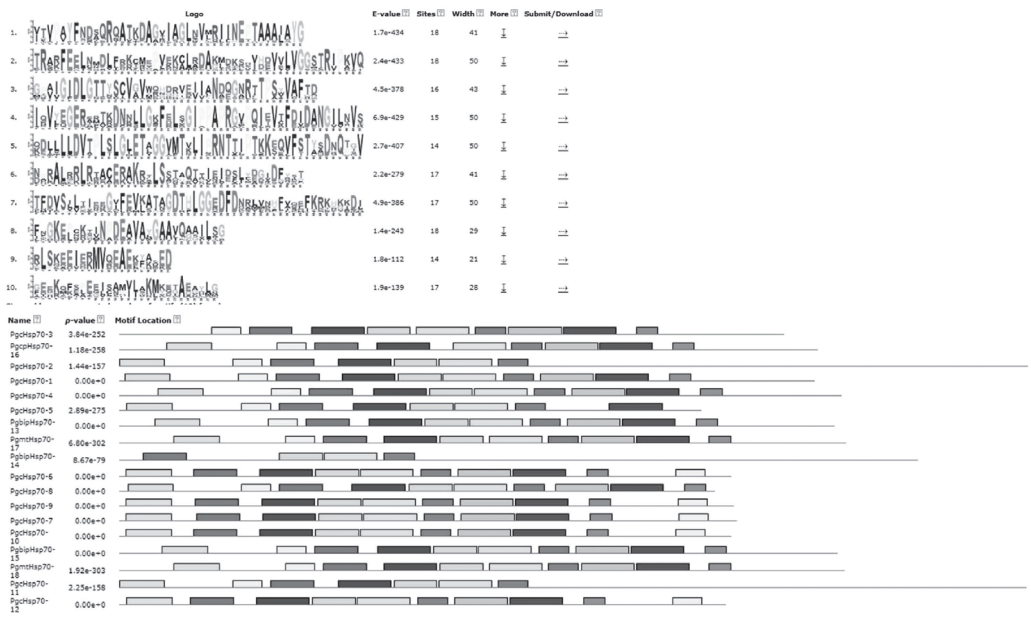

Fig. 4: Conserved protein motifs distribution in 18 PgHsp70s. Conserved motifs were analyzed by MEME Web serve using their respective protein sequences. Ten conserved motifs were identified, and different motifs are assigned different colors

Genome-wide characterizationof *PgHsp70* gene family

S. No.	Gene name	Acc. No. Genome/ GenBank	Chromosome location	Nucleotide			Protein						Localization	DBD
				ORF (bp)	Introns	Exons	Protein (aa)	M.Wt(daltons)	pI	Instability index	GRAVY	Aliphatic Index	TM helices	WOLF pSORT	
1	PgcHsp70-1	Pgl_GLEAN_10025719	1	1950	0	1	649	71069.5	5.13	33.14	-0.417	81.63	0	Cytoplasam	8-617
2	PgcHsp70-2	Pgl_GLEAN_10004706	1	2547	5	6	848	93777.37	5.17	40.4	-0.467	78.23	0	Cytoplasam	3-688
3	PgcHsp70-3	Pgl_GLEAN_10002651	1	1863	6	7	620	66352.91	4.8	26.59	-0.327	88.37	0	Cytoplasam	1-580
4	PgcHsp70-4	Pgl_GLEAN_10006422	2	2025	1	2	674	73706.53	5.33	30.59	-0.401	85.52	1	Cytoplasam	39-653
5	PgcHsp70-5	Pgl_GLEAN_10009874	2	1632	1	2	543	59773.3	8.28	35.35	-0.298	84.01	0	Cytoplasam	10-540
6	PgcHsp70-6	Pgl_GLEAN_10003711	4	1716	1	2	571	62449.43	4.97	33.82	-0.439	82.54	0	Cytoplasam	9-71 / 71-540
7	PgcHsp70-7	Pgl_GLEAN_10028496	5	1731	1	2	576	62997.08	5.16	33.18	-0.461	82.67	0	Cytoplasam	9-63 / 62-543
8	PgcHsp70-8	Pgl_GLEAN_10016341	5	1671	1	2	556	60963.56	5.39	36.24	-0.194	88.09	0	Cytoplasam	11-554
9	PgcHsp70-9	Pgl_GLEAN_10016343	5	1722	1	2	573	62611.62	5	33.66	-0.447	82.08	0	Cytoplasam	9-62 / 61-542
10	PgcHsp70-10	Pgl_GLEAN_10005520	6	1716	1	2	571	62353.42	4.97	32.47	-0.415	82.35	0	Cytoplasam	9-71 / 71-540
11	PgcHsp70-11	Pgl_GLEAN_10024296	7	2541	8	9	846	93616.12	5.17	44.19	-0.457	78.98	0	Cytoplasam	3-689
12	PgcHsp70-12	Pgl_GLEAN_10030022	7	1701	2	3	566	62112.22	4.98	33.78	-0.444	83.25	0	Cytoplasam	10-75 / 76-537
13	PgbipHsp70-13	Pgl_GLEAN_10018072	2	2004	7	8	667	73439.11	5.07	26.52	-0.474	86.24	1	ER	36-643
14	PgbipHsp70-14	Pgl_GLEAN_10006025	3	2238	11	12	745	82823.38	5.28	41.29	-0.549	82.13	0	ER	1-590
15	PgbipHsp70-15	Pgl_GLEAN_10030426	6	2013	0	1	670	73388.85	5.17	25.64	-0.395	85.73	1	ER	43-651
16	PgcpHsp70-16	Pgl_GLEAN_10004328	1	1959	6	7	652	70026	5.12	29.61	-0.319	84.62	0	Chloroplast	47-275 / 298-614
17	PgmtHsp70-17	Pgl_GLEAN_10033371	2	2037	5	6	571	62449.43	4.97	33.82	-0.439	82.54	0	Mitochondria	54-647
18	PgmtHsp70-18	Pgl_GLEAN_10007459	7	2034	5	6	677	72743.45	5.83	38.03	-0.324	84.93	0	Mitochondria	54-647

Table 1. *In silico* Characterization of pearl millet *Hsp70* genes and proteins

Discussion

When plants are subjected to different biotic and abiotic stress conditions, they display stress tolerance mechanisms by expressing genes like *Hsp70s* that playan importantrole (25,26). Hsps70s have the chaperonic function and play vital roles in many cellularprocesses underboth stress and control conditions. Genome-wide analysis of Hsp70 family revealed 14 *Hsp70* genes in *Arabidopsis*(13), 24 in rice (14), 34 in poplar (27), 61 in soybean (15), 21 in pepper (16), 29 in *Brachypodium* (18), 27 in *Setaria* (17) and 16 in quinoa (28). This indicates that this protein number varies from species to species.In pearl millet, 18 *Hsp70* genes were identified but the number appears less compared to other members of Poaceae family. PgHsp70 proteins are classified into 4 sub-classes, all of them possess the conserved domains at the C and N-termini, similar to *Setaria*Hsp70 (17). The *Hsp70* proteins are located in different sub-compartments of cells (29), probably to protect different cellular proteins. Based upon the sub-cellular localizations, the *PgHsp70* proteinsare categorized to 4 sub-groups; group I with 12 proteins in cytoplasm/nucleus, group II with 4 proteins in mitochondria, group III with 3 proteinsin endoplasmic reticulum and group IV with 1proteinlocalized in chloroplast. Similarly, in rice, *OsHsp70* proteins are localized innucleo/ cytosol (11 proteins), endoplasmic reticulum/Bips (6), mitochondria (3), andchloroplast (2). In*Arabidopsis*, 5 proteins were found in nucleo/ cytoplasm, 2 in plastid, 3 each in mitochondria and endoplasmic reticulum (13, 14). Kose (29) demonstrated that the cytosolic Hsp proteins movedto nucleus underheat stress, and the nuclear *Hsp70s* prevented DNA fragmentation and hence lead to high temperature tolerance. Cytoplasmic Hsp70 genes possess 1 or no introns, whereasorganellar *Hsp70s* have multiple introns with few exceptions (25).

These observations are akin to the present study. In *Sorghum bicolor Hsp70* also,multiple introns were observed, similar to previous reports (13, 16), implying that the exon/intron pattern of *Hsp70* family is not conserved among diverse

plants. Multiple numbers of introns in *PgHsp70s* may play a role in evolutionary process or have a regulatory role for imparting tolerance under diverse abiotic stress conditions (25).

Intandem/regional duplications, two or more genes are noticed on the same chromosome, while in segmental duplication, gene duplications are observed on different chromosomes (30).The gene duplication events play an important role in *Hsp70* family gene expansion in *Pennisetum glaucum*. A total of 7 events were observedin pearl millet, but 5 duplication events in *Sloanum*) (28), 8 in *Quinoa* (28), and 24 in *Glycinemax* (15). Semon et al. (31) pointed out that gene duplications, and chromosomal segments play a crucial role in the evolution of genome structure. In the present investigation, out of the 7 events, 6 were segmental duplications indicating their role in gene family expansion. Similarly, Zhang et al. (15) noticed 19 segmental duplications out of the 24 in *Glycinemax*. *In silico*analysis of *PgHsp70* promoters using the software Plant Care revealed multiple *cis*-acting elements,indicating that these

Table 2. Non-synonymous to synonymous substitution ratios ofPgHsp70 genes

PgHsp70 gene 1	Chromosome number	PgHsp70 Gene 2	Chromosome number	Number of non-synonymous sites (N)	Number of synonymous sites (S)	Non-synonymous substitution rate (d_N)	Synonymous substitution rate (d_S)	d_N/d_S
PgcHsp70-1	1	PgcHsp70-9	5	1430.7	288.3	4.871	0.0492	99
PgcHsp70-2	1	PgcHsp70-11	7	1973.4	564.6	0.4032	0.3335	1.209
PgcHsp70-3	1	PgcpHsp70-16	1	1503.4	356.6	5.9324	0.0599	99
PgcHsp70-5	2	PgcHsp70-8	5	1264.8	364.2	1.2098	1.018	1.1884
PgcHsp70-6	4	PgcHsp70-12	7	1410.5	287.5	6.4921	0.0656	99
PgbipHsp70-13	2	PgbipHsp70-15	6	1530.3	470.7	3.046	2.8728	1.0603
PgmtHsp70-17	2	PgmtHsp70-18	7	1579	452	0.0623	0.0585	1.0637

Table 3. Non-synonymous to synonymous substitution ratios of PgHsporthologs of pearl millet, Sorghum, Oryza, Zea mays and Arabidopsis

Pg Hsp70 Gene	Ortholog Gene	No. non-synonymous sites (N)	No. synonymous sites (S)	Non-synonymous substitution rate (dN)	Synonymous substitution rate (dS)	dN/dS
Pgl_GLEAN_10016343	Sb09g022580	1430.2	288.8	4.9101	0.0496	99
Pgl_GLEAN_10025719	Os03g16860	1615.3	331.7	5.0131	0.0506	99
Pgl_GLEAN_10003711	Sb08g018750	1401.1	311.9	6.0958	0.0616	99
Pgl_GLEAN_10030022	At5g02500	1409.9	288.1	7.6815	0.0776	99
Pgl_GLEAN_10005520	Sb03g039360	1347.5	365.5	2.9632	1.3942	2.1254
Pgl_GLEAN_10028496	Os12g38180	521.8	123.2	7.8399	0.0792	99
Pgl_GLEAN_10016341	Sb01g039510	1290	378	2.8908	1.6094	1.7961
Pgl_GLEAN_10006422	Sb01g010460	1626	396	4.052	8.7376	0.4637
Pgl_GLEAN_10018072	Sb04g001140	1650.2	350.8	6.3938	0.0646	99
Pgl_GLEAN_10002651	Sb08g009580	1492.1	367.9	6.0458	0.0611	99
Pgl_GLEAN_10006025	Sb04g030160	1857.8	377.2	6.5645	0.0663	99
Pgl_GLEAN_10004706	Sb09g005580	1909.3	529.7	0.6553	0.4468	1.4668

promoters couldregulate transcription of the downstream genes under diverse stress conditions, perhaps in a developmental stage-specific and tissue specific manner.

Studies from the past have shown that *Hsp70* genes were expressed variedly in response to different abiotic stress conditions (32,6). This study has been further extended to investigate the expression of *PgHsp70* genes in high VPD, low VPD and normal conditions. The results revealed that *PgcHsp70-1* showed a significantly upregulated expression in response to high VPD stresses which are inconsistent from the previous studies of Devi et al. (32). These findings show the potential roles of *Hsp70s* in the regulation of abiotic stress. However, this has not been validated in the present study.

Conclusions

A genome-wide scanning of *Pennisetum glacum* genome using the tools of bioinformatics resulted in the identification of 18 *Hsp70* genes in pearl millet. These Hsps are categorized into four subfamilies: *PgcHsp70* (12 proteins), *PgcpHsp70* (3 proteins), *PgbipHsp70* (1 protein) and *PgmtHsp70* (2 proteins) based on their subcellular localizations. Phylogenetic relationship revealed that *PgHsp70s* are closely related to *Sorghum Hsp70s.* Motifs at both C- and N-terminiare evolutionarily conserved in all the members. *In silico* promoter analysis showed the presence of several *cis*-elements which indicate that they play a key role under abiotic stress conditions. In high VPD stress,VPD insensitive ICMR-1122 cultivar showed higher expression in leaf and root tissues in comparison with VPD sensitive ICMR-1152 cultivar. In low VPD and normal conditions also, VPD insensitive ICMR-1122 displayed higher expression levels in leaf and root tissues when compared to VPD sensitive ICMR-1152. *PgcHsp70-1* exhibited maximum expression in all the conditions in comparison with other genes with the highest response in high VPD conditions. Our studies provide a point of reference for the functional validation of *Hsp70* family genes in pearl millet crop in the coming times.

Author contributions

PSR and VV designed the experiments, KD, PSR, PBM and PS executed the study, PSR, KD, NM and PBK analyzed data. PSR, PBK, NM and KD wrote the manuscript and critically evaluated.

Conflict of interest

The authors declare that they have no conflict of interest.

Acknowledgements

PSR acknowledges the Department of Science and Technology, Government of India for the research grant award through INSPIRE Faculty (Award No. IFA11-LSPA-06). Thanks to SISU theme for the sequence extraction and AgriGenome for analyzing the expression data. This work was undertaken as part of the CGIAR Research Program on Grain Legumes & Dryland Cereals (CRP-GLDC). ICRISAT is a member of the CGIAR Consortium.

References

1. Rathore, S., Singh, K., & Kumar, V. (2016). Millet grain processing, utilization and its role in health promotion: A review. *International Journal of Nutrition and Food Sciences*, *5*(5), 318-329.

2. Nambiar, V. S., Dhaduk, J. J., Sareen, N., Shahu, T., & Desai, R. (2011). Potential functional implications of pearl millet (*Pennisetum glaucum*) in health and disease. *Journal of Applied Pharmaceutical Science*, *1*(10), 62.

3. Yadav, D. N., Chhikara, N., Anand, T., Sharma, M., & Singh, A. K. (2014). Rheological quality of pearl millet porridge as affected by grits size. *Journal of food science and technology*, *51*(9), 2169-2175.

4. Sade, F. O. (2009). Proximate, anti-nutritional factors and functional properties of processed pearl millet (Pennisetum glaucum). *Journal of Food Technology*, *7*(3), 92-97.

5. Jaybhaye, R. V., Pardeshi, I. L., Vengaiah, P. C., & Srivastav, P. P. (2014). Processing and technology for millet based food products: a review. *Journal of Ready to Eat Food*, *1*(2), 32-48.

6. Reddy, P. S., Mallikarjuna, G., Kaul, T., Chakradhar, T., Mishra, R. N., Sopory, S. K., & Reddy, M. K. (2010). Molecular cloning and characterization of gene encoding for cytoplasmic Hsc70 from Pennisetum glaucum may play a protective role against abiotic stresses. *Molecular genetics and genomics*, *283*(3), 243-254.

7. Reddy, P. S., Thirulogachandar, V., Vaishnavi, C. S., Aakrati, A., Sopory, S. K., & Reddy, M. K. (2011). Molecular characterization and expression of a gene encoding cytosolic Hsp90 from Pennisetum glaucum and its role in abiotic stress adaptation. *Gene*, *474*(1-2), 29-38.

8. Reddy, P. S., Sharma, K. K., Vadez, V., & Reddy, M. K. (2015). Molecular cloning and differential expression of cytosolic class I small Hsp gene family in Pennisetum glaucum (L.). *Applied biochemistry and biotechnology*, *176*(2), 598-612.

9. Nitnavare, R. B., Yeshvekar, R. K., Sharma, K. K., Vadez, V., Reddy, M. K., & Reddy, P. S. (2016). Molecular cloning, characterization and expression analysis of a heat shock protein 10 (Hsp10) from Pennisetum glaucum (L.), a C 4 cereal plant from the semi-arid tropics. *Molecular biology reports*, *43*(8), 861-870.

10. Kummari Divya, Pooja Bhatnagar-Mathur, Kiran K. Sharma and Palakolanu Sudhakar Reddy. (2019) Heat Shock Proteins (Hsps) Mediated Signalling Pathways During Abiotic Stress Conditions.

11. Reddy, R. A., Kumar, B., Reddy, P. S., Mishra, R. N., Mahanty, S., Kaul, T., ... & Reddy, M. K. (2009). Molecular cloning and characterization of genes encoding Pennisetum glaucum ascorbate peroxidase and heat-shock factor: interlinking oxidative and heat-stress responses. *Journal of plant physiology*, *166*(15), 1646-1659.

12. Wang, X., Lu, Z., Gomez, A., Hon, G. C., Yue, Y., Han, D., ... & Ren, B. (2014). N 6-methyladenosine-dependent regulation of messenger RNA stability. *Nature*, *505*(7481), 117.

13. Lin, B. L., Wang, J. S., Liu, H. C., Chen, R. W., Meyer, Y., Barakat, A., & Delseny, M. (2001). Genomic analysis of the Hsp70 superfamily in Arabidopsis thaliana. *Cell stress & chaperones*, *6*(3), 201.

14. Sarkar, N. K., Kundnani, P., & Grover, A. (2013). Functional analysis of Hsp70 superfamily proteins of rice (Oryza sativa). *Cell stress and Chaperones*, *18*(4), 427-437.

15. Zhang, J., Liu, B., Li, J., Zhang, L., Wang, Y., Zheng, H.,& Chen, J. (2015). Hsf and Hsp gene families in Populus: genome-wide identification, organization and correlated expression during development and in stress responses. *BMC genomics*, *16*(1), 181.

16. Guo, M., Lu, J. P., Zhai, Y. F., Chai, W. G., Gong, Z. H., & Lu, M. H. (2015). Genome-wide analysis, expression profile of heat shock factor gene family (CaHsfs) and characterisation of CaHsfA2 in pepper (Capsicum annuum L.). *BMC plant biology*, *15*(1), 151.

17. Singh, R. K., Jaishankar, J., Muthamilarasan, M., Shweta, S., Dangi, A., & Prasad, M. (2016). Genome-wide analysis of heat shock proteins in C 4 model, foxtail millet identifies potential candidates for crop improvement under abiotic stress. *Scientific reports*, *6*, 32641.

18. Wen, F., Wu, X., Li, T., Jia, M., Liu, X., Li, P., ... & Yue, X. (2017). Genome-wide survey of heat shock factors and heat

shock protein 70s and their regulatory network under abiotic stresses in Brachypodium distachyon. *PloS one*, *12*(7), e0180352.

19. Varshney, R. K., Shi, C., Thudi, M., Mariac, C., Wallace, J., Qi, P., ... & Srivastava, R. K. (2017). Pearl millet genome sequence provides a resource to improve agronomic traits in arid environments. *Nature biotechnology*, *35*(10), 969.

20. Hu, B., Jin, J., Guo, A. Y., Zhang, H., Luo, J., & Gao, G. (2014). GSDS 2.0: an upgraded gene feature visualization server. *Bioinformatics*, *31*(8), 1296-1297.

21. Suyama, M., Torrents, D., & Bork, P. (2006). PAL2NAL: robust conversion of protein sequence alignments into the corresponding codon alignments. *Nucleic acids research*, *34*(suppl_2), W609-W612.

22. Bailey, T. L., Boden, M., Buske, F. A., Frith, M., Grant, C. E., Clementi, L., ... & Noble, W. S. (2009). MEME SUITE: tools for motif discovery and searching. *Nucleic acids research*, *37*(suppl_2), W202-W208.

23. Tamura, K., Stecher, G., Peterson, D., Filipski, A., & Kumar, S. (2013). MEGA6: molecular evolutionary genetics analysis version 6.0. *Molecular biology and evolution*, *30*(12), 2725-2729.

24. Lescot, M., Déhais, P., Thijs, G., Marchal, K., Moreau, Y., Van de Peer, Y., ... & Rombauts, S. (2002). PlantCARE, a database of plant cis-acting regulatory elements and a portal to tools for in silico analysis of promoter sequences. *Nucleic acids research*, *30*(1), 325-327.

25. Sung, D. Y., Vierling, E., & Guy, C. L. (2001). Comprehensive expression profile analysis of the Arabidopsis Hsp70 gene family. *Plant physiology*, *126*(2), 789-800.

26. Lee, J. H., Yun, H. S., & Kwon, C. (2012). Molecular communications between plant heat shock responses and disease resistance. *Molecules and cells*, *34*(2), 109-116.

27. Yer, E. N., Baloglu, M. C., Ziplar, U. T., Ayan, S., & Unver, T. (2016). Drought-responsive Hsp70 gene analysis in populus at genome-wide level. *Plant molecular biology reporter*, *34*(2), 483-500.

28. Liu, J., Wang, R., Liu, W., Zhang, H., Guo, Y., & Wen, R. (2018). Genome-wide characterization of heat-shock protein 70s from Chenopodium quinoa and expression analyses of Cqhsp70s in response to drought stress. *Genes*, *9*(2), 35.

29. Kose, S., Furuta, M., & Imamoto, N. (2012). Hikeshi, a nuclear import carrier for Hsp70s, protects cells from heat shock-induced nuclear damage. *Cell*, *149*(3), 578-589.

30. Schlueter, J. A., Scheffler, B. E., Jackson, S., & Shoemaker, R. C. (2008). Fractionation of synteny in a genomic region containing tandemly duplicated genes across Glycine max, Medicago truncatula, and Arabidopsis thaliana. *Journal of heredity*, *99*(4), 390-395.

31. Sémon, M., & Wolfe, K. H. (2007). Rearrangement rate following the whole-genome duplication in teleosts. *Molecular biology and evolution*, *24*(3), 860-867.

32. Devi, M. J., Sinclair, T. R., & Taliercio, E. (2015). Comparisons of the effects of elevated vapor pressure deficit on gene expression in leaves among two fast-wilting and a slow-wilting soybean. *PloS one*, *10*(10), e0139134.

Current Trends in Biotechnology and Pharmacy
Vol. 13 (2) 112-123, April 2019, ISSN 0973-8916 (Print), 2230-7303 (Online)

Endemic Brucellosis in Indian Animal and Human Populations: A Billion Dollar Issue

Manasa Machavarapu[1,2], Revathi Poonati[2], Prudhvi Chand Mallepaddi[2], Vinayachandu V Gundlamadugu[3], Sujaya Raghavendra[4], Kavi Kishor B Polavarapu[2,3] and Rathnagiri Polavarapu[1,2,3]

[1]Department of Biotechnology, Acharya Nagarjuna University, Guntur 522 510, Andhra Pradesh, India.
[2]Genomix Molecular Diagnostics Pvt. Ltd., Prashanthinagar, Kukatpally, Hyderabad 500 072, India.
[3]Genomix CARL Pvt. Ltd., Rayalapuram Road, Pulivendula-516 390, Kadapa, Andhra Pradesh, India
[4]Dr. Ram Manohar Lohia Hospital, New Delhi- 110 001, India
*For Correspondence - giri@genomixbiotech.com

Abstract

Brucellosis is a common and neglected zoonotic disease. It is endemic and still an uncontrolled public health problem in many developing countries including India. Present epidemiological data suggest that brucellosis is causing a major economic problem which burdens up to 3.4 billion US dollars per year. Due to insufficient awareness in public, safe livestock practices, trading the infected animals and economic burden of disease diagnosis and vaccination have led to persistence of brucellosis in the country. Paucity of epidemiological data obtained from previous survey programmes is not convincing enough with the degree of the disease prevalence in the country. Since India is sensitive from both religious and economic points of view, control of the disease has become a sensitive issue. Prevention of brucellosis is dependent on conducting adequate health education awareness and control programmes to address the disease depth of the issue in the country. This review discusses epidemiology, diagnostic methods, prevalence, and vaccines along with recent control measures adopted in Indian Scenario.

Key words: Brucellosis, animal populations, zonotic disease, small ruminants, insufficient awareness, paucity of epidemiological data, awareness and control programmes

Introduction

Brucellosis is an infectious zoonotic disease caused by Gram negative facultative intracellular bacterial organisms of the genus *Brucella*. *Brucellae* belong to α–2 subdivision of *proteobacteria.* They are Gram-negative, partially acid fast, aerobic, facultative intracellular coccobacilli or short rods. They are oxidase, catalase, nitrate reductase and urease positive. *Brucella* can infect a wide variety of animal species and human beings. The genus *Brucella* contains ten recognized species. Based on the host specificity and pathogenicity and host preference, six classical species are identified (1). They are *Brucella abortus*, *Brucella melitensis*, *Brucella suis, Brucella ovis, Brucella canis* and *Brucella neotamae* (2, 3). Recently, four new *Brucella* species are identified. They are *Brucella pinnipedalis* isolated from seals and *Brucella ceti* isolated from cetaceans (4), *Brucella microti* isolated from common voles (5), soil (6) and foxes (7) and *Brucella inopinata* isolated from breast implant (8). Worldwide the main pathogenic species are *B. abortus* responsible for bovine brucellosis, *B. melitensis* that causes caprine and ovine brucellosis and *B. suis* associated with swine brucellosis. These three species mainly cause abortions in animals. *B. abortus* preferentially infects cattle, *B.melitensis* sheep

and goats, *B. suis* pigs and *B. canis* dogs. Above species infect humans with *B.melitensis* being the most common.

Brucellosis is a dreadful and contagious disease of animals and characterized by abortion in females and to a lesser extent orchitis and infection of accessory sex glands in males and infertility in both the sexes. It has zoonotic importance in terms of its transmissibility to human beings. When brucellosis is identified in a herd, flock, region or country, international veterinary regulations impose restrictions on animal movement and trade, which results in huge economic loss. In order to control and eradicate brucellosis in cattle, small ruminants and pigs, many control programmes have been initiated and implemented worldwide (9). *B. ovis* and *B. canis* are responsible for ram epididymitis and canine brucellosis, respectively. In the case of *B. neotomae,* only strains isolated from desert wood rat (*Neotoma lepida*) in North America have been reported.

Brucellosis and epidemiology

Brucellosis is found worldwide, however it has been eradicated from many countries, but still it is the most serious problem in developing countries including India. The disease has considerable impact on animal and human health as well as socioeconomic impacts especially in rural areas where income relies largely on livestock breeding and dairy products. The rates of infection may vary from one country to another and between regions within the country. Brucellosis is widely prevalent throughout India among the bovine population both in farm and village animals causing economic losses up to 3.4 billion US dollars (10). In India, prevalence and disease spread is still increasing, though advances in diagnosis, therapy and vaccines have been made available. Serological survey of brucellosis was performed in 23 states of India. A total of 30,437 bovine samples were screened with Rose Bengal Plate Agglutination Test (RBPT) and Serum Tube Agglutination Test (SAT), which revealed 1.9% prevalence in cattle and 1.8% in

Table 1. Seroprevalence in different states of India.

State	Species	Prevalence	Reference
Rajasthan	Goats	11.45%	Kapoor *et al.,* 1985 (12)
	Humans	2.97%	
Nagaland	Over all	11% to 34%	Rajkhowa *et al*., 2005 (13)
Punjab	Buffaloes	13.4%	Dhand *et al*., 2005 (14)
	Cattle	9.9%	
Tamil Nadu	Over all	9.96% to 20.35%	Sulima, 2009 (15)
Rajasthan and Bihar	Cattle	8.58%	Singh *et al.,* 2007 (16)
	Goat	8.85%	
	Sheep	7.08%	
Arunachal Pradesh	Overall	18.98% to 23.29%	Shakuntala *et al*., 2016 (17)
Meghalaya	Over all	2.8 to 5.6%	Shakuntala *et al*., 2016 (17)
Gujarat	Over all	11.90% to 33.70%	Patel, 2014 (18)
Karnataka	Over all	45.80%	Jagapur, 2013 (19)
Uttar Pradesh	Over all	22.39%	Jagapur, 2013 (19)
Uttarakhand	Over all	8.57%	Jagapur, 2013 (19)

buffaloes (11). Seroprevalence of brucellosis in different states of India from previous reports was mentioned in the table 1. From the table, it is evident that prevalence reports were mainly concentrated on live stock species. Seroprevalence from rest of the states is not available at present.

Animal brucellosis : Brucellosis causes economic losses due to abortions, premature births, and decreased milk production in animals. Further, repeated breeding also may cause temporary or permanent infertility in livestock. Bovine brucellosis is widespread in India and appears to be on the increase in recent times, perhaps due to increased trade and rapid movement of livestock across different states (20). Free grazing and mixing with flocks of sheep and goats also contribute to wide disease spread of disease in animals, resulting in an outbreak of brucellosis. Clinical signs of the disease in animals include abortions, retained placenta, orchitis, epididymitis, rarely arthritis, with excretion of organisms in milk and uterine discharges. Diagnosis of disease depends on the isolation of the organism from milk, blood, abortion materials, udder secretions and tissues. Presumptive diagnosis can be carried out by assessing serological responses to *Brucella* antigens (21). All *Brucella* species may also infect wild life species. Classical species have been isolated from a great variety of wild species such as bison, elk, wild boar, fox, hare, feral swine, African buffalo, reindeer and caribou (22). In order to implement appropriate control methods to address wild life brucellosis, it is crucial to distinguish between spill over infection contracted from domestic animals and a sustainable infection (22). In the latter case, the concern of the livestock industry is to prevent the re-introduction of the infection in livestock (spill-back), particularly in regions or states that are "officially brucellosis-free". If the status of "officially brucellosis-free" is lost, domestic animals must be tested prior to being traded, which imposes huge costs.

Human brucellosis : Brucellosis is a significant zoonoses that causes veterinary and public health problems in India. In India, 80% of the population live in approximately 575,000 villages and thousands of small towns; have close contact with domestic or wild animal population owing to their occupation. Hence, human population stands at a greater risk of acquiring zoonotic diseases including brucellosis (23). Human brucellosis is predominantly transmitted through animal contact and also by consuming infected milk and meat products. Worldwide, reported incidence of human brucellosis in endemic disease areas varies widely, from <0.01 to >200 per 100,000 population. For example, Egypt, the Islamic Republic of Iran, Jordan, Oman, Saudi Arabia and Syrian Arab Republic reported a combined annual total of more than 90,000 cases of human brucellosis in 1990 (24). The low incidence reported in known brucellosis-endemic areas may reflect the absence or the low levels of surveillance and reporting (25). However in India, the true incidence of human brucellosis is unknown.

B. abortus, *B. melitensis*, *B. suis* and *B. canis* are the species that mainly infect humans. Consumption of undercooked traditional delicacies has been implicated in human brucellosis. Other route of infection for persons working in slaughter houses, laboratories and veterinarians is through skin wounds or by accidental ingestion. Hunters may be infected by skin abrasions or by accidental ingestion of organisms of animals that they have killed (26, 27). Inhalation is often responsible for a significant percentage of cases in abattoir employees (28). Laboratory acquired *Brucella* infection could be through accidental inhalation of aerosols and mucosal or skin contacts. Brucellosis is a major health hazard for the laboratory workers handling the cultures of the virulent or attenuated strains. The disease has been recognized as one of the common laboratory-transmitted infections and has been reported to occur in clinical, research, and production laboratories (Bouza *et al* 2005 (29); Centre for Disease Control and Prevention [CDC] 2008 (30)).

The presence of brucellosis in wild animals, with a potential for continuous transfer to domestic animals and from them to humans is another

epidemiological issue (31). *B. melitensis* has been identified in most of the recorded cases in humans. However, *B. abortus* and *B. suis* also cause substantial morbidity in the countries where domestic animals have persistent infection. *B. canis* is rarely seen in humans and *B. ovis*, and *B. neotamae* have not been identified in humans. Clinical signs and symptoms of human infection include continued or intermittent fever, chills, irregular fever of variable duration, with headache, profuse sweating, weakness and weight loss. Although brucellosis has been or close to being eradicated in developed countries, it is still a major public and animal health problem particularly in developing countries where livestock are major sources of food and income. Livestock expansion with uncontrolled transport, lack of veterinary support and vaccines favouring the disease are spreading. Many factors are associated with the current approaches of disease control, eradication or prevention in the country such as level of infection, reliability of diagnostic tests, surveillance, monitoring and effective vaccination programmes.

Brucellosis diagnosis : Diagnosis of brucellosis based on clinical signs is difficult, because they are also commonly observed in other diseases. The most important clinical feature of brucellosis is abortion in their first gestation. Usually, females abort only once and remain infected throughout their life time. So, clinical diagnosis of the disease in animals cannot be fixed on the basis of abortion, since many pathogens may cause abortions in animals. Clinicians practicing in endemic areas must be aware of the disease and develop a high degree of clinical suspension based on the history and epidemiological data. Otherwise, the disease may be misdiagnosed or diagnosis may be delayed, due to its deceptive nature. Therefore, laboratory testing is essential. Brucellosis diagnosis involves direct testing such as isolation and identification of *Brucella* species. Indirect testing includes detection of antibodies in blood and milk specific to *Brucella* antigens. The choice of testing depends upon the prevalence of the disease and epidemiological status of disease suspected animals in a country or region. Isolation of organisms and detection of *Brucella* species DNA are the methods that allow certainty of diagnosis.

Culture of *Brucella* species in the laboratory: Definitive diagnosis of brucellosis is carried out by isolation and culture of organism from the clinical samples. Laboratory diagnosis of disease by culture method is slow due to slow growth of *Brucella* in culture media (32, 33). Bacteriological method includes culturing of samples such as aborted foetal stomach contents, milk, blood, lymph nodes and vaginal discharges from suspected cases for isolation and identification of the infecting *Brucella* organisms (34, 35). The isolated organisms are further tested using molecular based tests. This sequence of confirmatory procedures is referred to as the "gold standard" method for identifying *Brucella* species (36).

Molecular detection of brucellosis : Molecular methods such as polymerase chain reaction (PCR) have been recently included in disease diagnosis. The advantages of PCR are numerous. Independent of the disease stage, it is more sensitive than blood culture and more specific than serological methods (37). Genus specific PCR assays are generally adequate for the molecular diagnosis of human brucellosis (38). Molecular assays targeting the *IS711* insertion element, which is found in multiple copies within *Brucella* chromosomes, also improve analytical sensitivity (39). The *bcsp31* gene, coding for a 31-kDa immunogenic outer membrane protein conserved among all *Brucella* spp. is the most common molecular target in clinical applications (40). Such a genus-specific PCR can help to avoid false-negative results in patients infected with unusual species and biovars.

Serological methods of brucellosis detection Several serological methods have been tried and few of them have lasting effects. Rose Bengal Plate Agglutination Test (RBPT), Serum Tube Agglutination Test (SAT), Enzyme Linked Immunosorbent Assay (ELISA) are the most

common tests practiced in the laboratories now. Recently, Lateral Flow Assays (LFA) are also widely used in laboratories and in the field. According to OIE, Complement Fixation Test (CFT) and Competitive ELISA (cELISA) are the gold standard serological assays being used for disease diagnosis. Other important assays used for diagnosis include coombs agglutination test, radio immune assay, and fluorescent polarization assay.

Rose Bengal Plate Agglutination Test for brucellosis diagnosis : RBPT is a widely used diagnosis agglutination test. It is rapid and can be performed within 4 minutes on glass slide or plate with the help of an acidic-buffered antigen (pH 3.65 ± 0.05). This test has been introduced as screening test in the field because of its rapidity and simplicity. OIE considers agglutination tests are "prescribed tests for trade" (OIE 2009).

Serum Agglutination Test for diagnosis : SAT is the most popular and is recently being used worldwide as a diagnosis test. SAT measures the total quantity of agglutinating antibodies (IgM and IgG), and the quantity of specific IgG is determined by 2-mercaptoethanol (2ME). SAT titers above 1:160 are considered for diagnostic purposes in conjunction with a compatible clinical presentation. In endemic areas, a titre of 1:320 as cutoff may make the test more specific. The type of antibody is important, as IgG antibodies are considered a better indicator of active infection and the rapid fall in the level of IgG antibodies is said to be prognostic of successful therapy. Studies by researchers (41, 42) have shown persistence of various levels of SAT antibodies in many clinically cured patients.

Enzyme Linked Immunosorbent Assay test for diagnosis : ELISA are divided into two categories. One is indirect ELISA (iELISA) and another competitive ELISA (cELISA). ELISA is an effective method for diagnosing acute and chronic brucellosis and for detecting antibodies in CSF of patients with neurobrucellosis. The ELISA is as sensitive as Radio Immuno Assay (RIA) (43). In iELISA, mostly purified smooth LPS is used as an antigen but good deal of variation exists in the anti-bovine IgG conjugate (44). iELISA is highly sensitive but vulnerable to non-specific reactions with *Yersinia enterocolitica* O:9. In cELISA, monoclonal antibodies developed against specific epitope that are not shared with LPS of *Yersinia* are used to increase the specificity of the assay (45, 46).

Complement Fixation Test (CFT) for brucellosis diagnosis : CFT allows detection of anti-*Brucella* antibodies that are able to activate complement. Cattle immunoglobulins (Ig) that can activate bovine complement are the IgG and the IgM. According to available literature, this test is not highly sensitive but exhibits an excellent specificity (47, 48). Since the test is difficult to standardize, it is progressively being replaced by ELISAs (OIE 2009).

Fluorescence Polarization Assay (FPA) : During FPA test, serum samples are incubated with *Brucella* specific antigen labeled with flourescein isothiocynate. Large fluorescent complexes are formed in the presence of antibodies against *Brucella* species. In negative samples, antibodies do not form a complex and spin quickly, therefore cause greater depolarization of light. In the positive samples, antibodies specific to *Brucella* antigen form complexes and cause less depolarization of light than do in negative samples. Thus, the disease is detected based on light polarization.

Lateral flow assays (LFA) for diagnosing brucellosis : LFA is also called as rapid immuno chromatographic assay. *Brucella* IgG and IgM lateral flow assays (49) and protein-G based lateral flow assays (50) have been found to be rapid and simple with high sensitivity and specificity. These tests are simple, rapid and can be performed easily in point of care areas and health care centers as field tests. Thus, LFA has an edge over other diagnostic tests.

Spectrum of brucellosis disease

Department of Biotechnology (DBT), Ministry of Science and Technology, Government of India, has launched a "network project on brucellosis". The

mission of the network is to develop simple, rapid and convenient diagnostic kits like lateral flow assay (LFA) rapid detection kits (Figure 1) and indirect ELISA (iELISA) kits (Figure 2) and validate them at the National Reference Laboratories. These kits are currently being used in the field to understand the prevalence of brucellosis in a large spectrum. In the present study, a total of 14,343 samples were collected randomly from various parts of the country, including domestic animals, wild animals and humans involved in animal practices (Table 2). The data suggest that over all the disease seroprevalence is 15.15%. All these samples were categorized into three types based on the places of testing. They are Gosalas, unorganized village farms and organized dairy farms. Out of this data, screening of Gosalas, unorganized village farms, and organized dairy farms showed that the prevalence of the disease is 30.81%, 10.09% and 11.62% respectively.

In Gosalas, shelter less and unwanted cows gather from different places and become a reservoir for brucellosis and other infectious diseases. Due to insufficient awareness, any one of the cows from infected area/region with brucellosis easily transmits the disease to the other healthy animals present in Gosalas and neighbouring areas. In our study, screening of 4,085 animals from 10 Gosalas was carried out by LFA and iELISA tests which revealed that prevalence ranges from 10.24% to 30.81%. Screening of 4,695 animals for disease prevalence in organized dairy farms showed 5.24% to 17.82%. Contrarily, in unorganized village farms, the disease prevalence is less and ranged from 0.1% to 10.09%. Shome et al. (51) reported 0.58% to 20.17% in individual animal seroprevalence in organized farms. Examination of 4,580 animals by RBPT and ELISA tests from 119 dairy farms revealed high over all prevalence (65.54%) of the disease in herds than in individual animals in Punjab (34.15%) and Haryana (22.34%) (52). In unorganized farms, high prevalence (14.14%) was recorded in comparison with organized farms (3.23%) by Lone et al. (53). In contrast, other reports (54, 55) showed higher prevalence of

Fig. 1. Genomix Lateral Flow assay test kit for *Brucella* antibody detection in specimens

brucellosis among the organized farms compared to the rural unorganized farms. Radostits et al. (56) indicated that the prevalence of the disease depends upon diverse factors like management, housing, animal population density, size of farm, type of herd (self-raised or purchased from different sources), sanitary conditions and the method of disposal of infected animals.

Brucellosis and its significance in public health

Human brucellosis has serious public health consequences in endemic areas (57). In humans it represents a major public health hazard, which affects social and economic development in various countries. Animal health workers, butchers, farmers, and those who habitually consume raw milk and come in contact with animals are at high risk for catching brucellosis (58). Veterinarians and laboratory persons who work with *Brucella* cultures are also at high risk of getting infected.

Treatment, vaccination and control programmes

Brucellae are inaccessible to antibiotics as they are facultative, intracellular pathogens. Many antimicrobials are active against *Brucella* species; however, clinical efficacy does not always correlate with *in vitro* susceptibility (59). The treatment recommended by the World Health Organization for acute brucellosis in adults is rifampicin 600 to 900 mg and doxycycline100 mg

Vol. 13 (2) 112-123, April 2019, ISSN 0973-8916 (Print), 2230-7303 (Online)

Table 2. Test results of LFA and iELISA for brucellosis testing with field collected samples.

Species	No. of samples tested	No. of positive samples (%)
Cows and Bulls	4635	1264 (27%)
Buffaloes	4977	547 (10.9%)
Sheep and Goats	571	14 (2.4%)
Pigs	113	2 (1.8%)
Dogs	223	4 (1.8%)
Elephants	29	6 (20.6%)
Camels	55	6 (11%)
Humans	516	13 (2.5%)
Transterrestrial	3224	317 (9.8%)
Total samples	14,343	2,173 (15.15%)

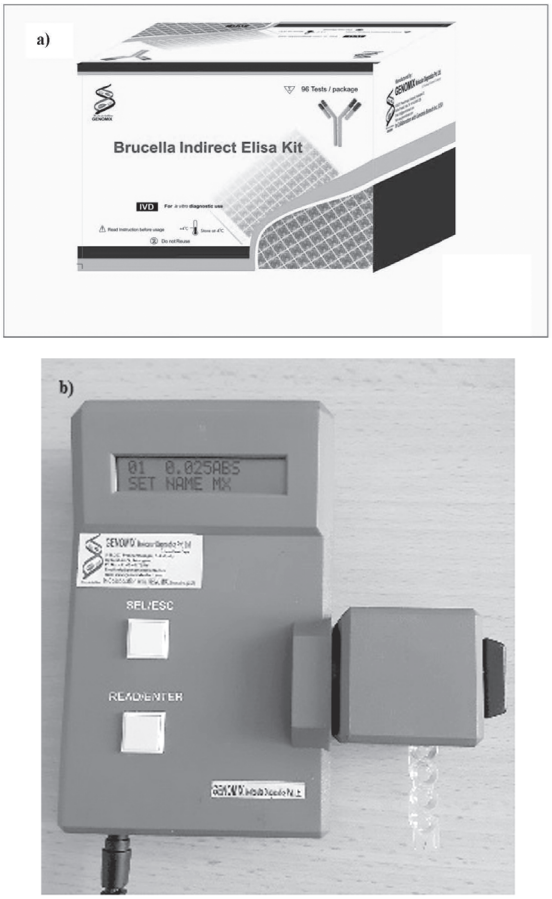

Fig. 2. Genomix indirect ELISA test kit for *Brucella* antibody detection with hand held ELISA reader (a) *Brucella* indirect ELISA kit (b) Handheld ELISA reader

twice daily for a minimum of six weeks (FAO/WHO 1986). Some still claim that a combination of intramuscular streptomycin (1 g/day for 2-3 weeks) with an oral tetracycline (2 g/day for 6 weeks) gives fewer relapses (60, 42). Trimethoprim-sulfamethoxazole (TMP/SMX) is a popular drug in many areas, used in triple regimens. Various combinations that incorporate ciprofloxacin and ofloxacin have been tried clinically, yielding similar efficacy to that of the classic regimens (61). For neurobrucellosis, combination therapy with two or three drugs - doxycycline, rifampicin, and TMP/SMX that penetrate central nervous system is recommended (62). In case of animals, the amount of drugs needed for the exercise outweigh the economic value of an animal. Most farmers do not have the capacity to continue with the treatment because it is time consuming and drugs very expensive. Therefore, vaccination of young animals has proved to be the best preventive measure.

There are a number of approaches in the control of brucellosis and eradication programmes which include vaccination of animals, surveillance, testing, quarantine and culling (63, 64). Animal vaccination, diagnosis (serological and molecular methods) and culling programmes have been implemented in many countries like USA, UK and Canada and freed the areas from disease for some

years, although incidental cases are reported due to relaxation of the above mentioned programmes. Other factor associated with high prevalence is increasing exchange of animals harbouring *Brucella* organisms (65, 66). Animal vaccination in endemic areas has been the most effective control method. An attenuated vaccine strain that induces a T-cell mediated immune response grants a more improved immunity than the killed vaccines (67). In many countries, S19 is a widely used vaccine for the control of the disease. Recently, RB51 developed from rough strain of *B. abortus* has been introduced into the market. However, S19 is still the most effective vaccine used to control brucellosis. The attenuated strain is a live vaccine that ignites the immune response of the vaccinated animal to resist *Brucella* infection by producing antibodies against the attacking organisms and getting rid of the dead organisms by phagocytes. The antibodies produced against the disease disappear from the systemic circulation in few months although lifelong immunity has been suggested so that the animal retains the resistance to disease for years (67). In India, S19 is produced in large scale and the most widely used. Testing and culling may help in screening and confirming suspected cases and at the same time getting rid of *Brucella* positive animals. While in some cases, cross reactions give false positives resulting into culling wrong animals. Therefore, caution must be exercised while testing for the disease diagnosis and subsequent culling.

How to address brucellosis in India

In India, lack of awareness, cost effectiveness of vaccination and lack of proper diagnosis of animals during trading, economic burden of screening the disease and vaccination of animals have led the persistence of brucellosis. Insufficient preventive measures and lack of awareness in rural areas as well as uncontrolled selling/transport of animals in open borders are resulting in high prevalence. Further, high prevalence is also due to armed conflicts and political instability in the country and previously unsuccessful eradication programmes in the country.

Since India is sensitive from both religious and economic points of view, culling the infected animals is not possible. This can be accounted for organized farms, unorganized village farms and Gosalas too. Prevention of human brucellosis should be focused mainly on the elimination of infection in animals and humans along with hygiene, vaccination and effective heating and pasteurization of dairy products. Although India has a policy for the control of brucellosis in dairy cattle, the present focus is very much towards the curative services rather than preventive. Veterinarians and other health care workers should take precautionary measures such as wearing protective clothes, gloves and masks while handling the still births, conception materials and cultures. Such measures can reduce the occupational risk of acquiring brucellosis (68). In general population, avoidance of unpasteurized dairy products, raw meat consumption can certainly prevent infection.

Conclusions

In India, brucellosis Prevalence is more in Gosalas, organized dairy farms according to the available data. As brucellosis transmitted from small ruminants poses a significant health risk factor, more efforts should be required to diagnose and control brucellosis in sheep and goats also. Organizing adequate awareness and disease control programmes on public health education on brucellosis, and risk factors can prevent rapid spreading of brucellosis. Quarantine of suspected or animals in transit must be screened for the disease in order to prevent transmission of brucellosis from region to region. Since animal brucellosis treatment is very expensive, one should encourage the mass vaccination of livestock. Animal owners should be taught about the importance of vaccination of their animals. In India, lack of awareness and limited availability of vaccines are the main causes for persistence of brucellosis. A paradigm shift from the current biomedical model to a socio-cultural model is imperative for the control and elimination of brucellosis in India. Brucellosis is a serious public

health challenge having socio-economic problems and an unaccounted financial burden which needs joint efforts, promotion of intersectoral action, regional and international cooperation, as well as technical and financial support (69).

Acknowledgements

We gratefully acknowledge the help and financial support of this study from the Department of Biotechnology (DBT), New Delhi, Government of India.

References

1. Oreno, E., Cloeckaert, A., Moriyon, I. (2002). Brucella evolution and taxonomy. Vet Microbiol. 90:209-27.
2. Alton, G. G., Jones, L.M., Angus, R.D., Verger, J.M. (1988). Techniques for the brucellosis laboratory. 1st edition. Paris: Institut National de la Recherche Agronomique.
3. Corbel, M.J., Banai, M., Genus, I. (1992). 173AL.In: Brenner DJ, Krieg NR, Staley JT, editors. Bergey's manual of systematic bacteriology. Vol 2. New York: Springer; 2005. p. 370-86.
4. Foster, G., Osterman, B.S., Godfroid, J., Jacques, I., Cloeckaert, A. (2007). Brucella ceti sp. nov. and Brucella pinnipedialis sp. nov. for Brucella strains with cetaceans and seals as their preferred hosts. Int J Syst Evol Microbiol. 57:2688-93.
5. Scholz, H.C., Hubalek, Z., Sedlacek, I., Vergnaud, G., Tomaso, H. (2008). Brucella microti sp. nov., isolated from the common vole Microtus arvalis. Int J Syst Evol Microbiol. 58:375-82.
6. Scholz, H.C., Hubalek, Z., Nesvadbova, J., Tomaso, H., Vergnaud, G., Le Fleche, P., *et al*. (2008). Isolation of Brucella microti from soil. Emerg Infect Dis. 14:1316-7.
7. Scholz, H. C., Hofer E., Vergnaud, G., Le Fleche, P., Whatmore, A.M. , Al Dahouk, S., *et al*. (2009). Isolation of Brucella microti from mandibular lymph nodes of red foxes, Vulpes vulpes, in lower Austria. Vector Borne Zoonotic Dis. 9:153-6.
8. Scholz, H. C., Nockler, K., Gollner, C., Bahn, P., Vergnaud, G., Tomaso, H., et al. (2010). *Brucella inopinata* sp. nov., isolated from a breast implant infection. Int J Syst Evol Microbiol. 60:801-8.
9. Manual of standards for diagnostic tests and vaccines. Paris: Office International des Epizooties (2009).
10. Singh, B. B., Dhand, N.K., Gill, J.P. (2015). Economic losses occurring due to brucellosis in Indian livestock populations. Prev Vet Med 119:211-5.
11. Isloor, S., Renukaradhya G. J., Rajasekhar, M. A. (1998). Serological survey of bovine brucellosis in India. *Rev. Sci. Tech.*, 17: 781-785.
12. Kapoor, P. K., Sharma, S. N., Rao, K. L. (1985)."Seroprevalence of brucellosis in goats and human being in Bikaner, (Rajasthan)". *Ind J Comp Microbiol ImmunolInfect Dis*, 6: 96-101.
13. Rajkhowa, S., Rahman, H., Rajkhowa, C., Bujarbaruah, K. M. (2005). Seroprevalence of brucellosis in mithuns (*Bos frontalis*) in India. Preventive Veterinary Medicine, 69 (1): 145-151.
14. Dhand, N. K., S. Gumber., B. B. Singh., Aradhana, M. S., Bali, H., Kumar, D., R, Sharma., J, Singh., K. S. Sandhu. (2005). A study on the epidemiology of brucellosis in Punjab (India) using Survey Toolbox. *Rev. Sci. Tech.,* 24: 879-885.
15. Sulima, M. (2009). Serological and molecular detection of Brucella infection in cattle. M.V.Sc. thesis submitted to Tamil Nadu Veterinary and Animal Sciences University, Tamil Nadu, India.
16. Singh, S. V., Singh, A. V., Shukla, N., Singh, P. K., Sohal, J. S., Gupta, V. K., Vihan, V.

S. (2007b). Sero-prevalence of Johne's disease in prospective young bulls of Hariana breed by indigenous ELISA kit, using protoplasmic antigen from Bison type genotype of *Mycobacterium avium* subspecies *paratuberculosis* of goat origin. *Indian J. Anim. Sci.,*77 (8): 659–662.

17. Shakuntala, I., S. Ghatak., R. Sanjukta., A. Sen., S. Das., A.K. Puro., A. Dutta., K. Kakoty. (2016). Incidence of brucellosis in livestock in North-Eastern India. *Int jour of Infec Diseeases,* 45S: 1-477

18. Patel, M. D., Patel, P. R., Prajapati, M. G., Kanani, A. N., Tyagi, K. K., and Fulsoundar, A. B. (2014). Prevalence and risk factor's analysis of bovine brucellosis in peri-urban areas under intensive system of production in Gujarat, India, *Veterinary World*, 7 (7):509-516.

19. Jagapur, R.V., Rathore, R., Karthik, K., and Somavanshi, R. (2013). Seroprevalence studies of bovine brucellosis using indirect-enzyme-linked immunosorbent assay (iELISA) at organized and unorganized farms in three different states of India, *Vet World*, 6 (8):550-553.

20. Renukaradhya, G. J., Isloor, S., Rajasekhar, M. (2002). Epidemiology, zoonotic aspects, vaccination and control/eradication of brucellosis in India. *Vet. Microbiol.* 90 183–195

21. World Health Organization (2006). Brucellosis in humans and animals WHO/CDS/EPR/(2006)7.

22. Godfroid, J. (2002). Brucellosis in wildlife. Rev Sci Tech, 21:277-86.

23. Mantur, B. G,. and Amarnath, S. K. (2008). Brucellosis in India- A review. *Journal of biosciences*, 33 (4):539-547.

24. Awad, R. (1998). "Human brucellosis in the Gaza Strip, Palestine" *East. Mediterr. Health J,* 4 225-233.

25. McDermott, J. J. and Arimi, S. M. (2002). Brucellosis in sub-Saharan Africa: epidemiology, control and impact. *Vet. Microbiol,* 90 111-134.

26. Seifert, H. S. N. (1996). Brucellosis. *Tropical Animal Health*

27. Radostits, O. M., Gay, C. C., Hinchcliff, K. W., Constable, P. D. (2007). Diseases associated with Brucella species. *Veterinary Medicine: A Textbook of the Diseases of Cattle, Horses, Sheep, Pigs and Goats*.

28. Robson, J. M., Harrison, M. W., Wood, R. N., Tilse, M. H., McKay, A. B. Brodribb, T. R. (1993). Brucellosis: re-emergence and changing epidemiology in Queensland *Med. J. Aust.* 159 153-158

29. Bouza, E., Sanchez-Carrillo, C., Hernangomez, S., Gonzalez, M. J. (2005). Laboratory- acquired brucellosis: a Spanish national survey. *J. Hosp. Infect.* 61 80-83

30. Centers for Disease Control and Prevention (CDC) 2008. (2006). Laboratory acquired brucellosis–Indiana and Minnesota. *MMWR Morb. Mortal. Wkly. Rep.* 57 39-42

31. Cutler, S. J., Whatmore, A. M., Commander, N. J. (2005). Brucellosis-new aspects of an old disease. *J. Appl. Microbiol.* 98 1270-1281

32. Yagupsky, P. (1999). Detection of *Brucella* in blood cultures. *Journal of Clinical Microbiology* 37 (11): 3437-3442.

33. Xavier, M. N., Silva, T. M., Costa, É. A., Paixão, T. A., Moustacas, V. S., Júnior, C. A. C., Santos, R. L. (2010). Development and evaluation of a species-specific PCR assay for the detection of *Brucella ovis* infection in rams *Veterinary Microbiology*, 145 (1): 158-164.

34. Quinn, P J., Carter, M. E., Markey, B., Carter, G. H. (1999). *Brucella* species. Veterinary Microbiology. Published by Elsevier Health Sciences, 261-267.

35. Anonymous. (2004a). Manual of Diagnostic tests and vaccines for terrestrial animals.

Office International Des Epizootics: Paris, France, 409-438.

36. Keid, L. B., Soares, R. M., Vieira, N. R., Megid, J., Salgado, V. R., Vasconcellos, S. A., Richtzenhain, L. J. (2007). Diagnosis of canine brucellosis: comparison between serological and microbiological tests and a PCR based on primers to 16S-23S rDNA interspacer *Veterinary research communications*, 31 (8): 951-965.

37. Al Dahouk, S., Sprague, L. D., Neubauer, H. (2013). New developments in the diagnostic procedures for zoonotic brucellosis in humans. *Rev Sci Tech*, 32 (1): 177-188.

38. Al Dahouk, S. and Nöckler, K. (2011). Implications of laboratory diagnosis on brucellosis therapy *Expert Rev. Anti. Infect. Ther.*9 (7): 833-845.

39. Bounaadja, L., Albert, D., Chénais, B., Hénault, S., Zygmunt, M. S., Poliak, S., Garin- Bastuji, B. (2009). Realtime PCR for identifi cation of *Brucella* spp.: a comparative study of *IS711*, *bcsp31* and *per* target genes. *Vet. Microbiol*.137 (1–2): 156-164.

40. Baily, G. G., Krahn, J. B., Drasar, B. S., Stoker, N. G (1992). Detection of *Brucellamelitensis* and *Brucella abortus* by DNA amplifi cation. *J. Trop. Med. Hyg*. 95 (4): 271-275.

41. Almuneef, M. and Memish, Z. A. (2002). Persistence of *Brucella* antibodies after successful treatment of acute brucellosis in an area of endemicity. *J. Clin. Microbiol.* 40: 231-3

42. Mantur, B. G., Biradar, M. S., Bidri, R. C., Mulimani, M. S., Veerappa., Kariholu, P., Patil, S. B., Mangalgi, S. S. (2006). Protean clinical manifestations and diagnostic challenges of human brucellosis in adults: 16 years' experience in an endemic area. *J. Med. Microbiol.* 55:897-903

43. Corbel, M. J. (1997). Brucellosis: an overview *Emerging Infectious Diseases*, 3: 213-221.

44. Saegerman, C., De Waele, L., Gilson, D., Godfroid, J., Thiange, P., Michel, P., *et al.* (2004). Evaluation of three serum i-ELISAs using monoclonal antibodies and protein G as peroxidase conjugate for the diagnosis of bovine brucellosis. Vet Microbiol. 100:91-105.

45. Nielsen, K.H., Kelly, L., Gall, D., Nicoletti, P., Kelly, W. (1995). Improved competitive enzyme immunoassay for the diagnosis of bovine brucellosis. Vet Immunol Immunopathol.46:285-91.

46. Weynants, V., Gilson, D., Cloeckaert, A., Denoel, P.A., Tibor, A., Thiange. P., *et al*. (1996). Characterization of a monoclonal antibody specific for Brucella smooth lipopolysaccharide and development of a competitive enzyme-linked immunosorbent assay to improve the serological diagnosis of brucellosis. Clin Diagn Lab Immunol, 3:309-14.

47. Emmerzaal, A., de Wit, J.J., Dijkstra, T., Bakker, D., van Zijderveld, F.G. (2002). The Dutch *Brucella abortus* monitoring programme for cattle: the impact of false-positive serological reactions and comparison of serological tests" Vet Q, 24:40-6.

48. McGiven, J. A., Tucker, J.D., Perrett, L.L., Stack, J.A., Brew, S.D., MacMillan, A.P. (2003). Validation of FPA and cELISA for the detection of antibodies to Brucella abortus in cattle sera and comparison to SAT, CFT, and iELISA" J Immunol Methods. 278:171-8.

49. Smits, H. L., Abdoel, T. H., Solera, J., Clavijo, E., Diaz, R. (2003). Immunochromatographic *Brucella*-specifi c immunoglobulin M and G lateral flow assays for rapid serodiagnosis of human brucellosis. *Clin. Diagn. Lab. Immunol.* 10:1141-1146

50. Manasa, M., Revathi, P., Prudhvi Chand, M., Maroudam, V., Navaneetha, P., Dhinakar Raj., P. B. Kavikishor., B.De., Rathnagiri, P. (2018). Protein-G based Lateral Flow assay for Rapid Serodiagnosis of Brucellosis in Domesticated Animals. *J. Immunoassay and Immunochem*, Nov 26: 1-10.

51. Shome R., Padmashree, B.S., Krithiga, N., Triveni, K., Sahay, S., Shome, B.R., Singh, P., Rahman, H. (2014). Bovine Brucellosis in organized farms of India - An assessment of diagnostic assays and risk factors. Adv. Anim. Vet. Sci. 2 (10): 557-564.

52. Chand, P. and Chhabra, R. (2013). Herd and individual animal prevalence of bovine brucellosis with associated risk factors on dairy farms in Haryana and Punjab in India. Trop. Anim. Hlth. Prod. 45(6): 1313-1319.

53. Lone, I. M, Baba, M. A, Shah, M. M, Iqbal, A. and Sakina, A. (2013). Seroprevalence of brucellosis in sheep of organized and unorganized sector of Kashmir valley, *Vet World* 6(8): 530-533.

54. Suresh, S., Ramakrishna, J., Saseendranath, M. R., Tresamol, P. V., and Bhat, M. N. (1993). Sero survey of bovine brucellosis in Tamilnadu: A recent study. *Cheiron* 22: 1-7.

55. Mehra, K. N, Dhanesar, N. S. and Chaturvedi, V. K. (2000). Sero-prevalence of brucellosis in bovines of Madhya Pradesh. *Indian Veterinary Journal*, 77: 571-573.

56. Radostits, O. M., Gay, C. C., Hinchcliff, K. W., Constable, P. D. (2007). Diseases associated with Brucella species. *Veterinary Medicine: A Textbook of the Diseases of Cattle, Horses, Sheep, Pigs and Goats*.

57. Corbel, M. J. (2006). *Brucellosis in humans and animals*. *World Health Organization*.

58. Chukwu, C. C. (1987). Differentation of Brucella abortus and Yersinia enterocolitica serotype 09 infections in cattle: The use of specific lymphocyte transformation and brucellin skin tests. *Veterinary Quarterly*, 9 (2): 134-142.

59. Hall, W. H. (1990). Modern chemotherapy for brucellosis in humans" *Rev. Infect. Dis.* 12**:** 1060-1099

60. Ariza, J., Gudiol, F., Pallares, R., Rufi, G., Fernandez-Viladrich, P. (1985). Comparative trial of rifampin-doxycycline versus tetracycline-streptomycin in the therapy of human brucellosis" *Antimicrob. Agents. Chemother.* 28**:**548-551

61. Karabay, O., Sencan, I., Kayas, D., Sahin, I. (2004). Ofloxacin plus rifampicin versus doxycycline plus rifampicin in the treatment of brucellosis: a randomized clinical trial (ISRCTN11871179). *BMC. Infect. Dis.* 4: 18

62. McLean, D. R., Russell, N., Khan, M. Y. (1992). Neurobrucellosis: clinical and therapeutic features. *Clin. Infect. Dis.* 15:582-590

63. Godfroid, J. (1992). Diagnosis of bovine brucellosis for its eradication" *Annals in Medicine in Veterinary*, 136: 429-434.

64. Madkour, M. M. (2001). *Madkour's brucellosis*. Springer Science & Business Media.

65. Hosie, B. D., O. M. Al-Bakri., R. J. Futter. (1985). Survey of Brucellosis on goats and sheep in Yemen Arab Republic" *Tropical Animal Health and Production*, 17:93-99.

66. Kiel, F. W., and Khan, M. Y. (1989). Brucellosis in Saudi Arabia" *Social Science & Medicine*, 29 (8): 999-1001.

67. Tizard, I. R. (2000). Veterinary Immunology-An Introduction" WB Saunders Company.

68. Young, E. J. (1995). An overview of human brucellosis" *Clin. Infect. Dis,* 21: 283-290.

69. Kumar, A. (2010). Brucellosis: Need of Public Health Intervention In Rural India" *Prilozi*. 31(1):219-31.

Current Trends in Biotechnology and Pharmacy
Vol. 13 (2) 124-145, April 2019, ISSN 0973-8916 (Print), 2230-7303 (Online)

Quantitative Structure-activity Relationship based Design, Synthesis, and Evaluation of Novel Diarylether Derivatives as a potent Acetylcholinesterase inhibitor and Antioxidant to treat Cognitive dysfunctions

Pavan Srivastava[a], Prabhash Nath Tripathi[a], Piyoosh Sharma[a] and Sushant K Shrivastava[a]*

[a]Pharmaceutical Chemistry Research Laboratory, Department of Pharmaceutical Engineering and Technology, Indian Institute of Technology (Banaras Hindu University), Varanasi-221005, U.P., India.
*For Correspondence - skshrivastava.phe@itbhu.ac.in

Abstract

Some promising acetylcholinesterase (AChE) inhibitors with an antioxidant potential were designed, synthesised, and evaluated for their role in treating cognitive dysfunctions. The *in silico* Gaussian-based quantitative structure-activity relationship (QSAR), virtual screening (VS), QikProp drug-likeliness prediction and docking pose filtration protocols were adapted to design and screen the novel series of diaryl ether derivatives. Further, the selected compounds were investigated for their molecular binding stability using molecular dynamics (MD) simulation analysis and molecular mechanics generalised born surface area (MM-GBSA). The identified hits were synthesised and evaluated for their *in vitro* AChE inhibition and antioxidant potential. Among all the synthesized compounds, the compound 39 was observed as potent AChE inhibitor (AChE IC_{50} = 1.30 ± 0.09 µm; Ki = 0.054 ± 0.009 µM), and also the antioxidant potential of compound 39 (52.9%) was observed significantly better than standard donepezil (<10%) and parallel to ascorbic acid (56.6%). Further, compound 39 ameliorated the scopolamine-induced cognitive impairment in the Y-maze and passive avoidance testsin mice models. *Ex vivo* and biochemical analysis established the brain AChE inhibitory potential and antioxidant properties of compound 39. The results signified compound 39 to be a promising lead for the treatment of cognitive dysfunctions.

Key words: QSAR; virtual screening; diaryl ether; acetylcholinesterase; antioxidant.

1. Introduction

The incidences of dementia due to Alzheimer's disease (AD) and other neurodegenerative disorders are increasing alarmingly with a rate of nearly ten million new cases per year(1). According to the World Health Organisation's report, approximately fifty million people around the globe are currently suffering from dementia(2), and these numbers are expected to increase drastically in the future. The lack of effective therapies for these neurodegenerative disorders creates an enormous burden on society.

The initial cognitive impairment (starting stage of dementia) is a transitional state between the decline in cognition (with ageing) and the early stage of neurodegenerative disease (3). The early interventional therapies at the primary stage may reduce the progression of AD and other neurodegenerative diseases.

The parasympathetic neurotransmitter acetylcholine (ACh) has been shown to strengthen the synaptogenesis of active neurons and the up-regulation of cognitive functions(4, 5). ACh is hydrolysed by acetylcholinesterase (AChE) into choline and acetic acid. The inhibitors of AChE impede the breakdown of ACh and improve the amount of neuronal ACh (6). Currently, AChE

inhibitors AChEIs are the first line therapeutics to be used to treat the AD worldwide. The other cholinesterase is butyrylcholinesterase (BChE), which is found in both the plasma and brain and is also capable of hydrolysing ACh and the other esters (7).

The studies revealed that an imbalance of reactive oxygen species (ROS) causes oxidative stress and could also promote dementia(8). Antioxidants enhance cognition by suppressing ROS during the early stages of dementia(9). However, all the trials based on using a single target to develop a new drug to treat dementia have failed in the last two decades (10).Therefore, investigating multi-targeted ligands that can act on two or more targets is an alternative strategy to treat dementia. Considering the significance of AChE and the oxidative stress hypothesis, the investigation of AChEIs with an antioxidant potential could be a promising strategy for the treatment of dementia.

In the pursuit towards the search for novel multi-targeted ligands, several studies have revealed that the diaryl ether presented in various natural and synthetic pharmaceuticals could be a good sub-structure for the design of novel compounds. Apart from its wide range of pharmacological activities, various derivatives were extensively studied for AChEIs (11-14) and antioxidants (15).

Herein, we designed new molecules using the contour maps generated from the field-based quantitative structure-activity relationship (QSAR). Moreover, selected compounds using *in silico* screening protocols like docking, drug likeliness, molecular mechanics generalised born surface area (MM-GBSA) and molecular dynamics (MD) studies were identified and synthesised. The screened potential hits were evaluated for their *in vitro* cholinesterase inhibition, propidium iodide (PI) displacement assay and antioxidant potential followed by *in vivo* Y-maze and passive avoidance tests, *ex vivo* AChE estimation and antioxidant potential.

2. Results and Discussion

Computational Studies

Gaussian-based QSAR investigation and designing considerations

The field-based QSAR method was performed with a definite set of parameters to calculate the Gaussian equations using electrostatic fields, steric fields, hydrophobic fields, hydrogen bond donor (HBD) and acceptor (HBA) fields. The partial least-squares (PLS) fitting procedure was used to establish the relationship between these five fields. A set comprising of thirty-four known AChEIs (12, 16) with IC_{50} data ranging from a low to high micromolar concentration was selected for training and test sets. Further, their pIC_{50} was calculated usingthe reported procedure to generate the QSAR model (17) (Table 1). The model resulted in the field fraction values 0.09, 0.38, 0.27, 0.14, and 0.10 that showed the contributions of the electrostatic, steric, hydrophobic, HBD, and HBA respectively. It was noteworthy that, steric and hydrophobic fields gave much higher field fractions indicating the steric and non-polar features as major contributors. The results of the PLS method have a high value for a leave-one-out cross-validation q^2 (q^2> 0.2) and a non-cross-validation r^2 (0.54 and 0.98), respectively. The other PLS statistics and field Gaussian parameter were also found within the range, which proposed that the QSAR model has a good predictive ability and were statistically significant. The correlation of the observed pIC_{50} values and estimated pIC_{50} values of the best model was plotted, and a significant correlation was observed.

The designing consideration was focused on the electrostatic, steric, hydrophobic, HBD, and HBAinformation as observed through the contour maps from the generated model based on diaryl ether nucleus. The contour map around the molecule with the highest activity was generated by plotting the various coefficients from the model.

The study of contour map around the most active compound **5** (AChE IC_{50} = 2.5 μM) gave a

fair idea about the modification required to increase the activity of parent compound (Fig. 1). This information was much valuable and suggested about the modification required to improve the activityof compound **5** (Fig. 2). Thus, four series were designed on the basis of information obtained through contour maps. In the I series, 1-chloro-3-nitro-2-phenoxybenzene, 3-chloro- 2-phenoxyaniline, 3-chloro-N-methyl-2-phenoxyaniline, and 3-chloro-N,N-dimethyl-2-phenoxyaniline were linked with the aromatic ring. In the III series, Schiff bases derivatives of amino acid methyl ester were designed. While, in the II and IV series, the reduced imines of the above compounds were designed. For ortho, meta, and para aromatic substitutions, we used various substituents from a different quadrant of the Craig plot. The substituents of the Craig plot were divided into four quadrants as per their hydrophobicity constant (π) on the X-axis and Hammett constant (σ)electron donor or acceptor on the Y-axis properties(18). Thus, a total of 698 molecules including the un-substituted derivatives were designed for the next VS, QikProp drug-likeliness prediction and docking studies(Fig. *3).*

In silico molecular docking study : The virtual screening of these derivatives was carried out in the glide module of Schrodinger to predict their consensual interaction at the active site of cholinesterase enzyme. To screen the best compound, the new 698 designed compounds were docked at the active site of AChE (PDB: 1EVE).

The crystal structure of enzyme revealed that the detailed understanding of active binding sites has a critical role in the designing of novel inhibitors for the treatment of AD. Amongst the various residues, the amino acids involved in the catalytic active site (CAS) and peripheral anionic site (PAS) were the most important and selected as a primary criterion of docking post processing for screening the potential hits. The docking result showed compounds of series I, II, and III having nitro group had significant interaction at PAS region of the AChE binding pocket in comparison

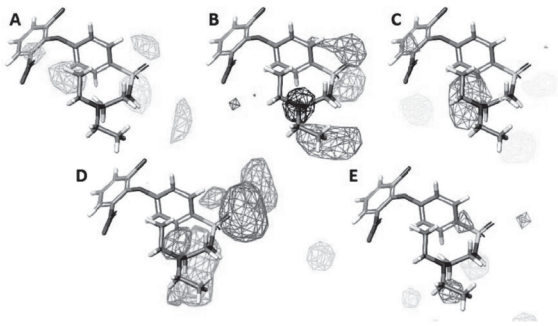

Fig. 1. Contour maps for the Gaussian-based QSAR model forcompound5 (A) Steric contour map, green (positive). (B) Electrostaticsteric contour map, blue (positive) and red (negative)(C) Hydrophobicsteric contour map, yellow (positive) and maroon(negative). (D) HBA contour map, orange (positive) and magenta(negative). (E)HBD contour region, sky blue(positive) and violet(negative).

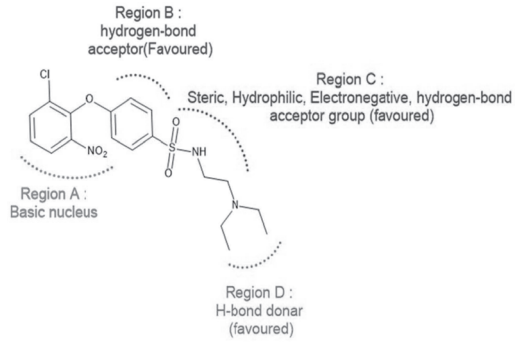

Fig. 2. Summary of favored information obtained from contour map around the most active compound 5.

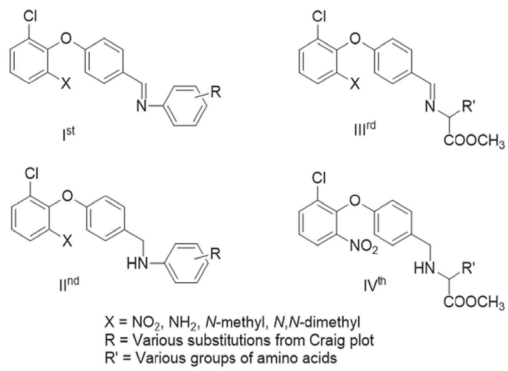

Fig. 3. Structures of designed compounds.

Vol. 13 (2) 124-145, April 2019, ISSN 0973-8916 (Print), 2230-7303 (Online)

to the other designed compounds. The nitro and bromo group from the first quadrant (σ, π), COOH group from the second quadrant (σ, -π), hydroxylgroup from the third quadrant (-σ, -π), and isopropyl group from the fourth quadrant (-σ, π) were shown best interaction among the different substituents. It was also noted that the para-substituted compounds were shown better interaction in comparison the meta or ortho substitution. Similarly, in the designed Schiff bases derivatives of serine, threonine, and tyrosine methyl esters had shown the best interaction. Thus, 15 compounds out of 698 designed compounds were selected for the next step on the basis of their significant interaction at the active site of the AChE.The binding model of compound **39**, compound **5,** and donepezil against AChE were represented in figure 4A, 4B, and 4C respectively

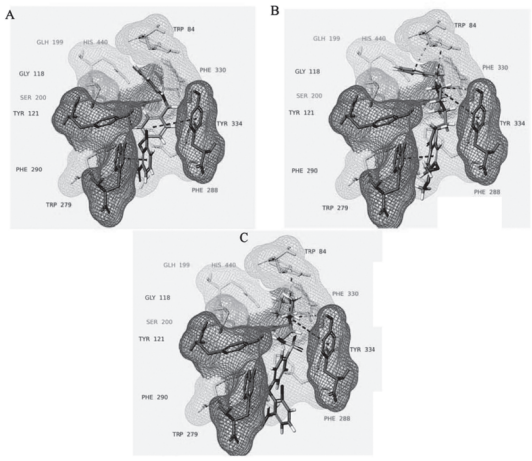

Fig. 4. *In silico* molecular docking simulations analysis of (A) The complex structure of compound 39 with AChE; (B) The complex structure of donepezil with AChE; (C) The complex structure of compound 5 with AChE; Red color represents the catalytic triad. Green color represents the anionic subsite site. Sky blue color represents acyl binding site. Purple color represents the PAS site. Graycolor represents the oxyanion hole. Receptor grid surface was generated around 5 Å distance. p-p interactions were represented by the red color dotted stick. p-cation interactions were represented by the green color dotted stick.

***In silico* drug-likeliness :** The drug likeliness physicochemical parameters i.e., caco-2 cell permeability (PPCaco), brain/blood partition coefficient (log BB), and ADME/Tox were predicted through QikProp module of Schrodinger 2016-1. The result showed that all the designed compounds were satisfied the *in silico* likeliness parameters.

MM-GBSA assay : MM-GBSA was used to rationalize the virtual screening results and prioritize the docking poses(19). The binding energy of the all identified hits on AChE was evaluated using Prime MM-GBSA module of Schrodinger 2016-1. The results of MM- GBSA indicated significant binding of diaryl ether derivatives in AChE and in the range of -85.45 to -28.22 kcal/mol.

Molecular dynamics simulations : Molecular dynamic (MD) simulation study was carried out to monitor the structural variations in the form of ligand-protein interactions and conformations(20). Molecular dynamics simulation runs of 50 ns were performed for docked protein-ligand complexes of the compound 33, compound 39, and compound 45, as a representative compound from each series to confirm the stability and validate molecular docking. The ligand-protein RMSD observed in the course of simulation exhibited deviation for the early 10 ns, and 23 ns respectively for compound 39 and compound 45 due to the early protein structural stabilization. While the RMSD for compound 33 exhibited unstable dynamics during the whole simulation. The Simulation interaction diagram of all docked complex demonstrated the simulations and the interactions with respect to protein and ligand upto 50 ns. The backbone structural deviations values, observed for the latter phase were non-significant and observed under the range of (1.5-11 Å), (3-5 Å: Fig.5), and (2.5-4.3 Å) respectively for compound 33, 39, and 45 respectively.

Thus, the complexes in AChE for compound **39** and compound **45** exhibited a stable-state dynamics for the remaining period, indicated that the ligands were not left their initial binding site.

The results indicated that 50 ns of the simulation were enough for stabilizing these complexes. However, the dynamics study for compound **33** exhibited unstable RMSD with respect to the protein and its binding pocket and these results were further supported by their *in vitro* studies later.

The Protein-Ligand Contacts stacked bar chart for compound **39** in Fig.6&7 showed the normalized interactions including hydrophobic (Trp84, Trp279, Phe330, Phe331, Tyr334), H-bonding (Tyr121), water bridge (His440) and ionic interaction (Asp285). The Ligand-Protein Contacts diagram (Fig. 7) showed a schematic diagram of the compound **39** interacting with AChE during MD simulation. The stacked bar chart showed that compound **39** interacted with His440 (29%) at CAS and with Trp84 (65%), Phe330 (56%) at anionic subsite. The MD simulation of Serine Schiff base containing compound **45** showed 40% and 31% contact time with His440 and Ser200 respectively at CAS, with Trp121 (32%), and Tyr334 (35%) at PAS and with Phe330 (33%) at anionic subsite. The overall results of MD simulation indicated that amino acid residue of PAS and anionic subsite was contributing more toward the stabilization of diaryl nucleus and the results were in the accordance of docking studies.

Thus, based on the QSAR model, docking, drug likeliness, MM-GBSA, and dynamics studies, 15 compounds were screened and selected. Further using the best QSAR model, the activity of the designed compounds against AChE was generated (pIC_{50}). Predicted IC_{50} of newly designed compounds indicated that it would be effective to synthesize these molecules and further validate the model by testing them *in vitro*.

Chemistry : Diaryl ether derivative compound **23** was synthesized by reacting 1-chloro-2-fluoro-3-nitrobenzene with parahydroxybenzaldehyde using Williamson ether synthesis(21). The sodium hydride was used as a strong base to generate the alkoxide ion from parahydroxybenzaldehyde in cold conditions. The formation of diaryl ether was well characterized by ^{1}H NMR and ^{13}C NMR spectroscopy. In the second step, the compound **23** was allowed to react with various amines (**24-29**) and amino acid esters (**45-47**) to form the Schiff base under acidic and basic conditions respectively. The compound (**30-35**) was further reduced to a secondary amine using sodium borohydride (**36-41**). The presence of Schiff base was confirmed by the characteristic singlet peak at 8-9 ppm, that and it was disappeared in the reduced compound with the appearance of two new peaks of CH_2 and NH proton at 4.4 ppm and 5.4 ppm respectively.

***In vitro* studies**

***In vitro* AChE Studies and structuralactivity relationship :** The Ellman's method (22) is a quick reliable and accurate procedure to check the rate of hydrolysis inhibited by the test compound using acetylthiocholine iodide as a substrate and DTNB as a reagent. All synthesized compounds were tested for the AChE inhibition. Compound 39 was found to be the most active (AChE IC_{50} = 1.30 ± 0.09 μM; BChE IC_{50} = 24.1 ± 0.9 μM). Almost all the designed fifteen compounds showed AChE inhibition property(except 32, 45, 46, and47) (AChE IC_{50} Range = 1.3 to >50 μM; BChE IC_{50} Range = 4.71 to >50 μM)(Table 2).

Propidium iodide (PI) is a PAS-AChE (fluorescent) specific inhibitor. When PI bounds to the PAS region of AChE resulted in the increased fluorescent intensity. If an inhibitor bound specifically to the PAS and displace the PI from PAS-AChE complex, resulted in decreased fluorescent intensity. Therefore, the best compound **39** was also studied for enzyme kinetic study and propidium iodide displacement assay (23). It displaces 14.4 % of propidium iodide from the PAS region confirms it's binding at PAS.The most active AChEI compound **39** was subjected to enzyme kinetic study which displayed competitive inhibition (Ki = 0.054 ± 0.009 μM) using Lineweaver–Burk plot (24).

The SAR of synthesized derivatives was summarized in figure 8. The *in vitro* studies showed that the modification in the basic 1-chloro-3-nitro-

Vol. 13 (2) 124-145, April 2019, ISSN 0973-8916 (Print), 2230-7303 (Online)

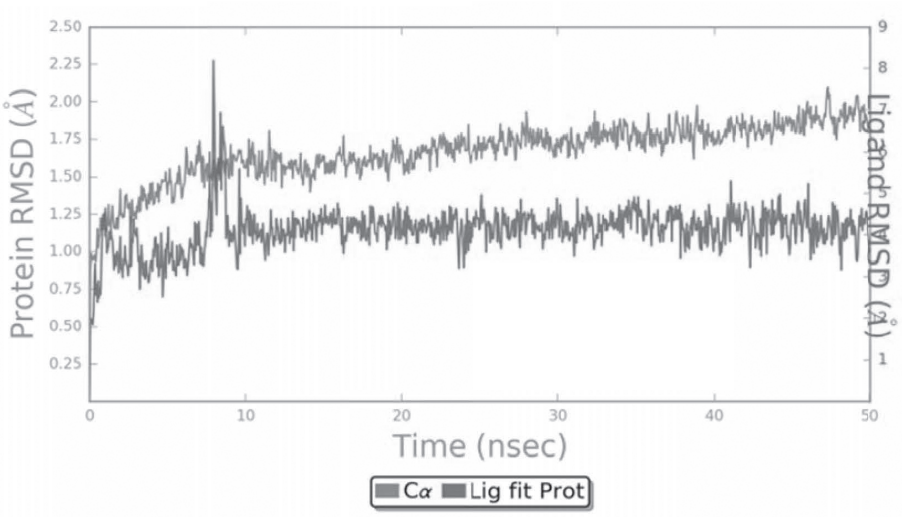

Fig 5. RMSD fluctuations of protein backbone (blue) and compound **39** (red) for 50 ns simulation run on AChE proteins.

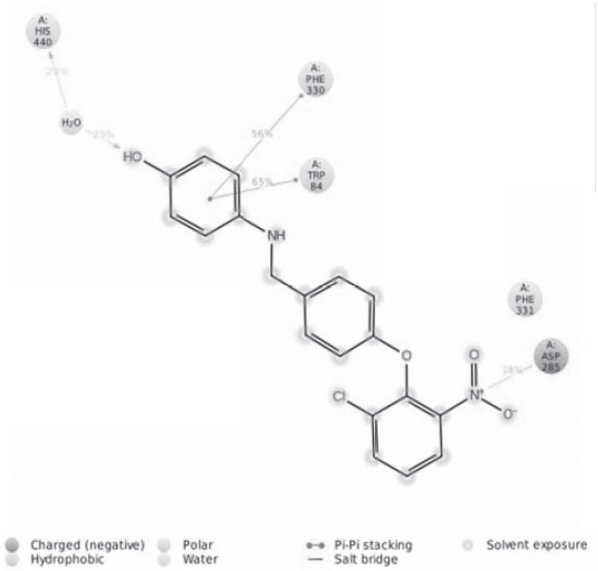

Fig. 6. A schematic representation showing the interaction of compound **39** with active siteamino acid residues of AChE.

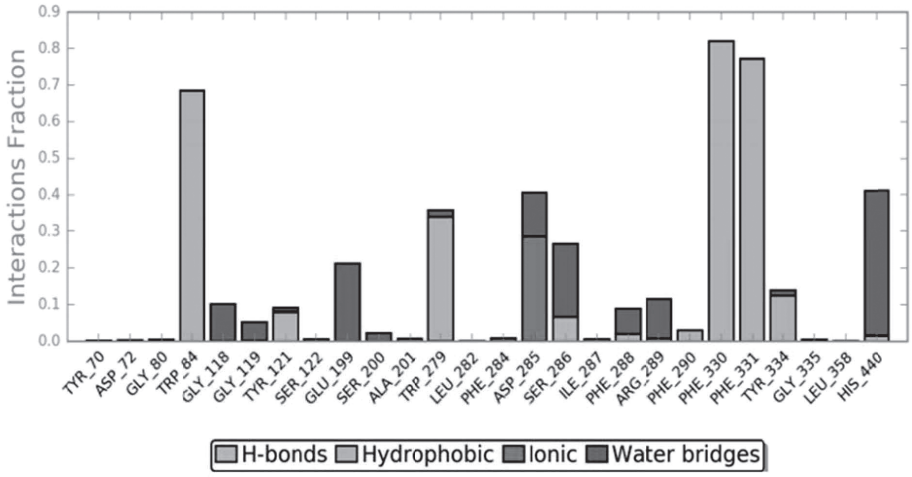

Fig. 7. Stacked bar chart representation of compound **39** with active site amino acidresidues of AChE showing different colors for different types of interactions (Green- H-bonding; Gray- Hydrophobic; Blue- Water bridges; Pink- Ionic interactions).

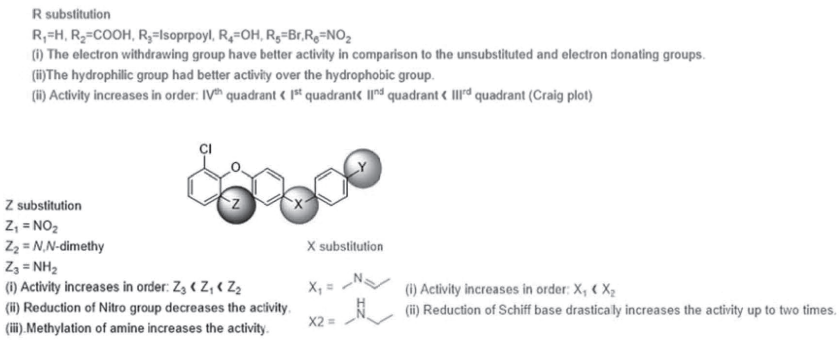

Figure 8. Structure-activity relationship (AChE)of diaryl ether derivatives.

2-phenoxybenzene reduces the activity. The structural-activity relationship (SAR) of compounds (**30-41**) indicated that the reduction of the Schiff base increases the activity two-fold. It was also observed that the para substitution increases the activity many folds as compared to unsubstituted analogs. Various substituents at the para position from the different quadrant of the Craig Plot provide significant insight intoSAR regarding the substitution required for AChE inhibition. The descending order activity is summarized as OH > COOH> NO_2>Br > isopropyl substitutions. Further, it was observed that the substitution from Ist Quadrant substitution (the electron withdrawing (ó) and hydrophobic substituent (ð)) was most active against AChE in comparison to the other quadrant substitution and the unsubstituted analogs. Further, the Schiff base of amino acid esters (**42-44)** (AChE IC_{50} = >50 µM; BChE IC_{50} = >50 µM) had not shown any significant inhibitory activity against AChE *in vitro*.

***In vitro* antioxidant studies and structural-activity relationship :** All the synthesized compounds were tested for its antioxidant activity using a quick and reliable 1,1-diphenyl-2-picrylhydrazyl (DPPH) method (25). The ascorbic

acid was used as the standard and around 10 compounds among 15 compounds exhibited significant antioxidant potential whereas the standard donepezil was not exhibited antioxidant activity (<10%). Interestingly, the compound **39** having highest AChE inhibition(AChE IC_{50} = 1.30 ± 0.09 μM) was also the compound with maximum antioxidant activity (52.9 ± 2.6 %) as compared to the ascorbic acid (56.6 ± 3.1 %).

The SAR indicated that the substituent, as well as spacer, affects the antioxidant activity. The imine had the lower antioxidant potential as compared to the methanamine spacer linked derivatives, and Schiff base derivative of amino acid esters. The various substitutions at the para position of the aromatic ringhave also influenced the activity. The phenolic OH group had the maximum antioxidant potential as compared to the other substitutions.

Blood-brain barrier permeation assay : The *in vitro* parallel artificial membrane permeability assay(26) (PAMPA) was performed for compound 39to predict its blood-brain barrier permeation. Verapamil, diazepam, progesterone, atenolol, dopamine, lomefloxacin, alprazolam, chlorpromazine, and oxazepam were used as controls (to validate the PAMPA-BBB model) to determine *in vitro* permeability (P_e) along with compound 39. P_e (10^{-6} cm s^{-1}) values greater than 4 signified the high permeability of compound. The donepezil (7.54 ± 0.42) and compounds 39 showed appreciable CNS permeability (5.57 ± 0.68).

***In vivo* studies**

Y-maze test : Y-maze spontaneous alternation experiment was used as the behavioral model to test the animal's spatial working memory. The animal was injected scopolamine to inhibit the memory before the commencement of the experiment and since the hippocampus was involved in the task of the model, Y-maze experiment directly indicated the improvement of learning and memory behavior of the mice treated with compound 39.

Spontaneous alteration score was determined for the compound **39** at three doses (1, 5, and 20 mg/kg) and compared to scopolamine, donepezil, and control-treated group (Fig. 9 A). The results showed improvement in alternation score at a dose of 5 mg/kg for compound **39.** Moreover, at the dose 1 mg/kg, donepezil showed significant alternations as compared to thescopolamine treated group.

The novel arm entry was performed to check the anxiety and cainophobia behaviors of mice (Fig. 9B). The mice treated with compound **39** had spent their most of period in exploring the new arm at the dose of 1 and 5 mg/kg, while the scopolamine-treated mice spend more time at the center of the maze. At the dose of 5 mg/kg, compound **39** showed significant differences with scopolamine treated group while the differences were not significant as compared to the donepezil. Thus, compounds **39** showed a significant increase in the working memory and declined in the anxiety without altering the locomotive behavior of mice.

Passive avoidance test : In passive avoidance test the shock was given in the acquisition phase and during the retention phase, transfer latency periods were recorded. The significant difference was observed in the transfer latency time for acquisition trail in comparison to the retention trial for the compound 39 (1, 5, and 20 mg/kg) and donepezil-treated group, while no significant difference was observed for the scopolamine treated group (Figure 9C). Thus compound 39 exhibited a significant increase in transfer latency time in comparison to scopolamine treated group.

Rotarod performance test : The rotarod study was performed to examine the motor learning and motor coordination of the animals. Treatment groups were tested for fall off time (seconds) before and after treatment by rotarod apparatus to check the neurotoxicity. The compound 39 showed the non-significant difference between fall off time before and after treatment on rota rods suggestive of the lack of any side effect on the motor system

of the animals, while diazepam treated group was observed to be neurotoxic.

Neurochemical analysis

Ex vivo evaluation of AChE : The rate of hydrolysis of ACh in the brain was determined for compound 39 (5 mg/kg), donepezil, control, and scopolamine treated group in the *ex vivo* experiment using the Ellman assay protocol. The results revealed that there was a significant difference in the rate of hydrolysis for compound39 (5 mg/kg) and donepezil compared to the scopolamine treated group (Figure 10A). These results also reflected the ability of compound 39 to cross the blood-brain barrier.

***Ex vivo* evaluation of oxidative stress biomarkers :** To evaluate the antioxidant potential, we had performed different *ex vivo*

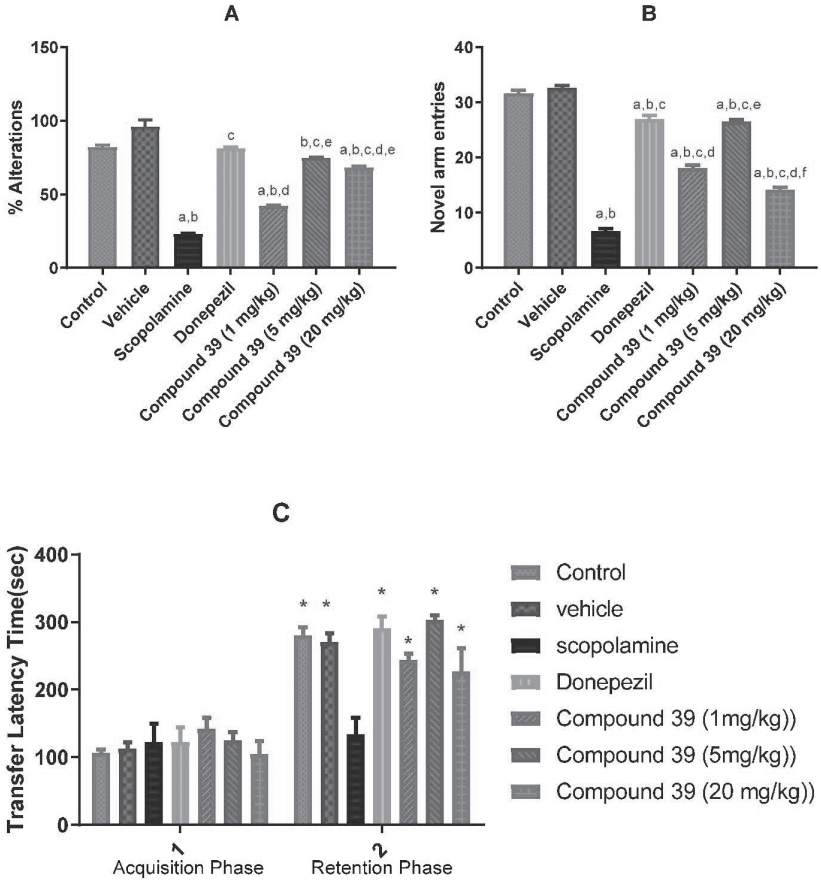

Fig. 9. The in vivo learning and memory test effect of compound 39+ scopolamine (1, 5 , and 20 mg/kg), donepezil (1 mg/kg) and scopolamine (A) Percentage alteration; (B) novel arm entry; Values were expressed as Mean ± SEM, n=6, a $p<0.05$ compared to control; b $p<0.05$ compared to vehicle; c $p<0.05$ compared to scopolamine; d $p<0.05$ compared to donepezil + scopolamine; e $p<0.05$ compared to compound 39+ scopolamine at dose of 1 mg/kg; f $p<0.05$ compared to compound 39+ scopolamine at dose of 5 mg/kg.Values were expressed as ± SEM; Significance wasdetermined by one-way ANOVA, followed by Tukey's test. (C) The effect of scopolamine-induced alteration in the passive avoidance Test. Values are expressed as ± SEM (n = 6); Significance was determined by two-way ANOVA, followed by Tukey's test.* $p<0.001$ compared to respective acquisition Trial.

biochemical test including thiobarbituric acid (TBA) assay, hydrogen peroxide (H_2O_2) assay, reduced glutathione (GSH) assay, superoxide dismutase (SOD) assay to determine malonaldehyde (MDA)/mg protein, catalase activity, GSH level, nitrite level, and SOD unit/mg protein respectively for control, scopolamine, compound 39 (5 mg/kg dose), and donepezil-treated group to check their effect on oxidative stress.

The *ex vivo* experiment showed a significant decreased oxidative stress among the group treated with compound **39**(5 mg/kg) as compared to donepezil and scopolamine treated group, revealing its antioxidant property (Fig. 10B-10F). However, the donepezil-treated group showed no improvement in oxidative stress and found non-significant as compared to scopolamine treated group. Hence, the compound **39** was found to be better than donepezil concerning counteracting oxidative stress induced by scopolamine along with improved learning and memory.

3. Conclusion

Some diaryl ether derivatives were computationally designed and synthesized as potential AChE inhibitor with significant antioxidant property parallel to ascorbic acid. We have evaluated the most potent compound for improving the learning and memory behavior and the results were compared with the standard drug donepezil. Since the design of the molecules was based on Craig plot and Gaussian-based QSAR, therefore, their structure-activity relationship gave useful insights to further enhance and modify the potential of molecules in the future. The most potent compound **39** showed the significant reversal of cognitive deficits and antioxidant potential at the dose of 5 mg/kg, compared to standard drug donepezil in animal models. These results also showed the excellent predictive ability

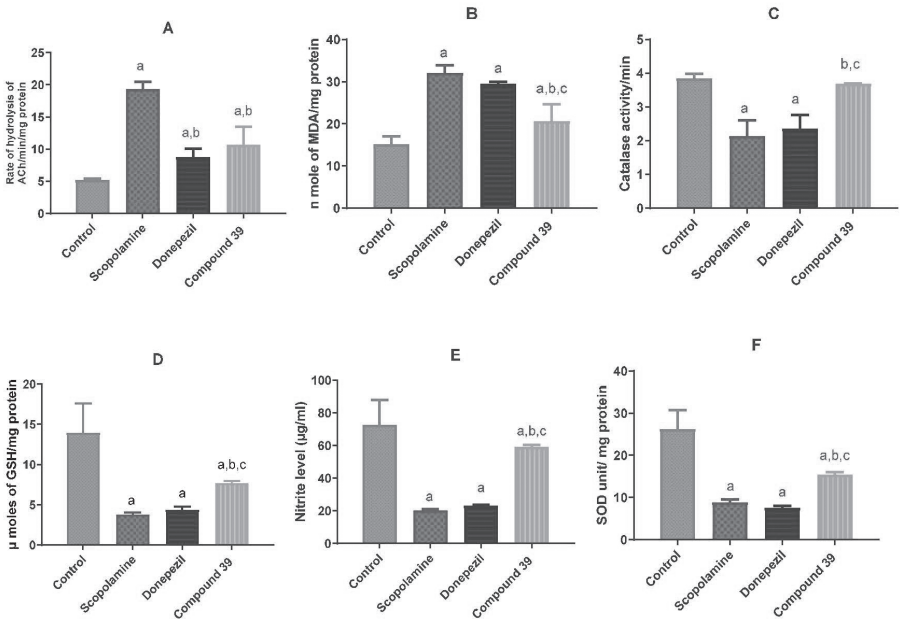

Fig. 10. The ex vivoAChE and antioxidant effect of compound 39 (5 mg/kg), donepezil (1 mg/kg) and scopolamine(A)Rate of hydrolysis of ACh; (B) Lipid peroxidation assay; (C) Catalase activity; (D) Reduced glutathione assay; (E) Nitrite level (F) Superoxide dismutase (SOD) assay; a $p<0.05$ compared to control; b $p<0.05$ compared to scopolamine; c $p<0.05$ compared to donepezil. Values are expressed as Mean ± SEM; Significance was determined by one-way ANOVA, followed by Tukey's test.

Vol. 13 (2) 124-145, April 2019, ISSN 0973-8916 (Print), 2230-7303 (Online)

Table 1. Compound structure,pIC_{50}, and results of Gaussian QSAR model.

Compound Number	Structure	Set	pIC_{50}
1[a]	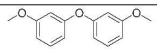	training	7.72
2[a]	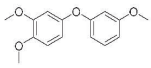	test	7.92
3[a]	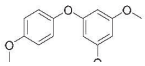	training	7.77
4[a]	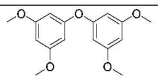	test	7.81
5[b]	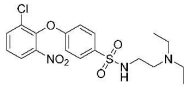	training	5.60
6[c]	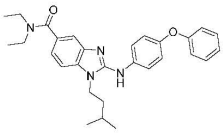	training	4.41
7[c]	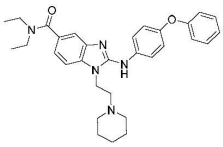	training	2.90
8[d]	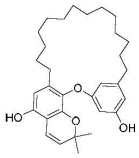	training	5.46
9[d]	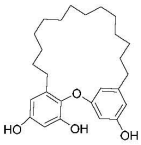	test	5.46
10[d]	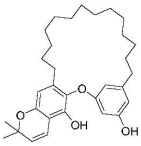	training	5.44

Vol. 13 (2) 124-145, April 2019, ISSN 0973-8916 (Print), 2230-7303 (Online)

11[e]	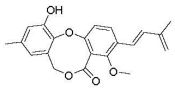	test	5.79
12[e]	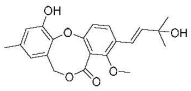	training	3.00
13[e]	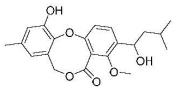	training	3.00
14[e]	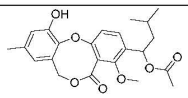	training	3.00
15[e]	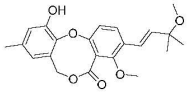	training	3.00
16[f]	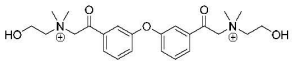	training	2.99
17[f]	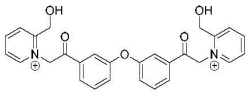	test	3.10
18[f]	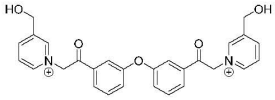	training	5.53
19[f]	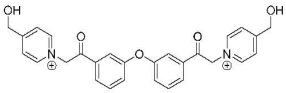	training	4.92
20[f]	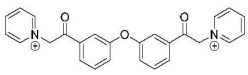	test	5.49

[a](11), [b](12), [c](13), [d](40), [e](41), [f](14)

and accuracy of our Gaussian-based 3D-QSAR model. Thus, the present study provided a useful class of AChE inhibitors having antioxidant potential with promising therapeutic applications against dementia.

4. Material and Methods

Computational study : Field-based 3D QSAR, Molecular docking, QikProp Molecular Mechanics-Generalized Born Surface Area (MM-GBSA) approach and molecular dynamics studies were performed on Phase, Glide, QikProp, Prime, and Desmond modules of Schrodinger 2018-1 respectively using the standard protocol and following the procedure adopted before (27, 28). The crystallographic structures of human AChE in complex with donepezil available in the protein data bank (PDB) (http://www.rcsb.org/pdb/home/home.do) were selected with accession codes 1EVE.

Chemistry

Instrumentation and chemicals : FT-IR spectra were recorded on Bruker ECO-ATR (Alpha). ^{1}H-NMR (500 MHz) and ^{13}C-NMR spectra (125 MHz) were recorded on a BrukerAvance FT-NMR spectrophotometer at room temperature using TMS as an internal standard. Elemental analyses (C, H, N) were performed using EXETER CE-440. All the chemicals were purchased from Sigma-Aldrich (India) and were used without further purification. Thin layer chromatography monitored the progress of the reactions on Merck silica gel 60 F254 aluminum sheets (Merck, Germany).

Synthesis : Synthesis of 4-(2-chloro-6-nitrophenoxy)benzaldehyde (23): 4-hydroxy-benzaldehyde (22) (0.040 mol) and 1-chloro-2-fluoro-3-nitrobenzene (21) (0.040 mol) was dissolved in THF in cold condition followed by portion wise addition of sodium hydride (60 % dispersion in mineral oil; 0.040 mol) in reaction. The reaction mixture was stirred at room temperature under inert atmosphere for 4 h. Completion of the reaction was monitored by TLC. After the completion of the reaction, the solvent was evaporated and the product was extracted using ethyl acetate. The organic layer was evaporated and subjected to column chromatography using 10% EtOAc/Hexane to afford the product 4-(2-chloro-6-nitrophenoxy) benzaldehyde (23). Yield 90%; ^{1}H NMR (500 MHz, DMSO-d_6) **δ** 9.92 (s, 1H), 8.19 (m, 1H), 8.17 (m, 1H), 8.09 – 7.92 (m, 2H), 7.66 (m, 1H), 7.11 – 7.09 (m, 2H).^{13}C NMR (125 MHz, DMSO-d_6) **δ** 191.99, 159.74, 144.88, 140.31, 134.31, 132.81, 132.58, 132.19, 128.38, 126.85, 126.04, 118.94, 118.73; Anal. $C_{13}H_8ClNO_4$: C, 56.24; H, 2.90; N, 5.04; Found: C, 56.27; H, 2.84; N, 5.01.

General preparation for the synthesis of compounds (30-35) (29) : The compound 23 (0.003 mol) was refluxed with various amines (0.003 mol, 24-29) using two drops of glacial acetic acid as catalyst and ethanol as a solvent. The reaction mixture was refluxed until the completion of the reaction. After completion of the reaction, the solvent was evaporated and recrystallized using methanol to obtain the target compounds (30-35).

1-(4-(2-chloro-6-nitrophenoxy)phenyl)-N-phenylmethanimine (30): ^{1}H NMR (500 MHz, $CDCl_3$) **δ** ^{1}H NMR (500 MHz, Chloroform) **δ** 8.54 (s, 1H), 7.95 (m, 1H), 7.64 (m, 1H), 7.58 – 7.44 (m, 2H), 7.35 – 7.28 (m, 4H), 7.24 (m, 2H), 7.08 – 6.93 (m, 2H). ^{13}C NMR (125 MHz, $CDCl_3$) **δ** 163.06, 158.22, 151.07, 144.88, 140.31, 133.07, 132.81, 131.21 – 130.81, 129.42,129.02, 128.38, 126.85, 126.04, 125.41, 121.29, 121.08, 120.23, 119.84 ; Anal. $C_{19}H_{13}ClN_2O_3$: C, 64.69; H, 3.71; N, 7.94; Found: C, 64.65; H, 3.76; N, 7.95.

4-((4-(2-chloro-6-nitrophenoxy) benzylidene) amino) benzoic acid (31): ^{1}H NMR (500 MHz, DMSO-d_6) **δ** 12.45 (s, 1H), 8.80 (s, 1H), 8.15 – 7.97 (m, 3H), 7.73 – 7.54 (m, 3H), 7.54 – 7.45 (m, 2H), 7.26 (m, 1H), 7.01 – 6.86 (m, 2H). ^{13}C NMR (125 MHz, DMSO-d_6) **δ** 168.95 , 163.06 , 158.22 , 158.04 , 144.88 , 140.31 , 133.07 , 132.81 , 131.68, 131.46 , 131.21, 130.81, 128.38, 127.93, 126.8, 126.04, 120.23, 119.84, 117.48, 117.26 ; Anal. $C_{20}H_{13}ClN_2O_5$: C, 60.54; H, 3.30; N, 7.06; Found : C, 60.51; H, 3.26; N, 7.10.

1-(4-(2-chloro-6-nitrophenoxy) phenyl)-N-(4-isopropylphenyl)methanimine (32): ^{1}H NMR (500

Table 2. IC_{50} values of the synthesized derivatives and antioxidant activity.

Comp. code	AChE IC_{50} (µM) ± SEM	BChE IC_{50} (µM) ± SEM	Selectivity Index[a]	Reduction % of DPPH ± SEM at 10 µM
30	40.7 ± 2.1 µM	>50 µM	-	<10%
31	5.6 ± 0.3 µM	34.9 ± 1.4 µM	6.20 ± 0.5	<10%
32	>50 µM	>50 µM	-	<10%
33	2.3 ± 0.12 µM	14.9 ± 0.7 µM	6.47 ± 0.4	41.5 ± 2.3
34	7.8 ± 0.8 µM	>50 µM	-	<10%
35	12.2 ± 1.1 µM	27.0 ± 2.0 µM	2.2 ± 0.8	<10%
36	20.3 ± 1.4 µM	>50 µM	-	25.5 ± 2.6
37	1.7 ± 0.09 µM	15.3 ± 1.1 µM	9.0 ± 0.9	26.8 ± 0.6
38	48.5 ± 3.3 µM	>50 µM	-	23.2 ± 1.1
39	1.3 ± 0.09 µM	24.1 ± 0.9 µM	18.5 ± 1.2	52.9 ± 2.6
40	16.5 ± 1.6 µM	>50 µM	-	28.1 ± 2.0
41	12.2 ± 1.0 µM	4.71 ± 0.13	0.38 ± 0.04	26.1 ± 1.2
45	>50 µM	>50 µM	-	18.7 ± 1.1
46	>50 µM	>50 µM	-	18.0 ± 0.6
47	>50 µM	>50 µM	-	45.5 ± 2.5
Donepezil*	0.04 ± 0.01	15.24 ± 0.88	381 ± 6.33	<10%
Ascorbic acid	nd	nd	nd	56.6 ± 3.1

Values are expressed in the mean ± SEM (n=3); [a]IC_{50}(BChE)/IC_{50}(AChE); nd (not determined)

MHz, $CDCl_3$) δ 8.53 (s, 1H), 7.94 (m, 1H), 7.64 (m, 1H), 7.58 – 7.43 (m, 2H), 7.36 – 7.23 (m, 5H), 7.09 – 6.94 (m, 2H), 3.07 (m, 1H), 1.41 – 1.27 (d, 6H). ^{13}C NMR (125 MHz, $CDCl_3$) δ 163.06, 158.22, 148.50, 145.86, 144.88, 140.31, 133.07, 132.81, 131.21, 130.81, 128.38, 126.85, 126.66, 126.45, 126.04, 123.56, 123.16, 120.23, 119.84, 34.20, 23.57, 23.17 Anal. $C_{22}H_{19}ClN_2O_3$: C, 66.92; H, 4.85; N, 7.09; Found: C, 66.89; H, 4.81; N, 7.13.

4-((4-(2-chloro-6-nitrophenoxy) benzylidene)amino) phenol (33)

^{1}H NMR (500 MHz, $CDCl_3$) ä 8.59 (s, 1H), 7.93 (m, 1H), 7.93 – 7.75 (m, 4H), 7.40 (m, 1H), 7.75 (m, 1H), 7.15 – 7.14 (m, 3H), 6.92 (m, 1H), 4.65 (s, 1H).^{13}C NMR (125 MHz, $CDCl_3$) δ 163.06 , 158.18 (d), 144.81 (d), 140.31 , 133.07 , 132.81 , 131.21, 130.81 , 128.38 , 126.85 , 126.04, 122.78, 122.57, 120.23, 119.84, 116.98, 116.77 ; Anal. $C_{19}H_{13}ClN_2O_4$: C, 61.88; H, 3.55; N, 7.60; Found: C, 61.91; H, 3.51; N, 7.57.

N-(4-bromophenyl)-1-(4-(2-chloro-6-nitrophenoxy)phenyl)methanimine (34): ^{1}H NMR (500 MHz, $CDCl_3$) δ 8.60 (s, 1H), 7.95 (m, 1H), 7.65 (m, 1H), 7.62 – 7.45 (m, 4H), 7.27 – 7.16 (m, 3H), 7.10 – 6.96 (m, 2H). ^{13}C NMR (125 MHz, $CDCl_3$) δ 163.06 , 158.22 , 154.08, 144.88, 140.31, 133.07, 132.81, 132.09, 131.88, 131.21, 130.81, 128.38, 126.85, 126.04, 122.15, 121.93, 120.23, 119.84, 117.74 ; Anal. $C_{19}H_{12}BrClN_2O_3$: C, 52.87; H, 2.80; N, 6.49; Found: C, 52.83; H, 2.77; N, 6.43.

1-(4-(2-chloro-6-nitrophenoxy)phenyl)-N-(4-nitrophenyl)methanimine (35): ^{1}H NMR (500 MHz, $CDCl_3$) δ 8.56 (s, 1H), 8.26 – 8.12 (m, 2H), 7.94 (m, 1H), 7.63 (m, 1H), 7.62 – 7.44 (m, 4H), 7.24 (m, 1H), 7.07 – 6.93 (m, 2H). ^{13}C NMR (125 MHz, $CDCl_3$) ä 163.06, 158.22, 158.01, 144.88, 144.19, 140.31, 133.07, 132.81, 131.21, 130.81, 128.38, 126.85, 126.04, 125.58, 125.18, 121.67, 121.28, 120.23,119.84 ; Anal. $C_{19}H_{12}ClN_3O_5$: C, 57.37; H, 3.04; N, 10.56; Found: C, 57.40; H, 3.00; N, 10.51.

General preparation for the synthesis of compounds (36-41)(30): The compound 23 (0.003 mol) was refluxed with various respective amines (0.003 mol, 24-29) and ethanol as a solvent. The reaction mixture was refluxed until the completion of the reaction. After completion of the reaction, sodium borohydride (0.004 mol) was added portion wise with continuous stirring at 0–5 ^{0}C for 30 min. The solvent was evaporated after the completion of the reaction mixture and workup using ethyl acetate. The organic layer was evaporated and recrystallized using methanol to obtain the target compounds (36-41).

N-(4-(2-chloro-6-nitrophenoxy)benzyl)aniline (36): ^{1}H NMR (500 MHz, $CDCl_3$) δ 7.89 (m, 1H), 7.60 (m, 1H), 7.32 – 7.20 (m, 3H), 7.16 – 7.10 (m, 2H), 7.02 – 6.88 (m, 2H), 6.65 (m, 1H), 6.62 – 6.49 (m, 2H), 4.47 (d, 2H), 4.11 (s, 1H). ^{13}C NMR (125 MHz, $CDCl_3$) δ 154.77, 147.84, 144.88, 140.31, 134.53, 132.81, 129.31, 128.92, 128.38, 127.43, 127.22, 126.85, 126.04, 119.91, 119.52, 118.27, 114.35, 114.14, 46.86 ; Anal. $C_{19}H_{15}ClN_2O_3$: C, 64.32; H, 4.26; N, 7.90; Found: C, 64.29; H, 4.22; N, 7.87.

4-((4-(2-chloro-6-nitrophenoxy) benzyl)amino)benzoic acid (37)

^{1}H NMR (500 MHz, DMSO-d_6) ä 12.51 (s, 1H), ä 7.95 (m, 1H), 7.93 – 7.84 (m, 2H), 7.65 (m, 1H), 7.27 – 7.18 (m, 3H), 7.08 – 6.94 (m, 2H), 6.85 – 6.71 (m, 2H), 4.48 (d, 2H), 4.02 (s, 1H).^{13}C NMR (125 MHz, DMSO-d_6) δ 168.95, 154.96 – 154.66, 144.88, 140.31, 134.53, 132.81, 132.21, 132.00, 128.38, 127.43, 127.22, 126.85, 126.04, 120.79, 119.91, 119.52, 111.77, 111.37, 46.86 ; Anal. $C_{20}H_{15}ClN_2O_5$: C, 60.24; H, 3.79; N, 7.02; Found: C, 60.20; H, 3.81; N, 7.05.

N-(4-(2-chloro-6-nitrophenoxy)benzyl)-4-isopropylaniline (38): *^{1}H NMR (500 MHz, $CDCl_3$) ä 7.95 (m, 1H), 7.65 (m, 1H), 7.28 – 7.17 (m, 3H), 7.17 – 7.08 (m, 2H), 7.08 – 6.94 (m, 2H), 6.63 – 6.49 (m, 2H), 4.47 (d, 2H), 3.68 (s, 1H), 3.02 (s, 1H), 1.40 – 1.27 (m, 6H). ^{13}C NMR (125 MHz, $CDCl_3$) δ 154.77, 144.88, 143.59, 140.31, 138.11, 134.53, 132.81, 128.38, 128.25, 127.96, 127.43, 127.22, 126.85, 126.04, 119.91, 119.52, 116.60, 116.20, 46.86, 34.20, 23.57, 23.17 ; Anal. $C_{22}H_{21}ClN_2O_3$: C, 66.58; H, 5.33; N, 7.06; Found: C, 66.55; H, 5.36; N, 7.02.*

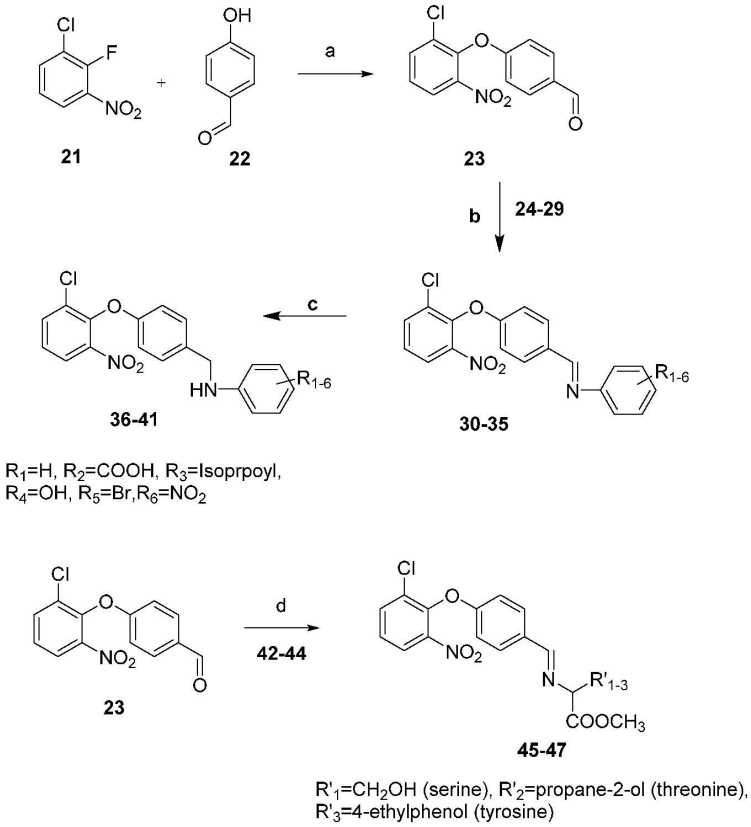

Scheme 1. Reagents and conditions: (a) THF, NaH, 25-35□C, 4 h; (b) ethanol, glacial acetic acid (catalytic amount) 60-65 □C, 12 h (**24-29** were various amines) (c) ethanol, glacial acetic acid (catalytic amount), $NaBH_4$ 60-65 □C, 12 h; (d) ethanol, triethylamine, 60-65□C, 48 h 42-44 **47** were serine, threonine, and tyrosine methyl ester respectively).

4-((4-(2-chloro-6-nitrophenoxy) benzyl)amino) phenol (39):*^{1}H NMR (500 MHz, $CDCl_3$)* **δ** *7.23 (m, 2H), 7.11 (m, 1H), 6.98 – 6.97 (m, 3H), 6.826 (m, 1H), 6.77 – 6.66 (m, 4H), 5.09 (s, 1H), 4.41 (d, 2H), 3.70 (s, 1H). ^{13}C NMR (125 MHz, $CDCl_3$)* **δ** *154.77, 151.27, 144.88, 140.72, 140.31, 134.53, 132.81, 128.38, 127.43 – 127.22, 126.85, 126.04, 119.91, 119.52, 117.49, 117.27, 115.48, 115.27, 46.86 ; Anal. $C_{19}H_{15}ClN_2O_4$; C, 61.55; H, 4.08; N, 7.56; Found: C, 61.53; H, 4.06; N, 7.51.*

4-bromo-N-(4-(2-chloro-6-nitrophenoxy) benzyl)aniline (40)

^{1}H NMR (500 MHz, $CDCl_3$) δ 7.91 (m, 1H), 7.61 (m, 1H), 7.39 – 7.26 (m, 2H), 7.26 – 7.15 (m, 3H), 7.01 – 6.87 (m, 2H), 6.51 – 6.37 (m, 2H), 4.47 (d, 2H), 4.00 (s, 1H).^{13}C NMR (125 MHz, $CDCl_3$) δ 154.77, 146.78, 144.88, 140.31, 134.53, 132.81, 132.14 – 131.75, 128.38, 127.43, 127.22, 126.85, 126.04, 119.91, 119.52, 115.59, 115.19, 109.18, 46.86 ; Anal. $C_{19}H_{14}BrClN_2O_3$: C, 52.62;

H, 3.25; N, 6.46; Found: : C, 52.58; H, 3.21; N, 6.42.

4-bromo-N-(4-(2-chloro-6-nitrophenoxy) benzyl) aniline (41)

^{1}H NMR (500 MHz, $CDCl_3$) δ 8.15 – 8.03 (m, 2H), 7.95 (m, 1H), 7.65 (m, 1H), 7.27 – 7.18 (m, 3H), 7.08 – 6.94 (m, 2H), 6.93 – 6.79 (m, 2H), 4.48 (d, 2H), 3.89 (s, 1H).^{13}C NMR (125 MHz, $CDCl_3$) δ 156.36, 154.77, 144.88, 140.31, 138.13, 134.53, 132.81, 128.38, 127.43, 127.22 ,126.85, 126.04, 125.56, 125.34, 119.91, 119.52, 114.50, 114.11, 46.86 ; Anal. $C_{19}H_{14}BrClN_2O_3$: C, 57.08; H, 3.53; N, 10.51; Found: C, 57.05; H, 3.55; N, 10.53.

General preparation for the synthesis of compounds (45-47) (31)

Various amino acid esters (0.003 mol, 42-44) were dissolved in ethanol and reaction mixture makes basic usingtriethylamine followed by addition of compound 23(0.003 mol). The reaction mixture was refluxed until the completion of the reaction. After completion of the reaction, the solvent was evaporated and recrystallized using methanol to obtain the target compounds (45-47).

2-((4-(2-chloro-6-nitrophenoxy) benzylidene)amino)-3-hydroxypropanoic acid (45)

^{1}H NMR (500 MHz, $CDCl_3$) δ 9.30 (s, 1H), 8.05 (m, 1H), 7.65 (m, 1H), 7.58 – 7.45 (m, 2H), 7.02 – 6.88 (m, 2H), 5.87 (s, 1H), 4.21 – 4.19 (m, 2H), 4.21 (m, 1H), 3.30 (s, 3H).^{13}C NMR (125 MHz, $CDCl_3$) δ 173.39, 161.40, 157.35, 144.78, 139.58, 133.44, 132.85, 130.52, 130.30 , 128.41, 127.28, 126.06, 119.96, 119.74, 76.29, 63.06 ; Anal. $C_{16}H_{13}ClN_2O_6$: C, 52.69; H, 3.59; N, 7.68; Found: C, 52.66; H, 3.63; N, 7.71.

2-((4-(2-chloro-6-nitrophenoxy) benzylidene)amino)-3-hydroxybutanoic acid (46)

^{1}H NMR (500 MHz, $CDCl_3$) δ 8.50 (s, 1H), 7.99 (m, 1H), 7.60 – 7.45 (m, 3H), 7.18 – 7.06 (m, 2H), 7.04 (s, 1H), 4.43 (s, 1H), 4.21 – 4.19 (m, 2H), 3.91 (m, 1H), 3.67 (s, 3H), 1.56 (m, 1H),.^{13}C NMR (125 MHz, $CDCl_3$) ä 175.13, 162.59, 157.38, 144.88, 140.31, 133.45, 132.81, 130.49, 130.27, 128.38, 126.85, 126.04, 120.01, 119.61, 81.26, 69.18, 21.08 ; Anal. $C_{17}H_{15}ClN_2O_6$: C, 53.91; H, 3.99; N, 7.40; Found: C, 53.89; H, 4.01; N, 7.44.

2-((4-(2-chloro-6-nitrophenoxy) benzylidene)amino)-3-(4-hydroxyphenyl)propanoic acid (47)

^{1}H NMR (500 MHz, $CDCl_3$) δ 8.78 (s, 1H), 7.89 (m, 1H), 7.61 (m, 1H), 7.53 – 7.38 (m, 2H), 7.24 (m, 1H), 7.10 – 6.92 (m, 2H), 6.84 (m, 1H), 6.80 – 6.66 (m, 2H), 4.39 (m, 1H), 3.78 (s, 3H), 3.57 (s, 1H), 3.28 – 3.01 (m, 2H). ^{13}C NMR (125 MHz, $CDCl_3$) δ 173.57, 163.76, 157.35, 156.71, 144.78, 139.58, 133.44, 132.85, 130.96, 130.75, 130.52, 130.30, 129.42, 128.41, 127.28, 126.06, 119.96, 119.74, 116.07, 115.86, 75.65, 35.94 ; Anal. $C_{22}H_{17}ClN_2O_6$: C, 59.94; H, 3.89; N, 6.35; Found: C, 59.90; H, 3.92; N, 6.39.

Pharmacology

In vitro assays

Estimation of cholinesterase activity : The IC_{50} value of all the compounds was examined on AChE obtained from the electric eel (E.C. 3.1.1.7) and butyrylcholinesterase obtained from human serum (E.C. 3.1.1.8) as per Ellman's method (22). Different concentrations of compounds from 10 nm to 100µm were selected to obtain inhibition of the enzymatic activity. A stock solution of Enzyme 2.5 unit/ ml was prepared. The final assay solution was prepared by mixing 25 µl 2.5 unit/mL of AChE and 10 µl of different concentrations of the compounds, followed by addition of 300µl 0.1 M phosphate buffer (pH 8.0), 50µl of 0.001 M 5,52 - dithiobis(2-nitrobenzoic acid), and 10µl of 0.0075 M of substrate (acetylthiocholine iodide, ATCh or butyrylthiocholine iodide, BTCh, respectively). The reaction was allowed to proceed for 10 min and absorbance measured at 412 nm for every 1 min. The blank assay consisted of all components except AChE to account for the non-enzymatic reaction. The reaction rates were compared, and the percent inhibition due to the increasing concentrations of the compound was calculated. The concentration of each test compound was

recorded in triplicate, and their IC_{50} values were determined graphically from percent inhibition curves. While determining the enzyme kinetics, different substrate concentration was used. The concentration of compound 39 was fixed at its IC_{50}. The Ki value was determined using the Lineweaver and Burk method(24).

DPPH (2, 2-diphenyl -1-picryl -hydrazyl) radical scavenging activity : DPPH assay was used to measure the antioxidant potential of the compound. 100 µl solution of test compound at several concentrations (10 nm to 100 µm) in methanol was mixed with 200 µl of 0.5 mM DPPH solution. After shaking vigorously, it was allowed to stand in the dark for 30 min at room temperature, and the reading was taken at 517 nm.

Propidium iodide displacement assay : Propidium Iodide displacement assay was used to measure the displacement of Propidium Iodide from the PAS of AChE in respect to the test compound. The 5U of the enzyme was prepared in 0.1 mMTris buffer. Different concentration of test compounds was added to the solution and incubated at room temperature for 20 hours. The 20 µM propidium iodide was added, and the fluorescence was measured after 10 min at excitation and emission wavelength 535 and 595 nm respectively (23).

PAMPA- BBB assay : The pore size of acceptor microplates with PVDF membrane was 0.45 mm and was glazed with porcine brain lipid in dodecane and buffer (pH 7.4) was poured in sufficient quantity. Compounds 39 and donepezil were dissolved in DMSO (5 mg/ml) and diluted up to 200 fold. The resulting solution was added to the donor well plate. The acceptor plate was placed cautiously above the donor plate and then incubated (18 h). The amount of drug in donor and acceptor plate was determined in UV (n = 3; scanned for at least five different wavelengths). Validation of PAMPA model was performed using drugs (mentioned in the discussion, purchased commercially) (32).

In vivo and ex vivo studies

Animals : The adult Swiss albino mice weighing 24-28 g were procured from the approved vendors. The protocol of the experiment and the number of mice required were approved by the animal ethical committee (Dean/2017/CAEC/92). Animals were maintained in environmentally controlled temperature (25 ± 2 °C) and humidity (65 ± 5 %RH) with 12 h light/dark cycles, and water ad libitum and commercial rodent feed were freely available.*Experimental design and drug administration*

Test compounds were suspended in 0.3% w/v sodium carboxymethylcellulose (CMC). The behavioural studies were performed in seven groups with each group having six mice as follows: (i) control (ii) vehicle (0.5 ml) (iii) scopolamine hydrobromide (3 mg/kg), (iv) donepezil (plus scopolamine hydrobromide) (1 mg/kg), (v), (vi), and (vii) compound 39 (plus scopolamine hydrobromide) (1, 5, 20 mg/kg respectively). Treatment was given once daily for seven consecutive days to the respective group of animals. Scopolamine hydrobromide was dissolved in distilled water and administer edintraperitoneally to mice after 30 min of drug treatment on the 7th day of the experiment.

Y-maze test: The Y-maze apparatus consists of three arms maze mostly used for the assessment of instant and short working memory in the rodents. After 30 min of 7th day treatment, scopolamine hydrobromide was administered intraperitoneally to all groups of mice except the control group. The mice of each group were kept at the center of the maze and allowed to explore all the three arms. The total arm entries and spontaneous alterations behavior were observed for each mouse over a period of 5 min. The "memory improvement score" can be calculated as % spontaneous alterations rate = (Number of alterations/(total arm entries – 2)) x 100(33).

Passive avoidance test: The experimental protocol was followed as mentioned above and the number of animal and route of drug administration remain the same. The animals were

trained in A rectangular box (48 ×23 × 27 cm;Columbus Instrument,PACS-30) having two compartments with electrifiable grid floor connected to a shock device which delivers scrambled foot shocks. In training phase mice was kept on the platform, and allowed to freely move to explore for 10 s and then allowed to return home, and the latency to descend was calculated. Immediately after this, an unavoidable footshock of 0.5 mA for 10 s was applied, and the mice were returned to the home cage. In the retention test, 24 h after the learning trial the mice were again placed on the platform and the step-down latency was measured. The test was ended when the mice remain on the platform. Acquisition period of 30 s was used for each mice and time of descent during the learning phase and the time during the retention test was measured(34).

Rotarod performance test *:* The same groups of animals used in the Y Maze and passive avoidance test were used for the minimal motor impairment measurement using the rotarod test on the next day. The mice were first trained to stay on a rotating rod at 6 rpm with a diameter of 3.2 cm and the experiment was performed on the same dayto measure the minimal motor impairment. Compound **39** and diazepam (5 mg/kg) were given orally 1h earlier experiment. The latency of mice to fall from the rotating rod was automatically measured using sensors(35).

Neurochemical analysis

Preparation of tissue homogenate : After the completion of the behavioral assessments, mice were sacrificed through the cervical dislocation, and the whole brain was isolated, washed with cold double distilled water, and again rinsed with a pre-cooled normal saline solution. Each whole brain was homogenized with 3 ml of 10 mM phosphate buffered saline (pH 7.4) in Teflon-glass homogenizer on ice-cold bath and centrifuged at 8050 ×g-force for 10 min at 4 ºC.

Lowry method of protein estimation : The alkaline copper solution was prepared as per the prescribed method. 0.2 ml of tissue homogenate and 1 ml of alkaline copper solution was mixed well in a test tube and allowed to stand at room temperature for 10-12 minutes. 0.1 ml of Phenol (Folin and Ciocalteu's) reagent (sd fine-chem limited) was mixed rapidly to the above homogenate mixture within two seconds. The absorbance was taken after 30 minutes at 750 nm and plotted against the standard curve to know per mg protein content of the sample(36).

Ex vivo study for the estimation of AChE : The tissue homogenate was accessed for estimation of AChE using Ellman's method as discussed previously. Firstly the Ellman's reagent was prepared by mixing 15ml of 0.1 M phosphate buffer (pH 7.4), 500 µl of DTNB, and 100 µl substrate. 300 µl of this solution was pipet out in the cuvette of 96 well microplates. Then 10 µl of supernatant was added to it, and the absorbance was measured at 412 nm, and the rate of hydrolysis was measured as Hydrolysed ACh/min/mg of protein(29).

Lipid peroxidation assay (Thiobarbituric acid reactive substances method) : The tissue homogenate was mixed with an equal amount of 0.1 M phosphate buffer pH 7.4 and incubated at 37 °C for 2 h. To the incubated mixture 10% cold trichloroacetic acid was added. The mixture was centrifuged at 1000 rpm for 1 min. The supernatant (1 ml) was taken in a test tube and mix with equal amount of 0.67% of TBA. The test tube was boiled for in water bath for 10 minutes, and an equal amount (1 ml) of double distilled water was added, and optical density of the solution was taken at 532 nm, and the absorbance was converted into the no. of moles of MDA/mg protein (37).

Estimation of catalase activity : 250 µl of the mixture was taken from a mixture of 1.95 ml of phosphate buffer (pH 7) and 1 ml of 30mM hydrogen peroxide solution added to the cuvette of the microplate. 5 µl of supernatant was added to it, and the result was expressed as hydrogen peroxide decomposed/min/mg protein(38).

Reduced Glutathione assay *:* 0.01 M DTNB was added to the mixture of homogenate and 4% sulphosalicylic acid which were earlier centrifuged

for 1200 rpm for 15 minutes at 4 °C in phosphate buffer and estimated at 412 nm. The standard GSH curve was plotted, and concentration was measured in µmol of GSH /mg of protein (39).

Estimation of nitrite : Nitrite was estimated using the Griess reagent (an equal mixture of 0.1% aqueous solution of napthylethylenediamine and solution of 1% sulphanilamide in 5% phosphoric acid). 250 µl of Griess reagent and 50 µl of supernatant were added in the well of the microplate. The standard curve of nitrite concentration was calculated using a sodium nitrite was plotted, and the nitrite level concentration in the sample was expressed as mg/ml(38).

Superoxide dismutase assay : Aqueous solution of 0.5 ml hydroxylamine hydrochloride (pH 6.0) was added to the solution containing 50 mM sodium carbonate (pH 10.2) and 0.1 mM EDTA, and 96 mM of Nitro-blue tetrazolium (NBT). 0.05 mL of homogenate was added to this mixture, and the change in absorbance was recorded at 560 nm per 30 s interval for 2 min. Results were expressed as SOD unit/mg protein.

Conflict of interest

The authors declare no conflict of interest.

Acknowledgments

The authors gratefully acknowledge the Indian Institute of Technology (Banaras Hindu University), Varanasi for the financial support and providing necessary infrastructural facilities to carry out the experiments. We are also thankful to the Department of Health Research, Ministry of Health and Family Welfares for approving Young Scientist Grant in newer areas of Drugs Chemistry (V25011/215-HRD/2016-HR).

References

1. Wolters, F. J. and Ikram, M. A. (2018) Epidemiology of Dementia: The Burden on Society, the Challenges for Research *Biomarkers for Alzheimer's Disease Drug Development*, pp. 3-14 (Springer).
2. Organization, W. H. (2018) Towards a dementia plan: a WHO guide.
3. Petersen, R. C. (2018) How early can we diagnose Alzheimer disease (and is it sufficient)?: The 2017 Wartenberg lecture, *Neurology*, 91, 395-402.
4. Hasselmo, M. E. (2006) The role of acetylcholine in learning and memory, *Current opinion in neurobiology*, 16, 710-715.
5. Shrivastava, S. K., Sinha, S. K., Srivastava, P. et al. (2018) Design and development of novel p-aminobenzoic acid derivatives as potential cholinesterase inhibitors for the treatment of Alzheimer's disease, *Bioorganic chemistry*.
6. Coloviæ, M. B., Krstiæ, D. Z., Lazareviæ-Pašti, T. D., Bond•iæ, A. M. and Vasiæ, V. M. (2013) Acetylcholinesterase inhibitors: pharmacology and toxicology, *Current neuropharmacology*, 11, 315-335.
7. Darvesh, S., Hopkins, D. A. & Geula, C. (2003) Neurobiology of but yrylcholines terase, *Nature Reviews Neuroscience*, 4, 131.
8. Luca, M., Luca, A. and Calandra, C. (2015) The Role of Oxidative Damage in the Pathogenesis and Progression of Alzheimer's Disease and Vascular Dementia, *Oxidative medicine and cellular longevity*, 2015, 504678-504678.
9. Mecocci, P., Boccardi, V., Cecchetti, R. et al. (2018) A Long Journey into Aging, Brain Aging, and Alzheimer's Disease Following the Oxidative Stress Tracks, *Journal of Alzheimer's Disease*, 62, 1319-1335.
10. Oset-Gasque, M. J. S. and Marco-Contelles, J. (2018) Alzheimer's Disease, the "One-Molecule, One-Target" Paradigm, and the Multitarget Directed Ligand Approach (ACS Publications).
11. Özbey, F., Taslimi, P., Gülçin, Ý. et al. (2016) Synthesis of diaryl ethers with acetylcholinesterase, butyrylcholinesterase

and carbonic anhydrase inhibitory actions, *Journal of enzyme inhibition and medicinal chemistry*, 31, 79-85.

12. Andersson, C. D., Forsgren, N., Akfur, C. et al. (2013) Divergent structure–activity relationships of structurally similar acetylcholinesterase inhibitors, *Journal of medicinal chemistry*, 56, 7615-7624.

13. Dolles, D., Hoffmann, M., Gunesch, S. et al. (2018) Structure–Activity Relationships and Computational Investigations into the Development of Potent and Balanced Dual-Acting Butyrylcholinesterase Inhibitors and Human Cannabinoid Receptor 2 Ligands with Pro-Cognitive in Vivo Profiles, *Journal of medicinal chemistry*, 61, 1646-1663.

14. Koelle, G. (1963) Handbuch der experimentellen Pharmakologie, Ergänzungswerk, XV, *Cholinesterases and anticholinesterase agents. Berlin-Göttingen-Heidelberg: Springer 1963a. Google Scholar*.

15. Vanucci-Bacqué, C., Camare, C., Carayon, C. et al. (2016) Synthesis and evaluation of antioxidant phenolic diaryl hydrazones as potent antiangiogenic agents in atherosclerosis, *Bioorganic & medicinal chemistry*, 24, 3571-3578.

16. Andersson, C. D., Hillgren, J. M., Lindgren, C. et al. (2015) Benefits of statistical molecular design, covariance analysis, and reference models in QSAR: a case study on acetylcholinesterase, *Journal of computer-aided molecular design*, 29, 199-215.

17. Selvaraj, C., Tripathi, S. K., Reddy, K. K. and Singh, S. K. (2011) Tool development for Prediction of pIC 50 values from the IC 50 values-A pIC 50 value calculator, *Current Trends in Biotechnology & Pharmacy*, 5.

18. Langdon, S. R., Ertl, P. and Brown, N. (2010) Bioisosteric replacement and scaffold hopping in lead generation and optimization, *Molecular Informatics*, 29, 366-385.

19. Cho, A. E., Guallar, V., Berne, B. J. and Friesner, R. (2005) Importance of accurate charges in molecular docking: quantum mechanical/molecular mechanical (QM/MM) approach, *Journal of computational chemistry*, 26, 915-931.

20. Bowers, K. J., Chow, D. E., Xu, H. et al. (2006) Scalable algorithms for molecular dynamics simulations on commodity clusters, Paper presented at the *SC 2006 conference, proceedings of the ACM/IEEE*.

21. Williamson, A. (1850) XLV. Theory of ætherification, *The London, Edinburgh, and Dublin philosophical magazine and journal of science*, 37, 350-356.

22. Ellman, G. L., Courtney, K. D., Andres Jr, V. and Featherstone, R. M. (1961) A new and rapid colorimetric determination of acetylcholinesterase activity, *Biochemical pharmacology*, 7, 88-95.

23. Peauger, L., Azzouz, R., Gembus, V. et al. (2017) Donepezil-based central acetylcholinesterase inhibitors by means of a “bio-oxidizable” prodrug strategy: design, synthesis, and in vitro biological evaluation, *Journal of medicinal chemistry*, 60, 5909-5926.

24. Lineweaver, H. & Burk, D. (1934) The determination of enzyme dissociation constants, *Journal of the American chemical society*, 56, 658-666.

25. Brand-Williams, W., Cuvelier, M.-E. and Berset, C. (1995) Use of a free radical method to evaluate antioxidant activity, *LWT-Food science and Technology*, 28, 25-30.

26. Ottaviani, G., Martel, S. & Carrupt, P.-A. (2006) Parallel artificial membrane permeability assay: a new membrane for the fast prediction of passive human skin permeability, *Journal of medicinal chemistry*, 49, 3948-3954.

27. Shrivastava, S. K., Sinha, S. K., Srivastava, P. et al. (2019) Design and development of novel p-aminobenzoic acid derivatives as potential cholinesterase inhibitors for the treatment of Alzheimer's disease, *Bioorganic chemistry*, 82, 211-223.

28. Srivastava, P., Tripathi, P. N., Sharma, P. et al. (2019) Design and development of some phenyl benzoxazole derivatives as a potent acetylcholinesterase inhibitor with antioxidant property to enhance learning and memory, *European journal of medicinal chemistry*, 163, 116-135.

29. Shrivastava, S. K., Srivastava, P., Upendra, T., Tripathi, P. N. and Sinha, S. K. (2017) Design, synthesis and evaluation of some N-methylenebenzenamine derivatives as selective acetylcholinesterase (AChE) inhibitor and antioxidant to enhance learning and memory, *Bioorganic & medicinal chemistry*, 25, 1471-1480.

30. Suvire, F. D., Sortino, M., Kouznetsov, V. V. et al. (2006) Structure–activity relationship study of homoallylamines and related derivatives acting as antifungal agents, *Bioorganic & medicinal chemistry*, 14, 1851-1862.

31. Feng, B., Lu, L. Q., Chen, J. R. et al. (2018) Umpolung of Imines Enables Catalytic Asymmetric Regio reversed [3+ 2] Cycloadditions of Iminoesters with Nitroolefins, *Angewandte Chemie International Edition*, 57, 5888-5892.

32. Di, L., Kerns, E. H., Fan, K., Mcconnell, O. J. & Carter, G. T. (2003) High throughput artificial membrane permeability assay for blood–brain barrier, *European journal of medicinal chemistry*, 38, 223-232.

33. Kwon, S.-H., Lee, H.-K., Kim, J.-A. et al. (2010) Neuroprotective effects of chlorogenic acid on scopolamine-induced amnesia via anti-acetylcholinesterase and anti-oxidative activities in mice, *European journal of pharmacology*, 649, 210-217.

34. Rush, D. K. (1988) Scopolamine amnesia of passive avoidance: a deficit of information acquisition, *Behavioral and Neural Biology*, 50, 255-274.

35. Seth, A., Sharma, P. A., Tripathi, A. et al. (2018) Design, synthesis, evaluation and molecular modeling studies of some novel N-substituted piperidine-3-carboxylic acid derivatives as potential anticonvulsants, *Medicinal Chemistry Research*, 27, 1206-1225.

36. Lowry, O. H., Rosebrough, N. J., Farr, A. L. & Randall, R. J. (1951) Protein measurement with the Folin phenol reagent, *Journal of biological chemistry*, 193, 265-275.

37. Wills, E. (1966) Mechanisms of lipid peroxide formation in animal tissues, *Biochemical Journal*, 99, 667.

38. Kulshreshtha, A. & Piplani, P. (2016) Ameliorative effects of amide derivatives of 1, 3, 4-thiadiazoles on scopolamine induced cognitive dysfunction, *European journal of medicinal chemistry*, 122, 557-573.

39. Jollow, D., Mitchell, J., Zampaglione, N. A. and Gillette, J. (1974) Bromobenzene-induced liver necrosis. Protective role of glutathione and evidence for 3, 4-bromobenzene oxide as the hepatotoxic metabolite, *Pharmacology*, 11, 151-169.

40. Beniddir, M., Simonin, A.-L., Martin, M.-T. et al. (2009) *Turrianes from Kermadecia rotundifolia as new acetylcholinesterase inhibitors*.

41. Wu, B., Ohlendorf, B., Oesker, V. et al. (2015) Acetylcholinesterase inhibitors from a marine fungus Talaromyces sp. strain LF458, *Marine biotechnology*, 17, 110-119.

Current Trends in Biotechnology and Pharmacy
Vol. 13 (2) 146-155 April 2019, ISSN 0973-8916 (Print), 2230-7303 (Online)

In Vitro Cytotoxicity and In Vivo Anti-Tumor Efficacy of CD13 Targeted Peptide – Monomethyl Auristatin E (MMAE) Conjugates

Md Zahir Uddin[†], Xiaoling Li[†] and Bhaskara Jasti[*†]
† University of the Pacific, Thomas J. Long School of Pharmacy, Department of Pharmaceutics and Medicinal Chemistry, 751 Brookside Road, Stockton, CA 95211, USA.
*For Correspondence - bjasti@pacific.edu

Abstract

A series of novel peptide ligands that specifically bind to tumor vascular endothelial CD13 receptor were designed, synthesized and evaluated for in vitro binding. In this study, peptide - monomethyl auristatin E (MMAE) conjugates were evaluated for their in-vitro cytotoxicity and mice in-vivo anti-tumor efficacy. The peptides [PEP20, GYPAY; and PEP173 GYPAVYLF] were synthesized by standard solid phase peptide synthesis method. The drug-linker conjugate maleimidocaproyl-valine-citrulline-p-aminobenzoyloxycarbonyl-monomethyl auristatin E (mc-vc-PABC-MMAE) was used to prepare the peptide-drug conjugates (PDCs). Formation of the PDCs was confirmed by ESI-MS (PEP20-MMAE, 1062.5 $[M+H+Na]^{+2}$; PEP173-MMAE, 828.9 $[M+2H+Na]^{+3}$) and the % purities of the PDCs after purification were higher than 98%. For in-vitro cytotoxicity study, CD13 +ve HT1080, CD13 –ve MCF7 and HEK293 (normal cells) cells were incubated with various concentrations of PDCs/ MMAE. The drug, MMAE, showed very high potency (low IC_{50} values) across all three cell lines (HT-1080 cells, IC_{50} 0.09358 nM; MCF-7 cells, IC_{50} 0.4250 nM; HEK-293 cells, IC_{50} 0.8354 nM). PDCs (PEP20-MMAE and PEP173-MMAE) showed significantly lower cytotoxicity than MMAE in all cell lines. PEP20-MMAE showed 5.2 and 4.3 times lower cytotoxicity in CD13 negative MCF-7 and control normal HEK-293 cells, respectively, when compared to that in CD13 positive HT-1080 cells. PEP173-MMAE was found to have approximately 2.4 times less cytotoxicity in both MCF-7 cells and HEK-293 cells as compared to HT-1080 cells. For the anti-tumor efficacy study, 975 nmol/kg, which is equivalent to 0.70 mg/kg of MMAE, was selected as the treatment dose. In the mice treated with only PBS, the tumor grew rapidly and reached approximately 450 mm^3 by day 28 after tumor implantation (Figure 5). MMAE, PEP20-MMAE, and PEP173-MMAE, all showed almost complete tumor regression during the study. PEP20-MMAE and PEP173-MMAE showed slightly higher tumor regression than MMAE, but the difference was not statistically significant. However, the PDCs exhibited much lower weight loss in mice as compared to the drug MMAE indicating lower side effects in vivo. The limited effectiveness of peptide drug conjugates in in vivo mice tumor model suggested the need of further research to achieve the optimal chemical configuration of the conjugates for in vivo targeting.

Key words : CD13, aminopeptidase N, Knob-Socket model, peptide-drug conjugate

Introduction

In cancer therapy, the primary objective of targeted drug delivery is to transport drug to the cancer sites while minimizing their exposure to normal tissues. Two key strategies have been extensively studied to achieve this goal, both of which rely on modifying the pharmacokinetic properties of the drug. The first strategy uses a delivery vehicle, like nanoparticles, that carries

Vol. 13 (2) 146-155 April 2019, ISSN 0973-8916 (Print), 2230-7303 (Online)

the drug and determines the drug biodistribution via its own physicochemical characteristics. The second one is the prodrug strategy, where covalent modification of the drug with a moiety that momentarily disguises the drug's bioactivity and confers desirable pharmacokinetic properties. The prodrug approach have several advantages over delivery vehicle approach: (a) significantly lower amount of inert materials that results in decreased metabolic burden of the patient (b) minimize premature drug release, (c) relatively straight forward and simple preparation/manufacturing (1, 2).

Peptide-drug conjugate (PDC) is an emerging type of prodrug (3). It is formed by covalent attachment of a specific peptide sequence to a drug through a linker. The use of peptides would enable the incorporation of many functionalities into PDCs. The amino acid sequences can be selected to regulate the physicochemical properties of the conjugate, as well as to impart active targeting towards a specific receptor expressed at the target cancer tissue. PDCs are biodegradable and generally show no or minimum undesired immunogenic responses because they are composed of amino acids and typically have short peptide sequences (3, 4). Different amino acid combinations allow simplistic preparation of different PDCs. A number of tumor targeting peptides have been developed till date for different types of cancers (5). The peptide sequence can be easily modified to facilitate drug conjugation and, to tune the conjugate molecule ionization and hydrophobicity, which in turn impact the bioavailability. Additionally, PDCs can be purified by simple HPLC technique because of their low molecular weight (3).

The main building blocks of a PDC include a cytotoxic drug, a targeting peptide ligand and a linker between them. The therapeutic efficacy of the PDC is primarily governed by the potency of the cytotoxic drug and the targeting efficiency of the conjugate. The process of synthesizing PDCs is generally fast and simple. Since an already approved drug can be selected as the therapeutic payload, the overall cost of production of PDCs is significantly lower than that of synthesizing a new drug (4).

Doxorubicin, chlorambucil, camptothecin, and paclitaxel are some of the chemotherapeutic drugs that have been used in PDC development (6). But these drugs are relatively low potency cytotoxic drugs. Currently, very potent cytotoxic agents, like auristatins, are used in drug conjugate development (7). Auristatins leads to cell apoptosis by inhibiting the polymerization of tubulin in dividing cells (8).

Design of a novel peptide-doxorubicin conjugate was reported by Soudy et al. They made two different conjugates having ester and amide bonds between doxorubicin and linker. The PDC with ester bond showed 4 times more toxicity than doxorubicin in MDA-MB-435 cells and 40 times better selectivity towards breast cancer cell lines when compared to normal cells (9). Polyak et al reported the development of integrin targeted cyclic RGD-PEG-Dox conjugate. The PDC inhibited the cell proliferation at lower IC_{50} as compared to doxorubicin or control conjugate without RGD peptide (10). An EGFR-binding peptide-doxorubicin conjugate was developed and evaluated in-vitro and in-vivo for anti-cancer efficacy. The study showed improved anticancer efficacy and lower systemic toxicity of PDC with EGFR upregulated tumor cells (11).

CD13, also known as aminopeptidase N (APN), is Zn+2 dependent cell surface ectopeptidase. CD13 consists of 967 amino acid residues. It has a short N-terminal intracellular domain, a single transmembrane region, and a large extracellular domain. CD13 is heavily glycosylated with carbohydrates that is at least 20% of the protein mass. It has at least five different isoforms with differential O-glycosylation sites (12-14). While there is very little or no CD13 expression in normal vessels, it is overexpressed in angiogenic vessels of the neoplastic tissues. Different tumor cells also express or overexpress CD13 receptor. In terms of malignant cell growth, CD13 is implicated in tumor cell invasion, differentiation, proliferation and apoptosis, motility

and angiogenesis (15-20). CD13 is overexpressed in many cancers like breast, kidney, prostate, ovarian, colon, gastric, pancreatic and thyroid cancer (21).

In this study, two PDCs were prepared by conjugating previously designed CD13 targeted novel peptides (22) (PEP20, GYPAY; and PEP173, GYPAVYLF) to the drug monomethyl auristatin E (MMAE) via cleavable linker, and the in vitro cytotoxicity and in vivo anti-tumor efficacy of the PDCs were evaluated. The peptides (PEP20; and PEP173) were found to selectively bind to the CD13 receptor in vitro with significantly higher affinity as compared to CNGRC(C1-C5) peptide ligand (22). The linker-drug construct contains a spacer, maleimidocaproyl (mc); a protease degradable dipeptide, valine-citrulline (vc); a self-immolative moiety, para-amino benzyloxycarbonyl (PABC); and the antimitotic drug, MMAE. This construct is termed as mc-vc-PABC-MMAE. The linker-drug construct can be conjugated to a cysteine residue in the peptide sequence using the specific thiol-maleimide coupling reaction (23, 24).

Materials and Methods

Preparation of peptide-drug conjugates

Synthesis: First, the peptides (PEP20-Ahx-Cys, GYPAY-Ahx-C; and PEP173-Ahx-Cys, GYPAVYLF-Ahx-C) were synthesized by standard solid phase synthesis method (25-27). The amino acids and coupling reagents were obtained from Chem-Impex (Wood Dale, IL, USA). The synthesis was started with Fmoc-L-Cys(Trt)-2-chlorotrityl resin to place a cysteine residue at the C-terminal. Fmoc group was removed in each step by treating the resins with solution of 20% piperidine in DMF. A spacer (e.g. 6-aminohexanoic acid/ Ahx) was added between the designed peptide sequence and the C-terminal cysteine residue. Coupling of subsequent amino acids was performed with 1-hydroxy-benzotriazole (HOBt) and diisopropyl-carbodiimide (DIC). Boc protected amino acids were used only for the last N-terminal amino acids to eliminate the necessity of final Fmoc deprotection step. Cleavage of the peptides were performed by treating the resins with trifluoroacetic acid – water – triisopropylsilane (95: 2.5: 2.5) cocktail for 3 hours. The obtained TFA-peptide solution was cooled and evaporated under nitrogen flow until it became thick viscous oily liquid. Ice cold ether was added to the oily liquid to precipitate the peptide. The peptides are then freeze dried and stored in “20° C freeze until further use. The peptides were used to synthesize the PDCs without further purification. The PDCs were prepared using thiol-maleimide coupling reaction. To synthesize each PDC, 5mg of the peptide was dissolved in 2.5 ml of PBS-ACN (70:30) mixture, and equimolar amount of mc-vc-PABC-MMAE (MuseChem, Fairfield, NJ, USA) was dissolved separately in 2.5 ml PBS-ACN (70:30) mixture. The peptide solution and the drug-linker solution were mixed thoroughly by vortexing. The pH of the reaction mixture was adjusted to 6.5 – 7 using HCl (aq). The reaction mixture was shaken for 1 hour at room temperature, and solidified by freeze drying.

Characterization: All the synthesized molecules (PEP20-MMAE; and PEP173-MMAE) were characterized by Electron Spray Ionization Mass Spectrometry (ESI-MS, API 3000, SCIEX, Ontario, Canada). The purity of the synthesized molecules was determined using high pressure liquid chromatography (HPLC) (Agilent Technologies, Santa Clara, CA, USA). The column used was Agilent Zorbax C18, 5 ìm, 4.6×150 mm, and the wavelengths used for detection were 210, 254 and 280 nm. The samples were eluted with a mobile phase consisting of water (A) and acetonitrile (B) using a linear gradient from 10 to 90% B over 30 to 35 minutes, at 1.0 mL/min flow rate. The synthesized PDCs were purified by collecting the appropriate peaks. The purified compounds were freeze dried and stored at -80° C until further use.

*In vitro cytotoxicity of peptide-drug conjugates:*The cytotoxicity study of MMAE (MedKoo Biosciences, Morrisville, NC, USA) and peptide-drug conjugates was performed using CD13 overexpressing HT-1080 cells, CD13 non-expressing MCF-7 cells, and a control normal cell line HEK293. The cells were purchased from

ATCC (Manassas, VA, USA) and were grown in 75 cm^2 flasks in DMEM (high glucose, with L-glutamine, and sodium pyruvate) (Thermo Fisher Scientific, Waltham, MA, USA) with 10% FBS (Gemini Bio-Products, West Sacramento, CA, USA) and 1% penicillin-streptomycin (Gemini Bio-Products) at 37° C and 5% CO2. The cells were detached using TrypLE Express (Thermo Fisher Scientific) and the cell density was counted using Scepter Automated Handheld Cell Counter (MilliporeSigma, Burlington, MA, USA). The cells were seeded into clear 96 well plates at 5000 cells/well (0.2 mL cell suspension/well) and incubated overnight to allow them to attach to the wells. Then the cells were incubated with MMAE or PDCs at various concentrations ranging from 0.0000302 to 30200 nM for 72 h at 37° C and 5% CO2 (in complete growth media). The Sulforhodamine B (SRB) Cell cytotoxicity assays were performed following the company recommended protocol (SRB assay kit, Abcam, ab235935). The SRB absorbance was measured at 490 nm wavelength by using a microplate reader (BioTek Instruments, Inc., VT, USA).

Percent cytotoxicity was calculated by the following formula:

$$Cytotoxicity\,(\%) = \frac{O.D.(DMSO) - O.D.(Smaple)}{O.D.(DMSO)} \times 100$$

Where,

O.D. (DMSO) = absorbance of the DMSO control after background correction.

O.D. (Sample) = absorbance of the sample after background correction.

The IC_{50} values of the compounds were determined using Graph Pad Prism 7 software (GraphPad Software Inc., CA, USA) with nonlinear regression dose-response - inhibition curve fit (variable slope four parameter).

In vivo anti-tumor efficacy of peptide-drug conjugates: The in vivo studies were performed as per the animal protocol (No. 17R02) reviewed and approved by the Institutional Animal Care and Use Committee, University of the Pacific, Stockton, CA, USA. Four to six weeks old female athymic nude mice (nu/nu) were purchased from Simonsen Laboratories (Santa Clara, CA, USA).

Determining maximum tolerated dose (MTD) of the drug MMAE: The MTD of the drug MMAE was determined in four to six weeks old female athymic nude (homozygous, nu/nu) mice. Five healthy mice were given a single dose of 0.375 mg/kg, 0.5 mg/kg, 0.7 mg/kg, 1 mg/kg, and 1.5 mg/kg of MMAE, respectively via tail vein injection using 29 gauge needles. Following administration, the mice were observed daily for their general health and the body weight was measured every three days.

Xenograft model: CD13 overexpressing HT-1080 cells were cultured as described before. On the day of tumor transplantation, cells were detached using TrypLE Express and re-suspended in DMEM. The cell density was counted using Scepter Automated Handheld Cell Counter. The cells were centrifuged at 125xG for 5 minutes and the supernatant was discarded. The cell pellet was washed once with sterile PBS and re-suspended in 50:50 PBS – Matrigel (High Concentration) (Corning Life Sciences, Tewksbury, MA, USA) so that 0.1 mL of the suspension contains approximately 1,000,000 cells. The cell suspension was maintained on ice until injection. All mice were anaesthetized using isoflurane. 0.1 mL of cell suspension was injected subcutaneously on the right flank of each mouse using a 27 gauge needle. Following inoculation, the mice were observed daily for their general health and tumor appearance.

Anti-tumor efficacy: Tumors in mice were grown to reach an average of approximately 100 mm^3. The tumor bearing mice were then divided in to four groups each having four mice. The groups were PBS group, MMAE group, PEP20-MMAE group, and PEP173-MMAE group. Treatment was started 9 or 12 days after cancer cell transplantation and was administered intravenously via tail vein using 29 gauge needles every 4 days for a total of 4 doses (q4d X 4). The dose was 975 nmol/kg for each compound which

is equivalent to 0.7 mg/kg MMAE. The greatest longitudinal diameter (L) and the greatest transverse diameter (W) of the tumor were measured using Vernier caliper every four days from the day of first dosing. Tumor volume was determined using the formula $(L \times W^2)/2$. The body weights were also measured every four days.

Results and Discussion

Preparation of peptide-drug conjugates: The anticipated binding mode of the peptides (PEP20, GYPAY; and PEP173, GYPAVYLF) under study indicates that the N-terminal side binds deep inside the peptide binding channel of CD13 (22). Therefore, a cysteine conjugation site was incorporated at the C-terminal side of the peptides. A spacer (6-aminohexanoic acid, Ahx) was added in between the peptide sequence and the cysteine conjugation site to have spatial separation between the targeting peptide moiety and the linker-drug moiety.

The peptides (PEP20-Ahx-Cys; and PEP173-Ahx-Cys) were conjugated to monomethyl auristatin E (MMAE), a highly potent but non-selective tubulin polymerization inhibitor, through a maleimidocaproyl-valine-citrulline-p-aminobenzoyloxycarbonyl (mc-vc-PABC) linker. The maleimidocaproyl (mc) part of the linker-drug motif (mc-vc-PABC-MMAE) utilizes maleimide chemistry for cysteine linkage, which takes advantage of exceptional reactivity of maleimide towards sulfhydryl groups to form stable thioester bond. Valine-citrulline (vc) dipeptide is an intracellular protease, cathepsin B, sensitive linker. This protease sensitive approach uses the main proteases found in the tumor cell lysosome for identification and cleavage of a specific peptide sequence. The para-amino benzyloxycarbonyl (PABC) moiety in the linker-drug motif is a self-immolative spacer (24, 28).

Formation of desired molecules was confirmed by ESI-MS as shown in table 1. In the mass spectra PEP20-Ahx-Cys and PEP173-Ahx-Cys were observed as singly charged species whereas the peptide drug conjugates PEP20-MMAE (PEP20-Ahx-Cys-mc-vc-PABC-MMAE), and PEP173-MMAE (PEP173-Ahx-Cys-mc-vc-PABC-MMAE) were observed as double and triple charged. The HPLC analysis of the purified PDCs showed greater than 98% purity (Table 1).

In vitro cytotoxicity studies: Cytotoxicity studies were carried out to evaluate the potency of the free drug, and the peptide drug conjugates. Percentage cytotoxicity was calculated using sulphorhodamine B assay. MMAE showed very high potency (low IC_{50} values) across all three cell lines (Table 2). For all three cells lines, PDCs (PEP20-MMAE and PEP173-MMAE) showed significantly lower cytotoxicity than MMAE in the cell culture medium (Figures 1, 2 and 3, and Table 2).

PEP20-MMAE showed 5.2 and 4.3 times lower cytotoxicity in CD13 negative MCF-7 and control normal HEK-293 cells, respectively, when compared to that in CD13 positive HT-1080 cells (Figures 1, 2 and 3, and Table 2). PEP173-MMAE was found to have approximately 2.4 times less cytotoxicity both in MCF-7 cells and HEK-293 cells as compared to HT-1080 cells (Figures 1, 2 and 3, and Table 2). The PDCs seemed to have specificity trend towards CD13 positive HT-1080 cells as evidence by the lower IC_{50} in the HT-1080 cells. However, as compared to the HT-1080 cells, the drug MMAE was also found to be 4.5 and 8.9 times less cytotoxic (in terms of IC_{50}) in MCF-7 cells and HEK-293 cells, respectively (Figures 1, 2 and 3, and Table 2). This indicates that the conjugation of peptide-linker construct to the drug decreased the potency of MMAE but did not improve its selectivity.

There could be several reasons behind the lower cytotoxicity of the PDCs as compared to MMAE. One possibility could be higher protein binding of the PDCs or interference by fetal bovine serum present in the cell culture medium in which the cells were incubated with PDCs/drug. Liraglutide, a human glucagon-like peptide-1, was reported to exhibit approximately 99% serum protein binding in vitro (29). Hsiao IL and Huang YJ observed significantly lower in vitro cytotoxicity of ZnO particles in serum containing medium as

compared to the serum free medium (30). A dual targeting NGR-peptide"drug conjugate also showed significantly lower in vitro cytotoxicity than the drug itself in serum containing medium (31). The designed peptides might also lost their targeting ability after conjugating to the linker-drug construct due to the large size of the construct. The size of the drug-linker construct (mc-vc-PABC-MMAE) is bigger than the peptides. While, the molar weight of PEP20-Ahx-Cys and PEP173-Ahx-Cys are 785.91 and 1145.3 g/mol, respectively, the molar weight of the linker-drug construct is 1316.6 g/mol. It has been reported that conjugation induced perturbations in the peptide structural microenvironment can lead to diminished binding affinity to the target receptor (4). Peng ZH and Kopeèek J have shown that the cell penetrating cyclic peptide iRGD (CRGDKGPDC) lose its targeting ability after conjugating to linker-drug (valproic acid) construct (32).

In vivo anti-tumor efficacy: To select the therapeutic doses of the compounds in the in vivo study a maximum tolerated dose (MTD) was determined. MMAE was injected into healthy female athymic nude mice at doses ranging from 0.375 mg/kg to 1.5 mg/kg (n=1 for all doses, except for 0.70 mg/kg n=2). General health and body weight of the mice were monitored for 15 days after injection (Figure 4). Doses up to 0.70 mg/kg of MMAE were well tolerated with no apparent sign of toxicity. At 1.0 mg/kg dose, the mouse experienced around 20% weight loss within 6 days of injection and then started regaining weight. The mouse returned to initial body weight

Table 1. MS and HPLC data for the peptides and PDCs

Molecule	MS (g/mol) Observed	HPLC Purity (%)
PEP20-Ahx-Cys	808.8 [M+Na]+	80.5
PEP173-Ahx-Cys	1144.2 [M-H]-	80.9
PEP20-MMAE (PEP20-Ahx-Cys-mc-vc-PABC-MMAE)	1062.9 [M+H+Na]+2	98.1
PEP173-MMAE (PEP173-Ahx-Cys-mc-vc-PABC-MMAE)	828.9 [M+2H+Na]+3	98.3

Table 2. *In-vitro* cytotoxicity study data

Cell Line	IC50 (nM)		
	MMAE	PEP20-MMAE	PEP173-MMAE
HT-1080 (CD13 +ve)	0.09358 ± 0.01086	92.54 ± 13.38	72.68 ± 9.910
MCF-7 (CD13 -ve)	0.4250 ± 0.08300	477.9 ± 89.67	175.0 ± 21.30
HEK-293 (normal cell line)	0.8354 ± 0.1101	399.7 ± 51.89	172.8 ± 23.93

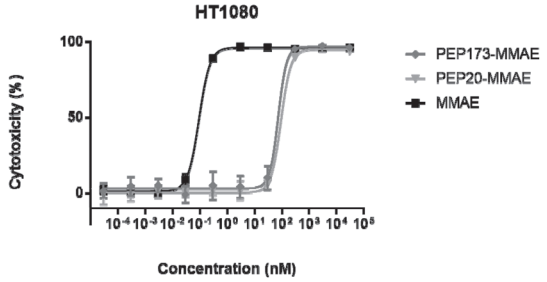

Fig. 1. Cytotoxicity of MMAE, PEP20-MMAE, and PEP173-MMAE in HT-1080 cells

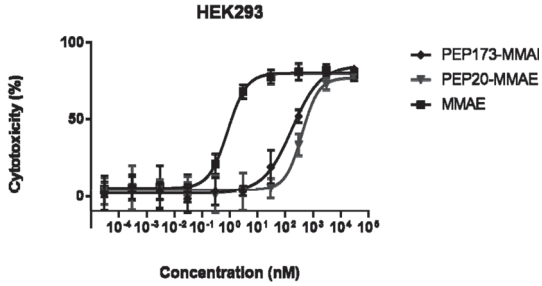

Fig. 3. Cytotoxicity of MMAE, PEP20-MMAE, and PEP173-MMAE in HEK-293 cells

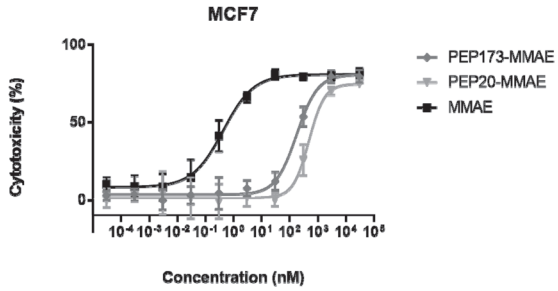

Fig. 2. Cytotoxicity of MMAE, PEP20-MMAE, and PEP173-MMAE in MCF-7 cells

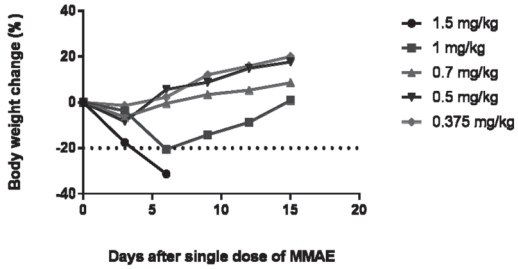

Fig. 4. MMAE tolerance in mice - MTD study

by day 15. The mouse receiving 1.5 mg/kg of MMAE lost more than 30% of the body weight by day 6 at which point the mouse was euthanized. Thus, the MTD of MMAE in female athymic nude mice (4-6 weeks old) was determined to be between 1.0 mg/kg and 1.5 mg/kg. The maximum tolerated dose (MTD) of dolastatin 10 in mice was reported to be approximately 0.45 mg/kg (33). Dolastatin 10 is a cytotoxic agent whose structure is similar to MMAE (34). Francisco et al reported the MTD of MMAE in SCID mice to be between 0.50 mg/kg and 1.0 mg/kg (23).

For the anti-tumor efficacy study, 975 nmol/kg, which is equivalent to 0.70 mg/kg of MMAE, was selected as the treatment dose (MMAE, PEP20-MMAE, and PEP173-MMAE). Treatment was started when the average tumor volume reached approximately 100 mm3 (9 or 12 days after tumor cell injection). Mice were administered with the drug, drug conjugates or PBS treatment every 4 days for a total of 4 doses (q4d x 4). In the mice treated with only PBS, the tumor grew rapidly and reached approximately 450 mm^3 by day 28 after tumor implantation (Figure 5). MMAE, PEP20-MMAE, and PEP173-MMAE all showed almost complete tumor regression during the study (Figure 5). PEP20-MMAE and PEP173-MMAE showed slightly higher tumor regression than MMAE, but the difference was not statistically significant. This insignificant difference in antitumor activity between the drug MMAE and PDCs may also be due to higher plasma protein binding of the PDCs or the diminished targeting ability of the peptides after conjugating with the larger linker-drug construct. Additionally, the degradation of PDCs in circulation by different enzymes may have contributed to this observation. Enzymatic degradation in systemic circulation has long been one of the major challenges for the peptide based drugs (35). van Hensbergen et al previously reported the CD13 targeted peptide-drug conjugate, Doxorubicin-CNGRC (C1-C5), to

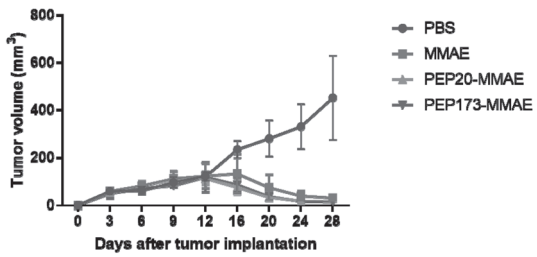

Fig. 5. Anti-tumor efficacy of the PDC's in mice

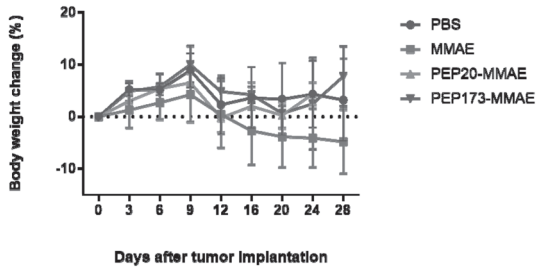

Fig. 6. Effect of PDC's on Body weight change (%) in mice

show no added advantage as compared to the drug, doxorubicin, in terms of in vitro cytotoxicity and in vivo antitumor effects (36).

Although, the PDCs have comparable anti-cancer efficacy in mouse as compared to the drug MMAE, the groups treated with PEP20-MMAE and PEP173-MMAE showed a body weight increase of 4% and 8%, respectively, even after fourth dose (25 and 28 days after tumor implantation) (Figure 6). On the other hand, the drug MMAE treated group lost body weight after dosing started and had a maximum weight loss of 10% after 28 days of tumor implantation (Figure 6). Weight loss is one of major adverse effects of anticancer agents due to high and non-selective cytotoxic potency (37). The PDCs (PEP20-MMAE and PEP173-MMAE) have shown significantly reduced side effects in terms of weight loss.

Conclusion

PDCs investigated showed limited effectiveness of peptide drug conjugates in vivo mice tumor model but reduced adverse effects, suggesting the need to improve the designed peptide-MMAE drug conjugates. Future research will focus on achieving the optimal chemical configuration of the conjugates for in vivo targeting and receptor mediated cellular uptake. The current computational simulation studies is limited to projecting binding of the peptides to the target protein. In future, peptide design with higher number of amino acids in the targeting moiety, and smaller linker-drug construct (especially small molecules) may be used to conserve the target binding ability of the PDCs.

References

1. Su, H., Koo, J.M. and Cui, H. (2015). One-component nanomedicine. Journal of Controlled Release, 219: 383-395.

2. Khandare, J. and Minko, T. (2006). Polymer–drug conjugates: progress in polymeric prodrugs. Progress in Polymer Science, 31(4): 359-397.

3. Wang, Y., Cheetham, A.G., Angacian, G., Su, H., Xie, L. and Cui, H. (2017). Peptide–drug conjugates as effective prodrug strategies for targeted delivery. Advanced Drug Delivery Reviews, 110-111: 112-126.

4. Vrettos, E.I., Mezõ, G. and Tzakos, A.G. (2018). On the design principles of peptide–drug conjugates for targeted drug delivery to the malignant tumor site. Beilstein Journal of Organic Chemistry, 14: 930-954.

5. Kapoor, P., Singh, H., Gautam, A., Chaudhary, K., Kumar, R. and Raghava, G.P.S. (2012). TumorHoPe: a database of tumor homing peptides. PLoS ONE, 7(4):e35187.

6. Gilad, Y., Firer, M. and Gellerman, G. (2016). Recent Innovations in Peptide Based Targeted Drug Delivery to Cancer Cells. Biomedicines, 4(2).

7. Alley, S.C., Zhang, X., Okeley, N.M., Anderson, M., Law, C., Senter, P.D. and

Benjamin, D.R. (2009). The pharmacologic basis for antibody-auristatin conjugate activity. Journal of Pharmacology and Experimental Therapeutics, 330(3): 932-938.

8. Doronina, S.O., Toki, B.E., Torgov, M.Y., Mendelsohn, B.A., Cerveny, C.G., Chace, D.F., DeBlanc, R.L., Gearing, R.P., Bovee, T.D., Siegall, C.B., Francisco, J.A., Wahl, A.F., Meyer, D.L. and Senter, P.D. (2003). Development of potent monoclonal antibody auristatin conjugates for cancer therapy. Nature Biotechnology, 21(7): 778-784.

9. Soudy, R., Gill, A., Sprules, T., Lavasanifar, A. and Kaur, K. (2011). Proteolytically stable cancer targeting peptides with high affinity for breast cancer cells. Journal of Medicinal Chemistry, 54(21): 7523-7534.

10. Polyak, D., Ryppa, C., Eldar Boock, A., Ofek, P., Many, A., Licha, K., Kratz, F. and Satchi-Fainaro, R. (2011). Development of PEGylated doxorubicin-E-[c(RGDfK)2] conjugate for integrin-targeted cancer therapy. Polymers for Advanced Technologies, 22(1): 103-113.

11. Ai, S., Duan, J., Liu, X., Bock, S., Tian, Y. and Huang, Z. (2011). Biological evaluation of a novel doxorubicin-peptide conjugate for targeted delivery to EGF receptor-overexpressing tumor cells. Molecular Pharmaceutics, 8(2): 375-386.

12. Wong, A.H.M., Zhou, D. and Rini, J.M. (2012). The X-ray crystal structure of human aminopeptidase N reveals a novel dimer and the basis for peptide processing. Journal of Biological Chemistry, 287(44): 36804-36813.

13. Luan, Y. and Xu, W. (2007). The structure and main functions of aminopeptidase N. Current Medicinal Chemistry, 14(6): 639-647.

14. O'Connell, P.J., Gerkis, V. and d'Apice, A.J. (1991). Variable O-glycosylation of CD13 (aminopeptidase N). Journal of Biological Chemistry, 266(7): 4593-4597.

15. Wickström, M., Larsson, R., Nygren, P. and Gullbo, J. (2011). Aminopeptidase N (CD13) as a target for cancer chemotherapy. Cancer Science, 102(3): 501-508.

16. Mina-Osorio, P. (2008). The moonlighting enzyme CD13: old and new functions to target. Trends in Molecular Medicine, 14(8): 361-371.

17. Pasqualini, R., Koivunen, E., Kain, R., Lahdenranta, J., Sakamoto, M., Stryhn, A., Ashmun, R.A., Shapiro, L.H., Arap, W. and Ruoslahti, E. (2000). Aminopeptidase N is a receptor for tumor-homing peptides and a target for inhibiting angiogenesis. Cancer Research, 60(3): 722-727.

18. Fukasawa, K., Fujii, H., Saitoh, Y., Koizumi, K., Aozuka, Y., Sekine, K., Yamada, M., Saiki, I. and Nishikawa, K. (2006). Aminopeptidase N (APN/CD13) is selectively expressed in vascular endothelial cells and plays multiple roles in angiogenesis. Cancer Letters, 243(1): 135-143.

19. Zhang, X. and Xu, W. (2008). Aminopeptidase N (APN/CD13) as a target for anti-cancer agent design. Current Medicinal Chemistry, 15(27): 2850-2865.

20. Hashida, H., Takabayashi, A., Kanai, M., Adachi, M., Kondo, K., Kohno, N., Yamaoka, Y. and Miyake, M. (2002). Aminopeptidase N is involved in cell motility and angiogenesis: its clinical significance in human colon cancer. Gastroenterology, 122(2): 376-386.

21. Corti, A. and Curnis, F. (2011). Tumor vasculature targeting through NGR peptide-based drug delivery systems. Current Pharmaceutical Biotechnology, 12(8): 1128-1134.

22. Uddin, M.Z., Li, X., Joo, H., Tsai, J., Wrischnik, L. and Jasti, B. (2019). Rational Design of Peptide Ligands Based on Knob–Socket Protein Packing Model Using CD13

as a Prototype Receptor. ACS Omega, 4(3): 5126-5136.

23. Francisco, J.A., Cerveny, C.G., Meyer, D.L., Mixan, B.J., Klussman, K., Chace, D.F., Rejniak, S.X., Gordon, K.A., DeBlanc, R., Toki, B.E., Law, C.L., Doronina, S.O., Siegall, C.B., Senter, P.D. and Wahl, A.F. (2003). cAC10-vcMMAE, an anti-CD30-monomethyl auristatin E conjugate with potent and selective antitumor activity. Blood, 102(4): 1458-1465.

24. Jain, N., Smith, S.W., Ghone, S. and Tomczuk, B. (2015). Current ADC Linker Chemistry. Pharmaceutical Research, 32(11): 3526-3540.

25. Amblard, M., Fehrentz, J., Martinez, J. and Subra, G. (2005). Fundamentals of modern peptide synthesis. Methods in Molecular Biology, 298: 3-24.

26. Amblard, M., Fehrentz, J., Martinez, J. and Subra, G. (2006). Methods and protocols of modern solid phase Peptide synthesis. Molecular Biotechnology, 33(3): 239-254.

27. Chandrudu, S., Simerska, P. and Toth, I. (2013). Chemical methods for peptide and protein production. Molecules, 18(4): 4373-4388.

28. Dubowchik, G.M., Firestone, R.A., Padilla, L., Willner, D., Hofstead, S.J., Mosure, K., Knipe, J.O., Lasch, S.J. and Trail, P.A. (2002). Cathepsin B-labile dipeptide linkers for lysosomal release of doxorubicin from internalizing immunoconjugates: model studies of enzymatic drug release and antigen-specific in vitro anticancer activity. Bioconjugate Chemistry, 13(4): 855-869.

29. Plum, A., Jensen, L.B. and Kristensen, J.B. (2013). In vitro protein binding of liraglutide in human plasma determined by reiterated stepwise equilibrium dialysis. Journal of Pharmaceutical Sciences, 102(8): 2882-2888.

30. Hsiao, I.L. and Huang, Y. (2013). Effects of serum on cytotoxicity of nano- and micro-sized ZnO particles. Journal of Nanoparticle Research, 15: 1829.

31. Enyedi, K.N., Tóth, S., Szakács, G. and Mezõ, G. (2017). NGR-peptide"drug conjugates with dual targeting properties. PLOS ONE, 12(6): e0178632.

32. Peng, Z. and Kopeèek, J. (2014). Synthesis and activity of tumor-homing peptide iRGD and histone deacetylase inhibitor valproic acid conjugate. Bioorganic & Medicinal Chemistry Letters, 24(8): 1928-1933.

33. Mirsalis, J.C., Schindler-Horvat, J., Hill, J.R., Tomaszewski, J.E., Donohue, S.J. and Tyson, C.A. (1999). Toxicity of dolastatin 10 in mice, rats and dogs and its clinical relevance. Cancer Chemotherapy and Pharmacology, 44(5): 395-402.

34. Poncet, J. (1999). The dolastatins, a family of promising antineoplastic agents. Current Pharmaceutical Design, 5(3): 139-162.

35. Böttger, R., Hoffmann, R. and Knappe, D. (2017). Differential stability of therapeutic peptides with different proteolytic cleavage sites in blood, plasma and serum. PLOS ONE, 12(6): e0178943.

36. van Hensbergen, Y., Broxterman, H.J., Elderkamp, Y.W., Lankelma, J., Beers, J.C.C., Heijn, M., Boven, E., Hoekman, K. and Pinedo, H.M. (2002). A doxorubicin-CNGRC-peptide conjugate with prodrug properties. Biochemical Pharmacology, 63(5): 897-908.

37. Wahlang, J.B., Laishram, P.D., Brahma, D.K., Sarkar, C., Lahon, J. and Nongkynrih, B.S. (2017). Adverse drug reactions due to cancer chemotherapy in a tertiary care teaching hospital. Therapeutic Advances in Drug Safety, 8(2): 61-66.

Current Trends in Biotechnology and Pharmacy
Vol. 13 (2) 156-162 April 2019, ISSN 0973-8916 (Print), 2230-7303 (Online)

Determination of Flecainide acetate and its degradation impurities by UPLC-MS

Geetha Bhavani K[a,b], Hari Babu B[c], Ramachandran D[c*], Srinivasu N[b#]
[a,b]JMJ College for Womens, Tenali, Andhra Pradesh, India.
Email: geethabhavanipurama@gmail.com
[b]Department of Science and Humanities, Vignan University, Vadlamudi, A.P., India
Email: navulurisrinivasu@gmail.com
[c]Department of Chemistry, Acharya Nagarjuna University, Nagarjuna Nagar, Guntur. A.P., India.
For correspondence: dittakavirc@gmail.com; Mob: +91-9866965335.

Abstract

A sensitive UPLC-MS method was developed for the determination of Flecainide acetate in the presence of four its related impurities (Impurities: A,B,D and E). The forced degradation study of Flecainide acetate was carried out under acidic, alkali, neutral and oxidative conditions. The degradation was observed under acidic, neutral and oxidative conditions and four degradation products (impurities) were observed. Successful chromatographic separation of Flecainide acetate and its degradation products were achieved on a Waters Acquity BEH C18 column (100 mm x 2.1 mm x 1.7µ) using a mobile phase of solvent A (10 mM Ammonium formate) and solvent B (acetonitrile) in gradient elution. The gradient program employed to achieve the separation was (T_{min}/%Solvent B): 0/15, 1/15, 3/90, 5/90, 7/15, 9/15. The flow rate was maintained at 0.3 mL/min. The impurities were characterized and the fragmentation pathways for the impurities were proposed.

Keywords: Flecainide acetate; Forced degradation; UPLC; ICH, LC-MS method.

Introduction

Flecainide acetate, N-(2-piperidinyl-methyl)-2,5-bis(2,2,2-trifluoroethoxy) benzamide monoacetate, is an anti-arrhythmic agent that is used to treat ventricular arrhythmias by blocking sodium causing a decreased intra-cardiac conduction velocity (1) and is brand under Tambocor. Forced degradation is a process where the natural degradation rate of a drug or drug product is accelerated by the application of an additional stress (2). Stress testing is designed to estimate degradation pathways and intrinsic stability of the drug molecule. The chemical structures of Flecainide acetate and its studied impurities are presented in Fig. 1.

Some regular chromatographic methods have been available in the literature for the determination of flecainide acetate in its bulk powder, in pharmaceutical formulations or in the presence of its enantiomer, metabolites or other antiarrhythmic drugs. In the last decade, four liquid chromatographic methods (3-6), one capillary zone electrophoretic method (7), one Thin Layer Chromatographic (TLC) method (8) have been reported. Only one spectro-fluorimetric method (9] and one electrochemical method (10) were reported. Also, the stability of flecainide acetate in an extemporaneously compounded oral suspension was studied by High Performance Liquid Chromatographic (HPLC) methods (11-12) and only one stability-indicating TLC-densitometry and HPLC methods (13) were reported. No stability indicating method for the analysis of Flecainide acetate and its impurities under stress degradation conditions using LC-MS has been reported. Therefore, the aim of the present study is designed to develop a LC-MS compatible procedure for the determination of Flecainide acetate in the presence of its related substances. The present contribution of the work was to

evaluate the opportunities offered by LC-MS for determining the impurities of the cited drug.

Materials and Methods

Chemicals and Reagents : Flecainide Acetate (purity e" 99%) bulk drugs were obtained as gift sample from a renowned manufacturer. 10 mM ammonium formate (Analytical- reagent grade) was purchased from Merck Pvt. Ltd., whereas acetonitrile (HPLC- grade) were purchased from Sigma Aldrich. All other reagents used like hydrochloric acid, hydrogen peroxide, and sodium hydroxide was of analytical grade (Merck Pvt. Ltd.). HPLC grade water (Milli Q water purification system) was used throughout the analysis.

Instrumentation and Chromatographic conditions : The separation was achieved on a UPLC separation module, Waters Acquity BEH C18 column (100 mm x 2.1 mm x 1.7µ) using a mobile phase of solvent A (10 mM Ammonium formate) and solvent B (acetonitrile) in gradient elution. The gradient program employed to achieve the separation was (T_{min}/ %Solvent B): 0/15, 1/15, 3/90, 5/90, 7/15, 9/15. The flow rate was maintained at 0.3 mL/min. The column temperature was maintained at 25 °C and the autosampler at 10 °C. The detection wavelength was 245 nm where the drug and the impurities showed optimum response for quantification and the injection volume was 2 µL. This method was transferred to LC-MS analysis by LC system to Agilent Q-TOF 6540 series, Agilent Technologies.

The capillary voltage applied was 4000 V. The temperature of the gas was set at 325 °C, using nitrogen as nebulizing gas and drying gas. Drying gas flow at 10 L/min, nebulizer pressure 40 psi and fragmentor 130 V. Mass spectra were acquired over an m/z range of 50-1000 and CID gas was high pure nitrogen (99.99 %). Mass Hunter Software was used for monitoring output signal, controlling acquisition and processing of the mass data.

Sample preparation for LC-MS analysis : Stress samples were collected and made up to volume with mobile phase whereas solid samples were directly dissolved and diluted with mobile phase. Sample concentration of 1 mg/mL was used to conduct degradation studies. All the samples were filtered through 0.22 µm membrane filter and injected into LC-MS system.

Forced degradation study : Forced degradation studies were performed as per ICH guidelines. All stress decomposition studies were performed with control solution i.e. prepared and treated similarly to the respective stress conditions without active component. Acidic degradation was performed by refluxing of sample at 1 mg/mL of 1 N HCl at 70 °C for 22 h. Alkaline degradation was performed by refluxing of sample with 1 mg/mL of 0.1 N NaOH at 70 °C for 28 h. The neutral degradation was performed by refluxing of sample with 1 mg/mL of H_2O for 48 h. Oxidative degradation was performed with 1 mg/mL of 10 % H_2O_2 at room temperature for 48 h. All the forced degraded samples were filtered and then injected into LC-MS system.

Results and Discussion

Optimization of the method : Flecainide Acetate is relatively non polar compound and was found to retain on traditional C18 bonded phases. To improve the selectivity and retention and further the peak shape bonded phases of stationary phase was tried. The initial trials were carried out with aqueous buffer solutions of pH 3.0, 4.0, 5.0, 5.5 and 6.0 with organic phase being methanol or acetonitrile. The method was optimized in keeping view of adequate separation of the impurities from the main peak.

Different columns with variable chemistries like Acquity CSH C18, Acquity HSS C18, Acquity HSS Cyano were tried with different combinations of mobile phase containing different proportions of buffer system and organic modifiers. The critical aspect of optimizing the method was based on the resolution obtained among the peaks. After a thorough screening of various buffers, organic modifiers and other chromatographic parameters the final separation was achieved on a Waters Acquity BEH C18 column (100 mm x 2.1 mm x 1.7 µ) using a mobile phase of solvent A (10 mM Ammonium formate)

and solvent B (Acetonitrile) in gradient elution. The final chromatogram of Flecainide acetate standard was shown in **Fig. 2**.

Forced degradation studies : In the present study, Flecainide acetate was subjected to different stress conditions, including acid, alkali and oxidative degradation as stated by International Conference on Harmonization guidelines (ICH, 2003). The drug shows the absence of degradation products under basic conditions **(Figure 3)**. Flecainide acetate was degraded upto 6.09 % and 25.95 % during neutral and peroxide degradation, respectively followed by formation of one major degradation product (Impurity-A) and the respective chromatograms are shown in **Figures 4 & 5**. Another degradation product (Impurity-D) was found under acidic condition and Flecainide acetate was degraded upto 4.55 % (**Figure 6**). The separation of all the impurities (Impurity-A, B, D & E) using the final optimized chromatographic conditions is shown in **Figure 7**, indicates the selectivity of the method.

The identification of impurity products was also very effective for knowing the pathways of impurity of drug substances or drug products. Therefore, the impurity products were subjected to LC-MS study to elucidate structural details. Results were tabulated in **Table 1** and mass spectrums were shown in **Figures 8 & 9**.

Mass spectrum shows pure drug at m/z 415.14, Impurity–A, with m/z 397.13 was obtained in neutral and peroxide degradation, Impurity–D

Table 1: Characterization of impurity products by LC-MS

Impurity products	Experimental mass	Best possible molecular formula
Impurity - A	397.13	$C_{17}H_{20}F_6N_2O_2$
Impurity - B	115.12	$C_6H_{15}N_2$
Impurity - D	319.04	$C_{11}H_8F_6O_4$
Impurity - E	409.09	$C_{17}H_{14}F_6N_2O_3$

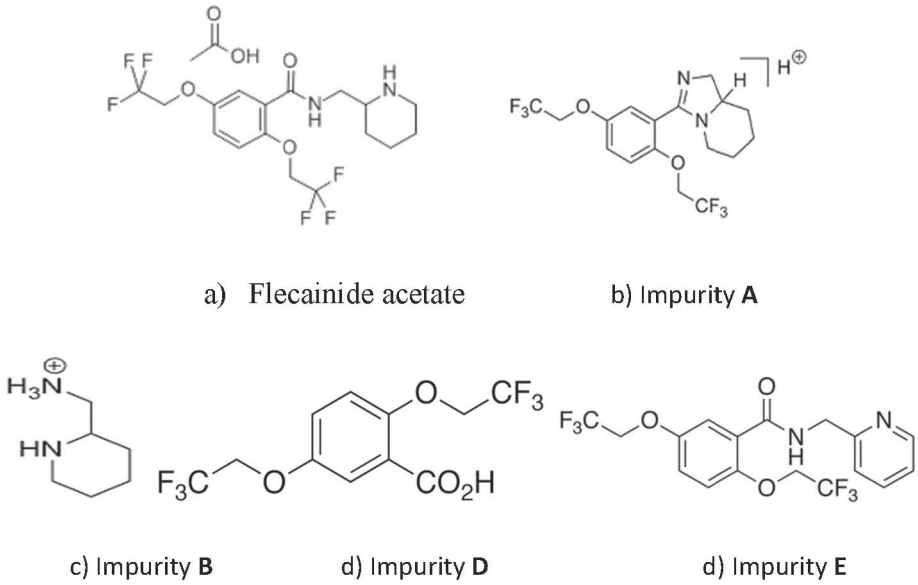

Fig. 1: Structures of Flecainide acetate and its impurities A, B, D & E

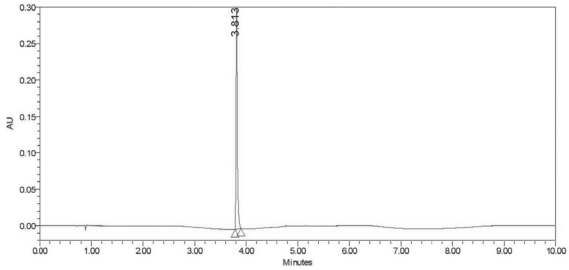

Fig. 2: Chromatogram of Flecainide Acetate standard

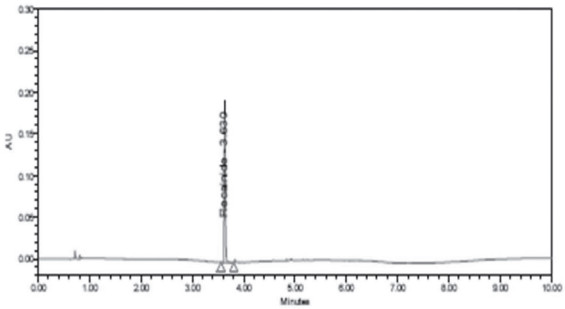

Fig. 3: Chromatogram of Flecainide acetate under base degradation

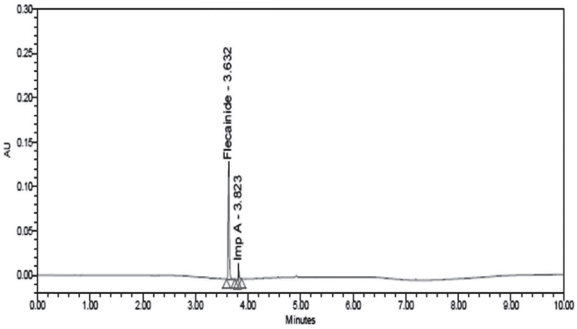

Fig. 4: Chromatogram of Flecainide Acetate under neutral degradation

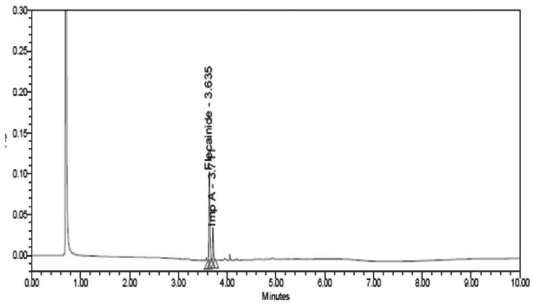

Fig. 5: Chromatogram of Flecainide Acetate under peroxide degradation

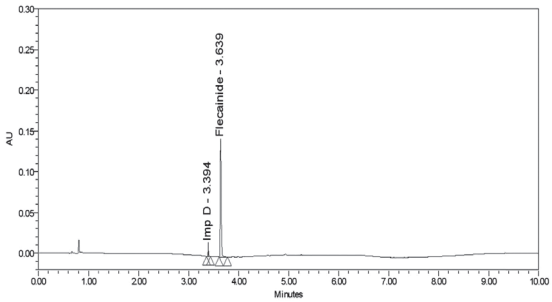

Fig. 6: Chromatogram of Flecainide Acetate under acidic degradation

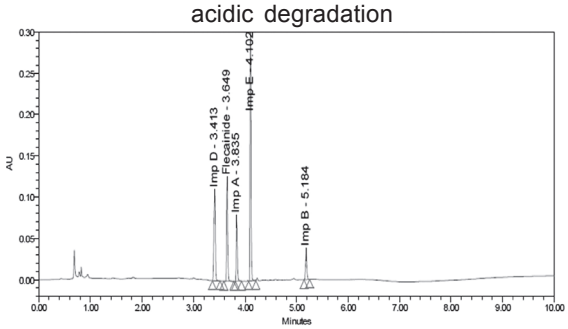

Fig. 7: Representative chromatogram showing the selectivity of the method

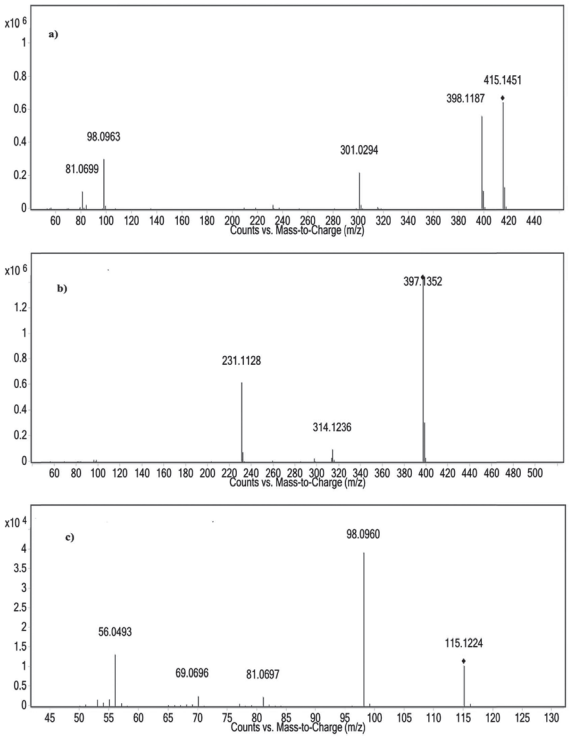

Fig. 8: MS/MS spectra of a) Flecainide acetate; b) Impurity A; c) Impurity B

Vol. 13 (2) 156-162 April 2019, ISSN 0973-8916 (Print), 2230-7303 (Online)

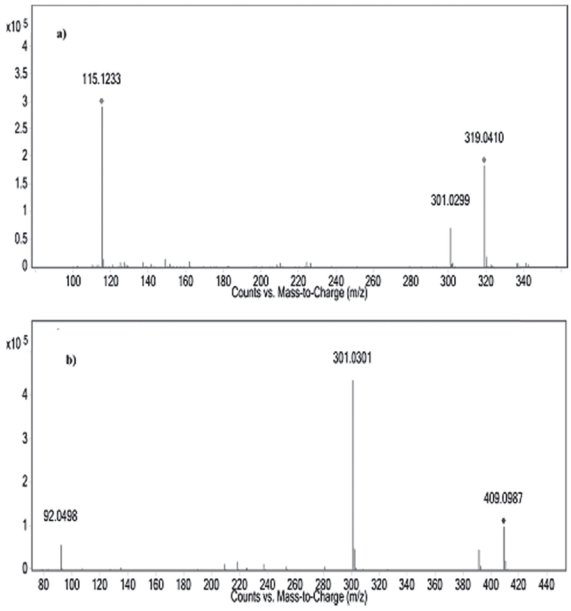

Fig. 9: MS/MS spectra of a) Impurity D; b) Impurity E

with m/z 319.04 in acidic degradation and Impurity–B & E with m/z 115.12, 409.09 along with A & D in mix and the fragmentation pathways of impurity products were shown in **Figures 10-13**.

Conclusion

The degradation behaviour of Flecainide acetate was studied under various stress conditions. The degradation study indicated that the selected drug was stable to alkali treatment while susceptible to neutral, peroxide and acidic stress. LC-MS study results reveal the formation of four impurity products in the chromatogram and the fragmentation pathways of the so used impurities were also identified. The developed method can be used to construct a profile for Flecainide acetate.

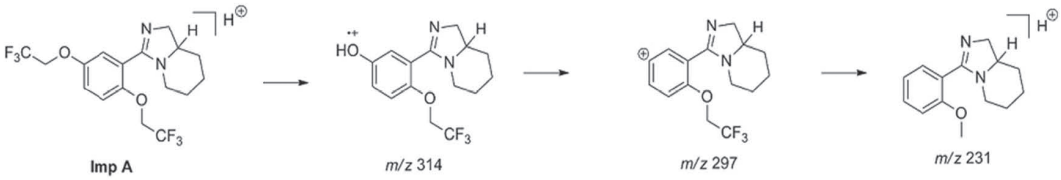

Fig. 10: Fragmentation pathway for Impurity A

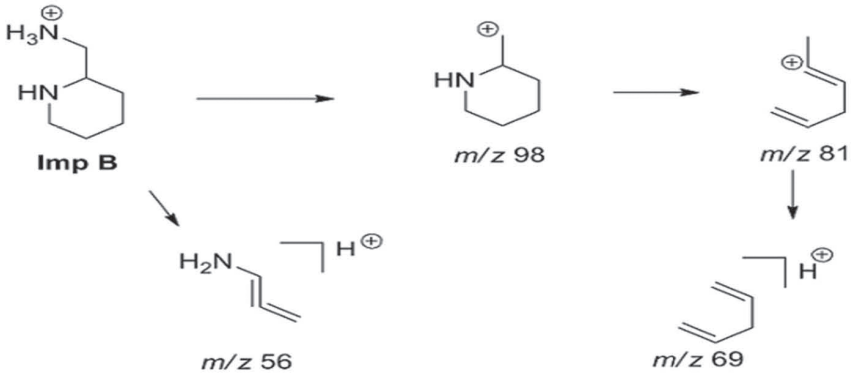

Fig. 11: Fragmentation pathway for Impurity B

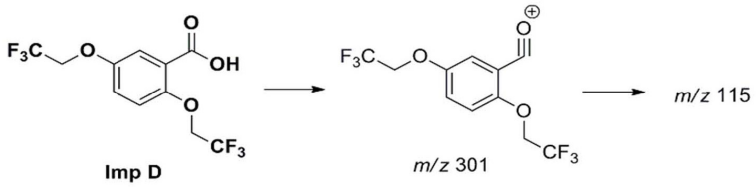

Fig. 12: Fragmentation pathway for Impurity D

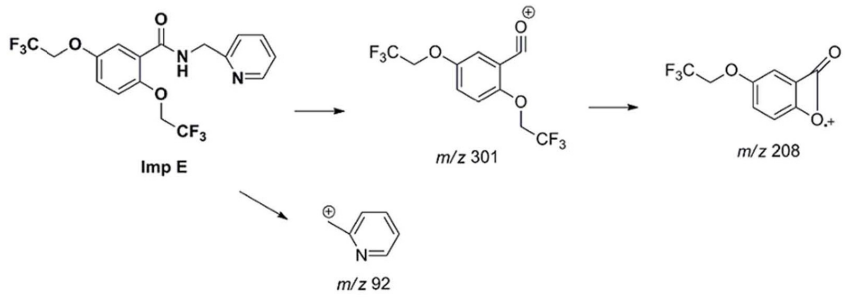

Fig. 13: Fragmentation pathway for Impurity E

Acknowledgements

The authors are thankful to Vignan University, Vadlamudi, Guntur and Acharya Nagarjuna University, Guntur for constant support.

Conflict of interest: The authors declare that there is no conflict of interests regarding the publication of this paper.

References

1] Levine, B., Chute, D. and Caplan, Y.H. (1990). Flecainide intoxication. *Journal of Analytical Toxicology* 14: 335–336.

2] Saxena, D., Damale, S., Joshi, A. and Datar, A. Forced degradation studies of amlodipine besylate and characterization of its major degradation products by LC-MS/MS. *International Journal of Life Sciences Biotechnology and Pharma Research* 3 (2014) 196-207.

3] Kristoffersen, L., Oiestad, EL., Opdal, MS., Krogh, M., Lundanes. E. and Christophersen, AS. (2007). Simultaneous determination of 6 beta-blockers, 3 calcium-channel antagonists, 4 angiotensin-II antagonists and 1 antiarrhythmic drug in post-mortem whole blood by automated solid phase extraction and liquid chromatography mass spectrometry: Method development and robustness testing by experimental design. *Journal of Chromatography B: Analytical Technology in Biomedicine and Life Sciences* 850: 147–160.

4] Lee, A., Choi, HJ., and Hyun, MH. (2010). Liquid chromatographic direct resolution of flecainide and its analogs on a chiral stationary phase based on (+)-(18-crown-6)-2,3,11,12-tetracarboxylic acid. *Chirality* 22: 693–698.

5] Sorensen, LK. (2012). A liquid chromatography–electrospray tandem mass spectrometry method for the determination of antiarrhythmic drugs and their metabolites in forensic whole blood samples. *Journal of Analytical Toxicology* 36: 116–122.

6] Doki, K., Sekiguchi, Y., Kuga, K., Aonuma, K., Kohda, Y. and Homma, M. (2014). Stereoselective analysis of flecainide enantiomers using reversed-phase liquid chromatography for assessing CYP2D6 activity. *Biomedical Chromatography* 28: 1193–1198.

7] Pietras, R., Kowalczuk, D., and Hopka³a, H. (2007). Simultaneous separation of 14 antiarrhythmic drugs and determination of mexiletine and flecainide by capillary zone electrophoresis. *Journal of AOAC International* 90: 977–986.

8] Pietras, R. and Kowalczuk. D. (2010). RP-TLC separation of antiarrhythmic drugs: Densitometric analysis of flecainide in tablets. *Journal of Planar Chromatography - Modern TLC* 23: 65–69.

9] Chang, SF., Miller, AM., Jernberg, MJ., Ober, RE. And Conard, GJ. (1983). Measurement of flecainide acetate in human plasma by an extraction spectro-photofluorometric method. *Arzneimittel-Forschung* 33: 251–253.

10] Stefan, RI., Baiulescu, GE., and Aboul-Enein, HY. (1997). Flecainide-selective membrane electrodes. *Analysis* 25: 39–42.

11] Wiest, DB., Garner, SS., Pagacz, LR. and Zeigler, V. (1992). Stability of flecainide acetate in an extemporaneously compounded oral suspension. *American Journal of Hospital Pharmacy* 49: 1467–1470.

12] Allen, LV. and Erickson, MA. (1996). Stability of baclofen, captopril, diltiazem hydrochloride, dipyridamole, and flecainide acetate in extemporaneously compounded oral liquids. *American Journal of Health-System Pharmacy* 53: 2179–2184.

13] El-Ragehy, NA., Hassan, NY., Tantawy, MA., and Abdelkawy, M. (2016). Stability-indicating chromatographic methods for determination of flecainide acetate in the presence of its degradation products; isolation and identification of two of its impurities. *Biomed. Chromatogr.,* 30: 1541-1548.

Current Trends in Biotechnology and Pharmacy
Vol. 13 (2) 163-177, April 2019, ISSN 0973-8916 (Print), 2230-7303 (Online)

Antigenotoxic effects of rutin against methotrexate genotoxicity in Swiss albino mice

Ashoka Ch [1] and Mohammed .S. Mustak[2]*
[1]Department of Zoology, Government Science College, Nrupathunga Road, Bangalore-560 001, Karnataka, India.
[2]Departments of Applied Zoology, Mangalore University, Mangalagangothri - 574 199 Mangalore, Karnataka, India.
*For Correspondence Address : msmustak@gmail.com; msmustak@mangaloreuniversity.ac.in

Abstract

Cancer chemoprevention with natural phytochemical compounds is an emerging strategy to prevent, impede, delay, or cure cancer. The aim of the study is to evaluate the anti-clastogenic potency of the rutin, a flavonoid to modulate the side effects induced by the anticancer drug Methotrexate. Methotrexate is an antimetabolite drug broadly used in the treatment of cancer and autoimmune diseases which causes an array of many side effects. Different doses of rutin (50, 100 and 150 mg/kg bw) were given once daily for five days orally and methotrexate (20mg/kgbw) was administered on the fourth day intraperitoneally. To understand the protective effect of rutin against methotrexate side effects, micronucleus test and chromosome aberration tests were performed at 48h post methotrexate administration. The results showed that 20mg/kgbw of MTX significantly induced MN in polychromatic erythrocytes ($p<0.05$) and resulted in significant increase in total chromosomal aberrations (41.8±3.70 %; $p<0.05$). Further, pre-treatment with the flavonoid rutin reduced the MNPCE and chromosomal aberrations in bone marrow and MN NCE in peripheral blood in comparison to MTX group. The Rutin supported the recovery from the mitotic suppression compared to MTX treated mice. Thus, the present study implies the major therapeutic use of rutin against genotoxic effects of methotrexate.

Keywords: Methotrexate, Rutin, Micronucleus, Mitotic Index, Polychromatic Erythrocytes, Chromosomal aberrations.

Introduction

In recent years, there have been considerable efforts to find naturally occurring substances that can inhibit, reverse, or retard mutagenesis (1-3). Flavonoids are a large group of plant secondary metabolites (4) that have attracted considerable interest because of their beneficial effects in humans; they have been reported to have antiviral (5), antiallergic (6), anti-inflammatory (7-9), antitumor (10-12), anti-radiation (13) and antioxidant activities (14,15). They are ubiquitous in fruits and vegetables that are regularly consumed by humans (16). More than 6000 different flavonoids (17) have been identified, many of which are responsible for their attractive colours of flowers(18) fruits and leaves. All these aspects justify the intense interest in flavonoids which has been manifested over several decades (19).

Methotrexate (MTX) is an anti-cancer drug developed during 1940s as a specific antagonist of folic acid, showing inhibitory effects on *de novo* synthesis of purine and pyrimidine nucleotides (20,21). Basic principle of therapeutic efficacy of

MTX is due to the inhibition of dihydrofolate reductase, a key enzyme in the folic acid metabolism (22). Studies have shown that MTX induce short and long term toxic effects including genotoxicity in mouse somatic and germinal cells (23). Previously, our study showed the cytogenetic toxicity of methotrexate in mouse bone marrow using chromosomal aberration, mitotic index and micronucleus assays (24). Studies have shown that Bone marrow (24), gastrointestinal mucosa and hair are particularly vulnerable to MTX (25). The MTX is not selective for the cancer cells, it can affect the normal tissues and so prolonged use of MTX has been associated with various organ toxicity (26). Recently, many secondary metabolites are tried to ameliorate the toxicity associated with MTX.The protective effects of vitamin E and Cornus mas fruit extract were studied on methotrexate-induced cytotoxicity in sperms of adult mice and jejunal mucosal damage in rats (27).Yuncu et al. 2015 (28) studied the p*rotective effects of vitamin E* and L-carnitine against *MTX*-induced injury in rat testis and reported the *elevation in malondialdehyde (MDA) levels and the amelioration in superoxide dismutase levels.* The compounds such as resveratrol and famotidine were also found significantly prevent the MTX induced elevation of the MDA, 8-OH/Guanosine and myeloperoxidase (MPO) parameters and decreased the levels of tGSH in the duodenal and jejunal tissues (29). The beta glucan, an antioxidant also showed protective effect on MTX induced testicular damage in rats (30).

Recently, more emphasis has been given to the discovery of genoprotective agents from the natural products and their isolated compounds against the damaging effects of chemicals. The Rutin (3,3',4',5,7-pentahydroxyflavone-3-rhamnoglucoside the flavonoid has the pharmacological properties like antioxidant, anti-inflammatory, anti-apoptotic, and anti-autophagic effects and have been exploited in human medicine and nutrition (31). Conventionally, it is used as an antimicrobial, antifungal, and anti-allergic agent. The recent studies have shown its multispectral pharmacological benefits for the treatment of various chronic diseases, such as cancer, diabetes, hypertension, and hypercholesterolemia (32-36). Further, studies demonstrated that orally administered rutin significantly attenuated memory deficits in Alzheimer's disease transgenic mice, by decreasing oligomeric Aβ level, increased super oxide dismutase activity and glutathione/glutathione disulphide ratio, reduced glutathione disulphide and MDA levels, and decreased IL-1 and IL-6 levels in the brain suggesting that rutin is a promising agent for Alzheimer's disease treatment (37,38). However, antigenotoxic effects of rutin against the MTX induced genotoxicity/ clastrogenic damage in Swiss albino mice were not yet studied. Therefore, the present study was aimed to evaluate protective role of rutin aganst the MTX induced the genotoxicity/clastogenecity through micronucleus assay and chromosomal abberations.

Materials and Methods

Chemicals: Methotrexate (MTX, $C_{20}H_{22}N_8O_5$, CAS No. 59-05-2; Batch No A1283L14) marketed by IPCA laboratories Mumbai, as Folitrax was used for the experiment. Colchicine ($C_{22}H_{25}NO_6$; CAS No.64-86-8; Batch No. T 823279) was purchased from SRL Ltd, Mumbai.Rutin trihydrate (CAS 250249-75-3; Batch No.000020566) was obtained from Himedia, India. All other chemicals were procured from Merck, SRL, Himedia, India.

Animals: Swiss albino mice belonging to the *Mus musculus* species inbred and maintained in the institutional animal house were used for the experiments. The animal experiments were conducted after obtaining the approval from the Institutional Animal Ethical Committee (IAEC) of Mangalore University. Care of the animals and experiments were conducted as per the guidelines of CPCSEA, (Committee for the Purpose of Control and Supervision of Experimentation on Animals) India. Animals were housed in polypropylene shoe box cages bedded with clean, dry paddy husk and kept in air-conditioned room at a temperature of 22± 2^0 C and relative humidity

50±15%. They were fed with a standard pelleted diet and water ad libitum. The 8-10 weeks old animals of both the sexes with an average body weight of 23±0.5 g were used for the experiments. In each experimental and control group, five animals were maintained.

Dose and treatment schedule: The LD_{50} value of methotrexate (MTX) for intra-peritoneal use has been reported as 50 mg/kg bw. in mice (datasheets.scbt.com/sc-3507.pdf). For the present study, we selected 20 mg/kg bw, dissolved in double distilled water and administered as a single dose in 0.2 ml quantity through intraperitoneal route. Double distilled water was used as a control. Rutin suspended in distilled water at different doses was orally administered. MTX was i.p injected only once on the 4th day of rutin treatment (The Study design is shown in table 1.)

Bone Marrow Micronucleus Test (MN Test): the bone marrow MN preparations were made from different groups (Group 1 to VIII) of experimental animals, following the modified method of Schmid (1973) (39). Rutin with Methotrexate groups (Groups VI, VII and VIII) were sacrificed after 24hr of Rutin treatment(48 h post MTX dosing). The bone marrow cells from thigh bones were flushed with 5% BSA into a centrifuge tube using a syringe and thoroughly mixed. The suspension was centrifuged at 1000 rpm for 15 minutes. The supernatant was discarded and a drop of fresh 5% BSA was added to the pellet. A thin smear was prepared in clean grease free slides. The slides were air dried and soon fixed in methanol for 10 minutes and stained with buffered (pH 6.8) May-Grunwald-Giemsa stain. Both the stains were filtered through a Whatman filter paper No. 1 (pore size 1.00 μ). Two thousand PCEs /animal were screened for MN and the corresponding normochromatic erythrocytes (NCEs) in the field were also scored to determine the MN frequency. PCEs are younger and NCEs are older erythrocytes. PCEs stain bluish and NCEs stain reddish orange in colour Fig.1.

Peripheral blood MN assay:The peripheral blood MN assay was done by using the method of Schlegel and MacGregor (40). The blood was drawn from the tail vein on the day of animal sacrifice(48h post MTX dosing) and thin smears were prepared on clean grease free slides. They were fixed in absolute methanol for 10 minutes. The slides were then stained with buffered 10 % Giemsa (pH-6.8) taken in vertical couplin jars. About 2000 NCE per animal were scanned for the presence of MN. The number of PCE corresponding to 2000 NCE was also determined (41).

Chromosomal Aberration (CA) Test: The chromosomal preparations were made following the method of Tjio and Whang (42). The condition of rutin and MTX administrations were the same as those used for the MN test.The animals were sacrificed 24 h post rutin treatment (48h after MTX dosing) The experimental animals were intraperitoneally injected with colchicine solution (2 mg|kgbw), before 1 h of sacrifice by cervical dislocation. The marrow cells were flushed from femur and tibia bones with 0.56% potassium chloride (KCl). The marrow suspension was thoroughly mixed with the hypotonic solution and left at room temperature for 30 minutes. After this, the suspension was centrifuged at 1000 rpm for 10 minutes and the pellet obtained was resuspended in 2 ml of 1:3 acetic-methanol fixative. The suspension was kept in room temperature for 45 minutes and centrifuged. The supernatant was discarded, and the fixative was again added, mixed thoroughly, incubated at room temperature for ten minutes and centrifuged. This step was repeated thrice. Finally, the pellet was suspended in appropriate amount of fixative and thoroughly mixed. 2-3 drops of suspension were dropped from a height of about 3 feet on clean, pre-chilled slides and flame dried. The slides were stained with buffered Giemsa (pH 6.8) and observed under microscope (Olympus BX51). 100 well-spread metaphases were screened from each animal for the presence of several types of chromosomal aberrations (Fig.2). From each animal, a total of 2000 cells were scored for the presence of dividing and non-dividing cells to determine the mitotic index values.

$$\text{Mitotic Index (MI)} = \frac{\text{Number of dividing cells} \times 100}{\text{Total number of bone marrow cells counted}}$$

Percentage reduction (%R) in the tests was calculated using the formula of Waters et al. (43,44): %R = [(mean in A - mean B)/(mean in A - mean in C)] × 100, where A is the group treated with MTX20 , B is the group treated with different doses of rutin plus MTX20 and C represents the control group.

Statistical Analysis: The data were expressed as mean ±S.D. The micronucleus induction data and chromosomal aberration data were analyzed statistically by analysis of variance (ANOVA). In cases in which $p < 0.05$, the Tukey's test compared treatment means. All data were processed using the statistical package SPSS 20.0 for Windows (IBM Corporation, Armonk, NY).

Results

The results of bone marrow micronucleus test are presented in table 2. The polychromatic erythrocytes (PCE) appear blue in colour and they are larger than the normochromatic erythrocytes (NCE). The NCEs stain orange red in colour (Fig.1B). In the control (Group I), the frequency of MN in PCEs was 0.15 ±0.07. In MTX treated animals it was significantly higher i.e 1.19±0.16 ($p<0.05$).The Rutin alone group (group II, III and IV) did not show any statistically significant difference in MN induction in PCEs compared to control group. The proportion of PCEs to the total erythrocytes were also like that of control group (Table.2). This indicates that the doses of rutin selected and the route of dosing in the present study do not pose any clastogenic threat to the bone marrow in the Swiss albino mice.MN in PCE was observed at all combinations, with the percent of MN reduction ranging between 17- 75 % (Table.2). The pre-treatment of rutin 100 mg/kg body weight showed Higher reduction (75%) in MNPCE when compared other doses of rutin against the MTX 20 group($p<0.05$).

In the peripheral blood micronucleus test, the frequency of MN NCE (Table.3 and Fig. 1-C,D) was increased in MTX treated mice compared to the control(distilled water) group($p<0.05$).The percentage frequency of PCE in MTX treated group was significantly decreased compared to control and rutin group. Pre-treatment with rutin has shown improvement in the PCE production. The % PCE has reached near a value of 2.

The results of chromosomal aberration test (CA) are presented in table 4 and 5. Significant increase in the percent aberrant cells was observed in MTX20 group (41.80±3.70) compared to the control group(4.6±2.30)(Table.5).Several types of aberrations such as gaps, breaks, exchanges, fragments, multiple aberrations, centromeric separation, centromeric associations, stickiness and pulverization has been observed . Metaphase plates containing two or more diverse types of aberrations were included under multiple aberrations. In our study high frequency of breaks were also observed and gaps, breaks and exchange aberrations are interlinked. These are the conventional type of aberrations which are included in every cytogenetic analysis. In the present study, MTX also produced significant rings (Fig.2. B; Fig. 3) and centric fusions (Fig. 2.D).Ring chromosomes as unusual circular chromosomes generally result from breaks at the ends of both chromosome arms with subsequent fusion of the broken ends to produce a continuous ring. In addition, significant centric fusion (Robertsonian translocation) (Fig.2.C) observed in the MTX treated groups, probably

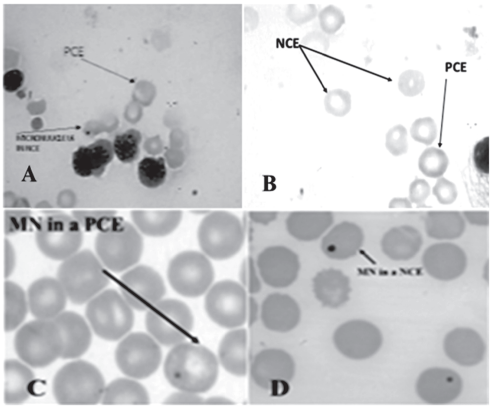

Figure 1.Photomicrograph showing micronucleus in erythrocytes. A- micronucleus in a NCE in the bone marrow smear preparation. B-PCE and NCE in the bone marrow smear preparation; C- micronucleus in a PCE in blood smear preparation; D- micronucleus in a NCE in blood smear preparation

originated from the fusion of two acrocentric chromosomes, due to action the drug.

The association of the two acrocentic chromosomes giving rise to a meta or submetacentric one by the fusion of centromere region is referred to as centric fusion or Robertsonian translocation. This phenomenon seems to be accenuated by exposure to MTX. The pre-treatment of rutin for five days, orally has shown some protection from the clastogenic action of MTX. When calculated, the % reduction of chromosomal aberrations in the combination group ranged from 20 -33 %(Table.5). Here , the 100 mg per kg dose has shown better reduction compared to other two doses.

The mitotic index (Fig.4) values of MTX alone were significantly ($p<0.05$) reduced when compared to the control group. This indicates the myelosuppression brought by the MTX in the haematopoietic stem cells. The three doses of

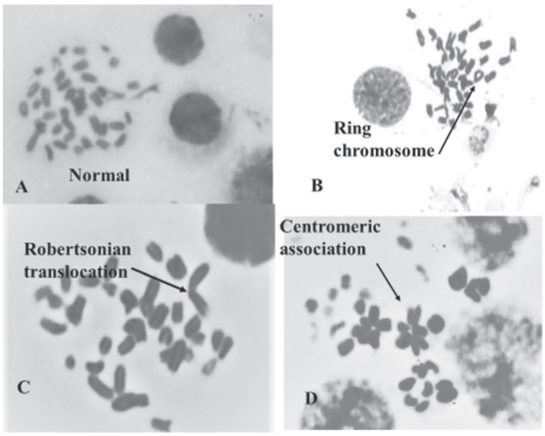

Fig. 2. Photograph (400X) showing diverse types of chromosomal aberrations induced by Methotrexate in the bone marrow cells of Swiss albino mouse. A. Normal Mataphase ; B. Ring chromosome ; C. Robertsonian translocation and D. Centromeric Association.

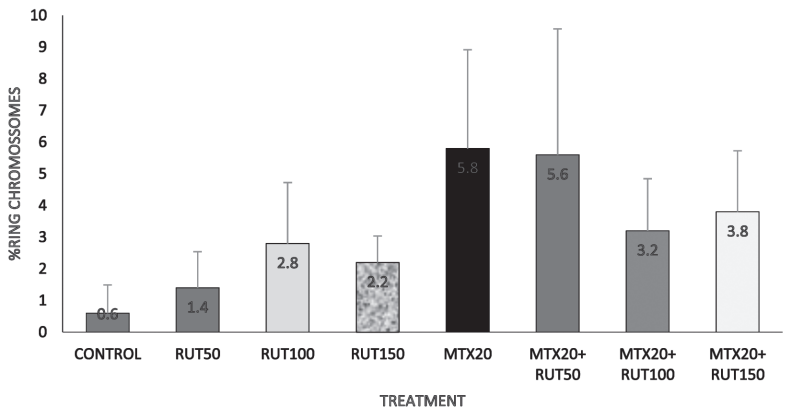

Fig. 3. Bar diagram depicting % ring chromosomes in rutin alone, Methotrexate alone and in combined groups of these two . Ring chromosome occurrence was more in the present in vivo study.

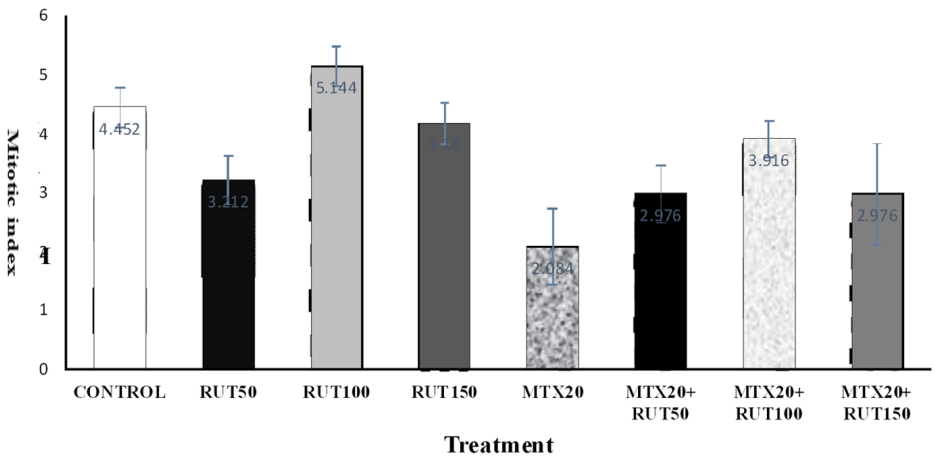

Fig. 4. The Bar diagram showing Mitotic Index in bone marrow of Methotrexate and rutin treated Swiss albino mice. MTX= Methotrexate (20mg/kg/ bw). RUT50-rutin 50mg/kg bw; RUT100-Rutin 100mg/kg bw; RUT150-Rutin 150mg/kg bw

rutin tested showed some effect on mitotic index.The rutin 100 mg per kg dose has shown increased value of mitotic index than the control group, whereas the other two doses , i.e., 50 mg per kg and 150 mg per kg showed some type of cytotoxicity as evidenced in the reduced mitotic index values. In combination group, all the three doses of rutin tested showed improved mitotic index values when compared to MTX alone group. Rutin 100 mg in combination with MTX showed a higher MI, suggesting mitogenic property.

Discussion

Despite of the development of diagnosis and therapy in medicine, many cancers are incurable. Only long-term treatment with harmful agents is available for these patients, such as MTX. MTX is a folate antagonist drug, and it is a structural analogue of folic acid. Therefore, it competes with folic acid (FA), the normal substrate for binding site on dihydrofolate reductase (DHFR), the key enzyme involved in the synthesis of DNA precursors. This will affect the nucleotide pool leading to perturbation in the DNA synthesis and cell proliferation (21). This may be the reason for the genotoxic damages such as chromosomal aberrations and micronucleus induction. The tissues with high cellular turnover are thus the most sensitive to the cytotoxic impact of MTX, which is responsible for its effectiveness as a chemotherapeutic agent, but also for many of its side effects such as mucositis, hair loss and cytopenias (45). The m*utagenic effects of MTX* have been attributed to a substantial proportion of cancer *chemotherapeutic agents (46).* In most cases, their cellular response is pleiotropic, making it challenging to develop these agents efficiently for potential therapeutic benefit (47). There is also absolute need to investigate for antimutagenic and anticarcinogenic potential of substances which could counteract the harmful chemotherapeutic agents. There are various plant-derived compounds improve the efficiency of cytotoxic agents, decrease their resistance, lower and alleviate toxic side effects. The interactions between dietary agents and chemotherapy drugs were studied using either in vitro cell systems or in vivo animal systems (48,49). Thus the concept of chemoprevention with natural or synthetic compounds to block, reverse or prevent the development of cancer has great appeal (50-52).

Table1. Description of *in vivo* study design opted in the present study.

Test group	Chemical	Dose
Group I (CONTROL):	double distilled water	0
Group II (RUT50)	rutin	rutin 50 mg/kg bw for five consecutive days.
Group III (RUT100)	rutin	rutin 100 mg/kg bw for five consecutive days.
Group IV (RUT150	rutin	rutin 150 mg/kg bw for five consecutive days
Group V (MTX20	Methotrexate	20 mg/kg bw dose of methotrexate (single i.p.)
Group VI (MTX20+RUT50	Methotrexate + rutin	rutin 50 mg/kg bw for five successive days+ MTX 20 mg
Group VII (MTX20+RUT100	Methotrexate + rutin	rutin 100 mg/kg bw for five successive days. +MTX 20 mg
Group VIII (MTX20+RUT150	Methotrexate + rutin	rutin 150 mg/kg bw for five successive days + MTX 20 mg

Table.2. Frequency of micronucleus and total MN in bone marrow cells of animals treated with different doses of rutin and MTX and their respective controls. a-compared with the control group ($p < 0.05$); b- compared with the MTX20 group ($p < 0.05$) RUT50-rutin 50mg/kgbw; RUT100-Rutin 100mg/kg bw; RUT150-Rutin 150mg/kg bw; MTX20 - Methotrexate 20 mg/kg bw

Treatment mg/kg	MNPCE± SD (%)	% Reduction	Total MN± SD (%)	% Reduction	P/N±SD
CONTROL	0.15 ±0.07		0.14±0.05 [b]		0.94±0.03 [b]
RUT50	0.14 ±0.08		0.14±0.02 [b]		0.97±0.44 [b]
RUT100	0.28 ±0.05		0.24±0.01 [b]		0.92±0.05 [b]
RUT150	0.40±0.11		0.30±0.08 [b]		0.88±0.06 [b]
MTX20	1.19 ±0.16[a]		0.78±0.10 [a, b]		0.51±0.03 [a]
MTX20+RUT50	0.62 ±0.16 [a, b]	54.8	0.32±0.07 [a, b]	71.81	0.54±0.05 [a]
MTX20+RUT100	0.41±0.09 [b]	75.00	0.47±0.07 [a, b]	48.44	0.74±0.05
MTX20+RUT150	1.01 ±0.34 [a]	17.31	0.69±0.19 [a]	14.06	0.60±0.04 [a]

Table 3. Peripheral blood MN test in animals treated with different doses of rutin and MTX. RUT50-rutin 50mg/kg bw; RUT100-Rutin 100mg/kg b. w; RUT150-Rutin 150mg/kg bw; MTX20 - Methotrexate 20 mg/kg bw. a-compared with the control group (p <0.05); b- compared with the MTX20 group (p <0.05)

Treatment/dose (mg/kg b w)	Mean%NCE±SD	Mean% PCE±SD	Mean% MN in NCE ±SD	% Reduction
CONTROL	97.92±0.28 [b]	2.08±0.28 [b]	0.05±0.03 [b]	
RUT50	97.48±0.32[b]	2.51±0.32[b]	0.06±0.04 [b]	
RUT100	97.59±0.24 [b]	2.41±0.27 [b]	0.10±0.03 [b]	
RUT150	97.90±0.19 [b]	2.09±0.19 [b]	0.09±0.04 [b]	
MTX20	98.93±0.12 [a]	1.06±0.12 [a]	0.25±0.09 [a]	
RUT50+MTX20	98.57±0.07 [a]	1.43±0.07 [a]	0.17±0.02 [a]	40.00
RUT100+MTX20	97.94±0.20 [b]	2.06±0.20 [b]	0.14±0.05	55.00
RUT150+MTX20	97.90±0.15 [b]	2.09±0.15 [b]	0.15±0.07	50.00

In the present study, we investigated anticlastogenic effect against genotoxicity of MTX, by the flavonoid rutin. Our result showed MTX 20mg/kg bw of induced significant total aberrant cells and MN in mouse bone marrow and peripheral blood erythrocytes at 48 h harvesting indicating it's genotoxic effects maintained for longer duration. Hall et al., (53) conducted in vivo clastogenicity and carcinogenicity assays in Sprague-Dawley with MTX. They reported that MTX did not induce conventional chromosome aberrations such as breaks, deletions, exchanges etc., and MTX significantly reduced the mitotic index values at higher doses which agreed with our observations. Hassanane et al., (54) also reported the anti genotoxicity of curcumin against methotrexate (10 mg/kg bw) in albino rats and observed significant chromosomal aberrations in MTX group and were similar to our present result. The methotrexate is reported to cause genotoxicity *in vivo* as well as *in vitro* systems (55). Keshava et al., (55) showed the chromosome damaging effects of MTX in V79 cells . They observed the aberrations such as gaps, breaks, fragments etc and the reduction in the mitotic index values in the MTX treated cells. The chromosome damage caused by the Methotrexate(Amethopterin) was found in cell cultures of patients who had been treated (56). Cytogenetic effects of MTX have also been reported in patients undergoing treatment for rheumatoid arthritis (57).

The MTX-induced micronuclei formation might be explained by the intracellular accumulation of the drug resulting in a continuous inhibition of deoxyribonucleotide triphosphate (dNTPs) synthesis, subsequently causing DNA lesions due to the inhibition of DNA repair. However, because insufficient dNTPs remain, DNA lesions induced by MTX genotoxicity present themselves as micronuclei (58-60).

Considering the toxicity of MTX in the therapy, the search is on for the substances which will help the patients to improve their health. Folinic acid(59)(Shahin, 2001), caffeic acid phenethyl

Table 4. The Effects of rutin on the frequency of different types of chromosomal aberrations induced by methotrexate in bone marrow cells of Swiss albino mice and controls at 48 hrs. RUT50-rutin 50mg/kg bw; RUT100-Rutin 100mg/kg b. w; RUT150-Rutin 150mg/kg bw; MTX20 - Methotrexate 20 mg/kg bw.GS - gaps; BS-breaks; EXS- exchanges; RS- rings; FS-fragments; MA-multiple aberrations; CF- centric fusion; CS- centromeric separation ;CS-centromeric associations ; St & Pul-stickiness and pulverization. a-compared with the control group ($p < 0.05$); b- compared with the MTX20 group ($p < 0.05$).
* From 100 metaphases/animal; 5 animals/group

Treatment (mg/kg bw)	Chromosomal aberration types Mean±SD										
	Gs	Bs	Ex	Rs	F	MA	CF	CS	CA	S&P	Total % * ±SD
CONTROL	0.60±0.54 [b]	0.40±0.89	0.40±0.54[b]	0.20±0.44[b]	0.20±0.89	0.20±0.890	0.40±0.44[b]	0.80±0.54	0.60±0.54	0.40±0.54[b]	4.60±2.30 [b]
RUT50	1.60±0.89[b]	1.40±1.14	2.20±1.30[b]	1.40±1.14[b]	0.20±0.440	0.60±0.89	1.20±1.30	0.80±0.83	1.60±1.14	0.00±0.00[b]	11.00±2.82 [b]
RUT100	0.60±0.89[b]	1.20±1.64	1.80±1.30[b]	2.80±1.92	1.00±1.73	0.40±0.54	1.80±0.83	1.40±1.34	0.80±1.30	0.40±0.54[b]	12.20±4.65 [b]
RUT150	1.2±0.83[b]	2.00±2.00	2.20±1.92[b]	2.20±0.83	0.60±1.30	0.20±0.44	2.20±1.92	2.40±2.60	2.20±2.28	0.40±0.54[b]	15.60±4.56 [b]
MTX20	9.0±3.67 [a]	2.00±2.00	7.00±3.08[a]	5.80±3.11[a]	0.20±0.44	0.20±0.44	5.40±4.03[a]	4.00±3.31	3.80±2.94	4.40±2.96[a]	41.8±3.70 [a]
MTX20+ RUT50	2.60±1.81 [b]	0.40±0.54	3.60±1.67	5.60±3.97[a]	1.60±1.34	0.20±0.44	8.00±4.47	0.00±0.00[b]	5.20±3.42[a]	6.20±2.58[a]	33.40±8.87 [a]
MTX20+ RUT100	3.60±1.94 [b],	1.00±1.73	4.40±1.94[a]	4.40±1.94	2.20±1.64	0.20±0.44	2.80±0.83	0.20±0.44[b]	5.00±4.30	5.40±1.51[a]	29.20±9.47[a]
MTX20+ RUT150	5.40±2.60[a]	5.80±1.78[a,b]	4.00±1.58	3.00±1.22	1.40±1.14	0.80±0.83	2.00±1.22	3.00±1.58	1.80±1.30	4.40±2.96[a]	34.20±6.41[a]

Table 5. The Effect of different doses of rutin on percentage reduction of chromosomal aberrations in Swiss albino mice. For each treatment 500 metaphase plates were analysed to obtain the mean % chromosomal aberrations and respective % reduction. RUT50-rutin 50mg/kg bw; RUT100-Rutin 100mg/kg bw; RUT150-Rutin 150mg/kg bw; MTX20 - Methotrexate 20 mg/kg bw. a-compared with the control group ($p < 0.05$);b- compared with the MTX20 group ($p < 0.05$)

Treatment/dose (mg/kg bw.)	% Aberrant cells (Mean ± SD)	% Reduction
CONTROL	4.6±2.30[b]	-
RUT50	11±2.82[b]	-
RUT100	12.2±4.49[b]	-
RUT150	15.6±4.56[b]	-
MTX20	41.8±3.70[a]	-
MTX20+ RUT50	33.4±8.87[a]	22.58
MTX20+ RUT100	29.2±5.89 [a,b]	33.87
MTX20+ RUT150	34.2±9.52 [a]	20.43

ester (61), vitamin A (62) and leucovorin (63), α-lipoic acid (64), silibinin(65), ambrex, a polyherbal formulation (66), Tinosporacordifolia *(67)*, phloridzin (68), gamma-irradiated basil(69),Vanillin and chlorophyllin (70), curcumin (71), vitamin E(72), berberine (73) are a few of the substances. In a recent experimentation, methotrexate induced genotoxicity was evaluated in combination of polyphenol extracts of Asteracanthalongifolia Nees. and Piperbetle Linn. (74) in Heteropneustes fossilis (fish) and observed an induction of MN highest in the MTX treated fishes after 21 days.

The flavonoid rutin is known for its many biological phenomena. It is also available for us through common diet components. Many research reports have shown beneficial effects of this flavonoid. Pre-treatment of rutin prevented deteriorative effects induced by cisplatin through a protective mechanism that involved reduction of increased oxidative stress as well as caspase-3, TNF-α and NFπB protein expression levels. Arjumand et al., 2011 found pre-treatment with rutin restoring the histopathological changes produced by cisplatin(75). Rutin attenuated gentamicin-induced renal damage by reducing oxidative stress, inflammation, apoptosis, and autophagy in rats (32). In our study, 100mg per kg dose showed on pre treatment ameliorates the MTX induced micronuclei formation in bone marrow and peripheral blood system. Further rutin also reduced the chromosomal aberrations and increased the mitotic index compared to MTX induced.

Conclusion

The MTX is a widely used anticancer drug and it is also being used in the treatment of various other ailments. Present study showed the protective role of rutin against the MTX induced genotoxicity using a mouse in vivo system. In the light of these observations, it is very essential to use MTX drug judiciously for human applications. Our study suggests that When it becomes very essential to use MTX drug, rutin can be supplied as protective supplementary agents may be included in the therapeutic regime to prevent the harmful effects of the drug. Rutin has a weak clastogenic effect, and in combination with MTX, it can enhance MTX's inhibitory effect on the MI and reduce CAs in bone marrow cells. This finding may direct attention to the beneficial effects of using rutin in chemotherapeutic approaches. In addition to its natural presence in the foods, rutin is also available as a supplement in the market.

Acknowledgement

The first author is very much thankful to his research supervisor (Late) Dr. K.K. Vijayalaxmi for her incessant support and blessings given in the true spirit of professional recognition through the work. The authors thank SAP-UGC, Department of Applied Zoology and Mangalore University for facilities provided throughout the work.

References

1. Chaudhary, G., Saini, M.R. and Goyal, P.K. (2007). Chemopreventive potential of Aloe vera against 7,12-dimethylbenz (a) anthracene induced skin papillomagenesis in mice. Integr. Cancer. Ther. 6: 405-412.

2. Lobo, V., Patil, A., Phatak, A. and Chandra, N. (2010). Free radicals, antioxidants and functional foods: Impact on human health. Pharmacognosy Reviews. 4 (8): 118–126.

3. Poornima, K. and Gopalakrishnan, V. K. (2014). Anticancer Activity of Tabernaemontana Coronaria against Carcinogen Induced Clear Cell Renal Cell Carcinoma. Chinese Journal of Biology. 2014: 584074

4. Falcone Ferreyra, M. L., Rius, S. P. and Casati, P.(2012). Flavonoids: biosynthesis, biological functions, and biotechnological applications. Frontiers in Plant Science. 3: 222.

5. Zakaryan, H., Arabyan, E., Oo, A., and Zandi, K. (2017). Flavonoids: promising natural compounds against viral infections. Archives of virology. 162 (9): 2539-2551.

6. Kawai, M., Hirano, T., Higa, S., Arimitsu, J., Maruta, M.,Kuwahara, Y., Ohkawara, T.,Hagihara, K.,Yamadori, T., Shima, Y., Ogata,A., Kawase,I. and Tanaka,T. (2007). Flavonoids and Related Compounds as Anti-Allergic Substances. Allergology International. 56: 113-123.

7. Hostetler, G., Riedl, K., Cardenas, H., Diosa Toro, M., Arango, D., Schwartz, S. and Doseff, A. I. (2012). Flavone deglycosylation increases their anti inflammatory activity and absorption. Molecular nutrition and food research. 56 (4): 558-569.

8. Mansourabadi, A. H., Sadeghi, H. M., Razavi, N. and Rezvani, E. (2015). Anti-inflammatory and analgesic properties of salvigenin, Salvia officinalis flavonoid extracted. Advanced Herbal Medicine. 1 (3): 31-41.

9. Carullo, G., Cappello, A. R., Frattaruolo, L., Badolato, M., Armentano, B. and Aiello, F. (2017). Quercetin and derivatives: useful tools in inflammation and pain management. Future medicinal chemistry. 9 (1): 79-93.

10. Bandele, O. J., and Osheroff, N. (2007). Bioflavonoids as poisons of human topoisomerase IIα and IIâ. Biochemistry 46 (20): 6097-6108.

11. Benavente-Garcia, O. and Castillo, J. (2008). Update on uses and properties of citrus flavonoids: new findings in anticancer, cardiovascular, and anti-inflammatory activity. Journal of agricultural and food chemistry. 56 (15): 6185-6205.

12. Lin, Y., Shi, R., Wang, X. and Shen, H. M. (2008). Luteolin, a flavonoid with potential for cancer prevention and therapy. Current cancer drug targets. 8 (7): 634-646.

13. Chatterjee, J., Nairy, R.K., Langhnoja, J., Tripathi, A., Patil, R.K., Pillai, P.P. and Mustak, M.S. (2018). ER stress and genomic instability induced by gamma radiation in mice primary cultured glial cells. Metab Brain Dis.

14. Nan, L., Kehui, O., Jiaoying, C., Wuying, Y. and Wenjun, W. (2014). Research on Anti-oxidant activity and hypolipemic mechanism of aloes flavonoids in mice. Food Nutr. Res. 2: 601-607.

15. Sripakdee, T., Mahachai, R. and Chanthai, S. (2017). Phenolics and Ascorbic Acid

Related to Antioxidant Activity of MaoFruit Juice and Their Thermal Stability Study. Oriental Journal of Chemistry. 33 (1): 74-86.

16. Chae, S. C., Lee, J.-H. and Park, S. U. (2013). Recent studies on flavonoids and their antioxidant activities. EXCLI Journal. 12: 226–230.

17. Panche, A. N., Diwan, A. D. and Chandra, S. R. (2016). Flavonoids: an overview. Journal of Nutritional Science. 5: e47.

18. Iwashina, T. (2015). Contribution to flower colors of flavonoids including anthocyanins: a review. Natural Product Communications. 10: 529-544.

19. Zielinska, D., Nagels, L. and Piskula, M.K. (2008). Determination of quercetin and its glucosides in onion by electrochemical methods. Anal Chim Acta. 617 (1-2): 22-31.

20. Chan, E.S. and Cronstein, B.N. (2002). Molecular action of methotrexate in inflammatory diseases. Arthritis Res. 4 (4): 266-73.

21. Hagner, N. and Joerger, M. (2010). Cancer chemotherapy: targeting folic acid synthesis. Cancer Management and Research. 2: 293–301.

22. Padmanabhan, S., Tripathi,D.N., Vikram,A., Ramarao,P. and Jena,G.B. (2008).Cytotoxic and genotoxic effects of methotrexate in germ cells of male swiss mice.Mutat. Res. 655: 59–67.

23. Padmanabhan S., Tripathi,D.N., Vikram,A., Ramarao,P. and Jena,G.B. (2009). Methotrexate-induced cytotoxicity and genotoxicity in germ cells of mice: Intervention of folic and folinic acid.Mutation Research. 673: 43–52.

24. Ashoka, CH. and Vijayalaxmi, K.K. (2016).Cytogenetic effects of methotrexate in bone marrow cells of Swiss albino mice. Int J Sci Res Edu. 4: 4828–34.

25. Burcu, B., Kanter, M., Orhon, Z.N., Yarali, O. and Karabacak, R. (2016). Protective Effects of Vitamin E on Methotrexate-Induced Jejunal Mucosal Damage in Rats. Anal Quant Cytopathol Histpathol. 38 (2): 87-94.

26. Abo-Haded, H. M., Elkablawy, M. A., Al-johani Zeyad, Al-ahmadi Osama, & El-Agamy, D. S. 2017. “Hepatoprotective effect of sitagliptin against methotrexate induced liver toxicity.” PLoS ONE 12 (3): e0174295.

27. Zarei, L., Sadrkhanlou, R., Shahrooz, R., Malekinejad, H., Eilkhanizadeh, B. and Ahmadi, A. (2014). Protective effects of vitamin E and Cornus mas fruit extract on methotrexate-induced cytotoxicity in sperms of adult mice. Veterinary Research Forum/ : Veterinary Research Forum/ : An International Quarterly Journal. 5 (1): 21–27.

28. Yüncü, M., Bükücü, N., Bayat, N., Sencar, L. and Tarakçioðlu, M. (2015). The effect of vitamin E and L-carnitine against MTX-induced injury in rat testis. Turk. J. Med. Sci. 45:Turk. J. Med. Sci. 45: 517–525.

29. Arslan, A., Ozcicek, F., Keskin Cimen, F., Altuner, D., Yarali, O., Kurt, N., ... Suleyman, H. (2015). Protective effect of resveratrol against methotrexate-induced oxidative stress in the small intestinal tissues of rats. International Journal of Clinical and Experimental Medicine. 8 (7): 10491–10500.

30. Koc, F., Erýsgýn, Z., Tekelýoglu, Y. and Takýr, S. (2018). The effect of beta glucan on MTX induced testicular damage in rats. Biotechnic and Histochemistry. 1-6.

31. Ganeshpurkar, A., and Saluja ,A.K. (2017). The Pharmacological Potential of Rutin(Review). Saudi Pharmaceutical Journal. 25: 149-164.

32. Kandemir, .M., Ozkaraca, M.,Yildirim, B,A., Hanedan,B., Kirbas,A., Kilic,K., Aktas,E.

and Benzer,F. (2015). Rutin attenuates gentamicin-induced renal damage by reducing oxidative stress, inflammation, apoptosis, and autophagy in rats.Ren Fail. 37(3): 518–525.

33. Ganeshpurkar, A. and Saluja ,A.K. (2017). The Pharmacological Potential of Rutin(Review).Saudi Pharmaceutical Journal. 25: 149-164.

34. Sharma, S.,Ali, A.,Ali,J.,Sahni,J.K. andBaboota,S. (2013). Rutin: therapeutic potential and recent advances in drug delivery.Expert Opinion on Investigationa Drugs. 22(8): 1063-1079.

35. Kumar, S. and Pandey,A.k. (2013). Chemistry and Biological Activities of Flavonoids: An Overview.The Scientific World Journal.2013:1-16.

36. Koval'skii, I. V.,Krassnyuk,I.I., KrassnyukJr,I.I.,Nikulina,O.I.,Belyatskaya,A.V.,. et al (2014). Mechanisms of Rutin Pharmacological Action (Review).Pharmaceutical Chemistry Journal.48(2): 73–76.

37. Li, A.N., Li, S., Zhang, Y., Xu, X.R., Chen, Y. and Li, H.B. (2014). Resources and biological activities of Natural Polyphenols. Nutrients. 6: 6020–6047.

38. Xu, P.X., Wang, S.W., Yu, X.L., Su, Y.J., Wang, T., Zhou, W.W., Zhang, H., Wang, Y.J. and Liu, R.T. (2014). Rutin improves spatial memory in Alzheimer's disease transgenic mice by reducing A beta oligomer level and attenuating oxidative stress and neuroinflammation. Behav. Brain Res. 264: 173–180.

39. Schmid, W. (1973). Chemical mutagen testing on in vivo somatic mammalian cells. Agent Action. 3: 77-85.

40. Schlegel, R.and MacGregor, J.T. (1982) The persistence of micronuclei in peripheral blood erythrocytes: detection of chronic chromosome breakage in mice. Mut .Res, 104: 367-369.

41. Ashoka, CH. and Mustak, M.S. (2018). Genotoxic Study of Chewing Leaf Tobacco in Swiss Albino Mice. Int. J. Life. Sci. Scienti. Res. 4 (1): 1620-1626.

42. Tjio, J.H. and J. Whang,J. (1962). Direct chromsome preparation of bone marrow cells. Stain Technology. 37: 17-20.

43. Waters, M.D., Brady, A.L., Stack, H.F. and Brockman, H.E. (1990). Antimutagenicity profiles for some model compounds. Mutat Res. 238 (1): 57-85.

44. Serpeloni, J.M., Grotto, D., Aissa, A.F., Mercadante, A.Z., Bianchi, Mde.L. and Antunes, L.M. (2011). An evaluation, using the comet assay and the micronucleus test, of the antigenotoxic effects of chlorophyll b in mice. Mutat Res. 725: 50–6.

45. Rajnics, P., Kellner, V.S., Kellner,A., Karadi,E., Kollar,B. andEgyed,M. (2017). The Hematologic Toxicity of Methotrexate in Patients with Autoimmune Disorders. Journal of Neoplasm. 2 (1): 1-6.

46. Szikriszt, B., Póti, Á., Pipek, O., Krzystanek, M., Kanu, N., Molnár, J., Ribli, D., Szeltner,Z., Tusnády, G.E., Csabai,I., Szallasi,Z., Swanton, C. and Szüts, D. (2016). A comprehensive survey of the mutagenic impact of common cancer cytotoxics. Genome Biology. 17: 99.

47. Müller, S. (2017). DNA damage-inducing compounds: Unraveling their pleiotropic effects using high throughput sequencing. Current medicinal chemistry. 24 (15): 1558-1585.

48. Sak, K. (2012). Chemotherapy and dietary phytochemical agents. Chemotherapy Research and Practice. 2012: 1-11.

49. Smith, M. L., Murphy, K., Doucette, C. D., Greenshields, A. L. and Hoskin, D. W. (2016). The dietary flavonoid fisetin causes

cell cycle arrest, caspase dependent apoptosis, and enhanced cytotoxicity of chemotherapeutic drugs in triple negative breast cancer cells. Journal of cellular biochemistry. 117 (8): 1913-1925.

50. Shu, L., Cheung, K. L., Khor, T. O., Chen, C. and Kong, A. N. (2010). Phytochemicals: cancer chemoprevention and suppression of tumor onset and metastasis. Cancer and Metastasis Reviews. 29 (3): 483-502.

51. Meiyanto, E., Hermawan, A. and Anindyajati, A. (2012). Natural products for cancer-targeted therapy: citrus flavonoids as potent chemopreventive agents. Asian Pacific Journal of Cancer Prevention. 13 (2): 427-436.

52. Batra, P. and Sharma, A. K. (2013). Anti-cancer potential of flavonoids: recent trends and future perspectives. 3 Biotech. 3 (6): 439-459.

53. Hall C., Tham,P.,Manandhar,M .,Cheng, M.,Noble,J.F. and Tatropoulos,M. (1988). Methotrexate:Assessment of in vivo clastogenicity and carcinogenicity. Toxicologic Pathology. 16(1): 10-21.

54. Hassanane, M.M., Ahmed,E.S., Shoman,Th.M. and Ezz-Eldin,A. (2010). Evaluation of the Genotoxicity and Antigenotoxicity of Curcumin by Chromosomal Aberrations and Biochemical Studies in the Albino Rats Exposed to Methotrexate. Global Veterinarie.4(20)185-189.

55. Keshava C., Keshava,N ., Whong,W.Z., Nath,J .and Ong,T.M. (1998). Inhibition of methotrexateinduced chromosomal damage by folinic acid in V79 cells.Mutation Res. 397: 221-8.

56. Lloyd, M.E., Carr, M., McElhatton, P., Hall, G.M. and Hughes, R.A.(1999). The effect of methotrexate on pregnancy, fertility and lactation. QJM. 92: 551-63.

57. Jarmalaite S., Dedonyte,V., Mierauskiene, J., Simkute,L., Ranceva,J., Butrimiene,I. (2008). Cytogenetic effects of treatment with methotrexate and infliximab in rheumatoid arthritis patients. BIOLOGIJA. 54: 7–11.

58. Goulian, M., Bleile,B. and Tseng.,B.Y. (1980). Methotrexate-Induced Misin corporation of Uracil into DNA. Proceedings of the National Academy of Sciences of the United States of America. 77 (4): 1956–1960.

59. Shahin, A., Ismail, M., Saleh, A.M.,Moustafa,H.A., Aboul-Ella,A.A. andGabr,H.M. (2001). Protective effect of folinic acid on low-dose methotrexate genotoxicity. Zeitschrift für Rheumatologie. 60 (2): 63–68.

60. Deng, H., Zhang,M., He,J., Wu,W., Jin, L., Zheng, W., Lou,J. and Wang, B. (2005). Investigating genetic damage in workers occupationally exposed to methotrexate using three genetic and-points. Mutagenesis. 20 : 351–357.

61. Uzar, E., Sahin, O., Koyuncuoglu, H. R., Uz, E., Bas, O., Kilbas, S., Yilmaz,H.R., Yurekli,V.A., Kucuker,H. and Songur, A. (2006). The activity of adenosine deaminase and the level of nitric oxide in spinal cord of methotrexate administered rats: protective effect of caffeic acid phenethyl ester. Toxicology. 218 (2-3): 125-133.

62. Sail, A. I., Al-Mahdawi, F. A., Al-Lami, M. Q. and Al-Jalabi, S. M. (2013). Protective Effect of Vitamin A against Oxidative Stress Caused by Methotrexate. Iraqi Journal of Science. 54 (3): 585-589.

63. Madhyastha, S., Prabhu, L. V., Saralaya, V. and Rai, R. (2008). A comparison of vitamin A and leucovorin for the prevention of methotrexate-induced micronuclei production in rat bone marrow. Clinics. 63 (6): 821-826.

64. Dadhania, V. P., Tripathi, D. N., Vikram, A., Ramarao, P. and Jena, G. B. (2010).

Intervention of á-lipoic acid ameliorates methotrexate-induced oxidative stress and genotoxicity: a study in rat intestine. Chemico-biological interactions.183 (1): 85-97.

65. Oufi, H. G. and Al-Shawi, N. N. (2014). The effects of different doses of silibinin in combination with methotrexate on testicular tissue of mice. European journal of pharmacology. 730 : 36-40.

66. Anila, R., Sathiya , S., Babu, C. S. and Rajkumar, J. (2015). In vitro and in vivo protective effects of ambrex, a polyherbal formulation, against methotrexate induced damages in hepatic cells. International Journal of Pharmacy and Pharmaceutical Sciences. 7 (8): 164-170.

67. Deepak, J. N., Rao, S., Byregowda, S. M., Vetrivel, M., Purushotham, K. M., Satyanarayana, M. L., Narayanaswamy, H. D. and Renukaprasad, C. (2015). Protective effects of Tinosporacordifolia against methotrexate induced oxidative damage in rat liver. Journal of Cell and Tissue Research. 15 (1): 4765

68. Khalifa, M. M., Bakr, A. G. and Osman, A. T. (2017). Protective effects of phloridzin against methotrexate-induced liver toxicity in rats. Biomedicine and Pharmacotherapy. 95: 529-535.

69. El Shahat, A. N., El-Shennawy, H. M. and El-Megid, M. H. A. (2017). Studying the protective effect of gamma-irradiated basil (Ocimum basilicum L.) against methotrexate- induced liver and renal toxicity in rats. Indian Journal of Animal Research. 51 (1): 135-140.

70. Keshava, C., Keshava, N., Whong, W.Z., Nath, J. and Ong,T.M. (1997). Inhibition of methotrexate-induced chromosomal damage by vanillin and chlorophyllin in V79 cells. Teratog. Carcinog. Mutagen. 17 (6): 313–326.

71. Salem, N. I. S., Noshy, M. M. and Said, A. A. (2017). Modulatory effect of curcumin against genotoxicity and oxidative stress induced by cisplatin and methotrexate in male mice. Food and Chemical Toxicology. 105: 370-376.

72. Dhanesha, M., Singh, K., Bhori, M. and Marar, T. (2015). Impact of antioxidant supplementation on toxicity of methotrexate: an in vitro study on erythrocytes using vitamin E. Asian J Pharm Clin Res. 8 (3): 339-343.

73. Mehrzadi, S., Fatemi,I., Esmaeilizadeh,M., Ghaznavi,H., Kalantar,H. and Goudarzi,M. (2018). Hepatoprotective effect of berberine against methotrexate induced liver. Biomedicine and Pharmacotherapy. 97 : 233–239.

74. Ghosh, S., Chatterjee, A., Mukhopadhyay, A. and Chakrabarti, P. (2017). Phytoremediation of methotrexate induced genotoxicity using polyphenol extracts of Asteracantha longifolia Nees. and Piper betle Linn. Journal of Pharmacognosy and Phytochemistry. 6 (3): 105-110.

75. Arjumand, W., Seth, A. and Sultana, S. (2011). Rutin attenuates cisplatin induced renal inflammation and apoptosis by reducing NFêB, TNF-α and caspase-3 expression in wistar rats. Food Chem Toxicol. 49 (9): 2013-21.

Current Trends in Biotechnology and Pharmacy
Vol. 13 (2) 178-189, April 2019, ISSN 0973-8916 (Print), 2230-7303 (Online)

Genetic Divergence and Phylogenetic Analysis of Fish Fauna from Lake Kolleru based on *COI* Sequences

Padmavathi P. and Gatreddi Srinu*
Department of Zoology & Aquaculture, Acharya Nagarjuna University
Nagarjuna Nagar - 522 510, Andhra Pradesh, India
*Corresponding author : gatreddisrinu@gmail.com

Abstract:

Lake Kolleru is one of the largest freshwater lakes in India and the only RAMSAR site of Andhra Pradesh. Due to several anthropogenic activities, it is currently experiencing an alarming decline in fish biodiversity. This emphasizes an immediate need for initiating research based on molecular tools in addition to traditional methods. The present study was aimed to evaluate the genetic diversity of Kolleru fishes and to compare them with their counter parts across India based on *COI* sequence data. The analysis was carried out by using 16 *COI* sequences of Kolleru fishes and 121 sequences of fishes belonging to other parts of India. The *COI* barcodes clearly distinguished all the fish species with higher inter-specific distance values than intra-specific K2P values. The average genetic distance within species, genus, family, and order was 0.16%, 2.45%, 5.30% and 13.71% respectively. Composition of four nucleotides and GC% at three codon positions were calculated and compared them with other retrieved *COI* sequences. NJ tree revealed distinct clades showing Kolleru sequences are clustered with other *COI* sequences of same species with significant bootstrap values. Hence, the *COI* sequence information is proved to be effective in genetic variation and phylogenetic assessment with respect to conservation of Kolleru fishes.

Keywords: Cytochrome Oxidase I, K2P distance, GenBank, Neighbour Joining tree

Introduction

India is well known for its rich natural heritage and harbours a unique biodiversity. India ranks twelfth among 17 megadiverse countries of the world. Even though the exact number of fish species is not known and unexplored because of several taxonomic impediments (1), it was estimated that India housed 2508 fish species (2), of which 856 belonged to freshwater inhabitants (3). India ranks ninth with a share of 8.9% in the world's fish diversity (4).

Lake Kolleru (81º 05" to 81º 21" E and 16º 32" to 16º 47"N) is one of the largest natural freshwater lakes in India with an extent of 245sq. km harbouring a rich diversity of fish fauna (5, 6). Kolleru wetland is a well known breeding ground for many riverine fishes as evident by the presence of robust number juvenile fishes especially the carps and air-breathing fishes (7,8). Since Kolleru is connected to Bay of Bengal *via* Upputeru drain, some marine and migratory fishes are also found in this lake (9, 10). The natural fishery of the lake was decline due to various man-made activities like over exploitation, heavy pollution due to industrial effluents into the lake, seasonal dry up, agricultural runoff with pesticides, and excessive weed growth (11, 12).

In addition to these, much of the lake bed and belt area is being converted into myriads of fish ponds owing to its shallow nature (mean depth 2m). At present, lake Kolleru is the hub of

aquaculture which makes Andhra Pradesh the second largest freshwater fish producing states in India. Pisciculture also caused ecological imbalance in lake by the introduction of invasive species and polluting the lake with aquaculture remnants (13, 14). It was reported that several fish species in lake Kolleru are on the verge of extinction (8). Future scenarios predicted that within next three decades, one-third of all freshwater fishes may get vanished (15), which is not exceptional for Kolleru as it contains a number of threatened and endemic fish species. The absence of three endemic species, *Rohtee ogilbii*, *Hypselobarbus dobsoni* and *Thynnichthys sandkhol* of the lake in recent times emphasizes the need for conservation of lake fauna (8). Fish resource estimates reported the presence of 4 endangered, 11 vulnerable and 1 rare species, which need to be conserved to protect them from extinction in near future (8). Most of the fishes of lake Kolleru are commercially important, of which 16 species are considered threatened and suggested to protect them to maintain the biodiversity of fishes (16, 17).

Diversity assessment based on whole DNA sequence, whether directly or indirectly by the analysis of proteins was used for species discrimination almost 50 years ago (18). Later on, single gene based analysis of ribosomal DNA was used extensively to investigate evolutionary relationships (19). Recently, Mitochondrial DNA (mtDNA) dependent molecular systematic studies were dominated. Mitochondrial DNA, with the characteristic feature of fast evolution rate than the nuclear DNA, has recently been used to elucidate genetic relationships for many species (20, 21, 22). Mitochondrial Cytochrome Oxidase I (*COI*) partial sequence based DNA Barcoding technique also gaining importance as a useful tool for investigating the genetic structure of species (23) apart from species identification and food authentication (24, 25, 26). DNA Barcoding data enabled the researchers to read the genetic information which can be used efficiently in proper management of species of ecosystem importance. A perusal of literature showed that no work has been done on the genetic diversity and molecular based phylogenetic studies of lake Kolleru fishes. Hence, the present study was undertaken to examine the genetic divergence of fish fauna in lake Kolleru. Focus was made to examine the genetic distances between inter-specific and intra-specific distance values of 16 *COI* sequences of Kolleru fishes retrieved from NCBI-GenBank. The data was analyzed and the phylogenetic position of Kolleru fishes was discussed.

Materials and Methods

Sequence analysis

GenBank accession numbers of 16 *COI* partial sequences belonged to 15 fish species of lake Kolleru and 121 sequences belonged to the same species from various parts of India were accessed from NCBI - GenBank available as on 15th October, 2017 with their taxonomic position have been presented in Table 1. By using the *COI* sequence data, genetic distance between lake Kolleru fishes and those of other parts of India was estimated. Care was taken to avoid bias in divergence assessment by giving preference to nearby geographical locations and then to distant geographical locations. Disequilibrium in taxa representation may result in skewness in divergence distributions. Taxa comparisons were standardized for a maximum of ten individuals per each species following the above criteria. Taxa with multiple denominations and taxonomic ranks, and suspected sequences that are derived from misidentification were omitted. A total of 137 sequences belonging to 15 species, 12 genera, 11 families and 5 orders were included in the analysis of the data.

The *COI* partial sequences obtained for each species were assembled and end-trimmed to a homologous region to avoid errors during sequencing and those sequences are subjected to alignment using ClustalW analysis tool (27). The *COI* partial sequences obtained for each species were manually verified for the presence of internal stop codons using the translate tool in ExPASy ProtParam tool by giving inputs related to vertebrate mitochondrial genome. Sequences

Table 1: GenBank Accession numbers of fish species from Kolleru and other parts of India

S.No	Family	Genus	Species	Accession Numbers*
Order: Anguilliformes				
1	Anguillidae	*Anguilla*	*bengalensis bengalensis*	**KR021973,** JX887591, JX887590, JX260829 JX260828, JX260827, JX260826, JX260825 KP897130, KM875502
2		*Anguilla*	*bicolor bicolor*	**KP979655,** KM875505, KM875504 KM875503, KY067460, KF182304, AP007236
Order: Cypriniformes				
3	Cyprinidae	*Esomus*	*danrica*	**KP939356,** KX245065, FJ459490, JN673955 FJ459486, KU738848, KJ936709, KX266826 KY290080, KU171302
4		*Laubuca*	*laubuca*	**KP939355,** KT353103
Order: Characiformes				
5	Serrasalmidae	*Piaractus*	*mesopotam-icus*	**KM519156,** JQ667515, KM519156,KM897518 GU701417, KM897143,KM897453, HQ420834 KP856756, KM519156
Order: Siluriformes				
6	Bagridae	*Mystus*	*bleekeri*	**KP939357,** JX983376, JX260918, JX260917 JX260916, KT896741, JN628904, KF824794 KF824797, KX266834
7	Clariidae	*Clarias*	*batrachus*	**KM519157,** JQ699207, KJ720696, JQ699208 KF742432, KJ959639, KF511567, FJ459459 JN628880, KF214293
8	Heteropneus-tidae	*Heteropneustes*	*fossilis*	**KR021972,** JX983313, JX983311, JX260882 JX260879, KX245084, JN628881, JN596578 GQ461897, GQ466395
9	Sisoridae	*Neotropius*	*atherinoides*	**KP939358,** JX901501, JN628927, KF824819 JN628910, KY290098, KY290041, KF824817 JN628890, JN628911
Order: Perciformes				
10	Eleotridae	*Eleotris*	*fusca*	**KP979654,** JX193751, KU692479, KT960773 KT960771, KT960769, KT960767, KT960768 KT960770, MF611583
11	Gobiidae	*Pseudapocryptes*	*elongatus*	**KT124739, KT124740,** KT378133, LC010470 MF594617, LC010471, LC010472, LC010480 LC010481, LC010482
12	Channidae	*Channa*	*punctata*	**KP979652,** JX983251, JX260843, KY290125 JN245990, EU342201, KX389275, KJ936637 KJ854469, KU761951
13		*Channa*	*striata*	**KP979651,** KP842452, KP842443, KJ538701 KJ538675, KY290120, KX389279, EU342204 HM117203, KP842455
14		*Channa*	*orientalis*	**KP979653,** JX983248, JX983245, KY290045 FJ459480, KJ936643, KJ937374 KJ847127 KF742420, KF742438
15	Cichlidae	*Etroplus*	*suratensis*	**KP939359,** FJ237544, JX260868, KP316238 KC858286, KF442186, KF442180, KF442165 KF372997, KF442191

*Accession number in bold indicates retrieved sequences of Kolleru fishes.

The *COI* partial sequences obtained for each species were assembled and end-trimmed to a homologous region to avoid errors during sequencing and those sequences are subjected to alignment using ClustalW analysis tool (27). The *COI* partial sequences obtained for each

with sufficient length (559 bp) were considered to bring uniformity in the analysis of all species. In order to bring homogeneity in some sequences, missing sequence parts were adopted from most conserved regions of the sequences available in NCBI GenBank for the same species.

Nucleotide composition (A, T, G & C) and GC content at different positions *i.e.* GC1, GC2 and GC3 (GC content in 3 codon positions) were calculated for homologous end-trimmed sequences using the software program MEGA V.7.0 (Arizona) (28). Inter- and intra-species evolutionary divergences in various hierarchical levels were analysed using Kimura's 2 Parameter (K2P) method (29). The variation in divergence was estimated following the bootstrap method with 1000 bootstrap replicate values. The pair-wise deletion option was selected to treat the gaps or missing data between each compared sequences. Mutation rates, polymorphic sites and genetic diversity between the populations (dataset I and II) and the total population was estimated using DnaSP v.5.0 software (30) by treating Kolleru fish *COI* sequences as population dataset I and other fish sequences as population dataset II. The evolutionary history of 15 Kolleru fishes was inferred by using Maximum Likelihood (ML) method based on Kimura 2 Parameter (K2P) model (29). Finally, the Neighbour Joining (NJ) tree was created to reveal K2P distance values among species of Kolleru and other parts of the country using K2P method and the values are represented as units of base substitutions per site (31).

Results

A total of 137 sequences were analyzed, of which 16 belonged to lake Kolleru and the remaining 121 belonged to other parts of India. Number of sequences used in this study ranged from two (*Laubuca laubuca*) to ten (remaining 14 species) based on the availability and uniform distribution in India. These are the only available sequences for Kolleru fish fauna from NCBI GenBank. The length of the available sequences ranged from 590 to 692 bp with an average of 629 bp. Moreover, no Indels (insertions and deletions) were found in the sequences and no stop codons were existed in the ExPASy ProtParam tool which indicates that all the available sequences code for functional mitochondrial *COI* gene without NUMTS (Nuclear Mitochondrial DNA). It was observed that the average genetic divergence within species, genera, family and order was 0.16%, 2.45%, 5.30% and 13.71% respectively (Table 2). The average congeneric distance is approximately 15-fold the average conspecific distance. Increasing genetic divergence was observed with increasing taxonomic levels, indicating a noticeable change in genetic divergence at the species boundaries. The inter species divergence values are represented in Table 3.

Nucleotide frequencies of *COI* sequences between Kolleru fishes and other retrieved sequences from different parts of India are presented in Table 4. The average nucleotide frequencies for all 15 species are as follows: A= 25.0%, T= 29.6%, G= 17.4%, C= 27.9%. The minimum, mean and maximum GC content for three codon positions of all 15 species are given in Table 4 and Figure 1.

Table 2: Summary of *COI* genetic divergence (K2 P percentage) of Kolleru fishes within various taxonomic levels

Comparison within taxonomic level	Mean±S.E.(%)	Maximum(%)
Species	0.16±0.40	2.30
Genera	2.45±1.32	20.40
Family	5.30±1.90	31.30
Order	13.71±2.40	31.30

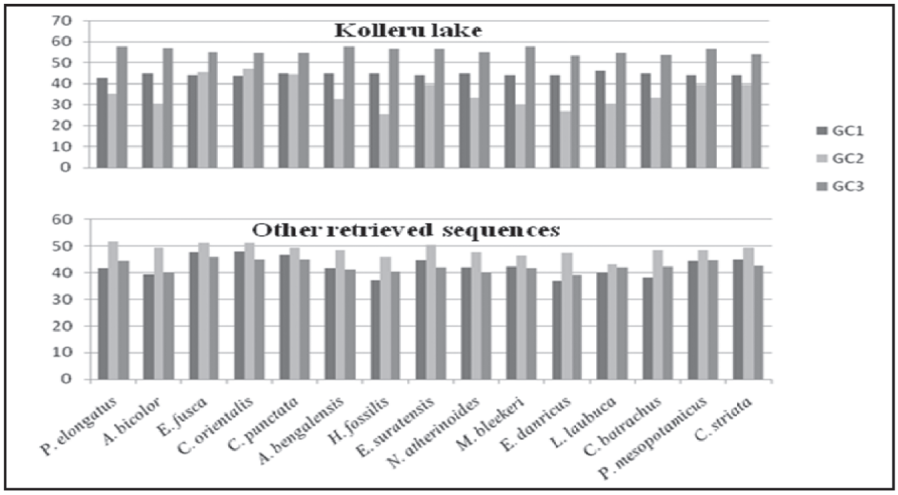

Figure 1: Variation in GC content (%) of *COI* sequences between Kolleru fishes and other retrieved sequences from different territorial parts. (GC1, GC2 and GC3: GC content in codon position 1, 2 and 3)

Table 3: Interspecies genetic divergence values of the 616 bp *COI* sequences, based on Kimura 2 parameter model. Pairwise divergences between species are below the diagonal and their standard error values are given above the diagonal.

S. No.	Species	1	2	3	4	5	6	7	8	9	10	11	12	13	14	15
1	*P. elongatus*		0.016	0.017	0.017	0.016	0.016	0.017	0.017	0.016	0.016	0.017	0.017	0.016	0.016	0.017
2	*A. bicolor*	**0.227**		0.015	0.017	0.017	0.010	0.016	0.017	0.016	0.016	0.016	0.017	0.017	0.015	0.016
3	*E. fusca*	**0.247**	**0.195**		0.016	0.016	0.015	0.016	0.016	0.016	0.016	0.016	0.017	0.016	0.016	0.016
4	*C. orientalis*	**0.268**	**0.242**	**0.208**		0.015	0.017	0.017	0.017	0.017	0.016	0.016	0.017	0.016	0.016	0.016
5	*C. punctata*	**0.244**	**0.218**	**0.187**	**0.177**		0.016	0.016	0.015	0.016	0.016	0.017	0.017	0.016	0.016	0.014
6	*A. bengalensis*	**0.227**	**0.063**	**0.193**	**0.237**	**0.206**		0.016	0.017	0.016	0.016	0.016	0.017	0.017	0.016	0.016
7	*H. fossilis*	**0.229**	**0.214**	**0.205**	**0.240**	**0.213**	**0.221**		0.016	0.015	0.016	0.016	0.017	0.014	0.015	0.016
8	*E. suratensis*	**0.247**	**0.229**	**0.195**	**0.229**	**0.198**	**0.227**	**0.219**		0.016	0.016	0.017	0.016	0.016	0.016	0.015
9	*N. atherinoides*	**0.242**	**0.211**	**0.195**	**0.224**	**0.208**	**0.209**	**0.170**	**0.214**		0.016	0.015	0.017	0.015	0.015	0.017
10	*M. bleekeri*	**0.227**	**0.203**	**0.196**	**0.219**	**0.211**	**0.213**	**0.172**	**0.203**	**0.131**		0.016	0.017	0.015	0.016	0.016
11	*E. danrica*	**0.252**	**0.196**	**0.208**	**0.226**	**0.214**	**0.214**	**0.190**	**0.219**	**0190**	**0.198**		0.017	0.015	0.015	0.017
12	*L. laubuca*	**0.286**	**0.256**	**0.265**	**0.263**	**0.265**	**0.260**	**0.260**	**0.250**	**0.255**	**0.260**	**0.253**		0.017	0.017	0.017
13	*C. batrachus*	**0.232**	**0.221**	**0.214**	**0.211**	**0.216**	**0.224**	**0.157**	**0.219**	**0.175**	**0.174**	**0.206**	**0.265**		0.016	0.016
14	*P. mesopotamicus*	**0.224**	**0.201**	**0.218**	**0.219**	**0.221**	**0.205**	**0.200**	**0.211**	**0.193**	**0.188**	**0.198**	**0.266**	**0.206**		0.017
15	*C. striata*	**0.235**	**0.229**	**0.208**	**0.196**	**0.153**	**0.226**	**0.216**	**0.200**	**0.214**	**0.203**	**0.218**	**0.271**	**0.219**	**0.227**	

The *COI* sequence data of lake Kolleru fishes contain more GC3 content followed by GC1 and GC2 except for *E. fusca* and *C. orientalis* in which GC2 is greater than GC1 whereas in other fish fauna, GC2 content is dominated followed by GC1 and GC3 in different fishes. The mean values of GC1, GC2 and GC3 codons are 44.3, 35.6 and 55.8 in lake Kolleru fishes and those of other fish fauna are 42.7, 48.9 and 42.5 respectively (Table 4). It is evident that the difference is more prominent in GC2 and GC3 rather than in GC1 content between Kolleru and other fish species. Highest mutation rate among all the species was observed in *A. bicolor bicolor* followed by *E. fusca*, *C. batrachus, C. orientalis* and *A. bengalensis bengalensis.* The same pattern was noticed in nucleotide diversity in total population (Table 5).

Table 4: Comparison of Nucleotide frequencies of COI sequences between Kolleru fishes and other retrieved sequences from different parts of India

	Within Lake Kolleru			**Other parts of India**		
	Min. %	Max. %	Mean±S.E. %	Min. %	Max. %	Mean±S.E. %
G	15.9	18.3	17.3±0.164	15.6	19.8	17.1±0.192
C	25.5	30.8	27.9±0.311	23.5	30.6	27.6±0.325
A	22.7	27.8	25.1±0.325	22.5	28.9	25.3±0.336
T	27.4	32.1	29.7±0.248	27.9	33.2	30.0±0.171
(G+C)	41.4	49.1	45.2±0.237	39.1	50.4	44.7±0.258

Table 5: DNA Divergence values between fish populations of Kolleru and other retrieved sequences

S. No.	**Name of the Species**	**No. of poly-morphic sites**	**No. of mutations**	**Avg. no. of Nucleotide differences between populations**	**Avg. no. of Nucleotide differences (k) in total population**	**Nucleotide diversity in total population**
1	*A. bengalensis bengalensis*	51	55	8.00	11.5	0.021
2	*A. bicolor bicolor*	308	314	64.8	105.4	0.180
3	*E. danrica*	6	6	0.7	1.3	0.002
4	*L. laubuca*	15	15	7.5	10	0.016
5	*P. mesopotamicus*	21	21	4.0	5.4	0.008
6	*M. bleekeri*	17	17	2.5	3.8	0.006
7	*C. batrachus*	110	118	18.3	28.0	0.046
8	*H. fossilis*	20	20	3.4	4.7	0.007
9	*N. atherinoides*	34	34	9.1	12.4	0.020
10	*E. fusca*	122	141	62.5	47.8	0.077
11	*P. elongatus*	25	25	15.4	9.1	0.027
12	*C. punctata*	67	71	11.1	16.2	0.026
13	*C. striata*	28	29	6.1	9.6	0.016
14	*C. orientalis*	84	91	22.3	28.5	0.040
15	*E. suratensis*	11	11	1.2	2.2	0.003

Fig. 2 represents the ML phylogenetic tree based evolutionary relationships among 15 species of lake Kolleru using K2P model. The higher average congeneric distance than the average conspecific distance has resulted in higher resolution in the ML tree among different species. Three species belonging to the family Channidae are clustered strongly (ML= 85%) with sub-clade formed by *Channa punctata* and *Channa striata*. Likewise, *COI* sequences belonging to the same species (*Pseudapocryptes elongatus*) and same genus (*Anguilla*) are clustered with maximum values (ML=100%). Species belonging to different species (*Esomus danricus* and *Laubuca laubuca*) are formed together with less clustering percentage (19%). Families belonging to the Order Perciformes (Eleotridae, Cichlidae & Channidae) and Order Siluriformes (Heteropneustidae, Clariidae, Sisoridae & Bagridae) are clustered under the same clade.

The NJ tree based on 137 partial *COI* sequences of fishes from different parts of the country along with *COI* sequences of Kolleru fishes resulted in the formation of different clusters wherein each cluster formed with one species irrespective of their source locations with significant bootstrap values (Fig. 3).

Discussion

The usage of *COI* sequence data in species diversity and phylogenetic assessment in addition to routine species identification is gaining immense importance in recent times (32, 33, 34). Due to the dearth of classical taxonomists to fulfil different levels of taxonomic studies (23), these molecular studies help to bring uniformity among scientific community to decipher the genetic diversity and phylogenetic assessments. In the present study on Kolleru fishes, the average K2P distance is more than 15-fold among congeneric level than conspecific individuals. This variation is almost double in confamilial species than congeneric individuals and even more (three fold) among the species belonging to different orders. This indicates sufficient genetic divergence beyond species level which can be referred to as barcoding gap (35). The average conspecific and congeneric values observed in the present study are lower than those of previous studies in both freshwater fishes (36) and marine fishes (37). Even with these lower values, the inter-hierarchical divergence can be successfully deciphered in lake Kolleru fishes and helps in defining threshold levels of interspecies demarcation especially in case of lakes with conservational importance. All the *COI*

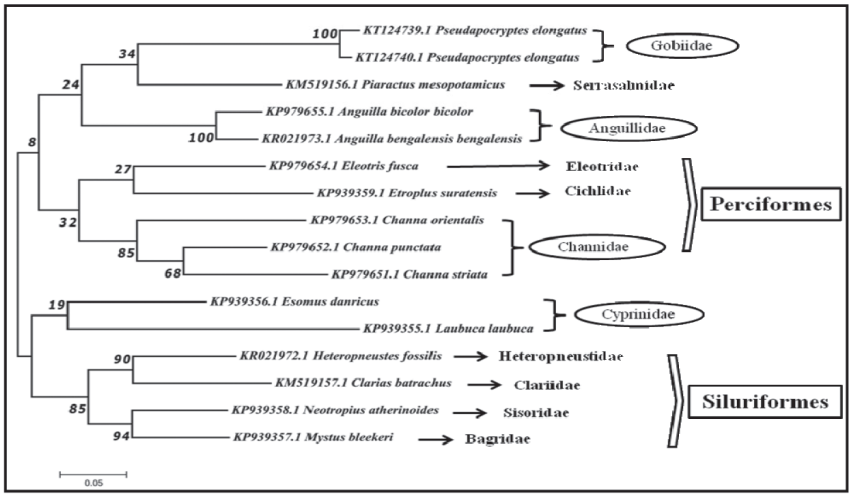

Figure 2: Unrooted K2P distance Maximum likelihood (ML) tree of *COI* partial sequences of lake Kolleru fishes using MEGA V.7.0

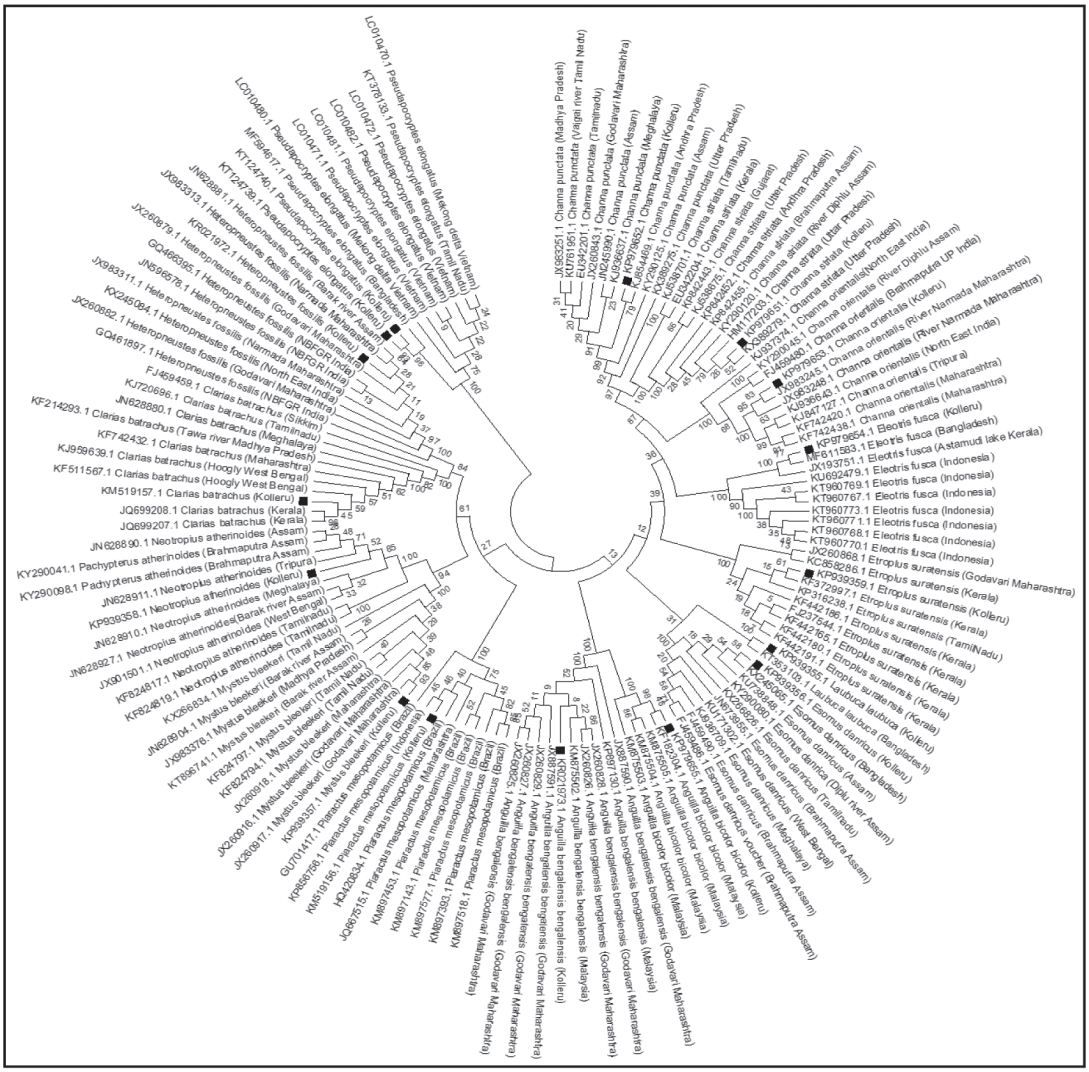

Figure 3: Circular K2P distance Neighbour Joining (NJ) tree constructed from *COI* partial sequences of Kolleru fishes and others using MEGA V.7.0

sequences of Kolleru fishes were simple and without any ambiguities. No indels were observed among any of the sequences indicating the absence of NUMTS (nuclear DNA sequences that are originated from mtDNA sequences and typically less than 600bp in length) (38). These results are in conformity with the earlier observations made by Ward *et al.* (2005) (39); Lakra *et al.* (2011) (37) and Viswambharan *et al.* (2015) (40). Bensasson et al. (2001) reviewed the occurrence of NUMTs in both animals and plants and reported their absence in fishes belonging to the order Actinopterygii (41). Mitochondrial genomes express reflective shifts in nucleotide usage among major taxonomic groups (42) and have consequential impact on phylogenetic analysis (43, 44). The GC content in *COI* sequences of lake Kolleru fishes found to

be 45.2 which is slightly lesser than the GC content of other parts of India (44.7) and it clearly shown that the nucleotide changes have been occurred more in GC3 followed by GC1 and GC2 codons. This revealed the fact that most synonymous mutations occur at GC3 followed by a few synonymous mutations at GC1 and almost negligible changes at GC2 codon (37). The mutational rate of the mitochondrial genome was proved to be higher than in the nuclear genome in the course of evolution (45, 46). The occurrence of relatively more types of mutations in GC3 may be attributed to the varying degrees of asymmetric skew in the frequencies of bases at 3rd codon position (47, 48). Number of mutations and polymorphic sites show drastic variations in different species of the total population which may be due to the changes in population over a period of time.

The *COI* sequence analysis has shown clear phylogenetic signal among all the 15 fishes of lake Kolleru (Fig. 2). The ML tree revealed distinct clusters formed by members of Perciformes, Cypriniformes and Siluriformes separately. The individuals of same species found to cluster under the same node (*Pseudapocryptes elongatus*) supported by higher bootstrap value (100) and same trend has been observed at genus level (*Anguilla* and *Channa*). The *COI* sequences clearly distinguished the taxonomic status of 15 fish species of lake Kolleru. Even when compared with fish sequences of other parts of the country, it formed distinguished clades irrespective of their source locations (Fig. 3). *COI* sequence information of lake Kolleru fishes is proved to be an efficient tool not only for species identification and delineating the species boundaries but also for constructing phylogenetic trees with clear phylogentic signal especially in the case of fresh water inland lakes having conservational importance like lake Kolleru. Among the IUCN listed species, 3 species are vulnerable *viz., Mystus bleekeri, Clarias batrachus* and *Heteropneustes fossilis,* and one species is endangered *viz., Anguilla bengalensis bengalensis* (8). Four out of the 15 species namely, *Channa orientalis, C. punctata, C. striata* and *Esomus danrica* were listed in Conservation Assessment and Management Plan (CAMP) workshop report (16). The report pointed the activities like fishing, loss of habitat, over exploitation and trade are the main culprits behind the gradual decrease in number of the species in lake. It is emphasized that by making use of the readily available molecular data, it is possible to assess the biodiversity and to design the conservational measures for fish fauna of lake Kolleru even by the non-taxonomists.

Acknowledgements

Authors are grateful to the authorities of Acharya Nagarjuna University for providing necessary facilities to carry out this work in the Department of Zoology and Aquaculture under the financial support of UGC-SAP- DRS Phase III. One of the authors (Mr. G. Srinu) is thankful to the UGC, New Delhi, Govt. of India for financial support under BSR (Basic Scientific Research) Fellowship.

References

1. Hoagland, K.E. (1996). The taxonomic impediment and the convention on biodiversity. *Association of Systematics Collections Newsletter*, 24(5), 61-62.
2. Eschmeyer, W.N., Fricke, R. and R. van der Laan (eds). Catalog of fishes: genera, species, references. (http://researcharchive.calacademy.org/research/ichthyology/catalog/fish-catmain.asp). Electronic version accessed on 15 Jan 2017. [This version was edited by Bill Eschmeyer.]
3. Froese, R. and Pauly, D., (2012). Fishbase (database). *World Wide Web Electronic Publications.* Available at: http://www.fishbase.org (accessed June 2012).
4. Levêque, C., Oberdorff, T., Paugy, D., Stiassny, M.L.J. and Tedesco, P.A. (2007). Global diversity of fish (Pisces) in freshwater. *In* Freshwater animal diversity assessment (pp. 545-567), Springer, Dordrecht.

5. Dutt, S. (1982). Ecodevelopment of Kolleru lake. Status position and approach document of INVOR. Visakhapatnam, Andhra Pradesh.

6. Rao, K.N., Krishna, G.M. and Malini, B.H. (2004). Kolleru lake is vanishing- a revelation through digital processing of IRS-1D LISS-III sensor data. *Current Science*, 86(9), 1312-1316.

7. Seshavatharm, V. and Venu, P. (1980). Some observations on the ecology of Kolleru lake. Wetland Ecology & Management, proceeding of the first international wetland conference, (pp. 35-44) New Delhi. India.

8. Barman, R.P. (2004). The Fishes of the Kolleru Lake, Andhra Pradesh, India with Comments on their Conservation. *Records of the Zoological Survey of India*, 103(1-2), 83-89.

9. Venkateswara Rao, K., Ramakrishnaiah, M. and Rama Raju, T. S. (2003). "The fish and fisheries of lake Kolleru" in *Lake Kolleru–Environmental status (Past and present),* BS Publications (pp. 168-184), Hyderabad, India.

10. Rao, G.V., Beebi, S.K. and Rao, P.M. (2006). Water quality studies of Kolleru lake, Upputeru river and Enamaduru drain. *Indian Journal of Environmental Protection*, 26(6), 537-545.

11. Shivaji Rao, T. (2003). Conflict between development and environment of Kolleru lake area. *In:* Y. Anajaneyulu and K. Durga Prasad (Eds.), *Lake Kolleru- Environmental status (past and present),* BS Publications (pp. 168-184) Hyderabad, India.

12. Basha, S.K.C., Gatreddi Srinu and Rao, G.L. (2017). Evolution of concept of sustainable development, its deterrence by emerging climate change and a way forward. *Ecology, Environment and Conservation,* 23(3), 1615-1622.

13. Leprieur, F., Hickey, M.A., Arbuckle, C.J., Closs, G.P., Brosse, S. and Townsend, C.R. (2006). Hydrological disturbance benefits a native fish at the expense of an exotic fish. *Journal of Applied Ecology*, 43(5), 930-939.

14. Woodford, D.J. and McIntosh, A.R. (2010). Evidence of source-sink metapopulations in a vulnerable native galaxiid fish driven by introduced trout. *Ecological Applications*, 20(4), 967-977.

15. Dudgeon, D., Arthington, A.H., Gessner, M.O., Kawabata, Z.I., Knowler, D.J., Lévêque, C., Naiman, R.J., Prieur-Richard, A.H., Soto, D., Stiassny, M.L. and Sullivan, C.A. (2006). Freshwater biodiversity: importance, threats, status and conservation challenges. *Biological reviews*, 81(2), 163-182.

16. Molur, S. and Walker, S. (1998). Report of the Workshop on "Conservation assessment and management plan for freshwater fishes of India", Published by Zoo outreach organization, CBSG, India 156p.

17. Menon, A.G.K. (1999). Checklist of the Freshwater Fishes of India. Records of the Zoological Survey of India, Occational paper No. 175, pp. 366.

18. Manwell, C. and Baker, C.M.A. (1963). A sibling species of sea-cucumber discovered by starch-gel electrophoresis. *Comparative Biochemistry and Physiology*, 10, 39-53.

19. Woese, C.R and Fox, G.E. (1977). Phylogenetic structure of the prokaryotic domain: the primary kingdoms. *Proc. of the National Academy of Sciences (USA)*, 97, 8392-8396.

20. Arnason, U., Gullberg, A. and Widegren, B. (1991). The complete nucleotide sequence of the mitochondrial DNA of the fin whale, *Balaenoptera physalus*. *Journal of Molecular Evolution*, 33(6), 556-568.

21. Keskin, E. and Can, A. (2009). Phylogenetic relationships among four species and a sub-species of Mullidae (Actinopterygii; Perciformes) based on mitochondrial cytochrome B, 12S rRNA and cytochrome oxidase II genes. *Biochemical Systematics and Ecology*, 37(5), 653-661.

22. Padmavathi, P. and Gatreddi Srinu. (2017). Emerging trends in DNA markers and their applications in Aquatic biodiversity with an emphasis on mitochondrial markers. *International Journal of Zoology Studies*, 2(6), 213-219.

23. Hebert, P.D.N., Cywinska, A. and Ball, S.L. (2003). Biological identifications through DNA barcodes. *Proceedings of the Royal Society of London B: Biological Sciences*, 270(1512), 313-321.

24. Haye, P.A., Segovia, N.I., Vera, R., de los Ángeles Gallardo, M. and Gallardo-Escárate, C. (2012). Authentication of commercialized crab-meat in Chile using DNA barcoding. *Food Control*, 25(1), 239-244.

25. Vartak, V.R., Narasimmalu, R., Annam, P.K., Singh, D.P. and Lakra, W.S. (2015). DNA barcoding detected improper labelling and supersession of crab food served by restaurants in India. *Journal of the Science of Food and Agriculture*, 95(2), 359-366.

26. Gatreddi Srinu and Padmavathi, P. (2016). DNA Barcoding: a torchbearer for sea food authentication in India. *Aquaculture Times*, 2(5), 22-23.

27. Thompson, J.D., Gibson, T.J., Plewniak, F., Jeanmougin, F. and Higgins, D.G. (1997). The CLUSTAL_X windows interface: flexible strategies for multiple sequence alignment aided by quality analysis tools. *Nucleic acids research*, 25(24), 4876-4882.

28. Kumar, S., Stecher, G. and Tamura, K. (2016). MEGA7: Molecular Evolutionary Genetics Analysis version 7 for bigger datasets. *Molecular biology and evolution*, 33(7), 1870-74

29. Kimura M. (1980). A simple method for estimating evolutionary rate of base substitutions through comparative studies of nucleotide sequences. *Journal of Molecular Evolution,* 16, 111-120.

30. Librado, P. and Rozas, J. (2009). DnaSP v5: a software for comprehensive analysis of DNA polymorphism data. *Bioinformatics*, 25(11), 1451-1452.

31. Saitou N. and Nei M. (1987). The neighbor-joining method: A new method for reconstructing phylogenetic trees. *Molecular Biology and Evolution*, 4, 406-425.

32. Duran, S., Palacin, C., Becerro, M.A., Turon, X. and Giribet, G. (2004). Genetic diversity and population structure of the commercially harvested sea urchin *Paracentrotus lividus* (Echinodermata, Echinoidea). *Molecular ecology*, 13(11), 3317-3328.

33. Knebelsberger, T., Dunz, A.R., Neumann, D. and Geiger, M.F. (2015). Molecular diversity of G ermany's freshwater fishes and lampreys assessed by DNA barcoding. *Molecular ecology resources,* 15(3), 562-572.

34. Singh, M., Verma, R., Yumnam, R. and Vishwanath, W. (2018). Molecular phylogenetic analysis of genus *Osteobrama* Heckel, 1843 and discovery of *Osteobrama serrata* sp. nov. from North East India. *Mitochondrial DNA Part A,* 29(3), 361-366.

35. Meyer, C.P. and Paulay, G. (2005). DNA barcoding: error rates based on comprehensive sampling. *PLoS biology*, 3(12), e422.

36. Chakraborty, M. and Ghosh, S.K. (2014). An assessment of the DNA barcodes of Indian freshwater fishes. *Gene*, 537(1), 20-28.

37. Lakra, W.S., Verma, M.S., Goswami, M., Lal, K.K., Mohindra, V., Punia, P.,

Gopalakrishnan, A., Singh, K.V., Ward, R.D. and Hebert, P.D.N. (2011). DNA barcoding Indian marine fishes. *Molecular Ecology Resources*, 11(1), 60-71.

38. Zhang, D.X. and Hewitt, G.M. (1996). Nuclear integrations: challenges for mitochondrial DNA markers. *Trends in ecology & evolution*, 11(6), 247-251.

39. Ward, R.D., Zemlak, T.S., Innes, B.H., Last, P.R. and Hebert, P.D.N. (2005). DNA barcoding Australia's fish species. *Philosophical Transactions of the Royal Society of London B: Biological Sciences*, 360 (1462), 1847-1857.

40. Viswambharan, D., Pavan-Kumar, A., Singh, D.P., Jaiswar, A.K., Chakraborty, S.K., Nair, J.R. and Lakra, W.S. (2015). DNA barcoding of gobiid fishes (Perciformes, Gobioidei). *Mitochondrial DNA*, 26(1), 15-19.

41. Bensasson, D., Zhang, D.X., Hartl, D.L. and Hewitt, G.M. (2001). Mitochondrial pseudogenes: evolution's misplaced witnesses. *Trends in ecology & evolution*, 16(6), 314-321.

42. Jermiin, L.S., Graur, D., Lowe, R.M. and Crozier, R.H. (1994). Analysis of directional mutation pressure and nucleotide content in mitochondrial cytochrome b genes. *Journal of Molecular Evolution,* 39(2), 160-173.

43. Philippe, H. and Laurent, J. (1998). How good are deep phylogenetic trees?. *Current opinion in genetics & development,* 8(6), 616-623.

44. Moreira, D., López-García, P. and Rodríguez-Valera, F. (2001). New insights into the phylogenetic position of diplonemids: G+ C content bias, differences of evolutionary rate and a new environmental sequence. *International journal of systematic and evolutionary microbiology,* 51(6), 2211-2219.

45. Oleinik, A.G. (2000). On the mutation rates of the mitochondrial and nuclear genomes of salmonid fishes. *Russian Journal of Marine Biology*, 26(6), 432-438.

46. Lynch, M. (2010). Evolution of the mutation rate. *Trends in Genetics*, 26(8), 345-352.

47. Faith, J.J. and Pollock, D.D. (2003). Likelihood analysis of asymmetrical mutation bias gradients in vertebrate mitochondrial genomes. *Genetics*, 165(2), 735-745.

48. Rocha, E.P., Touchon, M. and Feil, E.J. (2006). Similar compositional biases are caused by very different mutational effects. *Genome research*, 16(12), 1537-1547.

Current Trends in Biotechnology and Pharmacy
Vol. 13 (2) 190-198, April 2019, ISSN 0973-8916 (Print), 2230-7303 (Online)

Simple and rapid liquid chromatography–tandem mass Spectrometric (LC-MS/MS) method for the Simultaneous Determination of Pioglitazone and Glimepiride in human Plasma

D. S. S. Sai Praveen, *S. Asha, P. Ravi Kumar
[a] Dept. of Biotechnology, VFSTR (Deemed to be University), Vadlamudi, Guntur, A.P., India
[b]Dept. of Bio-Analytical R&D,AIZANT Drug Research Solutions, Hyderabad, Telangana, India
For correspondence : sai848@gmail.com

Abstract

A simple and rapid liquid chromatography-tandem mass spectrometric (LC-MS/MS) was proposed for the simultaneous determination of pioglitazone and glimepiride in human plasma.The analytes and the internal standards (IS) were extracted from 100 µL aliquots of human plasma *via* solid phase extraction (SPE). A mobile phase composed of 5 mM ammonium acetate (pH 3.0) and methanol (20:80, v/v) was used to chromatograph the analytes on a C_{18} column.The calibration curve obtained was linear (r^2 0.999) over the concentration range of 12.15–2418.27 ng/mL for pioglitazone and 2.00–500.61 ng/mL for glimepiride. The total run time was rapid with 2.5 min. and can analyze more samples in a day. All the validation results were complying with the recent USFDA guidelines.

Keywords
Pioglitazone; Glimepiride; Human plasma; LC/MS/MS; Chromatography; Validation.

Introduction

Pioglitazone is used for the treatment of type 2 *Diabetes mellitus* either alone or in combination with a sulfonylurea, metformin, or insulin [1],[2]. It selectively stimulates the nuclear receptor peroxisome proliferator-activated receptor gamma (PPAR-β) to modulate the transcription of the insulin-sensitive genes involved in the control of glucose and lipid metabolism [3]. The pharmacokinetics of pioglitazone does not differ significantly between healthy volunteers and patients with type 2 *Diabetes* [4].

Glimepiride is a sulfonylurea, hypoglycemic agent indicated for the treatment of type 2 *Diabetes mellitus*. The primary mechanism of action of glimepiride for lowering blood glucose appears to be dependent on stimulating the release of insulin from functioning pancreatic cells [5], [6].

The fixed dose combination of pioglitazone and glimepiride have been demonstrated in numerous clinical trials to be highly effective in reducing blood sugar and that the combined use might be more effective in treating type 2 *Diabetes mellitus* than a monotherapy [7], [8].This combination exerts more beneficial effects in patients with type 2 *Diabetes mellitus*. Duetact is a new single pill combination therapy of pioglitazone and glimepiride, approved by US FDA for the treatment of type 2 *Diabetes mellitus*.

Till date, two LC-MS methods [9], [10] have been reported for the simultaneous determination of pioglitazone and glimepiride in plasma samples. Ni *et al.,* 2014 [9] reported a method for the determination of pioglitazone and glimepiride simultaneously in human plasma. Another LC-MS

method proposed by Hess *et al.,* 2011 [10] describes simultaneous identification and quantification of 11 oral hypo-glycemic drugs in plasma including pioglitazone and glimepiride. Both the methods employed liquid-liquid extraction (LLE) technique to extract the analytes from plasma. However, these methods are having drawbacks like use of more plasma volume (e"0.2 mL), tedious sample extraction with LLE,use of non-polar solvents, evaporation, drying and reconstitution steps and longer chromatographic run time (>3 min). A good analytical method should be rapid with less analysis time, low volume of sample and efficient extraction to remove the endogenous matrix components [11], [12].

In the present paper, we propose a simple, rapid and selective LC-MS/MS method for the simultaneous determination of pioglitazone and glimepiride in human plasma. The method employs simple and efficient solid phase extraction (SPE) to extract the analytes from plasma. Also, the method uses isotope labeled compounds pioglitazone d4 (IS1) and glimepiride d4 (SI2) as internal standards (IS) for the quantitation of pioglitazone and glimepiride, respectively.Matrix effect related problems and variability in recovery between analytes and IS (Internal/Reference Standard) can be minimized using the isotope labeled compounds as an IS.

Materials and Methods

Chemicals and reagents : Reference samples of pioglitazone hydrochloride (99.6%), glimepiride (99.4%), pioglitazone d4 (99.5%) and glimepiride d4 (98.4%) were purchased from Vivan Life Sciences Ltd (Mumbai, India).The individual human plasma lots were obtained from Deccan's Pathological Labs, (Hyderabad, India). LC-MS grade water was prepared from Milli Q water purification system procured from Millipore (Bangalore, India). HPLC grade methanol was purchased from J.T Baker (Phillipsburg, USA). Analytical grade formic acid and ammonium acetate was also purchased from Merck (Mumbai, India).

Instrument conditions : An HPLC system (Shimadzu Corporations, Kyoto, Japan) coupled with API–4000 (AB Sciex, Applied Biosystems, Foster City, CA, USA) mass spectrometer was used for the study. A mixture of 5mM ammonium acetate (pH 3.0) and methanol (20:80, v/v) was used as mobile phase and delivered at a flow rate of 1.0 mL/min. An aliquot of 10 µL of processed samples were injected in to Zorbax SB C_{18}, 50* 4.6 mm, 3.5 µm analytical column which was kept at ambient temperature (20±5°C). The optimized parameters are listed in Table 1.

Sample preparation : All stock solutions were prepared in methanol at concentration of 1 mg/mL separately and stored at 2–8 °C in refrigerator. Further working solutions of analytes and IS were prepared in diluent (methanol and water, 80:20, v/v). Two separate stock solutions of pioglitazone and glimepiride were used for preparation of calibration standards (CC) and quality control (QC) samples in plasma. CC standards for pioglitazone in plasma were prepared at concentrations of 12.15, 24.30, 48.61, 121.52, 303.80, 607.59, 1215.18, 1813.70 and 2418.27 ng/ml. Similarly, for glimepiride in plasma, CC standards were prepared at concentrations of 2.00, 4.01, 10.01, 25.03, 50.06, 100.12, 200.24, 400.49 and 500.61 ng/ml.The QC samples were prepared at five different concentration levels of 12.22, 2.02 (lower limit of quantification, LLOQ), 32.16, 6.03 (low quality control, LQC), 321.64, 75. 35 (middle quality control, MQC–1), 1461.99, 251.18 (MQC–2) and 2182.07, 425.73 (high quality control, HQC) ng/mL for pioglitazone and glimepiride, respectively. All the prepared plasma samples were stored at –70 ± 10 °C. A combined working solution for IS1 (5000 ng/mL) and IS2 (2500 ng/mL) was also prepared in diluent.

All the frozen plasma samples were thawed at room temperature and vortexed for 10 s. A 100 µL aliquot of human plasma sample was mixed with 20 L of the internal standard working solution.Then 100 µL of water was added and samples were vortexed for 10 s.The sample mixture was loaded onto a Strata™ X 33µm

polymeric sorbent (30 mg/mL)that was pre-conditioned with 1.0 mL of methanol followed by 1.0 mL 50 mM ammonium acetate. The extraction cartridge was washed with 1.0 mL of water and 1.0 mL 50 mM ammonium acetate.The analytes were eluted with 0.5 mL of mobile phase and 10µL injected into the LC-MS/MS system.

Method validation : Method validation was carried out as per US FDA and EMEA guidelines [13], [14]. The parameters included carry over test, selectivity, specificity, linearity, precision and accuracy, sensitivity, matrix effect, recovery, dilution integrity and stability.

Results and Discussion

Method development : Tuning was done in positive and negative mode using 100 ng/mL solution of analytes. The high intense mass spectrum was obtained in positive mode. Hence, mass spectrometer was operated in positive ionization mode using ESI interface source. The ion spray voltage (ISV), source temperature, nebulizer gas (GS1) and (GS2) were suitably chosen to obtain reproducible and high response. Similarly, compound dependent parameters like De-clustering potential (DP), Collision energy (CE), and Collision cell exit potential (CXP) for each analyte were properly tuned by ramping the mass spectrometry conditions. The product ion mass spectra of pioglitazone, glimepiride, IS1 and IS2 are presented in the Fig. 1a, 1b, 1c and 1d respectively. LC–MRM technique was used for the quantification of analytes since it provides sensitivity and selectivity [15], [16].

Pioglitazone and glimepiride are having different physicochemical properties; hence it was difficult to develop a LC-MS/MS method simultaneously. It is necessary to select the proper mobile phase, analytical column and organic solvent. These parameters were suitably monitored to produce the better resolution from endogenous components which in turn affect sensitivity and reproducibility of the analytical method. In method

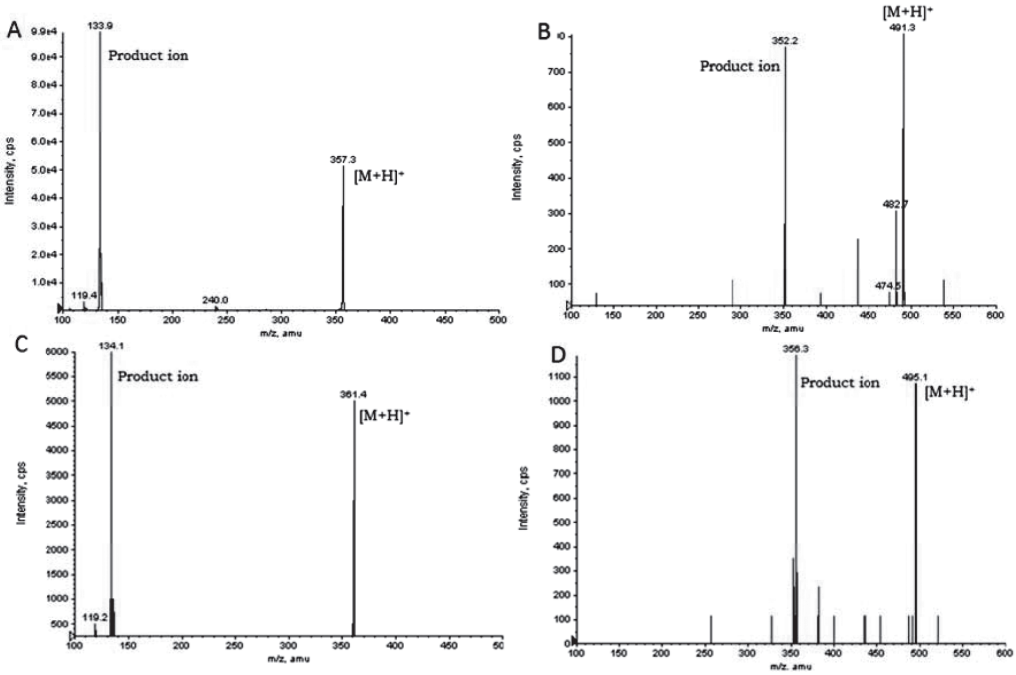

Fig. 1: Production mass spectra of [M+H]+ of (A) pioglitazone (B) glimepiride (C) pioglitazone-d4 (IS1) and (D) glimepiride-d4 (IS2)

development stage, many volatile buffers like ammonium acetate and ammonium formate with acid modifies such as acetic acid and formic acid and basic modifies like ammonia solution were tested for their suitability in combination with organic modifies namely acetonitrile and methanol. Also, different makes columns namely Hypurity advance, Zorbax SB C_{18}, Kromasil 100-5$C_{18,}$ Ace 3 $C_{18,}$ Alltima HP C_{18} and Zorbax XDB-phenyl were tested for their suitability with above volatile buffers in combination with organic modifiers. It was observed that 5 mM ammonium acetate (pH 3.0) and methanol (20:80, v/v) as the mobile phase was most appropriate to give best sensitivity, efficiency and peak shape for both analytes and the internal standards. Off all the columns tested, Zorbax SB C_{18}, 50 × 4.6 mm, 3.5 µm column gave good peak shape and response even at lowest concentration level for both the analytes.The flow rate was optimized to 1.0 mL/min. The retention time of pioglitazone, glimepiride, IS1 and IS2 (1.8, 0.7, 1.8 and 0.7 min, respectively) were low enough allowing a small run time of 2.5 min.

The reported methods have employed LLE to extract the pioglitazone and glimepiride from plasma. As a purpose to develop a novel and efficient extraction procedure, SPE was employed for the present work. Moreover, SPE give much cleaner extracts with minimal or no matrix effect. Among the different cartridges,StarataX polymeric sorbent, Oasis HLB, Bond ElutPlexa and Orpheus C_{18} extraction cartridges tested, StarataX polymeric sorbent cartridges were found to be best for the present purpose. The recovery for the analytes and the IS were good and reproducible. During the washing step, the cartridges were washed with 50 mM ammonium acetate to remove the endogenous matrix components efficiently. Stable labeled isotope standards of the analyte as an internal standard is suggested for bioanalytical assays to increase assay precision and limit variable recovery between analyte and the IS. Hence, pioglitazone d4 and glimepiride d4 were selected for the quantification of pioglitazone and glimepiride, respectively.

Chromatography and sensitivity : A representative chromatogram of blank sample, blank sample spiked with the respective IS and an LLOQ sample of pioglitazone and glimepiride were shown in Fig 2 and 3, respectively. No interference from endogenous plasma constituents with the analytes and the IS was observed in blank sample (Fig. 2a and 3a). Also, corresponding IS were not interfering with the analyte (Fig. 2b and 3b). To assess the method selectivity, six individual K2 EDTA plasma lots were screened to check the interference and all the lots were found to be free from interference. The lowest limit of reliable quantification (LLOQ) for the analytes was set at the concentration of 12.15 ng/mL for pioglitazone and 2.00 ng/mL for glimepiride. The precision and accuracy at LLOQ concentration were found to be 4.56% and 100% and 99.6% and 10.7% for pioglitazone and glimepiride, respectively.

Matrix effect and recovery **:** Matrix effect was checked in six lots of human plasma. Matrix effect expressed as IS normalized matrix factor (MF) was determined at LQC and HQC levels. The response of post–extraction spiked samples was compared with mean area of neat samples. The IS normalized matrix factor calculated for pioglitazone was 0.92 for LQC and 0.91 for HQC. Similarly, the IS normalized matrix factor calculated for glimepiride was 0.93 for LQC and 1.02 for HQC. The results indicate no significant matrix effect in all the plasma lots tested.

Recovery of pioglitazone and glimepiride was determined at low, medium and high quality control concentration. The mean area of extracted sample was compared with mean area of neat samples (n=6). The highest recoveries were obtained for analytes and the IS with the proposed SPE method. The mean overall recoveries (with the precision range) of pioglitazone, glimepiride, IS1 and IS2 were 96.9±1.73% (2.32-5.07%), 97.6±1.47% (6.6-12.9%), 93.9% (4.42-6.69%) and 92.0% (2.73-10.3%), respectively.

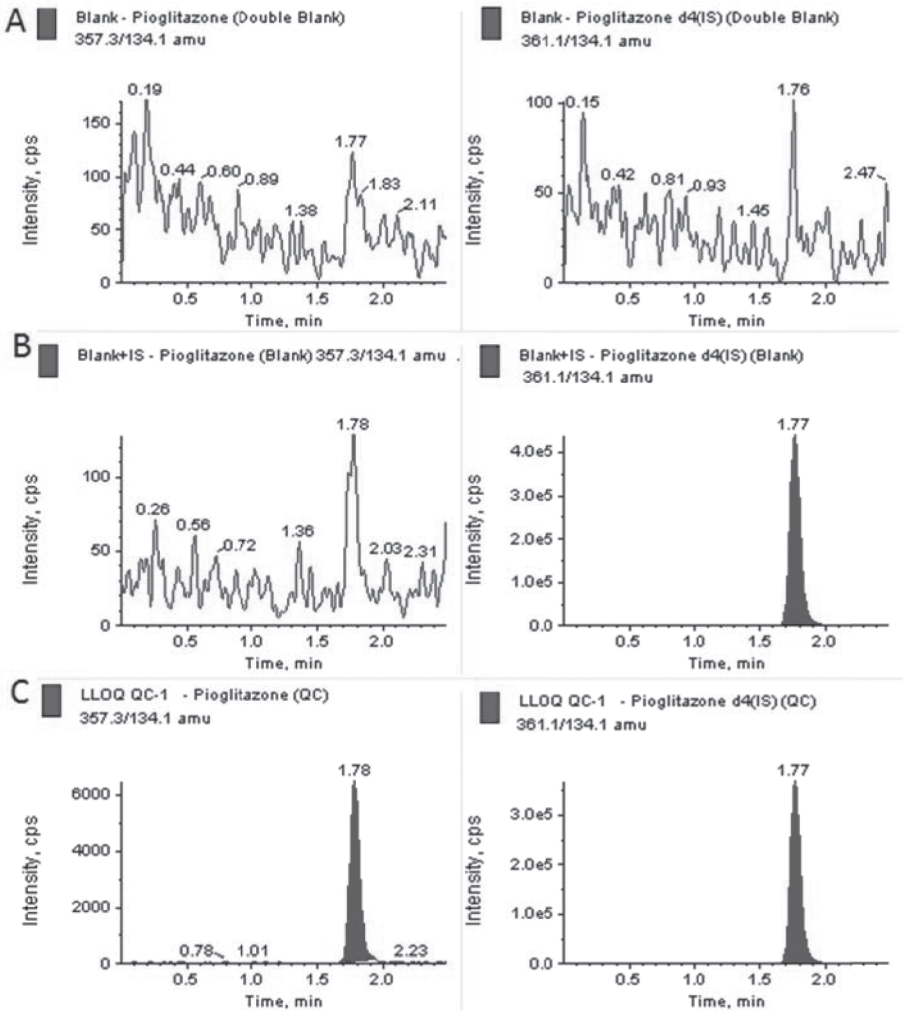

Fig. 2: Typical MRM chromatograms of pioglitazone (left panel) and IS (right panel) in human blank plasma (A), and human plasma spiked with IS (B), a LLOQ sample along with IS (C)

Linearity : The linearity for pioglitazone and glimepiride was established in the range of 12.15-2418.27 ng/mL and 2.00-500.61 ng/mL, respectively. A total of five calibration curves were generated during the validation. Each calibration curve contains blank samples, blank sample with the IS, nine non-zero calibration standards and five level of quality control samples (six at each level). Two weighting models (1/x and $1/x^2$) were compared and a regression equation with a weighting factor of $1/x^2$ of the drug to the IS concentration was found to produce the best fit for the concentration-detector response relationship for both pioglitazone and glimepiride in plasma. The correlation coefficient for each run of both the analytes was e" 0.99.

Precision,accuracy and dilution integrity: As shown in Table 2, the precision and accuracy of each analyte in the intra-day and inter-day runs were within ± 15% at LQC, MQC-1, MQC-2 and HQC concentrations and within ± 20% at LLOQ QCs. The upper concentration limit of pioglitazone and glimepiride can be extended

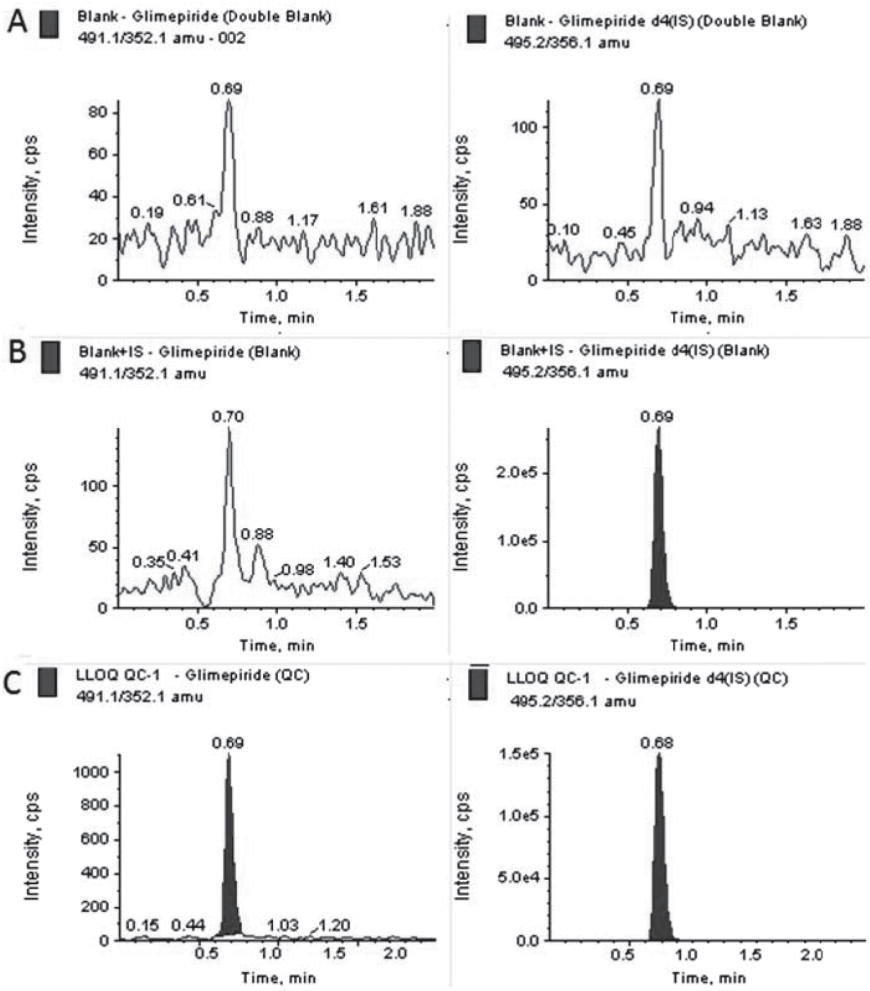

Fig. 3: Typical MRM chromatograms of glimepiride (left panel) and IS (right panel) in human blank plasma (A), and human plasma spiked with IS (B), a LLOQ sample along with IS (C)

to 4932 ng/mL and 826 ng/mL (2 times of ULOQ), respectively by using half (1:2) or quarter (1:4) dilution with screened human blank plasma. The precision and accuracy for pioglitazone at 1:2 dilutions were found to be 0.55 and 99.1%, and at 1:4 dilutions they were 0.78 and 110%, respectively. Similarly, the precision and accuracy for glimepiride at LQC concentration were found to be 6.73 and 98.6%, and at HQC level they were 8.59 and 96.8%, respectively. The dilution integrity results were deemed acceptable for 2 times and 4 times dilutions for both the analytes.

Stability studies : The stability of pioglitazone and glimepiride was evaluated in plasma as well as in processed samples. The stability was tested at LQC and HQC levels and the results are presented in Table 3. The mean % nominal values of the analytes were found to be within ±15% of the predicted concentrations for the analytes at their LQC and HQC levels.

Conclusions

In conclusion, the LC-MS/MS assay method described in this paper is rapid, simple, specific and sensitive for quantification of

Table 1. Main working parameters for Tandem mass–spectrometer.

Parameter	Analyte			
Mode of analysis	Pioglitazone Positive	IS1 Positive	Glimepiride Positive	IS2 Positive
Ion transition, m/z	357.30/134.10	361.10/134.10	491.10/352.10	495.20/356.10
Source temperature, °C	550	550	550	550
Dwell time per transition, msec	100	100	100	100
Nebulizer gas, psi	40	40	40	40
Turbolon gas, psi	40	40	40	40
Curtain gas, psi	40	40	40	40
Collision gas, psi	9	9	9	9
Ion spray voltage, V	5500	5500	5500	5500
Entrance potential, V	10	10	10	10
De-clustering potential, V	135	135	80	80
Collision energy, V	40	40	18	18
Collision cell exit potential, V	7	7	10	10
Resolution	Unit	Unit	Unit	Unit

Table 2: Precision and accuracy data for pioglitazone and glimepiride

QC		Intra–day precision and accuracy (n=12; 6 from each batch)			Inter–day precision and accuracy (n=30; 6 from each batch)		
Analytes	Concentration spiked (ng/mL)	Concentration found (mean; ng/mL)	Precision (%)	Accuracy (%)	Concentration found (mean; ng/mL)	Precision (%)	Accuracy (%)
Pioglitazone	12.22	12.14±0.92	7.58	99.32	12.54±0.86	6.85	102.57
	32.16	29.93±0.64	2.14	93.04	30.34±0.89	2.93	94.33
	321.64	326.10±4.40	1.35	101.39	325.62±5.48	1.68	101.24
	1461.99	1375.38±18.3	1.33	94.08	1368.15±25.91	1.89	93.58
	2182.07	2069.90±23.1	1.12	94.86	2040.17±40.27	1.97	93.50
Glimepiride	2.02	1.97±0.21	10.85	97.59	1.96±0.18	9.20	97.11
	6.03	6.12±0.60	9.85	101.60	5.95±0.53	8.90	98.63
	75.35	78.38±6.55	8.35	104.02	78.40±5.96	7.60	104.05
	251.18	258.82±22.48	8.69	103.04	253.49±16.98	6.70	100.92
	425.73	449.05±24.51	5.46	105.48	425.93±31.25	7.34	100.05

Table 3: Stability samples result for pioglitazone and glimepiride (*n*=6)

Analytes	Stability test	QC-Spiked concentration (ng/mL)	Mean ± SD (ng/mL)	Precision (%)	Accuracy/ Stability (%)
Pioglitazone	Auto-sampler (55 h)	30.17	30.61±0.44	1.42	95.17
		2250.36	1971.59±13.10	0.66	90.35
	Wet Extract (52 h)	30.17	30.64 ± 0.52	1.70	95.25
		2250.36	1967.27 ± 27.75	1.41	90.16
	Bench top (15 h)	30.17	29.42 ± 0.75	2.55	91.48
		2250.36	1961.22 ± 19.61	1.00	89.88
	Freeze-thaw (4 cycles)	30.17	30.30 ± 0.42	1.38	94.19
		2250.36	1988.52 ± 12.26	0.62	91.13
	Reinjection (36 h)	30.17	30.49 ± 0.58	1.89	94.79
		2250.36	1994.77 ± 15.42	0.77	91.42
	Long–term 60 days	30.17	30.60 ± 1.15	3.77	95.15
		2250.36	2016.62 ± 30.13	1.49	92.42
Glimepiride	Auto-sampler (55 h)	6.03	5.90±0.62	10.46	97.89
		425.73	460.96±17.29	3.75	108.28
	Wet Extract (52 h)	6.03	5.57±0.59	10.58	92.44
		425.73	463.36±23.98	5.18	108.84
	Bench top(15 h)	6.03	6.08±0.37	6.04	100.90
		425.73	440.98±24.33	5.52	103.58
	Freeze-thaw (4 cycles)	6.03	5.28±0.32	5.97	87.66
		425.73	447.73±36.21	8.09	105.17
	Reinjection(36 h)	6.03	6.21±0.25	4.02	103.08
		425.73	448.56±10.74	2.39	105.36
	Long–term (60 days)	6.03	5.84±0.33	5.72	96.89
		425.73	441.4237.81	8.57	103.69

pioglitazone and glimepiridein human plasma. This method was fully validated as per US FDA guidelines and is well suitable for pharmacokinetic or bioavailability/bioequivalence application. The method employed deuterated compounds as internal standards for quantification. The simple SPE method gave consistent and reproducible recoveries for the analytes from plasma. The proposed method is rapid with the chromatographic run time of 2.5 min and suitable for high–throughput bioanalysis of pioglitazone and glimepiride simultaneously. The advantages of the proposed method are (1) low plasma volume (only 100 µL) (2) simple and direct SPE method (3) rapid run time (2.5 min) thus large number of samples can be analyzed in short time.

Conflicts of interest : The authors declare that there are no conflicts of interest.

Acknowledgement

The authors gratefully acknowledge PCR Laboratories, Hyderabad for providing necessary facilities to carry out this work. We also thank management, VFSTR (Deemed to be University) for the support and encouragement.

References

1. Hanefeld M. Pharmacokinetics and clinical efficacy of pioglitazone. *International Journal of Clinical Practice* **121** (2001),pp 19.

2. Scheen AJ. Pharmacokinetics and clinical evaluation of the alogliptin plus pioglitazone combination for type 2 *Diabetes*. *Expert Opinion on Drug Metabolism and Toxicology* **11** (2015), pp1005.
3. Baughman TM, Graham RA, Wells-Knecht K, Silver IS, Tyler LO, Wells-Knecht M, Zhao Z. Metabolic activation of pioglitazone identified from rat and human liver microsomes and freshly isolated hepatocytes. *Drug Metabolism and Disposition* **33** (2005), pp 733.
4. Eckland DA, Danhof M. Clinical pharmacokinetics of pioglitazone. *Experimental and Clinical Endocrinology & Diabetes* **108** **(**2000), pp 234.
5. Rosskamp R, Wernicke–Panten K and Draeger E Clinical profile of the novel sulphonylurea glimepiride. *Diabetes Research and Clinical Practice* **31** (1996) pp 33.
6. Massi-Benedetti M. Glimepiride in type 2 *Diabetes mellitus*: a review of the worldwide therapeutic experience. *Clinical Therapeutics* **25** (2003), pp 799.
7. Tan M, Johns D, González Gálvez G, Antúnez O, Fabián G, Flores-Lozano F, Zúñiga Guajardo S, Garza E, Morales H, Konkoy C and Herz M. Effects of pioglitazone and glimepiride on glycemic control and insulin sensitivity in mexican patients with type 2 *Diabetes mellitus*: A multicenter, randomized, double-blind, parallel-group trial. *Clinical Therapeutics* **26** (2004),pp 680.
8. Hiroi S, Sugiura K, Matsuno K, Hirayama M, Kuriyama K, Kaku K, and Kawakami K. A multicenter, phase III evaluation of the efficacy and safety of a new fixed-dose pioglitazone/glimepiride combination tablet in Japanese patients with type 2 *Diabetes*.*Diabetes Technology and Therapeutics* **15** (2013),pp 158.
9. Ni XJ, Wang ZZ, Shang DW, Zhang M, Hu JQ, Qiu C and Wen YG. Simultaneous determination of glimepiride and pioglitazone in human plasma by liquid chromatography-tandem mass spectrometry and its application to pharmacokinetic study. *Journal of Chromatography* B **960** (2014), pp 247.
10. Hess C, Musshoff F and Madea B. Simultaneous identification and validated quantification of 11 oral hypoglycemic drugs in plasma by electrospray ionization liquid chromatography-mass spectrometry. *Analytical and Bioanalytical Chemistry* **40** (2011), pp 33.
11. Matta MK, Pilli NR, J V L N SR. A validated liquid chromatography and tandem mass spectrometric method for simultaneous quantitation of tenofovir, emtricitabine and efavirenz in human plasma and its pharmacokinetic application. *Acta Chromatogrica*, 27 (2015), pp 27-39.
12. Putluru SP, Matta M K, Ahire D, Subramanian M, Sinz M, Mandlekar S. A novel liquid chromatography tandem mass spectrometry method for the estimation of bilirubin glucuronides and its application to *in vitro* enzyme assays. *Drug Metabolism Letters*, 10 (2016), pp 264-269.
13. US DHHS, FDA and CDER. Guidance for Industry: Bioanalytical Method Validation. US Department of Health and Human Services, Food and Drug Administration, Center for Drug Evaluation and Research and Center for Veterinary Medicine: Rockville, MD, 2001.
14. Guideline on bioanalytical method validation, Science and Medicinal Health, European Medicines Agency (EMEA), EMEA/CHMP/EWP/192217/2009; 2011.
15. Matta MK, Pilli NR, Inamadugu JK, Burugula L, J V L N SR. Simultaneous quantification of lamivudine, zidovudine and nevirapine in human plasma by liquid chromatography – tandem mass spectrometry and its application to a pharmacokinetic study. *ActaPharmacologicaSinica B*. **2** (2012), pp 472-480.
16. Matta MK, Burugula L, Pilli NR, Inamadugu JK, J V L N SR. A novel LC-MS/MS method for simultaneous quantification of tenofovir and lamivudine in humanplasma and its application to a pharmacokinetic study. *Biomed Chromatogram*, **26** (2012), pp 1202-1209.

Current Trends in Biotechnology and Pharmacy
Vol. 13 (2) 199-211, April 2019, ISSN 0973-8916 (Print), 2230-7303 (Online)

Topical and Transdermal Benefits of Nanostructured Lipid Carriers

Ashwini M*[1], Srividya R[2], Shaanya Johl [3]
KRUPANIDHI COLLEGE OF PHARMACY
12/1, Chikkabellandur, Carmelaram, Post, Varthur Hobli, Bengaloru - 560 035
Correspondence : ashwinipreetham2@gmail.com

Abstract:

Lipid based carriers (solid lipid nanoparticles-SLN and nanostructured lipid carriers-NLC) were developed at the beginning of the 90s and has been extensively used for topical and transdermal delivery of pharmaceuticals and cosmeceuticals. Among them, NLC's are widely accepted for maintaining drug stability, improving drug therapy, solubilizing poorly water soluble drugs, achieving controlled and sustained drug delivery and reduced toxicity. This review article discusses different formulations and characterization techniques and discusses how NLCs can penetrate the skin barrier. Further, overview on the current state of the art of NLCs as therapeutic and cosmetic formulations are also discussed in detail. The study highlights the reported data on oral bioavailability and toxicological studies and how these NLC's can be employed as promising drug delivery systems for novel treatments in the near future.

Keywords: Nanostructured Lipid Carrier, transdermal drug delivery, topical drug delivery nanoparticles, penetration.

Introduction

Among the various delivery systems, drug delivery through skin can be considered as one of the convenient routes of administration (1). Skin drug delivery can be either dermal (topical) or transdermal. Dermal delivery includes application of drug directly at the site of action (skin surface), resulting in higher localized drug concentration with reduced systemic drug exposure. In transdermal drug delivery, the drug is delivered through the layers of the skin to reach the systemic circulation (2). One of the key advantages of transdermal drug delivery is improved patient acceptance or compliance compared to other routes of administration (3).

The major obstacle associated with the transdermal delivery system is the challenges offered by the Stratum Cornea (SC), whose molecular architecture permits only selected molecules to penetrate through it (4). Hence several new technologies have been developed to increase the transdermal permeation of drugs. Some of the important strategies used to enhance transdermal absorption are by using physical enhancers like ultrasound, iontophoresis, electroporation, magnetophoresis, microneedle, or by using chemical permeation enhancers such as sulphoxides, azones, glycols, alkanols, terpenes etc. or by the most important vesicular systems which include liposomes, niosomes, transfersomes, microemulsion and lipid nanoparticles (5).

The physical permeation enhancement methods are invasive and expensive, whereas the chemical enhancers cause skin irritation which may damage the skin permanently. These facts made the vesicular system more popular than the physical and chemical enhancement methods (5). The conventional vesicular systems like liposomes faces various stability issues which caused formulators to focus on lipid nanoparticles (6). Solid lipid nanoparticles (SLN) and nanostructured lipid carriers (NLC) are the two lipid nanoparticles which are extensively used for topical and transdermal delivery of drugs (7).

Recently NLCs are gaining more attention as it overcomes the complications connected with SLNs such as drug expulsion during storage and limited drug loading. In addition to this, the occlusive effect and use of lipid components in NLCs reduce the barrier function of SC, thus making them suitable for enhancing transdermal permeability (8).

2. Transdermal skin penetration

Nano lipid carriers penetrate into the skin by three basic pathways.

1. Channeling through the hair follicles and the sweat glands i.e. transappendageal.
2. Transcellular intake by direct permeation through the cell membrane of the epidermis.
3. Intercellular route involving passage through the gaps between the epidermal cells.

The nano size of these carriers promotes close association with stratum cornea of the skin, which permits topical spreading of the formulation causing occlusion and hydration of the skin. This leads to the widening of the gaps between the corneocytes. In addition, the presence of surfactants in these carriers causes alteration of the skin structures which further accelerates the penetration of the drug moieties. It is also hypothesized that the lipid richness of the epidermis may cause exchange of lipids with the nano carriers, thus adding to the penetration enhancement (10).

3. Advantages of Nanostructured Lipid Carriers (11)

* Prevention of chemical degradation of encapsulated drugs which improves drug stability.
* Site specific delivery to obtain control and targeted drug release.
* Improved drug loading capacity.
* Biocompatible and biodegradable lipids which results in reduced cyto and systemic toxicity.
* Holds both lipophilic and hydrophilic drugs.
* Reduced usage of organic solvents.
* Cost affective.

4. Disadvantages of Nanostuctured Lipid Carriers (12)

· Polymorphic changes of lipids may lead to drug expulsion on storage.
· Physical changes like gelation and formation of super cooled melts.
· Sterilization issues, specially formulations used for parentral purpose.
· Insufficient data on clinical studies related to NLC.

5. Types of NLC (13**,** 14)

a) **Type I: Highly imperfect solid matrix:** In this type of NLCs, a blend of solid and liquid lipids are used. The structural difference of lipids leads to imperfect, disarranged and disordered matrix. This structural disarrangement offers a lot of space for the accommodation of the drug.

b) **Type II: Multiple oil/fat/water carriers*:*** The main drawback of SLNs is drug expulsion due to the poor solubility of drug in the solid lipid. To overcome this, in NLCs, liquid lipids are used in large amounts, based on the fact that drugs are more soluble in liquid lipid than solid lipid. Use of liquid lipids leads to formation of minute nano compartments of oils which can accommodate large amount of drugs.

c) **Type III: Amorphous Matrix*:*** In this type of NLCs, crystallization is avoided by mixing solid lipids with special lipids like medium chained triglycerides, so that the matrix formed is not crystalline but amorphous in nature.

6. Method of preparation (25**,** 26)

* High-Pressure Homogenization Method
* Ultrasonic Emulsion Evaporation Method
* Solvent Dispersion
* High-Temperature Emulsion Evaporation-Low-Temperature Curing
* Microemulsion Method
* Phase Inversion Temperature (PIT) method
* Double emulsion technique
* Melt Emulsification Method

7. Lipids used in NLCs

Lipids used in NLCs are biocompatible and

biodegradable i.e. lipids which belong to the Generally Regarded As Safe (GRAS) category (10). Nanostructure lipid carriers (NLCs) contain both solid and liquid (oil) lipids in defined ratio. The structural imperfection of NLC is due to the presence of Liquid Lipids (oil), which converts the perfect crystalline structure of the solid lipid to a crystal lattice with many spaces, thus resulting in greater drug encapsulation and drug loading (27).

The solid lipids commonly used for NLCs include glyceryl palmitostearate, glyceryl behenate, steroids (e.g. cholesterol) and waxes (e.g. cetyl palmitate). Liquid lipids used are Caprylic/Capric triglycerides (C8/C10), Vitamin E and it's derivatives, Monoacylglycerols, oleic acid, isopropyl myristate, paraffin oil, 2- octyl dodecanol, propylene glycol, dicaprylocaprate (Labrafac®), Soya lecithin, Squalene. Generally digestible oils from natural sources are preferred. For topical delivery, use of oleic acid, linoleic acid, and decanoic acid will give an additional benefit as they are penetration enhancers. Liquid lipids and solid lipids for the preparation of NLCs are selected based on the relative drug solubility (28,29).

Surfactants used to prepare NLCs are usually selected based on their emulsification capacity (12). Hydrophilic, Lipophilic and Amphiphilic emulsifiers are used to stabilize the lipid dispersions.

Hydrophilic emulsifiers used are Pluronic® F68 (poloxamer 188), Pluronic® F127 (poloxamer 407), Tween 20, Tween 40, Tween 80, polyvinyl alcohol, Solutol® HS15, trehalose, sodium deoxycholate, sodium glycocholate, sodium oleate.

Lipophilic emulsifiers used are Myverol® 18-04K, Span 20, Span 40, Span 60 Amphiphilic emulsifiers used are Egg lecithin, soya lecithin, phosphatidylcholines, phosphatidy lethanolamines, Gelucire® 50/13 (28, 29, 30).

8. Cosmetic Benefits of NLC

Recognition of NLCs in cosmetic industry is due to its pearlaceous morphology and nano size. Their composition, high drug pay load, stability, protective and occlusive property makes them popular in this field (31). Some of the important benefits are mentioned below.

8.1 Occlusive effect : The lipid nano particles form a single layered film on the skin because of its high lipid composition and submicron size. Adhesive action due to the film formation prevents the water loss from the skin thus producing a moisturizing effect (32). This feature is effectively used in anti-aging formulations where moisture retention is the most important requirement (33)

Skin aging can be due to intrinsic or extrinsic factors. Intrinsic aging occurs with age and is inevitable. This is due to decreasing sweat/ oil glands, collagen and elastin which makes skin less elastic and more fragile. The occlusive effect of NLCs on skin causes rapid hydration and may improve the elasticity (34).

Lucia Montenegro et al. formulated a gel of NLCs containing rosemary essential oil (EO). Rosemary essential oil (EO) contains flavonoids and terpenes and hence possesses numerous therapeutic activities such as antioxidant, anti-inflammatory, fungicidal, antimicrobial, and anticancer activities. Studies have showed that rosemary essential oil (EO) can be used to treat many skin disorders. Skin hydration and improvement in skin elasticity was proven from the *in vivo* study, making it a suitable candidate for topical formulations (35).

8.2. Protective action against UV rays : The crystallinity of NLCs aids in the protection of the skin from harmful UV radiations. This property can be attributed to the light scattering property of their crystalline structure. This inherent property can be synergized by inclusion of a sunscreen agent into NLCs (36, 37). UV-blocking materials of ethylhexyl methoxycinnamate, oxybenzone, and avobenzone, were formulated into NLCs as a sun screen formulation by Chen et al. The Sun Protection Factor (SPF) and UVA-protection factor (PFA) was 51.5 and three stars respectively for

the optimized formulation. The crystallinity index of the optimized formulation was found to be maximum, further emphasizing it's UV blocking ability (38).

8.3. Aesthetic Appearance : The presence of lipid dispersion gives an elegant appearance to these nano carriers. This may be due to the whitening effect of the lipid (39). The undesired pigment of vitamin E was masked by formulating it into SLNs. So, the incorporation of active ingredients of cosmetics into NLCs/SLNs improve the customer acceptance by giving it an attractive appearance (40).

8.4. Stability improvement : The improvement of stability of the active ingredients, incorporated into NLC is attributed to the presence of spatially unlike lipids. These dissimilar lipids lead to a highly disarranged moleculular structure which has high encapsulation ability. This uniqueness of the NLC Matrix is used to encapsulate drugs which are unstable or undergo physical or chemical degradation (41,42). Solubility of the drug in the lipids is an important criteria for attaining this stability. So the lipid must be selected based on its ability to solubilize the drug (12,43).

A novel whitening agent Phenylethyl resorcinol was formulated into NLCs to overcome the drawback of photo degradation by Kim et al. The encapsulation efficiency was 93.1 ± 4.2% and loading capacity was 8.5 ± 0.4%. The stability test was performed for 3 months at 4 °C in the dark and 25 °C under daylight and the results showed excellent photo stability of the NLC loaded Phenylethyl resorcinol. The tyrosinase activity was efficiently reduced in melanoma cells indicating development of effective whitening agents (44).

8.5. Use of NLCs in perfumes : Perfumes are sweet-smelling liquids made from essential oils extracted from flowers and spices and are used to give an attractive/pleasant smell to one's body (45). Rapid loss of perfume action due to evaporation of the solvent is a major challenge in formulation of perfumes. Incorporating perfumes into emulsions containing oils is one approach to prolong their effect. Substituting lipid mixtures for liquid lipids (oil) of o/w emulsions leads to the formation of a solid matrix. This may result in slower release of the perfumes from this matrix compared to the emulsion (46). Hence NLCs could be used for the incorporation of perfumes

Perfumes like CA, CT and Kenzo was loaded into NLC by Aiman Hommoss. Panel nose test was performed to confirm its suitability. Perfume intensity was evaluated for 3, 6, 18, 24, 28 and 48 h. The towels treated with softeners containing the perfume-loaded NLC (Kenzo NLC) showed high intensity (47). Table 2 gives the cosmetic applications of NLCs.

9. Dermal Benefits of NLC : Local delivery of drug to the skin by NLC is a major interest of study; as it is aimed in providing site specific action. The Main advantage of targeted delivery is that it avoids systemic exposure of the drug. Reduced systemic reach of drug reduces the toxicity associated with it. The formulation used for local action should be designed in such a way that the drug must not reach the viable dermis, as it may be absorbed by the capillaries into the blood (53,54, 55).

In order to attain the topical action of NLCs, they must be incorporated into aqueous or semi solid dispersion. Incorporation of viscosity enhancers (hydroxypropyl methylcellulose, xanthan gum, hydroxypropyl methylcellulose, chitosan and Carbopol®) will be useful to attain the required consistency. The popularity of NLCs in topical applications is due to its ability to incorporate huge amount of drugs in the disordered matrix. These nano carriers on application achieve close contact with the stratum corneum due to its nano size. This will increase the drug flux and cause the drug to accumulate in the skin appendages resulting in the release of the drug in a controlled fashion to the site of action (28,56).

Broad range therapeutic molecules which show systemic adverse effects can be delivered through this formulation for obtaining efficient management of the disease, Betamethasone

Table No 1: Evaluation of NLCs

Test Parameter	Objective/Method	Reference
Particle size	Photon Correlation Spectroscopy (PCS) based on laser light diffraction	15
Poly dispersability index	Measures the particle size distribution	16
Entrapment efficiency	Total drug encapsulated within NLCs can be determined by UV spectroscopy	17
FT-IR Spectroscopy	Used to determine the compatibility between the excipients and active moiety	18
Zeta potential	Measures the electric potential of a particle determined by Dynamic Light Scattering (DLS) principle (electrophoresis measurement).	19
Shape	Involves determination of lamellarity of particles by Scanning electron microscopy (SEM)	20 21
Morphology Crystalline index	Atomic Force Microscopy (AFM) Differential scanning calorimetry (DSC)and X ray diffraction	22 23
Drug release	*In vitro* diffusion method	24

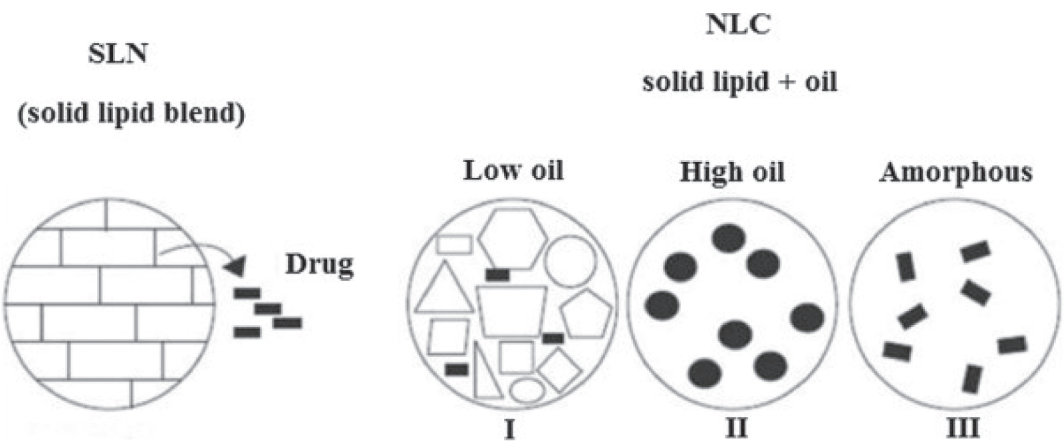

Figure 1: Representation of drug accommodation in SLN and NLC (13, 14)

Table No 2: Cosmetic Applications of NLCs

Active ingredient	Lipids used	Use	Method of preparation	Outcomes	Reference
Ascorbyl palmitate	Witepsol1 E85 Miglyol1 812	Anti -oxidant, Moisturizer	High pressure homogenization.	Moisturizing effect and skin penetration effect of Ascorbyl palmitate encapsulated in SLNs and NLCs was studied on 10 female Caucasian volunteers, the results proved to be better compared to the placebo.	48
1.2 Coenzyme Q10	Cetylpalmitate, Miglyol 812	1.3 Anti-ageing	1.4 High pressure homogenization	1.5 Tape-stripping test showed that Coenzyme Q10-loaded NLCs had improved skin penetration compared to the reference emulsion and liquid paraffin	49
1.6 Coenzyme Q10 and retinaldehyde co-loaded	Compritol 888 ATO Isopropyl Myristate	Management of wrinkles	high shear homogenization	1.7 Anti-wrinkle effect was studied by applying the formulation on wrinkle induced mice. Reduction in the epidermal thickness and recovery from wrinkle was observed.	50
CA, CT and Kenzo	Apifil, Dynasan 116 and Precifac ATO 888	Perfume	High pressure homogenization	Panel nose test confirmed slower release of the perfume with high intensity from the lipid matrix of the NLC	47
Oxybenzone	Glyceryl monostearate Miglyol 812 and oleic acid	Sun screen	Solvent diffusion method.	Oxybenzone-loaded NLC gel showed higher *in vitro* sun protection factor and erythemal UVA protection factor with very low irritation tendency to the skin.	51
Phenylethyl resorcinol	Glycerol monostearate olive oil were	Skin whitening	Hot-melted ultrasonic method.	Tyrosinase activity was significantly reduced by PR-NLCs, skin whitening effect was proven	44
Titanium dioxide (TiO2)	Dynasan 118 Dynasan 114, cetyl palmitate, Compritol 888 carnauba wax ,Miglyol 812,	Sunscreen	High pressure homogenization	UV blocking ability was assessed by measuring β-carotene concentration. The concentration was higher in TiO_2-loaded NLC cream compared to the conventional	47
	Decyl oleate			cream. Hence it was proved that lesser concentration of TiO_2 was required for the activity.	
Tretinoin	stearic acid oleic acid	Skin anti-aging	Hot melt probe sonication method	The optimum tretinoin NLC formulation showed slow release for about 360 min and lesser skin irritation as compared to the marketed gel formulation.	52

Table No 3: Dermal Application of NLC

Active ingredient	Lipids used	Use	Method used	Outcomes	Reference
Betamethasone dipropionate (BD)	Precirol ATO 5, oleic oil	Atopic dermatitis (AD).	Melt emulsification	The skin retention study was proved by the tissue distribution test, which showed order of BD distribution as skin > muscle > blood.	57
Clobetasol propionate	Compritol® ATO 888 and oleic acid	Eczema	Hot high-pressure homogenization technique	Carrageenan-induced hind paw inflammation method was used to compare the anti-inflammatory activity of C -NLCs with marketed formulation. The formulation showed appreciable reduction in inflammation, in a sustained manner.	59
Dutasteride	Stearic acid Phosal® 53 MCT	Benign Prostate Hyperplasia (BPH) to promote hair Growth	Melt-dispersion & ultrasonication method	A slow release for first 12 h was seen with DST- NLCs coated with CSO-SA. *In vivo* diffusion studies proved low permeability of the formulation into the blood, indicating good skin retention.	60
Halobetasol propionate (Hb)	Precirol, LAS	Vitiligo	High pressure homogenization	Larger particles with small polydispersity index were obtained by increasing the lipid composition. The encapsulation efficiency was greater than 90 % and size was less than 200 nm	61
2 Lidocaine (LID)	Compritol 888 ATO and Precirol ATO 5	Local anesthetic	Ultrasound dispersion	*In vivo* test included comparison of the guinea pig response to the pinprick test by LID SLN gel, LID NLC gel, and a marketed	62

dipropionate loaded nanostructured lipid carriers were formulated by Kong X et al., using precirol ATO 5 and oleic oil (OA) through the melt emulsification method. The optimum W/O ointment of BD-NLC showed highest skin retention and with very minimal amount of drug in the blood . Hence it was concluded that topical administration of BD-NLC can be affectively used to treat atopic dermatitis with reduced systemic side effects **(57).**

Thymol, a constituent of thyme oil from the plants of the Thymus genus is proven to have anti-inflammatory, antibacterial, antioxidant, anesthetic and antipsoriatic activity. Pivetta T et al. encapsulated thymol in NLCs using natural lipids - Illipe butter and Calendula oil through the sonication method. The NLCs were incorporated into gels to give them an appropriate rheological nature. *In vivo* studies indicated effective anti-inflammatory and anti-psoriatic activity in mouse models of skin inflammation and imiquimod-induced psoriasis (58). Table 3 gives the dermal application of NLC

10. Transdermal benefits of NLC : Non invasiveness, easy administration, maintenance of steady plasma drug concentration and avoidance of degradation by GIT are the important features of TransDermal Delivery System (TDDS). These advantages has made TDDS more popular and one of the most patient accepted systems

Table No 4: Transdermal applications of NLCs

Active ingredient	Lipids used	Use	Method used	Outcomes	Reference
Diclofenac	Glyceryl monostearate, lanolin PEG-75 Phospholipon® 90G Precirol® ATO 5	Anti-inflammatory and analgesic	Hot homogenization followed by ultra-sonication	Diclofenac NLC Gel 1 with particle size of 50 nm showed effective *in vivo* anti-inflammatory activity.	75
Meloxicam (MLX)	Cetylpalmitate, caprylic acid	Osteoarthritis and rheumatoid arthritis)	Microemulsion template strategy	MLX-NLC dispersed in carbapol 940. MLX NLC gel showed promising anti-inflammatory action by inhibiting edema by 78.23 % in carrageenan induced rat paw edema after 24h	76
Methotrexate (MTX)	Stearic acid Gelucire ® 50/13	Rheumatoid arthritis	Hot micro-emulsion method by using high shear homogenizer	Effective reduction in the concentration of pro inflammatory cytokinines by MTX NLC gel compared to MTX gel (marketed)	77
Pioglitazone	Apifil labrasol	Antihyperglycemic	Hot homogenizati-on followed by ultrasonication	*In vivo* anti diabetic study was carried out for Piosys tablet (marketed tablet) and Pioglitazone NLC-based transdermal therapeu tic system (PNLG-TTS). The blood glucose reduction by PNLG-TTS was up to 101.87 mg for 24 h and from Piosys tablet 108.87 mg at 6 h.	78
5 Sildenafil citrate	Cetyl palmitate Cremophor® RH 40	Erectile dysfunction	High-shear homogenization	SLNs and NLCs of sildenafil were compared for transdermal permeation. Due to smaller particle size of NLCs, better permeation potential was observed.	79
Simvastatin and Olanzapine	Oleic acid and Tripalmitin	Schizophrenia	Hot High Pressure Homogenization (HPH) technique,	Cytotoxic study was carried out to study the toxic effect of the Patch by evaluating viability of cell in HaCat cell line. The results proved reduction in cytotoxic effect of simvastatin by the lipid nanoparticles.	(3)

as compared to the conventional oral and intravenous systems (67,68 ,69).

The most important task of TDDS is penetration through the stratum corneum which is a protective barricade of skin. As discussed earlier, NLCs are an effective method for improving the skin penetration. This penetration enhancement is due to the hydration effect caused by the adhesive action of these carriers . In addition, their nano size gives an additional advantage; felicitating it to creep through the skin barriers and reach the systemic circulation (70).

The advent of NLCs owes to the drawbacks associated with the first generation lipid particulate system i.e. Solid Lipid Nanoparticles. NLCs hold good drug loading capacity and prevents drug expulsion and improves the stability. NLCs forms a depot at the site of application and releases the drug in a controlled pattern thus used in chronic disease conditions (41,71,72,73).

Bhaskar K et al. formulated flurbiprofen loaded NLCs and SLNs for transdermal delivery. The prepared lipid particles were incorporated into a hydrogel to ease topical application .The blood samples were collected from the tail vein of the wistar albino rat at regular intervals and pharmacokinetic and pharmacodynamic parameters of hydro gel and oral formulations were compared. The hydrogels with the NLCs and SLNs of flurbiprofen showed sustained release for nearly 24 hours when compared to the oral formulation. The gel edifice of the formulation was responsible for the slow sustain release and prolonged anti-inflammatory activity (74). Table 4 gives the transdermal applications of NLCs .

11. Conclusion

The advantage of NLCs over the conventional nano systems have made them a promising mode of drug delivery. The cosmetic industry has seen a massive increase in their usage. The number of marketed NLC cosmetics has increased since their invention. Increased patient compliance and improved bioavailability has made transdermally administered NLCs more accepted. NLCs for pulmonary and ocular delivery are gaining importance and has great potential for the near future.

Abbreviation

AFM: Atomic Force Microscopy
CA: It is the natural green apple fragrance provided by the company PharmaSol (Berlin, Germany).
CSO-SA: chitosan oligomer-stearic acid
CT: It is the natural lemon fragrance provided by the company Quest PharmaSol (Berlin, Germany).
Kenzo: It is a mixture of volatile oils provided by the company Kimex (Seoul, South Korea)
DSC: Differential scanning calorimetry
GRAS: Generally regarded as safe
PIT : Phase inversion temperature
SEM: Scanning electron microscopy
SLN: Solid lipid Nanoparticles
SPF: Sun protection factor
TDDS: Transdermal drug delivery system
TiO_2: Titanium Dioxide
U V: Ultraviolet

Acknowledgement:

The authors express their sincere gratitude to The Management, Krupanidhi Group of Institutions for supporting the work through Krupanidhi Research Incubator Centre (K-RIC) program under the Krupanidhi College of Pharmacy and to Dr. S. Parthasarathi, Accendere, CL Educate Ltd.

Reference

1. Prausnitz, M. R. and Langer, R. (2008).Transdermal drug delivery. *Nat. Biotechnol.* **26,** 1261–1268.
2. Brown, M. B., Martin, G. P., Jones, S. A. and Akomeah, F. K. (2006). Dermal and Transdermal Drug Delivery Systems/ : Current and Future Prospects. 175–187. doi:10.1080/10717540500455975
3. Mendes, M., Nunes, S. C. C., Sousa, J. J., Pais, A. A. C. C. and Vitorino, C. (2017). Expanding Transdermal Delivery with Lipid Nanoparticles: A New Drug-in-NLC-in-Adhesive Design. *Mol. Pharm.* **14,** 2099–2115.
4. Moser, K. (2001).Passive skin penetration enhancement and its quantification in vitro. *Eur. J. Pharm. Biopharm.* **52,** 103–112.
5. Benson, H. A. E. (2005).Transdermal drug delivery: penetration enhancement techniques. *Curr. Drug Deliv.* **2,** 23–33.
6. Mennini, N., Cirri, M., Maestrelli, F. and Mura, P. (2016).Comparison of liposomal and NLC (nanostructured lipid carrier) formulations for improving the transdermal delivery of oxaprozin: Effect of cyclodextrin complexation. *Int. J. Pharm.* **515,** 684–691.
7. Garcês, A., Amaral, M. H., Sousa Lobo, J. M. and Silva, A. C. (2018). Formulations based on solid lipid nanoparticles (SLN) and nanostructured lipid carriers (NLC) for cutaneous use: A review. *Eur. J. Pharm. Sci.* **112,** 159–167.

8. Hirlekar, R., Garse, H. and Kadam, V. (2011).Solid Lipid Nanoparticles and Nanostructured Lipid Carriers: A Review. *Curr. Drug ther.* **6,** 240–250.

9. Scheuplein, R. J. (1967). Mechanism of Percutaneous Absorption: II. Transient Diffusion and the Relative Importance of Various Routes of Skin Penetration. *J. Invest. Dermatol.* **48,** 79–88.

10. Kaur, S., Nautyal, U., Singh, R., Singh, S. and Devi, A. (2015). Nanostructure Lipid Carrier (NLC): the new generation of lipid nanoparticles. *Asian Pac. J. Heal. Sci.* **2,** 76–93.

11. Iqbal, M. A. *et al.* (2012).Nanostructured lipid carriers system: Recent advances in drug delivery. *J. Drug Target.* **20,** 813–830.

12. Negi, L. M., Jaggi, M. and Talegaonkar. (2014). S. Development of protocol for screening the formulation components and the assessment of common quality problems of nano-structured lipid carriers. *Int. J. Pharm.* **461,** 403–410.

13. Üner, M. and Yener, G. (2007). Importance of solid lipid nanoparticles (SLN) in various administration routes and future perspectives. *Int. J. Nanomedicine* **2,** 289–300.

14. Selvamuthukumar, S. and Velmurugan, R. (2012). Nanostructured Lipid Carriers: A potential drug carrier for cancer chemotherapy. *Lipids Health Dis.* **11.**

15. Elmowafy, M. *et al.* (2017). Atorvastatin-loaded nanostructured lipid carriers (NLCs): strategy to overcome oral delivery drawbacks. *Drug Deliv.* **24,** 932–941.

16. Zhuang, C.-Y. (2010). Preparation and characterization of vinpocetine loaded nanostructured lipid carriers (NLC) for improved oral bioavailability. *Int. J. Pharm.* **394,** 179–185.

17. Tofani, R. P., Sumirtapura, Y. C. and Darijanto, S. T. (2016). Formulation, characterisation, and in vitro skin diffusion of nanostructured lipid carriers for deoxyarbutin compared to a nanoemulsion and conventional cream. *Sci. Pharm.* **84,** 634–645.

18. Sharma, A., Sood, A., Mehta, V. and Malairaman, U. (2016). Formulation and physicochemical evaluation of nanostructured lipid carrier for codelivery of clotrimazole and ciprofloxacin. 9**.**

19. Rizwanullah, M., Amin, S. and Ahmad, J. (2017).Improved pharmacokinetics and antihyperlipidemic efficacy of rosuvastatin-loaded nanostructured lipid carriers. *J. Drug Target.* **25,** 58–74.

20. Das, S., Ng, W. K. and Tan, R. B. H. (2012).Are nanostructured lipid carriers (NLCs) better than solid lipid nanoparticles (SLNs): Development, characterizations and comparative evaluations of clotrimazole-loaded SLNs and NLCs? *Eur. J. Pharm. Sci.* **47,** 139–151.

21. Intakhab Alam, M. (2011).Nanostructured Lipid Carrier Containing CNS Acting Drug: Formulation, Optimization and Evaluation. *Curr. Nanosci.* **7,** 1014–1027.

22. Tamjidi, F., Shahedi, M., Varshosaz, J. and Nasirpour, A. (2013).Nanostructured lipid carriers (NLC): A potential delivery system for bioactive food molecules. *Innov. Food Sci. Emerg. Technol.* **19,** 29–43.

23. Jia, L.-J. (2010).Preparation and characterization of silybin-loaded nanostructured lipid carriers. *Drug Deliv.* **17,** 11–18.

24. Gokce, E. H. (2012).Resveratrol-loaded solid lipid nanoparticles versus nanostructured lipid carriers: evaluation of antioxidant potential for dermal applications. *Int. J. Nanomedicine* **7,** 1841–50.

25. Li, Q. (2017). A Review of the Structure, Preparation, and Application of NLCs, PNPs, and PLNs. *Nanomater. (Basel, Switzerland)* 7.

26. Ganesan, P. and Narayanasamy, D. (2017).Lipid nanoparticles: Different preparation techniques, characterization, hurdles, and strategies for the production of solid lipid nanoparticles and nanostructured lipid carriers for oral drug delivery. *Sustain. Chem. Pharm.* 6, 37–56.

27. Naseri, N., Valizadeh, H. and Zakeri-Milani, P. (2015). Solid Lipid Nanoparticles and Nanostructured Lipid Carriers: Structure, Preparation and Application. *Adv. Pharm. Bull.* 5, 305–13.

28. Beloqui, A., Solinís, M. Á., Rodríguez-Gascón, A., Almeida, A. J. and Preat, V. (2016). Nanostructured lipid carriers: Promising drug delivery systems for future clinics. *Nanomedicine Nanotechnology, Biol. Med.* 12, 143–161.

29. Purohit, D. K., Nandgude, T. D. and Poddar, S. S. (2016).Nano-lipid carriers for topical application: Current scenario. *Asian J. Pharm.* 10, 1–9.

30. Natarajan, J., Vvsr, K. and De, A. (2016). Nanostructured Lipid Carrier (NLC): A Promising Drug Delivery System. *Glob. J. Nanomedicine* 1.

31. Souto, E. B. and Müller, R. H. (2008). Cosmetic features and applications of lipid nanoparticles (SLN®, NLC®). *Int. J. Cosmet. Sci.* 30, 157–165.

32. Loo, C. (2013).. Effect of compositions in nanostructured lipid carriers (NLC) on skin hydration and occlusion. *Int. J. Nanomedicine* 8, 13–22.

33. Estanqueiro, M., Conceição, J., Amaral, M. H. and Sousa Lobo, J. M. (2014). Characterization, sensorial evaluation and moisturizing efficacy of nanolipidgel formulations. *Int. J. Cosmet. Sci.* 36, 159–166.

34. Ma, G. *et al.* Anti-aging cosmetics and its efficacy assessment methods Related content Nitrogen and Phosphorus Pollutants in Cosmetics Wastewater and Its Treatment Process of a Certain Brand Final report of the key comparison CCQM-K106: Pb, As and Hg measurements in cosmetic (cream) Anti-aging cosmetics and its efficacy assessment methods.

35. Montenegro, L. (2017). Rosemary essential oil-loaded lipid nanoparticles: In vivo topical activity from gel vehicles. *Pharmaceutics* 9, 1–12.

36. Müller, R. ., Radtke, M. and Wissing, S. (2002). Nanostructured lipid matrices for improved microencapsulation of drugs. *Int. J. Pharm.* 242, 121–128.

37. Jain, P., Rahi, P., Pandey, V., Asati, S. and Soni, V. (2017). Nanostructure lipid carriers: A modish contrivance to overcome the ultraviolet effects. *Egypt. J. Basic Appl. Sci.* 4, 89–100.

38. Chen, P. C., Huang, J.-W. and Pang, J. (2013). An Investigation of Optimum NLC-Sunscreen Formulation Using Taguchi Analysis. *J. Nanomater.* 1–10 .

39. Aljarada, H., Pyo, M., Müller, R. H. & Keck, C. SmartLipids formulation for " natural " skin whitening.

40. A. Dingler, R. P. Blum, H. Niehus, A., Blum, R. P., Niehus, H., Müller, R. H. and Gohla, S. (1999). Solid lipid nanoparticles (SLNTM/ LipopearlsTM) a pharmaceutical and cosmetic carrier for the application of vitamin E in dermal products. *J. Microencapsul.* 16, 751–767.

41. Jain, S., Patel, N., Shah, M. K., Khatri, P. and Vora, N. (2017). Recent Advances in Lipid-Based Vesicles and Particulate Carriers for Topical and Transdermal Application. *J. Pharm. Sci.* 106, 423–445.

42. Khan, S. (2015).. Nanostructured lipid carriers: An emerging platform for improving oral bioavailability of lipophilic drugs. *Int. J. Pharm. Investig.* 5, 182.

43. Ûner, M. (2006). Preparation, characterization and physico-chemical properties of Solid Lipid Nanoparticles (SLN) and Nanostructured Lipid Carriers (NLC): Their benefits as colloidal drug carrier systems. *Pharmazie* 61, 375–386.

44. Kim, B.S. (2017).The Improvement of Skin Whitening of Phenylethyl Resorcinol by Nanostructured Lipid Carriers. *Nanomaterials* 7, 241.

45. *& quot; DIRECTIVE 2003/15/EC & quot;*

46. Rainer H. Müller, Sven Staufenbiel, C. M. K. , (2014). Lipid Nanoparticles (SLN, NLC) for innovative consumer care & household products. *H&PC Today - Household Pers. Care Today* .

47. Hommoss, A. (2008). Nanostructured lipid carriers (NLC) in dermal and personal care formulations Inaugural-Dissertation.

48. Uner, M., Wissing, S. A., Yener, G. and Müller, R. H. (2005).Skin moisturizing effect and skin penetration of ascorbyl palmitate entrapped in solid lipid nanoparticles (SLN) and nanostructured lipid carriers (NLC) incorporated into hydrogel. *Pharmazie* 60, 751–5.

49. Müller, J. P. R. H. Coenzyme Q10-loaded NLCs: preparation, occlusive properties and penetration enhancement.

50. Nayak, K., Katiyar, S. S., Kushwah, V. and Jain, S. (2018). Coenzyme Q10 and retinaldehyde co-loaded nanostructured lipid carriers for efficacy evaluation in wrinkles. *J. Drug Target.* 26, 333–344.

51. Sanad, R. A., Abdelmalak, N. S., Elbayoomy, T. S. and Badawi. (2010) .A. A. Formulation of a novel oxybenzone-loaded nanostructured lipid carriers (NLCs). *AAPS PharmSciTech* 11, 1684–94.

52. Ghate, V. M., Lewis, S. A., Prabhu, P., Dubey, A. and Patel, N. (2016). Nanostructured lipid carriers for the topical delivery of tretinoin. *Eur. J. Pharm. Biopharm.* 108, 253–261.

53. Dubey, A. & Kamath, J. Nano Structured lipid carriers/ :A Novel Topical drug delivery system. *Int. J. PharmTech Res.* 4, 705-714.

54. Pardeike, J., Hommoss, A. and Müller, R. H. (2009). Lipid nanoparticles (SLN, NLC) in cosmetic and pharmaceutical dermal products. *Int. J. Pharm.* 366, 170–184.

55. Jaiswal, P., Gidwani, B. and Vyas, A. (2016).Nanostructured lipid carriers and their current application in targeted drug delivery. *Artif. Cells, Nanomedicine, Biotechnol.* 44, 27–40.

56. Müller, R. H., Petersen, R. D., Hommoss, A. and Pardeike, J. (2007). Nanostructured lipid carriers (NLC) in cosmetic dermal products. *Adv. Drug Deliv. Rev.* 59, 522–530.

57. Kong, X., Zhao, Y., Quan, P. and Fang, L. (2016). Development of a topical ointment of betamethasone dipropionate loaded nanostructured lipid carrier. *Asian J. Pharm. Sci.* 11, 248–254.

58. Pivetta, T. P. (2018). Development of nanoparticles from natural lipids for topical delivery of thymol: Investigation of its anti-inflammatory properties. *Colloids Surfaces B Biointerfaces* 164, 281–290.

59. Nagaich, U. and Gulati, N. (2016). Nanostructured lipid carriers (NLC) based controlled release topical gel of clobetasol propionate: design and in vivo characterization. *Drug Deliv. Transl. Res.* 6, 289–298.

60. Noor, N. M., Sheikh, K., Somavarapu, S. & Taylor, K. M. G. Preparation and characterization of dutasteride-loaded nanostructured lipid carriers coated with stearic acid-chitosan oligomer for topical delivery. *Eur. J. Pharm. Biopharm.* 117, 372–384 .

61. Lv, J. and Calpena, A. (2016).The exploration of therapeutic target of vitiligo based on butin. *J. Clin. Exp. Dermatol. Res.* 07.

62. Pathak, P. and Nagarsenker, M. (2009). Formulation and evaluation of lidocaine lipid nanosystems for dermal delivery. *AAPS PharmSciTech* 10, 985–92.

63. Aliasgharlou, L., Ghanbarzadeh, S., Azimi, H., Zarrintan, M. H. and Hamishehkar, H. (2016). Nanostructured Lipid Carrier for Topical Application of N-Acetyl Glucosamine. *Adv. Pharm. Bull.* **6,** 581-587.

64. Zhao, J. (2016). Podophyllotoxin-Loaded Nanostructured Lipid Carriers for Skin Targeting: In Vitro and In Vivo Studies. *Molecules* 21, 1549.

65. Iqbal, B., Ali, J. and Baboota, S. (2018). Silymarin loaded nanostructured lipid carrier: From design and dermatokinetic study to mechanistic analysis of epidermal drug deposition enhancement. *Journal of Molecular Liquids* 255.

66. Gaba, B. (2015). Nanostructured lipid carrier system for topical delivery of terbinafine hydrochloride. *Bull. Fac. Pharmacy, Cairo Univ.* 53, 147–159.

67. Alkilani, A. Z., McCrudden, M. T. C. and Donnelly, R. F. (2015).Transdermal Drug Delivery: Innovative Pharmaceutical Developments Based on Disruption of the Barrier Properties of the stratum corneum. *Pharmaceutics* **7,** 438–70 .

68. Merkle, H. P. (1989).Transdermal delivery systems. *Methods Find. Exp. Clin. Pharmacol.* **11,** 135–53.

69. Budhathoki, U., Gartoulla, K. and Shakya, S. (2016).Formulation and Evaluation of Transdermal Patches of Atenolol. *Indones. J. Pharm.* **27,** 196.

70. Palmer, B. C. & DeLouise, L. A. (2016). Nanoparticle-enabled transdermal drug delivery systems for enhanced dose control and tissue targeting. *Molecules* **21,** 7–9.

71. Uchechi, O., Ogbonna, J. D. N. and Attama, A. A. Nanoparticles for Dermal and Transdermal Drug Delivery. doi:10.5772/58672

72. Vvsr, K., De, A. and Natarajan, J. (2017).Glob J Nanomed Nanostructured Lipid Carrier (NLC): A Promising Drug Delivery System. 1.

73. M Surya Tej, K. V. (2016).Nano structured lipid carrier based drug delivery system. *J. Chem. Pharm. Res.* 8, 627–643.

74. Bhaskar, K., Anbu, J., Ravichandiran, V., Venkateswarlu, V. and Rao, Y. M. (2009). Lipid nanoparticles for transdermal delivery of flurbiprofen: Formulation, in vitro, ex vivo and in vivo studies. *Lipids Health Dis.* **8,** 1–15.

75. Nguyen, C. N., Nguyen, T. T. T., Nguyen, H. T. and Tran, T. H. (2017).Nanostructured lipid carriers to enhance transdermal delivery and efficacy of diclofenac. *Drug Deliv. Transl. Res.* **7,** 664–673.

76. Khurana, S., Jain, N. K. and Bedi, P. M. S. (2013).Development and characterization of a novel controlled release transdermal delivery system based on nanostructured lipid carriers gel for meloxicam. *Life Sci.* **93,** 763–772.

77. Garg, N. K., Singh, B., Tyagi, R. K., Sharma, G. and Katare, O. P. (2016). Effective transdermal delivery of methotrexate through nanostructured lipid carriers in an experimentally induced arthritis model. *Colloids Surfaces B Biointerfaces* 147, 17–24.

78. Alam, S. (2016). Nanostructured lipid carriers of pioglitazone for transdermal application: From experimental design to bioactivity detail. *Drug Deliv.* **23,** 601–609.

79. Elnaggar, Y. S. R., El-Massik, M. A. and Abdallah, (2011). O. Y. Fabrication, appraisal, and transdermal permeation of sildenafil citrate-loaded nanostructured lipid carriers versus solid lipid nanoparticles. *Int. J. Nanomedicine* **6,** 3195–205.

Current Trends in Biotechnology and Pharmacy
Vol. 13 (2) 212-231, April 2019, ISSN 0973-8916 (Print), 2230-7303 (Online)

Plant Defensins : Tissue Specific Expression Leading to Distinctive Functions

Arunima Pothana[1, 2], Pooja Bhatnagar-Mathur[1], Richa K Yeshvekar[1,3], Kiran K Sharma[1*]
[1]International Crops Research Institute for the Semi-Arid Tropics (ICRISAT), Patancheru, Hyderabad, 502324, Telangana, India.
[2] Jawaharlal Nehru Technological University, Kukatpally, Hyderabad, 500 085, India.
[3] Centre for Plant Sciences, University of Leeds, Leeds LS2 9JT, United Kingdom
*Corresponding Author : k.sharma@cgiar.org

Abstract

Plant defensins are small, cysteine-rich cationic antimicrobial peptides that possess biological activity towards a broad range of pathogenic organisms. These defense peptides are ubiquitous within the plant kingdom and acts as the first line of plant defense. Plant defensins are expressed in several plant tissues, such as seedlings, leaves, tubers, ûowers, pods, roots and fruits. They are mainly secreted at peripheral layers of cells and play an integral role in protecting storage, developmental and reproductive parts of the plants, against pathogen attack or injury as part of a systemic defense response. The expression of plant defensins might be constitutive or can be induced in response to pathogenic attack, abiotic stress or downstream to hormone signaling pathways. Moreover, most defensins are localized and expressed in particular tissues, performing very specific functions, thereby bestowing various benefits in respective hosts. From past few years plant defensins have become interesting and important candidates in transgenic technology, owing to their multifunctional but specific biological roles, especially for their broad-spectrum antifungal activity. This review summarizes about the biological roles displayed by plant defensins when constitutively over expressed in targeted tissues of transgenic plants, under the control of tissue specific promoters, and the predominant role exhibited by plant defensins in defense and developmental processes of plants.

Key words : Plant defensins, tissue specific, constitutive, floral organs, fruit specific, antifungal activity, promoter induced, genetic engineering, transgenic plants.

1. Introduction

Plant defensins are endogenous antimicrobial polypeptides that form an important component of the plant innate immune system. They are produced as the first line of defense in response to invading pathogens (1, 2, 3). In addition, some plant defensins are also induced in response to environmental stress such as drought, salinity (4, 5, 6), and signaling molecules, including methyl jasmonate (MJ), ethylene (ET) and salicylic acid (SA). These plant defensins have multifarious functions such as antifungal, antibacterial and antiviral activities. They also act as protease inhibitors, leading to insecticidal activity (7, 8). The multifunctional roles exhibited by many plant defensins include growth inhibitory effects against microbial pathogens such as bacteria (gram positive and gram negative bacteria), virus, fungi, protozoa and yeast (9, 2, 10, 11) inhibitors of digestive enzymes like α-amylases and serine proteases, anti-herbivore (12, 13), in abiotic stress tolerance (14, 15), heavy metal tolerance (16), plant development, protection of storage and reproductive organs (17, 18, 19, 8), ion channel blockers in mammalian and microbial cell walls (20, 21), antiproliferic activity (22, 7), boosting the herbicide property of

BAR gene (23, 24), antiparasitic activity (25) and root growth inhibition activities (26). The most widely studied and reported biological role of plant defensins is their antifungal role.

Plant defensins form a small gene family comprised of around 15 to 50 defensins per plant species (27). So far more than 1200 plant defensins have been identified from plant species such as *Arabidopsis thaliana, Medicago truncatula, Brassica rapa, Vitis vinifera*, many legumes and grass species (28, 3). The occurrence of multiple copies of defensins across the genome can be attributed to gene duplication events (29). However, sub-functionalization and neo-functionalization of these duplicate genes over the year lead to vast functional diversity on the defensin family. Though most plant genomes have multiple defensin genes, it is intriguing how only few members of the family are responsible for a specific function (30). For example, two defensins *MtDef1* and *MtDef2* identified from *M. truncatula* show difference in antifungal activity (31), suggesting that different defensins may be play specific functional roles.

The functional specificity of defensins can be reviewed at three levels, (i) tissue specific expression of defensin genes in response to particular conditions (ii) distinct subcellular localization of the protein and (iii) structure-dependent activity with respect to target molecules. There are numerous reports that describe the structures of various plant defensins, and their interactions with potential target molecules (17). Moreover, the mode of action of defensins and related pathways has also been studied. The specificity in biological roles of individual plant defensins can be attributed not only to the large structural disparity in the patterns of interconnected cysteine loops and disulphide bridges (10, 32), but also to their distinct spatio-temporal expression patterns. Although members of the defensin family are expressed ubiquitously throughout the plant organs such as seeds, leaves, tubers, flowers, pods, roots and fruits, individual members are usually expressed in specific organs or in response to particular stimuli (33, 30). For example, defensins play an integral role in protecting storage, developmental and reproductive parts of plants, through high expression in the epidermal cells and stomatal cells, which are likely to be the initial points of pathogen attack or injury (34, 3). Expression of most plant defensins is tissue-specific and developmentally regulated, thereby allowing them to perform specific biological functions (35, 36). Although the protein structures and their contribution to the mode of action of defensins have been well reported (37, 30, 28, 38, 39, 3), a detailed account on tissue specific expression of defensins are lacking. This review summarizes how the tissue specific expression imparts more specificity to the function of individual defensins.

2. Structure of plant defensins

Plant defensins were initially identified in the seeds of wheat and barley and were grouped as distant members of the thionin family due to homogeneity in molecular mass, amino acid sequence and the number of cysteine residues (40, 17, 10, 3). However, later studies revealed that these proteins differed in structure, pattern of disulfide bridges and spacing of cysteine residues, demonstrating that they were not a part of thionins, but an independent family (17, 2, 41). In subsequent years these peptides were termed as plant defensins after the identification and characterization of two novel antifungal proteins from *Raphanus sativus Rs-AFP1* and *RsAFP2* (40). Plant defensins are small, globular, cysteine rich cationic peptides with molecular masses between 5-7 kDa (37, 42, 43, 38, 44). The three-dimensional structure of plant defensins is highly conserved with a pattern of eight cysteine residues stabilized by four disulphide bonds, interconnected with three antiparallel beta-sheets and one alpha-helix which is in turn stabilized by a structural motif CS-$\alpha\beta$ (28, 45).

Plant defensins can be classified in to two groups based upon the structure of the mature transcript. The first consists of a signal peptide with size 25-30 amino acid residues, an acidic rich precursor protein (except *Ha-DEF1*, *Lm-def*, *PCP-A1* and *TAD1*) and a mature peptide, basic

in nature with about 45-54 amino acids (37, 30). The signal peptide helps in targeted subcellular localization and mitigates the biological activity of mature peptide when required. The mature peptide is composed of eight strictly conserved cysteine residues that are intended in four intrachain disulfide bridges responsible for the stabilization of the typical defensin structure. These intra-connected disulfide bridges form the CS-$\alpha\beta$ motif that is responsible for typical antimicrobial activity exhibited by plant defensins (28, 45, 46). Although most plant defensins contain four disulphide bridges in its structure, some peptides *PhD1* and *PhD2* from *Petunia hybrid*, contain the fifth disulphide bridge interconnecting the α-helix and the β1-strand, further improves stability of the defensin peptide structure (47). The second group of defensins has an additional carboxy-terminal pro-domain, observed especially in solanaceous species.

X- ray crystallography studies of certain defensins such as *R. sativus* (*RsAFP1*), *Nicotiana alata* (*NaD1*), *Pachyrrhizus erosus* (*SPE10*), *P. hybrida* (*PhD1*), *Pisum sativum* (*Psd1*) and *Saccharum officinarum* (*Sd5*) (48, 49, 47, 50, 51, 52) revealed that carboxy-terminal domain is composed of high content of acidic and hydrophobic amino acids (33 amino acids) along with signal peptide and mature defensin domain (30). This acidic nature of the pro-domain is used to neutralize the basic nature of the mature defensin domain leading to neutrally charged peptide. In addition, carboxy terminal domain also acts as a targeting sequence for sub-cellular sorting, post-translational proteolytic processing and intermolecular steric chaperone (47, 30). Another highly conserved motif found in the plant defensin structure is the γ-core. This motif comprises of two antiparallel β-sheets with an interposed turn region called the $\beta2\beta3$ loop. The β-core is cationic amphipathic motif contains specific residues proline and cysteine, that contributes to the secondary structure and amphipathicity of the motif (53). This motif plays an important role in the antifungal activity of defensin peptides, by inducing effective membrane permeabilization in susceptible fungi (54, 55, 2).

Multifunctional roles and mechanisms of action displayed by plant defensins is been illustrated in detail, along with the signaling cascades and pathways using case studies *RsAFP1* and *RsAFP2* from *R. sativum*, Psd1 from *P. sativum* pods, *MsDef1* from *M. sativa*, and *MtDef4* from *M. truncatula*, and *NaD1* from *N. alata*, *DmAMP1* from the seed of *Dahlia merkii*, *HsAFP1* antifungal peptide *Heuchera sanguinea* (28, 2, 3). The proposed mechanisms include three steps, first is receptor-mediated internalization- defensins specifically interacts with the lipid rafts of fungal plasma membrane composed of sphingolipids and phospholipids, the most common spingolipids is glucosylceramide (GlcCer) (56, 2). Different plant defensins have been shown to interact with different classes of sphingolipids, for example the plant defensin *RsAFP2* from *R. sativam* interacts with GlcCer (57), whereas the plant defensin *DmAMP1* from *D. merkii* interacts with mannosyl di-inositol phosphoryl ceramide ($M(IP)_2C$) (58) . In contrast, the plant defensins *NaD1* from *N. alata* was recently shown to interact with a variety of phospholipids, including phosphatidyl inositol mono-/bis-/tri-phosphates, phosphatidyl serine and phospatidic acid, but not with sphingolipids (59). Second is membrane translocation- upon interaction plant defensins are either internalized in to the fungal cell and interact with intracellular targets, or they stay at the cell surface and induce alteration of membrane integrity and distorts the membrane permeability (60, 61). The third is membrane permeabilization thus results in an increased Ca^{2+} uptake and K+ efflux and ultimately leads to cell death through induction of signaling cascades (62, 63). Kushmerick et al. (1998) have described the ability of plant defensins *1-zeathionin* and *2-zeathionin*, isolated from *Zea maize* kernels in block Na^+ ion-channel on fungal membrane, which leads to fungal membrane impermeability followed by fungal death. Likewise the ability of *MsDef1* isolated from *M. sativus* seed tissue to block L-type Ca^{2+} channels of fungal membranes. A specific γ-core motif (RGFRRR) is been identified in the *MtDef4* sequence acts as translocation

tissue specific expression leading to distinctive functions

Vol. 13 (2) 212-231, April 2019, ISSN 0973-8916 (Print), 2230-7303 (Online)

signal required for fungal cell entry (64). Alternatively, ROS production and oxidative stress, most often play a role in defensin-mediated cell death, as has been reported in *RsAFP2, HsAFP1, DmAMP1*, and *NaD1* defensins (52, 65, 66, 67).

3. Tissue specific localization and expression of plant defensins:

Plant defensins are widely distributed in various tissues across the plant. At least one defensin gene is expressed in each plant tissue and some tissues show expression of two or more defensins. The tissue specific localization and expression patterns of these peptides unfold the critical roles they play in defense and development of plants (68). Plant defensins have been identified in leaves, tubers, flowers, pods, seeds, germinating seeds, seedlings and also localized in other peripheral sites like xylem, stomata, and stomata cells, parenchyma cells, where they are expressed either constitutively or upon pathogenic infection, by mechanical wounding and other stress responses (69) Fig. 1. Overall, most of plant tissues constitutively express two or more defensin genes, implying that each defensin is expressed under specific conditions or in specific tissues and display target-oriented functions (Table-1).

Amongst the numerous plant defense peptides isolated from a variety of plant species certain deliver tissue specific expression, for instance four defensin genes isolated and characterization from *Heliophila coronopifolia* (*Hc-AFP1-4*), have a tissue-specific expression patterns confirmed by differential gene expression studies in the native host. The peptides *Hc-AFP1* and *3* expressed in mature leaves, stems and flowers, whereas *Hc-AFP2* and *4* are exclusively expressed in seed pods and seeds. All four peptides were active against two test pathogens *Botrytis cinerea, Fusarium solani,* but displayed different levels of antipathogenecity and modes of action. The expression patterns of the peptides suggests role in protecting vegetative and reproductive structures against pathogen attack, but their roles in plant developmental and physiological processes have not been clearly distinguished yet (8).

3.1 Seedlings : *SPI1*defensin (PR-12)-like protein from *Picea abies*, was found to be expressed only in the radicles, roots, stem, and aerial part of seedlings, but was not detectable in the embryo (70). In more mature plants, expression was observed in leaves most predominantly in epithelial cells such as guard cells of stomata (71), since stomata are the main entryway used by many

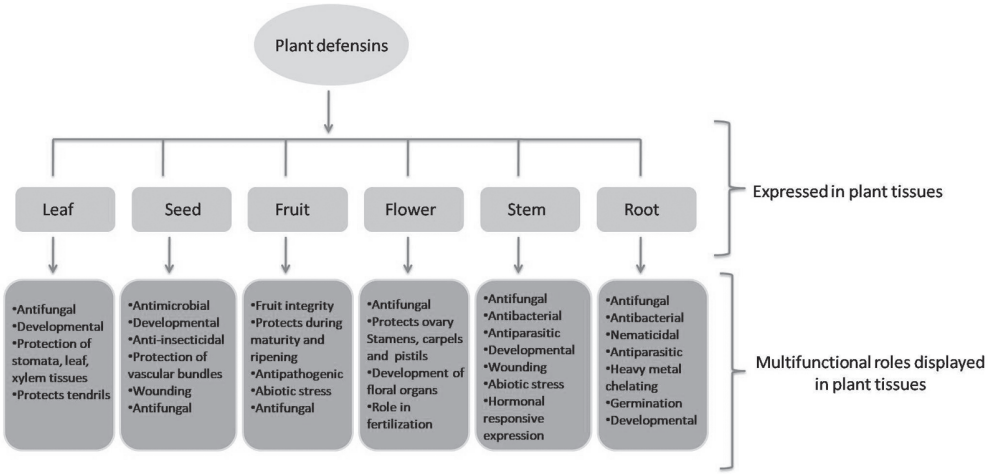

Fig.1. Schematic representation of multifunctional roles displayed by plant defensins in various tissues.

Vol. 13 (2) 212-231, April 2019, ISSN 0973-8916 (Print), 2230-7303 (Online)

Table 1. Overview of defensin genes from various plant sources, there tissue specific expression leading to characteristic biological activity and transgenic applications.

Plant species	Defensin gene	Expressed in Tissues	Induced by signaling compounds	Transgenically expressed in	Biological role	References
Arabidopsis thaliana	*Pdf2.2, Pdf2.3, Pdf 1.2, Pdf2.1* *Thi2.1*	seedlings, roots, leaves, stems, flowers. flower	MJ, ET JA		antifungal activity, nematicidal activity developmental role,	(99, 100, 72) (87)
Brassica campestris, Brassica pekinensis	*BSD1*	flowers			protecting reproductive organs	(82)
Brassica juncea	*Bjdefensin*	leaf, roots	JA		induced by biotic and abiotic stresses	(96)
Brassica oleracea	A1(*PCP-A1*)	flower			development of floral organs	(88)
Capsicum annuum	*J1-1* *CaDef*	fruit leaf		*Solanum esculentum*	antifungal activity	(91, 108)
Citrullus lanatus	*Cldef2.2*	leaves, roots, stems	MJ, SA, ET		antifugal activity	(95)
Carica papaya	*pdf1.1, pdf1.2*	fruit	MJ		protects vegetative and reproductive tissues	(101)
Fragaria ananassa	*FaDef1*	fruit			antifungal activity	(92)
Heliophila coronopifolia	*Hc-AFP2,4* *Hc-AFP1*, 3	seed leaves, stems , flowers			protecting vegetative, reproductive organs, antifungal activity	(8)

tissue specific expression leading to distinctive functions

Medicago truncatula	*DEFLs MtDef1.1, MtDef2.1 MtDef4.2*	root, seeds	MJ	*Triticum aestivum Arachis hypogeae*	antipathogenic activity antifungal activity	(77, 78, 79, 80)
Medicago sativus	*MsDEF1*	seed	MJ		antifungal activity	(31)
Nicotiana alata	*NaD1*	flowers			protects of the reproductive organs	(47)
Nicotiana megalosiphon	*NmDef*	leaf		*Nicotiana tobacum, Solanum tuberosum*	inhibits oomycetes	(112)
Oryza sativa	*CAL1* *PRP1* promoters	root Leaf, stem, grain		*Triticum aestivum, Oryza sativum*	chelating Cd ions protecting storage and reproductive organs	(81) (36)
Picea abies	*SPI1*	radicles, roots, stem, seedlings, leaves			antifungal activity	(70, 71)
Pisum sativum	*Psd1*	pods			antipathogenic role	(62)
Pisum sativum	*DRR230-a, DRR230-b, DRR230-c*	leaves, stems, flowers			antipathogenic activity	(74)
Prunus persica	*PpDfn1*	bark			antifungal activity	(93)
Picea glauca	*PgD PgD1 promoters*	leaf, roots	JA	*Arabidopsis thaliana*	antifungal activity	(102, 114)
Pinus sylvestris	*Sp-AMP2*	leaf		*Nicotiana tobacum*	inhibits necrotrophic pathogens	(113)

Raphanus sativus	*RsAFPs*	seeds		*Niotiana tobacum, Oryza sativum*	antifugal activity	(40, 109)
Solanum lycopersicum	*DF1*, *DF2* *DEF2*	leaf leaf , seed			antifungal activity, protection of developmental and storage organs	(73)
Sorghum bicolor		leaf, roots			insecticidal activity, antifungal activity	(90)
Triticum aestivum	*PDF3, PDF5, PDF30* *PRP1*	seed leaf, stem, grain		*Oryza sativum*	antipathogenic activity, protecting storage, reproductive organs	(75, 36)
Torenia fournieri	LURE	flowers			role in pollen tube attractants during fertilization	(18)
Vitisvinifera	*VvAMP2*	flowers			antifungal activity, protects the reproductive organs	(86)
Vigna unguiculata	*VuDEF*	seed			insecticidal activity	(12)
Vigna radiate	*VrD1*	seed			insecticidal activity	(9, 94)
Wasabi japonica	*WD*	root		*Nicotiana tobacum, Lycopersicum esculentum*	antifungal activity	(107)
Zea Maize	*1-zeathionin, 2-zeathionin*	kernels			antifungal activity	(20)
Zea mays	ZmES4	flowers			role in pollen tube attractants during fertilization	(19)

tissue specific expression leading to distinctive functions

leaf infecting fungal pathogens. Likewise, *A. thaliana* defensins *Pdf2.2* and *Pdf2.3* were expressed in seedlings, roots, leaves, stems, and flowers. Besides *Pdf2.1* gene was strongly expressed in syncytia region of roots in host plants, which is a feeding site of beet cyst nematode *Heterodera schachtii,* apart from the feeding site it was expressed only in siliques but *not in other healthy tissues*. Hence the promoter of the *Pdf2.1* gene turned out to be an interesting candidate to drive root specific expression of nematocidal products that would subsequently inhibit syncytium development (72). In addition, *A. thaliana* defensin *Pdf1.2* may be induced in response to ET and MJ further protects the host by minimizing attack of phytopathogenic fungus *Verticillium dahlia.*

3.2. Shoots and leaves : Defensins and defensin-like peptides are functionally diverse and are commonly presented as an immune reaction between plant and pathogen. High expression levels of the defensin (*DF1* and *DF2*) transcripts were observed in *Solanum lycopersicum* leaf tissues collected from the plants grown in soil treated with *Trichoderma viridae* and *Bacillus subtilis* as biological control agents to suppress the activity of the pathogenic fungi *Fusarium oxysporum* and *Rhizoctonia solani* (73). Lai and colleagues studied about the expression levels of three homologous *Pisum sativum* defensin genes *DRR230-a*, *DRR230-b, DRR230-c* in various *P. sativum* tissues under biotic stress. Relatively high levels of *DRR230-a* and *DRR230-c* transcripts are present in mature leaves and stems, with intermediate expression levels in young leaves, tendrils and flowers, and low levels in roots and pods (1, 74). Three specific defensin genes *PDF3, PDF5,* and *PDF30* expressions were investigated in shoot tissues of seven commercial Egyptian *Triticum aestivum* varieties: Misr1, Giza168, Sakha94, Sids1, Gemmiza7, Gemmiza11, and Shandawel1 during seed germination, showed that there was difference in defensin gene expression among the seven varieties. This included absence of *PDF5* expression in Sids1and *PDF30* expression in Gemmiza7, Misr1 showed lowest and Shandawel1 gave the highest expression levels of the three studied genes. Other varieties represented various degrees of expression for the three genes (75). The observations can be related to the resistance of *T. aestivum* varieties to diseases and abiotic stresses, would certainly contribute information for wheat breeding programs and variety evaluation.

3.3 Roots Mitra and Long, (2004) reported that majority of defensins and defensin like proteins (*DEFLs*) were expressed in root nodules and seeds in *M. truncatula*, since they are the nutrient rich sources, composed of large amounts of protein, polysaccharides, and lipids that provide energy and raw materials for germination and development of the seedling, and also most vulnerable sites for attack of multitude soil pathogens to attack (77). Therefore nodule-speciûc *DEFLs* are engage in complex synergistic interactions with other AMPs to increase their efficiency against broad spectrum microbial population invitro and in field conditions as well (78, 79, 80). Defensins and defensin like proteins also play heavy metal remediating role, by accumulating toxic metal in edible plant parts while producing safe and nutritious edible by-products. Similarly defensin-like protein *CAL1* (cadmium (Cd) accumulation in leaf 1) is expressed preferentially in root exodermis and xylem parenchyma cells of *Oryza sativa*. *CAL1* acts by chelating Cd in the cytosol and facilitating Cd secretion to extracellular spaces, hence lowering cytosolic Cd concentration while driving long-distance Cd transport via xylem vessels. *CAL1* does not allow Cd or other heavy metals accumulation in rice grains, thus providing an efficient molecular tool to agriculture biotechnology, to develop *O. sativa* varieties that produce safe grains while remediating paddy soils (81).

3.4 Flower Several plant defensins and other *DEFLs* are highly expressed in flowers (Lay et al., 2003). These flower abundant antimicrobial peptides were shown to be crucial for plant reproduction, playing different functions during flower fertilization. In *Brassica campestris*

and *Brassica pekinensis* defensin 1 (*BSD1*) was expressed only in stamens of flowers (82). Flower-specific expression of defensin genes was also observed in solanaceous plants like, *N. tabacum* (83), *N. alata* (47), and *N. paniculata* (84). This suggests that flower specific defensin genes are more likely to protect the reproductive organs from effective pathogenic attack. The expression patterns of *N. alata* plant defensin (*NaD1*) was observed in floral organs like anthers, pistils, ovaries and petals of ornamental *N.tobaccum* flowers, and barely expressed in any other organs. *NaD1* expression was highest in young floral buds and decreased significantly as the flower matures. It is noteworthy that this peptide was expressed in the outermost layers of the sepals and petals and in tissues that surround the pollen or pollen tubes. The location of *NaD1* is consistent with its defense role as it protects the germ cells against possible damage by invading pathogens (47). Similar expression patterns were observed in two other floral defensins *FST*, *TPP3* (83, 85). According to Lay et al. (2003), floral defensins are of two types in solanaceous plants. One with C-terminal pro-domain which is deposited in the vacuoles this type is present only in floral buds, and the other type that does not have the C-terminal pro-domain is produced in epithelial layers of cells (47). *V. vinifera* defensin like peptide *VvAMP2* is highly conserved peptides with 10 cysteine residues, and active against the fungal pathogen *Botrytis cinerea*. Quantitative expression analysis revealed that *VvAMP2* and related *DEFLs* are specifically expressed in *V. vinifera* inflorescences, highly expressed in pollen/ stamen, and weak expression was observed in calyptrae and carpels suggesting a role in *V. vinifera* fertilization (86). Similarly *LURE* and *ZmES4*, *DEF* like genes from *Torenia fournieri* and *Zea mays* are highly expressed in the gametophyte synergid cells and functions as pollen tube attractants during fertilization (18, 19).

Plant defensins are also induced in response to plant hormones in floral tissues. For example, the flower defensin *Thi2.1* in *A. thaliana* can be induced by abiotic stress mediated by the activation of SA induction within the systemic acquired resistance pathway (87). In flowers the induction of defensins may also be correlated with flower development suggesting that other factors may be involved in flower defensin gene transcription. An intriguing defensin transcript, Pollen coat protein class A1(*PCP-A1)*, from *B. oleracea*, accumulate in microspores in flower and associated with self-incompatibility systems, further studies are required to elucidate its exact role (88). Certain transcriptional reprogramming like inverse regulation or antisense suppression occurs in host tissues occurs during plant defense activation against pathogenic attack. Stotz et al. (2009) reported the defensin gene *DEF2* expression was observed in developing flowers tissues in *S. lycopersicum*, constitutive over expression of *DEF2* enhances foliar resistance against *B. cinerea* and displayed inversely regulations like reduces pollen viability and seed production, alterations in various developmental and storage organs (73).

3.5 Seed and fruit Recently, microarray analysis in two model plants *A. thaliana* and *M. truncatula* showed a set of defensins and defensin-like genes were expressed specifically in seeds or fruits (89). Plant defensins play a very important role in protection of seed and seedlings from soil borne pathogens (40) *R. sativum* seeds with pathogens infected or mechanically damaged seed coats showed 30 folds increased expression of defensin genes. Various experiments on the location of plant defensins within the seed revealed that they are located in high levels in the peripheral cell layers and in the spaces between different seed organs, middle lamellae of the cell walls of the different seed tissues. Like the other defensins *RsAFPs* is localized in seeds organs where the first contacts with invading fungal pathogens occur. Furthermore, defensin peptides (*Psd1*) isolated from the seed of *P. sativum*, was shown to be localized primarily in vascular bundles and epidermal tissues of *P. sativum* pods, which are the first barriers to pathogen invasion (62). Plant defensins has an important activity like anti-insecticidal inhibition (12). They could interfere

tissue specific expression leading to distinctive functions

with α-amylase enzyme secreted in the insect gut and seize the insect energy derived from the starch degradation activity. Three defensin peptides $SI\alpha_1$, $SI\alpha_2$ and $SI\alpha_3$ isolated and characterized from these seed tissue of plant *Sorghum bicolor* inhibited the amylase activity of insects *Periplaneta americana* and *Locusta migratoria migratorioides* and attributes weak antifungal activity against fungus *Aspergillus oryzae* (90).

Fruits are especially vulnerable to pathogen infection at the fully ripe stage due to significantly high amount of nutrient rich material are stored in fruits, therefore, the putative extracellular localization of antimicrobial proteins like plant defensins enhances the chances of the maintenance of fruit integrity and seed maturation (91). The defensin peptides *J1-1* isolated from *Capsicum annum* is associated with fruit specific expression, but not in other tissues such as leaf, stem, root, flower. Protein levels of *J1-1* were gradually increased in the fruits from the early stage of the ripening to maturity, because this stage is more prone to the infection of anthracnose pathogen, *Colletotrichum gloeosporioides.* Furthermore *J1-1* defensin gene expression levels were likely increased both transcriptional and translationally in infected fruits during ripening. This peculiar characteristic of the *C. annum* defensin was further exploited in developing transgenic *C. annum* plants overexpressing *J1-1*, as expected the products showed increased tolerance to anthracnose fungus (91).

Semi quantitative expressions of defensin genes from *Fragaria ananassa* (*FaDef1*) were analyzed in root, stem, leaf, flower, and fruit tissues in three cultivars namely, Queenelisa, Camarosa, and Paros. The results revealed that higher amount of *FaDef1* expression was observed in developed fruits compared to that of immature fruit, and there was no observable expression in the root. Moreover, *FaDef1* is responsive to biotic and abiotic stress signal compounds and showed significant resistance against *B. cinerea* (92). Hence these peptides may be used as a candidate gene for engineering plants against gray mold. *Prunus persica* defensin gene (*PpDfn1*) is expressed in bark tissues of an year-old shoots, and is also expressed in early fruit development stages. A recombinant version of *rDFN1* was expressed in the yeast, *Pichia pastoris*, the obtained protein inhibited germination of the fungal pathogens *Penicillium expansum* and *B. cinerea*, but not the Gram-negative bacterium *Erwinia amylovora* (93).This study clearly indicated that both physiological role and antifungal potential exhibited by plant defensins in specific tissues. Defensins *VuDEF* expressed in seeds of *Vigna unguiculata* and defensin *VrD1* from *Vigna radiata* expressed in the germinating seed exhibited anti-insecticidal activity against α-amylase enzyme activity in insects *Acanthoscelides obtectus*, *Callosobruchus maculates, Zabrotessub fasciatus*, *Tenebrio molitor* (12, 9, 94).

3.6 Hormone-responsive constitutive expression Defensin-like protein from *Citrullus lanatus Cldef2.2*, had high amino acid homology with the *A. thaliana PDF2* cluster and is close to *AtPDF2.5.* The expression profiles revealed that expression was observed in all the examined tissues, including leaves, roots, and stems, the highest expression level was observed in roots. The protein abundance was observed in various tissues especially when subjected to SA, MJ and ET, also to *F. oxysporum* challenge (95). Similarly, the gene expression studies of *Bjdefensin* gene from source *B. juncea* revealed that the transcript levels of *Bjdefensin* gene increased significantly upon *Alternaria* infection, Jasmonic acid and wounding treatments but was not induced by SA. Consequently, the *Bjdefensin* promoter (2.5 kb) was isolated and cloned upstream of GUS gene in pORER2 vector. In silico studies of *Bjdefensin* promoter showed many important conserved cis-elements, responsive to biotic and abiotic stresses. Histochemical GUS assay showed pathogen-inducible expression of *Bjdefensin* promoter after fungal infection and also induced by JA and wounding (96).

Effect of fungal infection, wounding, various plant hormones and chemicals induces the accumulation of plant defensin transcripts in various tissues (97). As per the literature

chemicals such as mercuric chloride, MJ, ET and paraquat led to the induction of defensin gene expression (97). In *M. truncatula* defensin genes *MtDef1.1* and *MtDef2.1*are highly expressed in dry mature seed and are strongly induced by exogenous MJ application in young seedlings but not by ET or SA (98). Interestingly in closely related *M. sativa*, defensin gene expression is not observed by treatment with MJ, and down-regulated expression was observed by ET treatment (98). The *Arabidopsis* defensin gene *PDF1.2,* has been shown to be induced strongly in leaves by MJ and ET, but not by SA (99, 100). The data presented here suggest that some aspects such as induction of defensin genes via hormones applications or chemicals may not be uniform in inter and interspecific plant species. Similarly, *pdf1.1* and *pdf1.2* is induced in fruit, peel and leaf tissues of papaya upon cold stress and MJ treatment, which suggests the presence of analogous defense mechanisms in the vegetative and fruit tissues of plants (101, 102). Pervieux et al. (2004) demonstrated that *Picea glauca* Defensin 1 (*PgD1*) is up-regulated by wounding and JA in leaf and root tissues, more importantly, that recombinant *PgD1* displays antifungal activity against *Cylindrocladium floridanum*, *F. oxysporum,* and *Nectria galligena* (102).

4. Tissue specific expression of defensin genes in transgenic plants Certain attempts have been made by deploying heterologous defense peptides in many susceptible plants as tools to enhance their disease-resistance capability (103). Although most of them were not so successful, few of them were inspiring in the search for new alternatives (79, 104). The reasons behind might be low expression levels, or low half-life of the transgene or transgene product inactivation by host proteolytic enzymes (105, 106). Numerous studies have demonstrated the efficient role of plant defensins when cloned and expressed in different host plants and assayed against various pests and pathogen exists, most of them were efficacious in invitro and field conditions (2). As already discussed, plant defensin genes are induced by biotic, abiotic factors, during seed germination, flowering and hormonal treatments. They might be constitutively expressed, or show tissue-specific and developmentally regulated expression patterns (35, 36, 17, 19, 47). Plant defensins have been recognized as prominent candidates for generating transgenic crops due to their multifunctional role to pave ways for generating durable resistance against broad range phytopathogens. To validate the presumed role, plant defensins from distinctive plant sources have been cloned and transgenically expressed in various hosts (97, 1, 79). The first attempt was made to evaluate transgenic tobacco plants expressing antifungal defensin genes *Rs-AFP2* source from radish, high levels of peptide expression in leaf and root tissues was observed in transgenic plants, and showed an increasing resistance towards *Alternaria longipes* in invitro assays (40).

Wasabi defensin gene (0.5 kb) gene expression driven by the root-specific *LjNRT2* and *AtNRT2.1* promoters were overexpressed in the roots of transgenic *N. tobaccum* and *S. esculentum* plants showed stable integration and expressed in the root tissues but not in the leaf tissues. In fungal bioassays all transgenic plants showed increased resistance towards *F. oxysporum* compared to non-transformed plants. The study suggests that LjNRT2 and AtNRT2.1 promoters triggered the antifungal gene expression in the roots tissues and conferred increased resistance to the root pathogen *Fusarium oxysporum*. The transgenic products are safe in terms of biosafety issues since the roots of *Solanum esculentum* are not edible (107). Similarly, transgenic *Solanum esculentum* plants expressing the *Capsicum annum* defensin gene (*CaDef*) under the control of CaMV 35S promoter, accumulated defensin peptide in the leaf tissue showed enhanced ability in effective growth inhibition of fungi *Fusarium* sp. and *Phytophthora infestans* in vitro (108).

Jha and Chatoo, (2009) performed a successful attempt of generating transgenic *O. sativa* plants expressing cleavable chimeric gene

constructs consists of a leader peptide and two *Dm-AMP1* and *Rs-AFP2*, defensin genes from the seeds of *D. merckii* and *R. sativus*, driven by control of single maize ubiquitin promoter, peptides were targeted to express at the extracellular spaces of leaf and root tissues. Plants transformed with polyprotein construct showed 70-90% significant disease resistance against *Magnaporthe oryzae* and *Rhizoctonia solani* pathogens (109). Similarly, transgenic *Triticum aestivum* genotypes expressing a chimeric gene encoding an apoplast-targeted antifungal plant defensin *MtDef4.2* from *M. truncatula*, displayed resistance leaf rust pathogens without affecting the root colonization of a beneûcial arbuscular mycorrhizal fungus *Rhizophagus irregularis*. Histo-pathological analysis suggested the presence of both pre- and post-haustorial resistance to leaf rust in these transgenic lines expressing plant defensin *MtDef4.2* can provide substantial resistance to leaf rust disease in transgenic *T. aestivum* without negatively impacting its symbiotic relationship with the beneûcial mycorrhizal fungus (110). Similarly transgenic *Arachis hypogeae* genotypes expressing *Medicago* defensin genes *MtDef4.2, MsDef1* in seed tissues showed enhanced resistance against *Aspergillus flavus* infection and low to non existence levels of aflatoxin accumulation (111). Constitutive expression of *NmDef02* gene derived from *N. megalosiphon*, in leaf tissues of transgenic *N. tobaccum* and *S. tuberosum* plants delivered enhanced resistance against various plant microbial pathogens, including the oomycete *Phytophthora infestans*, causal agent of potato late blight disease, under greenhouse and in field conditions (112).

In addition plant defensins isolated from forest tree species contribute to sustainable forestry practices and the improvement of commercially grown trees to combat many microbial pathogens (113). These AMPs elevate host defense and can be used as molecular markers for resistance breeding. Transgenic *N. tobaccum* plants expressing the gene encoding *Pinus sylvestris* antimicrobial protein *Sp-AMP2,* gene showed enhance resistance and reduced lesions size caused by the necrotrophic pathogen *B. cinerea*. The transcript of *Sp-AMP2* was abundantly secreted in extracellular spaces of leaf and root tissues in most transgenic lines. This study provides an insight into the role of *Sp-AMP2* and its functional and ecological significance in the regulation of plant–pathogen interactions (113). The characterization of tissue-specific and pathogen-inducible promoters is essential for localized expression of defense-related genes. Transgenic *T. aestivum* and *O. sativa* plants were developed through the stable transformation with four defensin promoters pathogen responsive and resistance genes (*PRPI) promoter* from *T. aestivum* and *O. sativa* source, along with GUS reporter gene as fusion constructs. The promoters were active before and at anthesis in both transgenic *T. aestivum* and *O. sativa* plants with activity mainly concentrated in the ovary. In transgenic *O. sativa*, GUS activity was also observed in vascular tissue of lemma and anthers. After fertilization, GUS was strongly expressed in the outer cell layers of the pericarp and in vascular bundle of the grain. *T. aestivum* promoters were active in transgenic rice embryos, roots and coleoptiles. All *T. aestivum* and *O. sativa* promoters were strongly induced by wounding in leaf, stem and grain of transgenic *O. sativa* plants. These results suggest that *PRPI* promoters will be useful for tissue specific targeting and accumulation of proteins for resistance towards pathogens in vulnerable tissues of developing and germinating grains (36). Furthermore, *P. glauca* Defensin 1 (*PgD1*) promoter fragment fused to the uidA gene (GUS) was cloned, characterized in *A. thaliana* and *P. glauca* to analyse spatio-temporal promoter activity. The transgenic plants were subjected JA, wounding and infection by the hemibiotrophic pathogen *Pseudomonas syringae, Ceratocystis resinifera*, showed an up-regulation of both endogenous defensin and PgD1:GUS transgene, in transgenic spruce embryos, expression was clearly restricted to the shoot apical meristem. In *Arabidopsis*, leaves, flowers, guard cells and trichomes showed upregulation of transgene, and

also resistance against infection with the necrotrophic pathogen *Ceratocystis resinifera* and wounding (114). This study demonstrated that inspite of being expressed in evolutionarily divergent hosts *A. thaliana* and *P. glauca*, the promoter fragment appears relatively conserved and fully functional in regulatory mechanism and the defence signaling pathways. A defensin like ORF from *Mytilusedulis chilensis* driven by 35S promoter transformed in to *N. tobacum* plants, showed reasonably good transgene expression in leaf tissues not in other tissues, further offered detectable resistance to *N. tobacum* leaves when challenged with *Pseudomonas syringae* tissues (115).

Conclusions

Plant defensins are important components of the plants innate immunity, and exhibit protective antimicrobial role in various plant tissues and organs. Plant defensins are ubiquitous among different plant species, and are localized in wide range of plant organs, including seeds, leaves, pods, flowers and tubers. The tissue specific localization of plant defensins play a vital role in protection and development of plants, where they are expressed either constitutively or induced upon fungal infection, abiotic stress conditions or mechanical wounding. Plant defensins are mostly secreted in the periphery layers of plant organs, since these locations are consistently prone to stress, they are activated in the initial defense response against pathogens and inturn activate other antimicrobial pathways. Furthermore, plant defensins display an array of biological activities including protein translation inhibition activities and enzyme inhibitors of α-amylases and proteases, antiproliferic, antiparasitic and heavy metal remediation and many more. Considering the broadspectrum antipathogenic activity, tissue specific expression and various developmental roles of plant defensins, they are considered as prominent candidates in agricultural and pharmaceutical biotechnology. For last two decades tremendous scientific efforts were made and progress has been achieved, by using genetic engineering technology in plants. Expression of antimicrobial peptides in specific tissues towards fungal pathogens and their role in enhanced resistance to combat the infection attracted the scientific community. Engineering tissue-specifically expressed plant defensins or pathogen-inducible promoters, to develop the transgenic traits that are effective against a broad range of pathogens. Utilization of chimeric defensin peptides and polypeptide construct shows double impact to enhanced disease resistance. Successful evaluation of transgenic plants for their efficacy against pathogenic attack invitro and in field conditions is a prerequisite to augment in on-going disease management practices. Transgenic plants with targeted expression of defensin genes with enhanced disease resistance can become an integral component of food security and disease management programs in the future.

Acknowledgments

AP acknowledges the Department of Science and Technology, Govt. of India for the fellowship through the INSPIRE FELLOWSHIP, Code No. IF120374

References

1. Wang, Y., Nowak, G., Culley, D., Hadwiger, L. A., and Fristensky, B. (1999). Constitutive expression of pea defense gene DRR206 confers resistance to blackleg (Leptosphaeria maculans) disease in transgenic canola (*B. napus*), Molecular plant-microbe interactions, 12 (5): 410-418.
2. Lacerda, A., Vasconcelos, É. A. R., Pelegrini, P. B., and Grossi-de-Sa, M. F. (2014). Antifungal defensins and their role in plant defense, Frontiers in microbiology, 5: 116.
3. Parisi, K., Shafee, T. M., Quimbar, P., van der Weerden, N. L., Bleackley, M. R., and Anderson, M. A. (2018). The evolution, function and mechanisms of action for plant defensins, In Seminars in cell & developmental biology, Academic Press.
4. Mittler, R. (2006). Abiotic stress, the field environment and stress combination, Trends in plant science, 11(1): 15-19.

5. Takeuchi, H., and Higashiyama, T. (2011). Attraction of tip-growing pollen tubes by the female gametophyte, Current opinion in plant biology, *14*(5): 614-621.

6. Ramegowda, V., and Senthil Kumar, M. (2015). The interactive effects of simultaneous biotic and abiotic stresses on plants: mechanistic understanding from drought and pathogen combination, Journal of plant physiology, 176: 47-54.

7. Lin, P., Wong, J. H., and Ng, T. B. (2010). A defensin with highly potent antipathogenic activities from the seeds of purple pole bean, Bioscience reports, 30(2): 101-109.

8. De Beer, A., and Vivier, M. A. (2011). Four plant defensins from an indigenous South African Brassicaceae species display divergent activities against two test pathogens despite high sequence similarity in the encoding genes, BMC research notes, 4(1): 459.

9. Pelegrini, P. B., and Franco, O. L. (2005). Plant γ-thionins: novel insights on the mechanism of action of a multi-functional class of defense proteins, The international journal of biochemistry and cell biology, 37(11): 2239-2253.

10. Tam, J., Wang, S., Wong, K., and Tan, W. (2015). Antimicrobial peptides from plants, Pharmaceuticals, 8(4): 711-757.

11. Kraszewska, J., Beckett, M. C., James, T. C., and Bond, U. (2016). Comparative analysis of the antimicrobial activities of plant defensin-like and ultrashort peptides against food-spoiling bacteria, Applied and environmental microbiology, AEM-00558.

12. Chen, K. C., Lin, C. Y., Kuan, C. C., Sung, H. Y., and Chen, C. S. (2002). A novel defensin encoded by a mungbean cDNA exhibits insecticidal activity against bruchid, Journal of agricultural and food chemistry, 50(25): 7258-7263.

13. Choi, M. S., Kim, Y. H., Park, H. M., Seo, B. Y., Jung, J. K., Kim, S. T., and Kim, C. K. (2009). Expression of BrD1, a plant defensin from *B. rapa*, confers resistance against brown plant hopper (Nilaparvata lugens) in transgenic rice, Molecules and cells, 28(2): 131-137.

14. Moreira, R., Medri, M. E., Neumaier, N., Lemos, N. G., Pimenta, J. A., Tobita, S., and Abdelnoor, R. V. (2010). Soybean physiology and gene expression during drought, Genetics and molecular research, 9(4): 1946-1956.

15. Ahmed, N. U., Park, J. I., Jung, H. J., Seo, M. S., Kumar, T. S., Lee, I. H., and Nou, I. S. (2012). Identification and characterization of stress resistance related genes of *B. rapa*, Biotechnology letters, 34(5): 979-987.

16. Mirouze, M., Sels, J., Richard, O., Czernic, P., Loubet, S., Jacquier, A., and Marquès, L. (2006). A putative novel role for plant defensins: a defensin from the zinc hyper accumulating plant *A. halleri*, confers zinc tolerance, The plant journal, 47(3): 329-342.

17. Stotz, H. U., Thomson, J., and Wang, Y. (2009). Plant defensins: defense, development and application, Plant signaling & behavior, 4(11): 1010-1012.

18. Okuda, S., Tsutsui, H., Shiina, K., Sprunck, S., Takeuchi, H., Yui, R., and Kawano, N. (2009). Defensin-like polypeptide LUREs are pollen tube attractants secreted from synergid cells, Nature, 458(7236): 357.

19. Amien, S., Kliwer, I., Márton, M. L., Debener, T., Geiger, D., Becker, D., and Dresselhaus, T. (2010). Defensin-like ZmES4 mediates pollen tube burst in maize via opening of the potassium channel KZM1, PLoS biology, 8(6): e1000388.

20. Kushmerick, C., de Souza Castro, M., Santos Cruz, J., Bloch, C., and Beirão, P. S. (1998). Functional and structural features of ã zeathionins, a new class of sodium channel blockers, FEBS letters, 440(3): 302-306.

21. Ramamoorthy, V., Zhao, X., Snyder, A. K., Xu, J. R., and Shah, D. M. (2007). Two

mitogen activated protein kinase signalling cascades mediate basal resistance to antifungal plant defensins in Fusarium graminearum, Cellular microbiology, 9(6): 1491-1506.

22. Wong, J. H., and Ng, T. B. (2005). Sesquin, a potent defensin-like antimicrobial peptide from ground beans with inhibitory activities toward tumor cells and HIV-1 reverse transcriptase, Peptides, 26(7): 1120-1126.
23. Huffaker, A., Pearce, G., and Ryan, C. A. (2006). An endogenous peptide signal in Arabidopsis activates components of the innate immune response, Proceedings of the National Academy of Sciences, 103 (26): 10098-10103.
24. Wang, W. Z., Yang, B. P., Feng, C. L., Wang, J. G., Xiong, G. R., Zhao, T. T., and Zhang, S. Z. (2017). Efficient sugarcane transformation via bar gene selection. Tropical plant biology, *10*(2-3), 77-85.
25. De Zélicourt, A., Letousey, P., Thoiron, S., Campion, C., Simoneau, P., Elmorjani, K., and Delavault, P. (2007). Ha-DEF1, a sunflower defensin, induces cell death in Orobanche parasitic plants, Planta, 226(3): 591-600.
26. Allen, A., Snyder, A. K., Preuss, M., Nielsen, E. E., Shah, D. M., and Smith, T. J. (2008). Plant defensins and virally encoded fungal toxin KP4 inhibit plant root growth, Planta, 227(2): 331-339.
27. Silverstein, K. A., Graham, M. A., Paape, T. D., and VandenBosch, K. A. (2005). Genome organization of more than 300 defensin-like genes in Arabidopsis, Plant physiology, 138(2): 600-610.
28. De Oliveira Carvalho, A., and Gomes, V. M. (2009). Plant defensins-prospects for the biological functions and biotechnological properties, Peptides, 30(5): 1007-1020.
29. Wu, Y., Gao, B., and Zhu, S. (2017). New fungal defensin-like peptides provide evidence for fold change of proteins in evolution, Bioscience reports, 37(1): BSR20160438.
30. Lay, F. T., and Anderson, M. A. (2005). Defensins-components of the innate immune system in plants, Current protein and peptide science, 6(1): 85-101.
31. Spelbrink, R. G., Dilmac, N., Allen, A., Smith, T. J., Shah, D. M., and Hockerman, G. H. (2004). Differential antifungal and calcium channel-blocking activity among structurally related plant defensins, Plant physiology, 135(4): 2055-2067.
32. Schmitt, P., Rosa, R. D., and Destoumieux-Garzón, D. (2016). An intimate link between antimicrobial peptide sequence diversity and binding to essential components of bacterial membranes, Biochimica et biophysica acta (BBA)-biomembranes, 1858(5): 958-970.
33. Thomma, B. P., Cammue, B. P., and Thevissen, K. (2002). Plant defensins, Planta, 216(2): 193-202.
34. Da Silva Conceição, A., and Broekaert, W. F. (1999). 12 Plant Defensins, Pathogenesis- related proteins in plants, 248.
35. Padovan, L., Scocchi, M., and Tossi, A. (2010). Structural aspects of plant antimicrobial peptides, Current protein and peptide science, 11(3): 210-219.
36. Kovalchuk, N., Li, M., Wittek, F., Reid, N., Singh, R., Shirley, N., and Hrmova, M. (2010). Defensin promoters as potential tools for engineering disease resistance in cereal grains, Plant biotechnology journal, 8(1): 47-64.
37. Broekaert, W. F., Terras, F. R., Cammue, B. P., and Osborn, R. W. (1995). Plant defensins: novel antimicrobial peptides as components of the host defense system, Plant physiology, 108(4): 1353.
38. Vriens, K., Cammue, B., and Thevissen, K. (2014). Antifungal plant defensins: mechanisms of action and production, Molecules, 19(8): 12280-12303.

39. Prema, G., and Pruthvi, T. (2012). Antifungal plant defensins, *Current Biotica*, 6: 254-270.

40. Terras, F. R., Eggermont, K., Kovaleva, V., Raikhel, N. V., Osborn, R. W., Kester, A., and Vanderleyden, J. (1995). Small cysteine-rich antifungal proteins from radish: their role in host defense, The plant cell, 7(5): 573-588.

41. Finkina, E. I., and Ovchinnikova, T. V. (2018). Plant defensins: Structure, functions, biosynthesis, and the role in the immune response, Russian journal of bioorganic chemistry, 44(3): 261-278.

42. Zhu, S., Gao, B., and Tytgat, J. (2005). Phylogenetic distribution, functional epitopes and evolution of the CSáâ superfamily, Cellular and molecular life sciences CMLS, 62(19-20): 2257-2269.

43. Aerts, A. M., François, I. E. J. A., Cammue, B. P. A., and Thevissen, K. (2008). The mode of antifungal action of plant, insect and human defensins, Cellular and molecular life sciences, 65(13): 2069-2079.

44. Francisco, G. C., and Georgina, E. (2017). Structural Motifs in Class I and Class II Plant Defensins for Phospholipid Interactions: Intriguing Role of Ligand Binding and Modes of Action, Journal of plant physiology and pathology, 5, 1: 2.

45. De Oliveira Dias, R., and Franco, O. L. (2015). Cysteine-stabilized áâ defensins: from a common fold to antibacterial activity, Peptides, 72: 64-72.

46. Cools, T. L., Struyfs, C., Cammue, B. P., and Thevissen, K. (2017). Antifungal plant defensins: increased insight in their mode of action as a basis for their use to combat fungal infections, Future microbiology, 12(5): 441-454.

47. Lay, F. T., Brugliera, F., and Anderson, M. A. (2003). Isolation and properties of floral defensins from ornamental tobacco and petunia, Plant physiology, 131(3): 1283-1293.

48. Bruix, M., Jimenez, M. A., Santoro, J., Gonzalez, C., Colilla, F. J., Mendez, E., and Rico, M. (1993). Solution structure of. gamma. 1-H and. gamma. 1-P thionins from barley and wheat endosperm determined by proton NMR: a structural motif common to toxic arthropod proteins, Biochemistry, 32(2): 715-724.

49. Fant, F., Vranken, W., Broekaert, W., and Borremans, F. (1998). Determination of the three-dimensional solution structure of *R. sativus* Antifungal Protein 1 by 1H NMR1, Journal of molecular biology, 279(1): 257-270.

50. De Paula, V. S., Razzera, G., Barreto-Bergter, E., Almeida, F. C., and Valente, A. P. (2011). Portrayal of complex dynamic properties of sugarcane defensin 5 by NMR: multiple motions associated with membrane interaction, Structure, 19(1): 26-36.

51. Song, X., Zhang, M., Zhou, Z., and Gong, W. (2011). Ultra-high resolution crystal structure of a dimeric defensin SPE10, FEBS letters, 585(2): 300-306.

52. Van der Weerden, N. L., and Anderson, M. A. (2013). Plant defensins: common fold, multiple functions, Fungal biology reviews, 26(4): 121-131.

53. Yount, N. Y., and Yeaman, M. R. (2006). Structural congruence among membrane-active host defense polypeptides of diverse phylogeny, Biochimica et biophysica acta (BBA)-biomembranes, 1758(9): 1373-1386.

54. Yount, N. Y., and Yeaman, M. R. (2004). Multidimensional signatures in antimicrobial peptides, Proceedings of the national academy of sciences, 101(19): 7363-7368.

55. Sagaram, U. S., Pandurangi, R., Kaur, J., Smith, T. J., and Shah, D. M. (2011). Structure-activity determinants in antifungal plant defensins MsDef1 and MtDef4 with different modes of action against Fusarium graminearum, PLoS One, 6(4): e18550.

56. Thevissen, K., Osborn, R. W., Acland, D. P., & Broekaert, W. F. (2000). Specific

binding sites for an antifungal plant defensin from Dahlia (*D. merckii*) on fungal cells are required for antifungal activity, Molecular plant-microbe interactions, 13(1): 54-61.

57. Terras, F. R., Schoofs, H. M., De Bolle, M. F., Van Leuven, F., Rees, S. B., Vanderleyden, J., and Broekaert, W. F. (1992). Analysis of two novel classes of plant antifungal proteins from radish (*R. sativus* L.) seeds, Journal of biological chemistry, 267(22): 15301-15309.

58. Osborn, R. W., De Samblanx, G. W., Thevissen, K., Goderis, I., Torrekens, S., Van Leuven, F., and Broekaert, W. F. (1995). Isolation and characterisation of plant defensins from seeds of Asteraceae, Fabaceae, Hippocastanaceae and Saxifragaceae, FEBS letters, 368(2): 257-262.

59. Poon, I. K., Baxter, A. A., Lay, F. T., Mills, G. D., Adda, C. G., Payne, J. A., and van der Weerden,N. L. (2014). Phosphoinositide-mediated oligomerization of a defensin induces cell lysis, Elife, 3, e01808.

60. Thevissen, K., Ghazi, A., De Samblanx, G. W., Brownlee, C., Osborn, R. W., and Broekaert, W. F. (1996). Fungal membrane responses induced by plant defensins and thionins, Journal of biological chemistry, 271(25): 15018-15025.

61. Nicolas, P. (2009). Multifunctional host defense peptides: intracellular targeting antimicrobial peptides, The FEBS journal, 276(22): 6483-6496.

62. Almeida, M. S., Cabral, K. M., Kurtenbach, E., Almeida, F. C., and Valente, A. P. (2002). Solution structure of *P. sativum* defensin 1 by high resolution NMR: plant defensins, identical backbone with different mechanisms of action, Journal of molecular biology, 315(4): 749-757.

63. Muñoz, A., Chu, M., Marris, P. I., Sagaram, U. S., Kaur, J., Shah, D. M., and Read, N. D. (2014). Specific domains of plant defensins differentially disrupt colony initiation, cell fusion and calcium homeostasis in Neurospora crassa, Molecular microbiology, 92(6): 1357-1374.

64. Sagaram, U. S., El-Mounadi, K., Buchko, G. W., Berg, H. R., Kaur, J., Pandurangi, R. S., and Shah, D. M. (2013). Structural and functional studies of a phosphatidic acid-binding antifungal plant defensin MtDef4: identification of an RGFRRR motif governing fungal cell entry, PLoS one, 8(12): e82485.

65. Aerts, A. M., François, I. E., Bammens, L., Cammue, B. P., Smets, B., Winderickx, J., and Thevissen, K. (2006). Level of M (IP) 2C sphingolipid affects plant defensin sensitivity, oxidative stress resistance and chronological life span in yeast, FEBS letters, 580 (7):1903-1907.

66. Aerts, A. M., François, I. E., Meert, E. M., Li, Q. T., Cammue, B. P., and Thevissen, K. (2007). The antifungal activity of RsAFP2, a plant defensin from *R. sativus*, involves the induction of reactive oxygen species in Candida albicans, Journal of molecular microbiology and biotechnology, 13(4):243-247.

67. Aerts, A. M., Bammens, L., Govaert, G., Carmona-Gutierrez, D., Madeo, F., Cammue, B., and Thevissen, K. (2011). The antifungal plant defensin HsAFP1 from Heuchera sanguinea induces apoptosis in Candida albicans, Frontiers in microbiology, 2: 47.

68. De Oliveira Carvalho, A., and Moreira Gomes, V. (2011). Plant defensins and defensin-like peptides-biological activities and biotechnological applications, Current pharmaceutical design, 17(38): 4270-4293.

69. Broekaert, W. F., Cammue, B. P., De Bolle, M. F., Thevissen, K., De Samblanx, G. W., Osborn, R. W., and Nielson, K. (1997). Antimicrobial peptides from plants, Critical reviews in plant sciences, 16(3): 297-323.

70. Fossdal, C. G., Nagy, N. E., Sharma, P., and Lönneborg, A. (2003). The putative

gymnosperm plant defensin polypeptide (SPI1) accumulates after seed germination, is not readily released, and the SPI1 levels are reduced in Pythium dimorphum-infected spruce roots, Plant molecular biology, 52(2): 291-302.

71. Kragh, K. M., Nielsen, J. E., Nielsen, K. K., Dreboldt, S., and Mikkelsen, J. D. (1995). Characterization and localization of new antifungal cysteine-rich proteins from *B. vulgaris*, Molecular plant microbe interactions, 8(3): 424-434.

72. Siddique, S., Wieczorek, K., Szakasits, D., Kreil, D. P., and Bohlmann, H. (2011). The promoter of a plant defensin gene directs specific expression in nematode-induced syncytia in Arabidopsis roots, Plant physiology and biochemistry, 49(10): 1100-1107.

73. Hafez, E. E., Hashem, M., Balbaa, M. M., El-Saadani, M. A., and Ahmed, S. A. (2013). Induction of New Defensin Genes in Tomato Plants via Pathogens-Biocontrol Agent Interaction, *Journal of plant pathology* and *microbiology*, 4: 167.

74. Lai, F. M., DeLong, C., Mei, K., Wignes, T., and Fobert, P. R. (2002). Analysis of the DRR230 family of pea defensins: gene expression pattern and evidence of broad host-range antifungal activity, Plant science, 163(4): 855-864.

75. Mona M. Elseehy. (2015). Expression of defensin genes in Egyptian wheat (*T. aestivum*) varieties during grain germination, Journal of agricultural chemistry and biotechnology, 6 (3): 65 -75.

76. Mitra, R. M., and Long, S. R. (2004). Plant and bacterial symbiotic mutants define three transcriptionally distinct stages in the development of the *M. truncatula*/ Sinorhizobium meliloti symbiosis, Plant physiology, 134(2): 595-604.

77. Wang, W., Cole, A. M., Hong, T., Waring, A. J., and Lehrer, R. I. (2003). Retrocyclin, an antiretroviral è-defensin, is a lectin, The journal of immunology, 170(9): 4708-4716.

78. Gao, A. G., Hakimi, S. M., Mittanck, C. A., Wu, Y., Woerner, B. M., Stark, D. M., and Rommens, C. M. (2000). Fungal pathogen protection in potato by expression of a plant defensin peptide, Nature biotechnology, 18(12): 1307.

79. Kanzaki, H., Nirasawa, S., Saitoh, H., Ito, M., Nishihara, M., Terauchi, R., and Nakamura, I. (2002). Overexpression of the wasabi defensin gene confers enhanced resistance to blast fungus (Magnaporthe grisea) in transgenic rice, Theoretical and applied genetics, 105(6-7): 809-814.

80. Zimmerli, L., Stein, M., Lipka, V., Schulze Lefert, P., and Somerville, S. (2004). Host and non host pathogens elicit different MT/ ET responses in Arabidopsis, The plant journal, 40(5): 633-646.

81. Luo, J. S., Huang, J., Zeng, D. L., Peng, J. S., Zhang, G. B., Ma, H. L., and Lin, H. X. (2018). A defensin-like protein drives cadmium efflux and allocation in rice, Nature communications, 9(1): 645.

82. Park, H. C., Kang, Y. H., Chun, H. J., Koo, J. C., Cheong, Y. H., Kim, C. Y., and Koo, Y. D. (2002). Characterization of a stamen-specific cDNA encoding a novel plant defensin in Chinese cabbage, Plant molecular biology, 50(1): 57-68.

83. Gu, Q., Kawata, E. E., Morse, M. J., Wu, H. M., and Cheung, A. Y. (1992). A flower-specific cDNA encoding a novel thionin in tobacco, Molecular and general genetics MGG, 234(1): 89-96.

84. Komori, T., Yamada, S., and Imaseki, H. (1997). A cDNA clone for ã-thionin from *N. paniculata* (accession no. AB005250; PGR97–132), Plant physiology, 115: 314.

85. Milligan, S. B., and Gasser, C. S. (1995). Nature and regulation of pistil-expressed genes in tomato, Plant molecular biology, 28(4): 691-711.

86. Nanni, V., Schumacher, J., Giacomelli, L., Brazzale, D., Sbolci, L., Moser, C., and Baraldi, E. (2014). Vv AMP 2, a grapevine flower specific defensin capable of inhibiting B otrytis cinerea growth: insights into its mode of action, Plant pathology, 63(4): 899-910.
87. Epple, P., Apel, K., & Bohlmann, H. (1997). ESTs reveal a multigene family for plant defensins in Arabidopsis thaliana, FEBS letters, 400(2): 168-172.
88. Tavares, L. S., Santos, M. D. O., Viccini, L. F., Moreira, J. S., Miller, R. N., and Franco, O. L. (2008). Biotechnological potential of antimicrobial peptides from flowers, Peptides, 29(10): 1842-1851.
89. Tesfaye, M., Silverstein, K. A., Nallu, S., Wang, L., Botanga, C. J., Gomez, S. K., and Katagiri, F. (2013). Spatio-temporal expression patterns of *A. thaliana* and *M. truncatula* defensin-like genes, Plos one, 8(3): e58992.
90. Bloch, C., and Richardson, M. (1991). A new family of small (5 kDa) protein inhibitors of insect á amylases from seeds or sorghum (Sorghum bicolor (L) Moench) has sequence homologies with wheat β purothionins, FEBS letters, 279(1): 101-104.
91. Seo, H. H., Park, S., Park, S., Oh, B. J., Back, K., Han, O., and Kim, Y. S. (2014). Overexpression of a defensin enhances resistance to a fruit-specific anthracnose fungus in pepper, Plos one, 9(5): e97936.
92. Zahirnejad, B., Bahramnejad, B., and Rostamzadeh, J. (2018). Isolation and Expression Analysis of a Defensin Gene from Strawberry (Fragaria× ananassa cv. Paros), Journal of agricultural science and technology, 20(6): 1243-1257.
93. Wisniewski, M. E., Bassett, C. L., Artlip, T. S., Webb, R. P., Janisiewicz, W. J., Norelli, J. L., and Droby, S. (2003). Characterization of a defensin in bark and fruit tissues of peach and antimicrobial activity of a recombinant defensin in the yeast, Pichia pastoris, Physiologia Plantarum, 119(4): 563-572.
94. Dos Santos, I. S., Carvalho, A. D. O., de Souza-Filho, G. A., do Nascimento, V. V., Machado, O. L., and Gomes, V. M. (2010). Purification of a defensin isolated from Vigna unguiculata seeds, its functional expression in Escherichia coli, and assessment of its insect á-amylase inhibitory activity, Protein expression and purification, 71(1): 8-15.
95. Zhang, M., Yang, X. P., Xu, J. H., Liu, G., Yao, X. F., Li, P. F., and Zhu, L. L. (2014). Cloning and differential expression analysis of defensin gene Cldef2. 2 from watermelon (Citrullus lanatus (Thunb.) Matsum. & Nakai), In XXIX International Horticultural Congress on Horticulture: Sustaining Lives, Livelihoods and landscapes (IHC2014): 1110 (pp. 49-56).
96. Rawat, S., Ali, S., Nayankantha, N. C., Chandrashekar, N., Mittra, B., and Grover, A. (2017). Isolation and expression analysis of defensin gene and its promoter from *B.juncea*, Journal of plant diseases and protection, 124(6): 591-600.
97. Terras, F. R., Penninckx, I. A., Goderis, I. J., and Broekaert, W. F. (1998). Evidence that the role of plant defensins in radish defense responses is independent of SA, Planta, 206(1): 117-124.
98. Hanks, J. N., Snyder, A. K., Graham, M. A., Shah, R. K., Blaylock, L. A., Harrison, M. J., and Shah, D. M. (2005). Defensin gene family in Medicago truncatula: structure, expression and induction by signal molecules, Plant molecular biology, 58(3): 385-399.
99. Penninckx, I. A., Eggermont, K., Terras, F. R., Thomma, B. P., De Samblanx, G. W., Buchala, A., and Broekaert, W. F. (1996). Pathogen-induced systemic activation of a plant defensin gene in Arabidopsis follows a SA-independent pathway, The plant cell, 8(12): 2309-2323.
100. Penninckx, I. A., Thomma, B. P., Buchala, A., Métraux, J. P., and Broekaert, W. F. (1998). Concomitant activation of MJ and ET response pathways is required for induction of a plant defensin gene in Arabid-

opsis, The Plant Cell, 10(12): 2103-2113.
101. Rivera-Domínguez, M., Astorga-Cienfuegos, K. R., Tiznado-Hernández, M. E., and González-Aguilar, G. A. (2012). Induction of the expression of defence genes in Carica papaya fruit by MJ and low temperature treatments, Electronic Journal of Biotechnology, 15 (5): 6-6.
102. Pervieux, I., Bourassa, M., Laurans, F., Hamelin, R., and Séguin, A. (2004). A spruce defensin showing strong antifungal activity and increased transcript accumulation after wounding and MJ treatments, Physiological and molecular plant pathology, 64(6): 331-341.
103. Castro, M. S., and Fontes, W. (2005). Plant defense and antimicrobial peptides, Protein and peptide letters, 12(1): 11-16.
104. Ponti, D., Mangoni, M. L., Mignogna, G., Simmaco, M., and Barra, D. (2003). An amphibian antimicrobial peptide variant expressed in *N. tabacum* confers resistance to phytopathogens, Biochemical journal, 370(1): 121-127.
105. Halpin, C., Cooke, S. E., Barakate, A., Amrani, A. E., and Ryan, M. D. (1999). Self processing 2A polyproteins–a system for co ordinate expression of multiple proteins in transgenic plants, The plant journal, 17(4): 453-459.
106. Owens, L. D., and Heutte, T. M. (1997). A single amino acid substitution in the antimicrobial defense protein cecropin B is associated with diminished degradation by leaf intercellular fluid, Molecular plant-microbe interactions, 10(4): 525-528.
107. Kong, K., Ntui, V. O., Makabe, S., Khan, R. S., Mii, M., and Nakamura, I. (2014). Transgenic tobacco and tomato plants expressing Wasabi defensin genes driven by root-specific LjNRT2 and AtNRT2. 1 promoters confer resistance against *F. oxysporum*, Plant biotechnology, 31(2): 89-96.
108. Zainal, Z., Marouf, E., Ismail, I., and Fei, C. K. (2009). Expression of the Capsicuum annum (chili) defensin gene in transgenic tomatoes confers enhanced resistance to fungal pathogens, American journal of plant physiology, 4(2): 70-79.
109. Jha, S., and Chattoo, B. B. (2009). Transgene stacking and coordinated expression of plant defensins confer fungal resistance in rice, Rice, 2(4): 143-154.
110. Kaur, J., Fellers, J., Adholeya, A., Velivelli, S. L., El-Mounadi, K., Nersesian, N., and Shah, D. (2017). Expression of apoplast-targeted plant defensin MtDef4.2 confers resistance to leaf rust pathogen Puccinia triticina but does not affect mycorrhizal symbiosis in transgenic wheat, Transgenic research, 26(1): 37-49.
111. Sharma, K. K., Pothana, A., Prasad, K., Shah, D., Kaur, J., Bhatnagar, D., Sudini, H. K. and Bhatnagar-Mathur, P. (2018). Peanuts that keep aflatoxin at bay: a threshold that matters, Plant biotechnology journal, 16(5):1024-1033.
112. Portieles, R., Ayra, C., Gonzalez, E., Gallo, A., Rodriguez, R., Chacón, O., and Enriquez, G. (2010). NmDef02, a novel antimicrobial gene isolated from *N. megalosiphon* confers high level pathogen resistance under greenhouse and field conditions, Plant biotechnology journal, 8(6): 678-690.
113. Jaber, E., Kovalchuk, A., Raffaello, T., Keriö, S., Teeri, T., and Asiegbu, F. O. (2017). A Gene Encoding Scots Pine Antimicrobial Protein Sp-AMP2 (PR-19) Confers Increased Tolerance against *B. cinerea* in Transgenic Tobacco, Forests, 9(1): 10.
114. Germain, H., Lachance, D., Pelletier, G., Fossdal, C. G., Solheim, H., and Séguin, A. (2011). The expression pattern of the *P. glauca* Defensin 1 promoter is maintained in *A. thaliana*, indicating the conservation of signalling pathways between angiosperms and gymnosperms, Journal of experimental botany, 63(2): 785-795.
115. Arenas, G., Marshall, S. H., Espinoza, V., Ramírez, I., and Peña-Cortés, H. (2006). Protective effect of an antimicrobial peptide from Mytilus edulis chilensis expressed in *N. tabacum* L, Electronic journal of biotechnology, 9(2): 0-0.

Vol. 13 (2) i - ii April 2019, ISSN 0973-8916 (Print), 2230-7303 (Online)

NEWS ITEM

IISc researchers dispatched directly proteins into cells, first of its kind

In a breakthrough that might have huge medical implications, researchers at Bengaluru's Indian Institute of Science (IISc) have used a novel strategy to directly deliver proteins into mammalian cells. Proteins are big molecules and so cannot enter the cells on their own. So a team led by Govindasamy Mugesh from the institute's Department of Inorganic and Physical Chemistry substituted a hydrogen atom of the protein with an iodine atom to achieve a nearly sixfold increase in protein uptake by cells.The increased protein uptake was seen even when the molecular weight of the protein was 28,000 dalton, meaning the protein was much bigger in size than most of the therapeutic small molecules.The researchers also tried replacing a hydrogen atom with an atom of bromine and chlorine but the uptake was way lower than when iodine was used.In the case of bromine, the uptake of proteins increased by only about two times, while the uptake increased only marginally when chlorine was used. The results were published in the journal Angewandte Chemie. Other researchers have tried tagging the protein with cell-penetrating peptides, supercharged proteins and even used virus-like particles to ferry the proteins into cells. But these approaches have severe limitations including altering the protein function inside the cell. For this reason, most of the applications involving proteins are directed to extracellular targets. Proteins inside the cells get impaired during diseased conditions such as neurodegenerative and cardiovascular disease. Supplementing the cellular protein in such cases becomes important and this is where the method used by the IISc team will come in handy.The team had to first synthesise a green fluorescent protein with one hydrogen atom being replaced with an iodine atom. Iodine forms a halogen bond with a specific receptor (caveolin) that transports the protein from the cell membrane surface to inside the cells. To be functionally useful, the proteins must enter the cytoplasm of the cell. However, the moment proteins are ferried into the cell by the receptor they are trapped inside the endosomes and transported to lysosomes, where the proteins are degraded. Significant decrease in protein concentration as measured by the fluorescence intensity was seen by the researchers after 24 hours.To overcome the problem of protein degradation, the team treated the cells with a peptide (ppTG21).

Detection of oral cancer is possible through lymph node biomarkers By looking out for five biomarkers, it is now possible to tell in advance if a person with oral cancer of the gum and cheek has lymph node metastasis even before surgery is undertaken, a study has found. The ability to correctly predict absence/presence of lymph node metastasis in oral cancer patients is 80-90% based on the five biomarkers, a team led by Partha Majumder from the National Institute of Biomedical Genomics, Kalyani, West Bengal, has found. As a result, an oral cancer patient can be spared of a neck dissection to investigate if the cancer has spread to the lymph nodes in case the five biomarkers are absent. Lymph node dissection increases morbidity. However, if the patient tests positive for even one biomarker then an aggressive treatment would be required. An oral cancer patient with cancer spread to the lymph node has a 50% lower chance of survival for five years or more compared with patients in whom it has not spread to the lymph node.

In oral cancer patients, the cancer cells tend to commonly spread to the lymph node in the neck. But not all oral cancer patients have the tendency for the cancer to spread to other organs (metastasis). So in some patients, the cancer would have spread to the lymph node even at an early stage of oral cancer, while in some patients with advanced (T4 stage) oral cancer, the cancer would not have spread.To find out what determines lymph node metastasis in oral cancer patients, the team studied two groups of patients — those with lymph node metastasis and those with advanced oral cancer but without lymph node metastasis. Totally, 72 patients belonging to these two groups were studied by a team led by Dr. Rajiv Sarin, Director of Advanced Centre for Treatment, Research and Education in Cancer (ACTREC), Tata Memorial Centre, Mumbai and co-author of the paper.The team found that lymph node metastasis was associated with five genomic biomarkers. The results were published in International Journal of Cancer.There are five genomic features or biomarkers of lymph node metastasis in oral cancer patients. Two of these are rare, heritable DNA changes in BRCA2 and FAT1 genes. The remaining three are non-heritable (somatic) DNA alterations. The somatic DNA alterations can occur in genes belonging to three different pathways — mitotic G2/M cell-cycle pathway, homologous recombination (HR) and non-homologous end joining (NHEJ) DNA-repair pathways. The protein product of FAT1 gene functions as an adhesion molecule that keeps the

cells together. In the case of cancer, cellular adhesion property is sometimes lost and the cells tend to spread. A cell duplicates to produce two daughter cells. Many genes are involved in this cell-cycle pathway, called mitotic G2/M pathway. If DNA of one or more genes of this pathway is altered, then many adverse cellular events take place. Most importantly, chromosomes become unstable and abnormal chromosomal changes occur, eventually leading to metastasis.

Researchers from JNCASR synthesised novel molecule for spinal cord injury

Spinal cord injury can now be repaired using a small molecule (TTK21) synthesised by a team led by Tapas Kumar Kundu from the Molecular Biology and Genetics Unit at Jawaharlal Nehru Centre for Advanced Scientific Research (JNCASR), Bengaluru, a study has found. The small molecule tested both on mice and rat models promoted regeneration and growth of new sensory and motor axons leading to recovery of sensory and motor functions in the animals with spinal cord injury.Since the small molecule cannot cross the blood–brain barrier and enter the brain, the researchers used 400 nanometre-size carbon nanospheres made using glucose, which is self-fluorescent, and attached the molecule to its surface. The non-toxic nature of the small molecule has already been demonstrated in animals.The JNCASR researchers in collaboration with a French team had in October 2018 used the same molecule to recover long-term memory in mice with Alzheimer's disease.When the spinal cord is injured, the tails (axons) of nerve cells that stretch up and down the spine are either damaged or even completely cut.

For the first time Black hole image was unearthed:

This image released on April 10, 2019 by Event Horizon Telescope shows a black hole. Scientists revealed the first image ever made of a black hole after assembling data gathered by a network of radio telescopes around the world. Photo: Event Horizon Telescope Collaboration/Maunakea Observatories. This image released on April 10, 2019 by Event Horizon Telescope shows a black hole. Scientists revealed the first image ever made of a black hole after assembling data gathered by a network of radio telescopes around the world. Scientists have been puzzling over invisible "dark stars" since the 18th century, but never has one been spied by a telescope, much less photographed.Astronomers on April 10 unveiled the first photo of a black hole, one of the star-devouring monsters scattered throughout the Universe and obscured by impenetrable shields of gravity. The image of a dark core encircled by a flame-orange halo of white-hot gas and plasma looks like any number of artists' renderings over the last 30 years. Scientists have been puzzling over invisible "dark stars" since the 18th century, but never has one been spied by a telescope, much less photographed. The supermassive black hole now immortalised by a far-flung network of radio telescopes is 50 million lightyears away in a galaxy known as M87.The unprecedented image — so often imagined in science and science fiction — has been analysed in six studies co-authored by 200 experts from 60-odd institutions and published on April 10 in Astrophysical Journal Letters.The Universe is filled with electromagnetic "noise", and there was no guarantee M87's faint signals could be extracted from a mountain of data so voluminous it could not be delivered via the Internet.

Post doc opportunities:

1. Tata Institute for Genetics and Society-Bengaluru, Karnataka: Post-doctoral Fellow with the Tata Institute of Genetics and Society, inStem, Bangalore, Karnataka.To be part of a team of scientists working on gene editing in mammalian stem cellsRefer concerned website.

2. Institute for Stem Cell Biology and Regenerative Medicine- Bengaluru, Karnataka: A post-doctoral fellow position is available for a candidate with cell and molecular biology expertise. The position is to work on the molecular mechanisms of Alzheimer's disease reporting to Prof.Mahendra Rao at inStem, Bengaluru Refer website instem.res.in

3. Indian Institute of Technology Hyderabad - Hyderabad, Telangana: Postdoctoral Position" on Stem Cell Engineering and Regenerative Medicine at eNARM Lab, Department of Biomedical Engineering, IIT Hyderabad. Refer iith.ac.in.

The 13th Annual Convention of ABAP & International Conference on

ENVIRONMENTAL SUSTAINABILITY, HUMAN HEALTH AND DEVELOPMENT

20 - 22nd December, 2019

First Circular

Jointly Organized by

Association of Biotechnology and Pharmacy

KNOWLEDGE IS POWER

and

Department of Biotechnology

VIGNAN'S

Foundation for Science, Technology & Research

UNIVERSITY

(Estd u/s 3 of UGC Act of 1956)

Venue: A-Block, Sangamam Seminar Hall
VFSTR, Vadlamudi-522213 A. P., India

Registered with Registrar of News Papers for India
Regn. No. APENG/2008/28877

Association of Biotechnology and Pharmacy

(Regn. No. 28OF 2007)

Printed, Published and owned by Association of Bio-Technology and Pharmacy # 6-69-64 : 6/19, Brodipet, Guntur - 522 002, Andhra pradesh, India. **Printed at :** Don Bosco Tech. School Press, Ring Road, Guntur - 522 007. A.P., India **Published at :** Association of Bio-Technology and Pharmacy # 6-69-64 : 6/19, Brodipet, Guntur - 522 002, Andhra pradesh, India.
Editors : Prof. K.R.S. Sambasiva Rao, Prof. Karnam S. Murthy